AD-A083 972 CAMBRIDGE UNIV (ENGLAND) DEPT OF CIVIL ENGINEERING F/G 8/13
CENTRIFUGAL MODELLING OF SOIL STRUCTURES. PART II. THE CENTRIFU--ETC(U)
JUN 79 D V MORRIS, A N SCHOFIELD DA-ERO-76-G-040
UNCLASSIFIED NL

1 OF 3
AD
A083972


NC

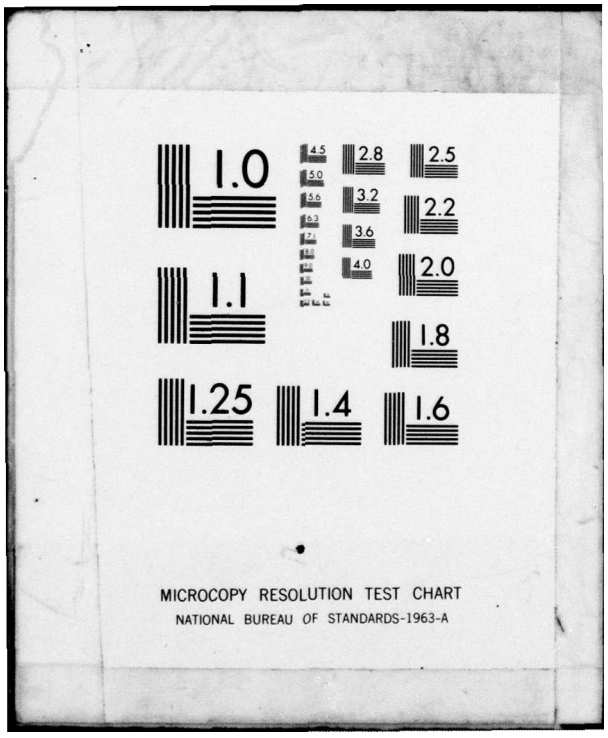
1.0
4.5
5.0
5.6
6.3
2.8
3.2
3.6
4.0
2.5
2.2
2.0
1.8
1.1
1.25
1.4
1.6
MICROCOPY RESOLUTION TEST CHART
NATIONAL BUREAU OF STANDARDS-1963-A

CENTRIFUGAL MODELLING OF SOIL STRUCTURES
PART II

THE CENTRIFUGAL MODELLING OF DYNAMIC SOIL-STRUCTURE INTERACTION AND EARTHQUAKE BEHAVIOUR

Final Technical Report

by

Derek Victor Morris

June 1979

EUROPEAN RESEARCH OFFICE

United States Army

London England

GRANT NUMBER DA-ERO - 76-G-040

A. N. Schofield

Approved for Public Release; distribution unlimited

Unclassified
SECURITY CLASSIFICATION OF THIS PAGE (When Data Entered)

REPORT DOCUMENTATION PAGE

READ INSTRUCTIONS BEFORE COMPLETING FORM

1. REPORT NUMBER (6)

2. GOVT ACCESSION NO. AD-A083972

3. RECIPIENT'S CATALOG NUMBER

4. TITLE (and Subtitle)
Centrifugal Modelling of Soil Structures. Part II. The Centrifugal Modelling of Dynamic Soil-Structure Interaction and Earthquake Behavior.

5. TYPE OF REPORT & PERIOD COVERED
Final Technical
6 May 76 - 5 May 79

6. PERFORMING ORG. REPORT NUMBER

7. AUTHOR(s) (10)
Derek Victor Morris
Andrew N. Schofield

8. CONTRACT OR GRANT NUMBER(s) (14)
DAERO-76-G-040

9. PERFORMING ORGANIZATION NAME AND ADDRESS
Department of Civil Engineering
Cambridge University
Cambridge, United Kingdom

10. PROGRAM ELEMENT, PROJECT, TASK AREA & WORK UNIT NUMBERS (16)
ITI61102BH57-01 (17) 01

11. CONTROLLING OFFICE NAME AND ADDRESS
U. S. Army Research & Standardization Group (Eur)
Box 65
FPO NY 09510

12. REPORT DATE (11)
June 1979

13. NUMBER OF PAGES
205

14. MONITORING AGENCY NAME & ADDRESS (if different from Controlling Office)
USAE Waterways Experiment Station
P. O. Box 631
Vicksburg, MS 39180

15. SECURITY CLASS. (of this report) (12) 022
Unclassified

15a. DECLASSIFICATION/DOWNGRADING SCHEDULE

16. DISTRIBUTION STATEMENT (of this Report) (15) DA-ERO-76-G-040
Distribution unlimited

17. DISTRIBUTION STATEMENT (of the abstract entered in Block 20, if different from Report) (9)
Final technical rept. 6 May 76-5 May 79,

18. SUPPLEMENTARY NOTES
411 742

19. KEY WORDS (Continue on reverse side if necessary and identify by block number)
Soil mechanics, centrifuge modelling, earthquakes, foundation stability, soil dynamics, dynamic modelling, geotechnical centrifuge

20. ABSTRACT (Continue on reverse side if necessary and identify by block number)
Accurate model tests of problems in soil mechanics may be carried out by the technique of centrifugal modelling, which preserves the correct magnitude and distribution of stress in the soil. There is a consistent set of rules to relate the behaviour of a full-size prototype to the behaviour of a model for both static test, and dynamic events. The object of this investigation was, firstly, to show that dynamic modelling was possible, and secondly, to use the technique for some initial studies of soil-structure dynamic interaction and
(Over)

DD FORM 1 JAN 73 1473 EDITION OF 1 NOV 65 IS OBSOLETE

Unclassified
SECURITY CLASSIFICATION OF THIS PAGE (When Date Entered)

earthquake motion. The first tests investigated the rocking behaviour of rigid towers, instrumented with accelerometers, on bases of varying sizes and geometries, resting on a foundation of dry sand. It was possible to measure the natural frequency and damping of the soil-structure system by perturbing such a tower-firstly, by detonating a small explosive charge on the tower - secondly, by recording its wind-induced motion. The natural frequency of circular foundations appeared to be satisfactorily predicted by a simple one-degree-of-freedom analysis, utilising equivalent elastic theory for the rotational foundation stiffness. However, agreement depended on the precise assumptions that were made about the magnitude and distribution of the soil stress(and hence soil modulus) under the foundation. The inelastic and yielding behavior of soil tends to reduce the rotational stiffness predicted by elastic theory. A suitalble empirical rule for small values of strain(below which the effect of strain softening is not important) is proposed. Current elastic theory for square foundations also appeared to be satisfactory, although values of stiffness for embedded foundations were over-estimated by theory. Interaction effects between adjacent towers appeared to be small. Large amplitudes of motion measurably decreased the base stiffness. It was also possible to verify the dynamic modelling laws indirectly, using differnt models of the same prototype. For subsequent test, a special apparatus was designed and constructed to model horizontal earthquake motion on the centrifuge. It may be described as a shaking table on a centrifuge, with an exponentially decaying horizontal motion provided by mechanical springs. Values of horizontal acceleration and frequency correspond to values suitably scaled-up from typical full size earthquakes. Miniature transducers were successfully used to record dynamic motions and pore pressures. Initial test on the earthquake motion of a rigid rocking tower on dry sand implied that a simple one-degree-of-freedom analysis was inadequate to describe the observed behavior, which was much more complex than initially imagined. Similar test with saturated fine sand showed generation of excess pore pressure under the foundation, and in one case, foundation failure. It was also shown both experimentally and theoretically that a simple quasi-static analysis grossly over-estimated the likelihood of towers "falling over" as a result of an earthquake producing high horizontal accelerations. Test on embankments of dry sand showed that they moved as a rigid body with little amplification of movement towards the crest, since in this case, their fundamental frequency was well above the earthquake frequency. Slip of surface material was observed for large values of horizontal acceleration and steep slopes, and this correlated with a simple stability analysis. Qualitative test on embankments of saturated fine sand clearly showed the cyclic generation of pore pressures inside the soil, non-uniform motion of the embankment in response to the base motion, and its failure by lateral spreading. There are some difficulties associated with the dynamic modelling of saturated soils, and careful attention must be given to the modelling laws if particular full size prototypes are to be modelled correctly.

THE CENTRIFUGAL MODELLING OF DYNAMIC SOIL-STRUCTURE INTERACTION AND EARTHQUAKE BEHAVIOUR

Derek Victor Morris

A Dissertation submitted for the Degree of
Doctor of Philosophy

at

Cambridge University
Cambridge
England

St. John's College
Cambridge
June 1979

Frontispiece - Typical damage after the 1964 earthquake in Niigata, Japan.

SYNOPSIS

Accurate model tests of problems in soil mechanics may be carried out by the technique of centrifugal modelling, which preserves the correct magnitude and distribution of stress in the soil. There is a consistent set of rules to relate the behaviour of a full-size prototype to the behaviour of a model, not only for static tests, but also for dynamic events. The object of this investigation was, firstly, to show that dynamic modelling was possible, and secondly, to use the technique for some initial studies of soil-structure dynamic interaction and earthquake motion.

The project used the geotechnical centrifuge at Cambridge University, England, and this will accept packages of almost one tonne in mass at a maximum acceleration of 155 g.

The first tests investigated the rocking behaviour of rigid towers, instrumented with accelerometers, on bases of varying sizes and geometries, resting on a foundation of dry sand. It was possible to measure the natural frequency and damping of the soil-structure system by perturbing such a tower - firstly, by detonating a small explosive charge on the tower, and secondly, by recording its wind-induced motion.

The natural frequency of circular foundations appeared to be satisfactorily predicted by a simple one-degree-of-freedom analysis, utilising equivalent elastic theory for the rotational foundation stiffness. However, agreement depended on the precise assumptions that were made about the magnitude and distribution of the soil stress (and hence soil modulus) under the foundation. The inelastic and yielding behaviour of soil tends to reduce the rotational stiffness predicted by elastic theory, and it was

possible to perform many centrifuge tests to quantify this effect. A suitable empirical rule for small values of strain (below which the effect of strain-softening is not important) is proposed.

Current elastic theory for square foundations also appeared to be satisfactory, although values of stiffness for embedded foundations were over-estimated by theory. Interaction effects between adjacent towers appeared to be small. Large amplitudes of motion measurably decreased the base stiffness. It was also possible to verify the dynamic modelling laws indirectly, using different models of the same prototype.

For subsequent tests, a special apparatus was designed and constructed to model horizontal earthquake motion on the centrifuge. It may be described as a shaking table on a centrifuge, with an exponentially decaying horizontal motion provided by mechanical springs. Values of horizontal acceleration and frequency correspond to values suitably scaled-up from typical full size earthquakes. Miniature transducers were successfully used to record dynamic motions and pore pressures.

Initial tests on the earthquake motion of a rigid rocking tower on dry sand implied that a simple one-degree-of-freedom analysis was inadequate to describe the observed behaviour, which was much more complex than initially imagined. Similar tests with saturated fine sand showed generation of excess pore pressure under the foundation, and in one case, foundation failure. It was also shown both experimentally and theoretically that a simple quasi-static analysis grossly over-estimated the likelihood of towers "falling over" as a result of an earthquake producing high horizontal accelerations.

Tests on embankments of dry sand showed that they moved as a rigid body with little amplification of movement towards the crest, since in this case, their fundamental frequency was well above the earthquake frequency. Slip of surface material was observed for large values of horizontal acceleration and steep slopes, and this correlated with a simple stability analysis.

Some qualitative tests on embankments of saturated fine sand clearly showed the cyclic generation of pore pressures inside the soil, non-uniform motion of the embankment in response to the base motion, and its failure by lateral spreading. There are some difficulties associated with the dynamic modelling of saturated soils, and careful attention must be given to the modelling laws if particular full size prototypes are to be modelled correctly. However, it is shown how these difficulties may be resolved.

It may be concluded that these tests have demonstrated that centrifugal modelling can be used successfully and relatively economically for experiments in dynamic soil mechanics, and have also provided interesting results on certain aspects of dynamic soil-structure interaction and earthquake engineering.

ACKNOWLEDGEMENTS

I am particularly grateful to Professor A.N. Schofield, the head of the Cambridge Soil Mechanics Group, to Dr. R.G. James as supervisor, to Professor R.V. Whitman who was a visitor in 1976/77, and indeed to all members of the Cambridge University Soil Mechanics Group, for their advice and assistance during this project.

Special mention must also be made of the support of Mr. R.E. Ward and his assistants Messrs. J. Doherty and W. Gwizdala, of Mr. A. Balodis for help with the electronic circuitry, of Mr. C. Collison for assistance in the operation of the centrifuge and Messrs. W. Gilman and T. Glyn of the Engineering Workshops for construction of the experimental equipment.

This research was supported by the European Research Office of the United States Army Corps of Engineers, and was part of a wider investigation into the environmental problems of liquefaction and earthquake behaviour.

I certify that, except where specific reference is made in the text to the work of others, the contents of this dissertation are original, and have not been submitted to any other university.

Derek V. Morris

June 1979 Derek V. Morris

CONTENTS

Illustrations

Illustrations (cont.)

Illustrations (cont.)

Photographs

Photographs (cont.)

CHAPTER 1

INTRODUCTION

In recent years, the technique of centrifugal modelling has attracted increasing attention in the model testing of soil mechanics problems. Properly conducted tests of this kind have certain fundamental advantages over conventional model tests, as the presence of centrifugal acceleration allows a scale model to duplicate the behaviour of a full size prototype much more accurately than a model at one gravity. The correct magnitude and distribution of stress in the soil is preserved, and there is a consistent set of rules to relate the behaviour of a prototype to a model. It seemed only logical, therefore, to attempt to extend this technique to include dynamic earthquake phenomena, and this was the main objective of the research described herein.

There are a number of additional reasons why this project was regarded as particularly important.

Firstly, the entire subject of earthquake phenomena has become very topical, as a result of recent prominent disasters. There is now a demand for proper evaluation of seismic risk, and an improved understanding of earthquake resistant design, and this demand will continue to increase with the prospect of ever more expensive and important construction (such as nuclear power plants) in areas that are both seismically active and environmentally sensitive.

Secondly, it has been extremely difficult to obtain reliable and relevant full-scale experimental data. Earthquakes

are naturally unpredictable, and on such an occasion, the collection of accurate measurements is usually an activity of low priority. Even when attempts are made to continuously monitor sites with comprehensive (and expensive) field instrumentation, the emphasis has been on monitoring the behaviour of structures, rather than soil, and the time-scale involved has been such that substantial deterioration of the instrumentation may often take place. Furthermore, earthquake records may differ quite radically from each other, and it would clearly be desirable (for parametric studies, for instance) to be able to take measurements that were repeatable.

Thirdly, conventional laboratory model tests, on shaking tables, for instance, have only been able to accommodate small models which involve stresses and strengths much smaller than at full-scale - so that in general, the properties of a prototype are not correctly modelled, and it is not obvious how to relate the behaviour of a model to the behaviour of a full-scale structure.

Fourthly, there are many serious difficulties in the theoretical analysis of earthquake behaviour. Analytic solutions provide a useful guide, but face severe problems in coping with anything other than simple geometries and uniform linear elastic material. Numerical solutions are more adaptable, but are expensive and face difficulties, in turn, in coping with true three-dimensional behaviour, plastic flow, discontinuities or slip in the soil. The performance, to date, of such computer analyses has been open to question, partly because the great number of assumptions and empirical constants

inherent in this process have meant that many alternative answers are frequently possible, and partly because there has been so little experimental data with which to validate such analyses.

For these reasons, the prime goal of this project was the design and construction of a special apparatus to model earthquake motion on a centrifuge. There is no theoretical objection to conducting dynamic tests on the centrifuge in this way, as the modelling laws are readily extended, and the method offers the prospect of producing experimental data relatively economically and repeatably.

This apparatus may conveniently be described as a shaking table on a centrifuge, and was used to investigate two immediate areas of research interest - the soil-structure interaction of model towers resting on dry and saturated sand, and the behaviour of both dry and saturated sand embankments subjected to a horizontal base movement.

It was also possible to carry out considerable preliminary work into the soil-structure interaction of a model tower, on the centrifuge, in a relatively simple fashion, and also to carry out an indirect verification of the dynamic modelling laws. These results are of considerable interest in their own right, and are described first.

CHAPTER 2

THE PRINCIPLES OF CENTRIFUGAL MODELLING

2.1 INTRODUCTION

The application of centrifugal model testing to soil mechanics was demonstrated as early as 1933 by Pokrovsky*, but only recently has much interest been shown in this technique in Western countries.

Centrifugal modelling relies on the fundamental equivalence of gravitational and inertial fields to set up a one-to-one correspondence between geometrically similar points in a full size prototype and in a model in a centrifuge.

If the linear modelling scale is defined as $n > 1$, then the general stress level under a depth z of soil of density ρ, is $z\rho g$. At the corresponding point in a centrifuge model, the linear dimension z is decreased to z/n, and the centrifugal (or quasi-gravitational) acceleration is increased to ng. The stress level at this point in the model will be the same as in the prototype. Similarly, the state of strain will be identical, if both

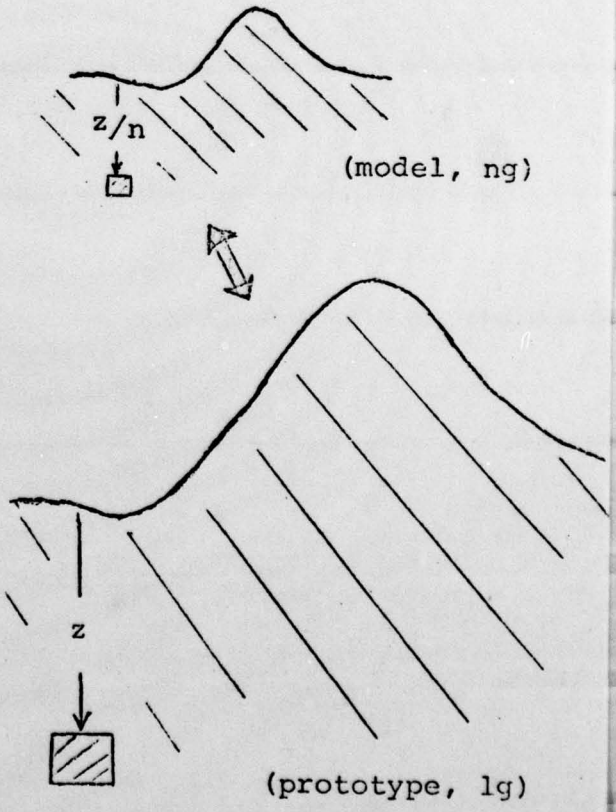

*POKROVSKY, G.I. (1933),"On the use of a centrifuge in the study of models of soil structures", Zeitschrift für Technische Physik, Vol. 14, No. 4 (in German).

the model and prototype are constructed of the same material.

This, then, is the basic tenet of centrifugal modelling. The pseudo-gravitational acceleration in a centrifuge soil model is increased to compensate for the reduction in size. Regarding soil as a continuum with identical bulk properties in the model and the prototype, there is, in principle, no immediate way that corresponding elements of soil can decide in which they are, as levels of stress, strain, pore-pressure, stress gradient, etc., are identical under this transformation. This equivalence is discussed in more detail in Appendix A.

As a result, most important aspects of the behaviour of a soil structure are correctly modelled, as illustrated by the following example.

Consider a slope of height h, constructed out of material of density ρ and cohesion Cu. The slope stability number $\frac{Cu}{h\rho g}$ will only be preserved in a model of identical material of height h/n, if, at the same time, g is increased to ng. Consequently the use of a centrifuge is vital in modelling cohesive materials. Various research workers, e.g. Bassett* (1973) have shown that the deformation and failure of clay embankments may be modelled centrifugally in a relatively straightforward fashion.

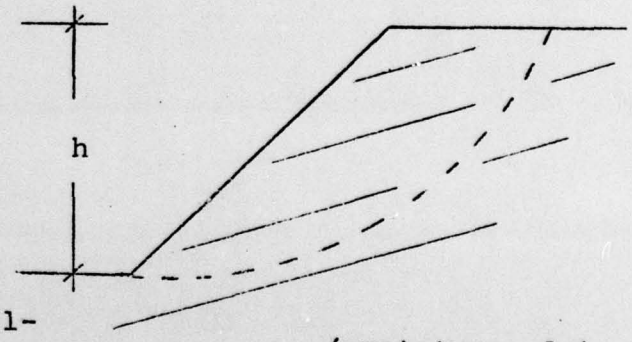

(prototype, lg)

(model, ng)

---

* BASSETT, R.H. (1973) "Centrifugal model tests of embankments on soft alluvial foundations" Proc. of 8th I.C.S.M.F.E., Vol. 2.2, Moscow.

The stability of a slope of cohesionless material, however, depends primarily on ϕ' (the angle of friction), which is not as sensitive to the general level of stress as the Taylor stability number. Indeed, it is often assumed constant, to justify the use of models at one gravity. Nevertheless, this is an approximation, for not only does ϕ' depend on the stress level, but so do many other parameters governing soil behaviour, such as the angle of dilation, the elastic modulus and the material damping.

It is, of course, possible to increase stress levels in a model by other means (e.g. by surcharge loading), but then the distribution of stress (and consequently of strength) is incorrect. Thus, in a conventional model, it is possible either to model the magnitude or distribution of stress and strength correctly - but not both. Centrifugal modelling enables both conditions to be satisfied simultaneously.

It is usually desirable to use the actual prototype soil in the model, so that the bulk material properties of a soil element are identical in both prototype and model. This is valid as long as the grain size is sufficiently small, compared to the size of such an element, that the element can still be considered as representative of the continuum in general - in other words, as long as the grain size is much smaller than the model size. If the soil is considered as a continuum in this fashion, then it is perfectly adequate (and indeed advantageous) to use the original material, and there is no need to "model" the soil in any way.

2.2 DYNAMIC MODELLING

Such principles extend to the modelling of time-dependent events, such as the time taken for the slip of an embankment. It has already been shown that in relating a model to a full-size prototype, the "dimension" of length is increased by the modelling scale n; and, as density is preserved, the "dimension" of mass is increased by n^3.

The constant acceleration formula $\ell = \frac{1}{2} gt^2$, may be re-written $t = \sqrt{\frac{2\ell}{g}}$. In the prototype, from basic principles, $\ell_{prototype} = n\ell_{model}$ and $g_{prototype} = (\frac{1}{n}) g_{model}$, so that

$$t_{prototype} = \sqrt{\frac{2n\ell_{model}}{(\frac{1}{n}) g_{model}}} = nt_{model}$$

On this basis, therefore, time is increased by n in going from the model to the prototype.

A distinction must be made in passing between true dynamic behaviour, and quasi-static modelling. The first of these involves some intrinsic time-scale of the model itself, such as the period of natural vibration, while the second would include the work reported by Rowe, Craig and Proctor* (1977), where a model was cyclically loaded, without the presence of inertial effects due to dynamic loading, and at a slower frequency than would be the case if the dynamic laws were strictly observed.

---

* ROWE, P. W.; CRAIG, W. H. and PROCTOR, D. C. (1977) "Dynamically loaded centrifugal model foundations", Proc. 9th I.C.S.M.F.E. (Tokyo)

In principle, the relationship between any variable in a full-scale structure and that in a centrifuge model is uniquely determined at this stage. However, it is shown in the next section that it is advisable to check that the important aspects of any particular model tests are modelled correctly under these rules. It is prudent therefore to look briefly at the modelling of earthquakes.

Any horizontal earthquake ground motion (after Fourier analysis) may be idealised as a horizontal sinusoidal motion of amplitude a with a circular frequency ω. The displacement is then given by the expression $a \sin \omega t$, and on the basis of previous analysis, it would be reasonable to model this motion by decreasing the amplitude of motion in proportion to the modelling scale, and by similarly increasing the frequency of vibration (as this has the dimensions of inverse time).

Two typical requirements may be made.

The first of these is that the dynamic shear stresses in a soil stratum are equal to those at full-scale. Considering the soil as a rigid body of density ρ, then the stress at a depth z is given by

$$\frac{\text{mass} \times \text{acceleration}}{\text{area}} = \frac{(\rho z^3) \times (-a\omega^2 \sin \omega t)}{z^2}$$

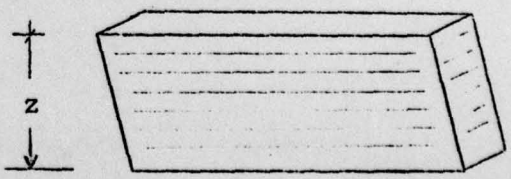

The peak stress in the model is thus

$$\propto (za\omega^2)_{\text{model}} = \frac{z_{\text{field}}}{n} \times \frac{a_{\text{field}}}{n} \times n^2\omega^2{}_{\text{field}}$$

$$= (za\omega^2)_{\text{field}}$$

Secondly, the tendency of the soil to generate excess pore pressures must be modelled correctly. This has been

shown experimentally by Silver and Seed* (1971) to be primarily a function of cyclic shear strain. The shear strain is simply the cyclic shear stress (just shown to be the same in the model as in the prototype) divided by the dynamic shear modulus (which is also the same for the identical soil material at the same level of confining pressure). Thus the cyclic shear strain at any point in the soil and the magnitude of any excess pore pressures generated should be the same in both model and prototype.

Lastly, considering experiments on soil structure interaction, these are usually described in terms of a dimensionless parameter $\omega r\sqrt{\frac{\rho}{G}}$. Now the density ρ and dynamic shear modulus G of the foundation material will be the same in both model and prototype if the material is at the same stress level. The circular frequency ω is increased in proportion to the modelling scale, while the foundation radius r is similarly decreased, so that this dimensionless parameter is the same for both cases.

Clearly, centrifugal modelling laws may confidently be extended to dynamic problems in soil mechanics without any great difficulties.

---

*SILVER, M.L. and SEED, H.B. (1971) "Volume changes in sands during cyclic loading" Proc. Am. Soc. of Civil Engineers, Vol.97, SM9.

2.3 FURTHER CONSIDERATIONS

The following table outlines the general principles for relating the behaviour of a centrifuge model to the equivalent full scale soil structure:-

Fundamental Dimensions	(Modelling scale n > 1)			
Length	in the model is	multiplied by	n	in the prototype
Mass	"	"	n^3	"
Time	"	"	n	"
Related Quantities				
Frequency	in the model is	multiplied by	$\frac{1}{n}$	in the prototype
Velocity	"	"	1	"
Acceleration	"	"	$\frac{1}{n}$	"
Force	"	"	n^2	"
Energy	"	"	n^3	"
Stress	"	"	1	"
Density	"	"	1	"
Strain	"	"	1	"

Unfortunately there are exceptions to these rules, as it is not possible to scale down completely all aspects of soil behaviour, since it is a two-phase substance. The most important of these exceptions is that of pore pressure dissipation time, which scales as the square of the modelling scale.

This follows logically by writing that this time $t = \frac{T_v H^2}{C_v}$ where T_v is a factor dependent only on the percentage of dissipation that has taken place, and C_v is the coefficient of consolidation of the soil, which is constant for a given soil. Thus, in a model, the maximum drainage path H will be reduced by the modelling scale n, and the drainage time will be reduced by a factor of n^2. As a result, careful thought must be given to modelling experiments that involve the interaction of dynamic events with pore pressure dissipation. For instance, if the coefficient of consolidation were increased by a factor n, then both measures of time would scale in the same way.

This is, in general, the only important such exception, and methods of dealing with this problem are discussed in Section 13.3. The reasons for these exceptions are explained in Appendix A. However, the implication is that it is not possible to assume categorically that the fundamental modelling laws as outlined above apply to all aspects of soil modelling, and that it is always necessary to check that the particular aspects of soil behaviour are being modelled correctly.

Even in circumstances where such difficulties do exist, however, it is still advantageous to use a centrifuge in model testing, because it is allows a prospective modeller to vary more model parameters than would be the case with models at 1 g .

Centrifuge models involving dynamic motion may be subjected to Coriolis accelerations. However this seldom causes major difficulties in practice. Appendix B discusses Coriolis effects in more detail.

Another anomaly peculiar to centrifuge models is the non-uniformity of the acceleration field. This problem is rarely of practical significance if the model size is small compared with the centrifuge radius (nor is it of theoretical significance as gravitational fields are themselves curved).

It is also instructive to note in the context of earthquake engineering, that the values of force and energy involved in the seismic motion of a full-scale soil mass are extremely large, and on these grounds alone, the prospect of conducting full-scale tests is remote. The use of a centrifuge model allows enormous reductions in the force and energy requirements (proportional to the square and cube of the modelling scale respectively) and effectively makes such experiments possible.

Finally, it should be stressed that, although it is desirable to "test" the method by direct comparison with equivalent field tests (e.g. Lyndon and Schofield 1978*), this is not necessary in <u>every</u> situation. It is often possible to provide indirect evidence of the validity of the modelling laws, for instance, by conducting tests of the same prototype at different modelling scales (as demonstrated in Section 6.4).

---

*LYNDON, A. and SCHOFIELD, A. N. (1978) "Centrifugal model tests of the Lodalen landslide", Canadian Geotechnical Journal, February 1978

In general, however, it is sufficient to show that centrifuge tests agree with theoretical analyses that are in their turn based on well documented field measurements. The mathematics of centrifugal modelling is well defined, and it need only be shown to be consistent within the overall framework of soil mechanics.

Further discussion of the general role of centrifugal model testing may be found in the paper by Schofield* (1978).

---

* SCHOFIELD, A.N. (1978) "Use of Centrifugal Model Testing to assess Slope Stability" Canadian Geotechnical Journal, February 1978

CHAPTER 3

THE CAMBRIDGE CENTRIFUGE FACILITY - A BRIEF DESCRIPTION

The University Engineering Department at Cambridge University, England, operates a centrifuge exclusively for geotechnical use. Plate 1 shows a sketch of the installation. The rotor is in a circular housing 10 metres in diameter, buried underground for safety. It is driven through an eddy current coupling by a 225 kW electric motor, and this enables rotational velocities of up to 185 r.p.m. to be achieved.

Plate 2 shows the centrifuge arm itself. Packages are generally mounted on swinging platforms at the end of the arm, allowing the resultant acceleration to remain approximately vertical with respect to the specimen at all times. These platforms hang from plain bearings, and are designed to swing up continuously under centrifugal acceleration, until resting on retaining stops at the end of the arm. The bearings are flexibly mounted in such a way that the platforms seat onto the end of the centrifuge arm at an acceleration of about 10 g, and any subsequent increase in centrifugal force on the package is then taken directly onto the centrifuge arm.

The maximum carrying capacity is 900 kg at an effective radius of about 4 metres, and the maximum centrifugal acceleration is 155 g - although tests are generally conducted at lower values of acceleration. A counter balance mass is mounted on an identical swinging platform on the other end of the arm. This mass may be altered, in order to keep out-of-balance forces on the centrifuge rotor within specified limits during each test.

Tests are monitored visually with a television camera mounted on the arm, close to the centre spindle, and the output may be recorded with a video tape recorder. There is also provision for external flash photography of samples, which can be used for photogrammetric determination of sample deformation.

The rotor is provided with hydraulic and electrical slip rings. Transducers of various kinds may be connected to these, and the slip rings may be used to drive electrical, hydraulic or pneumatic devices in the package or on the centrifuge arm. Signal output may be recorded with a data-logger or (particularly for dynamic experiments) with a multi-channel frequency-modulated tape recorder and/or a recording oscillograph.

The stresses in the rotor arm are monitored with strain gauges, and an accelerometer mounted at the effective package radius gives a continuous reading of the value of centrifugal acceleration throughout a test (this may also be calculated from the rotational velocity of the rotor).

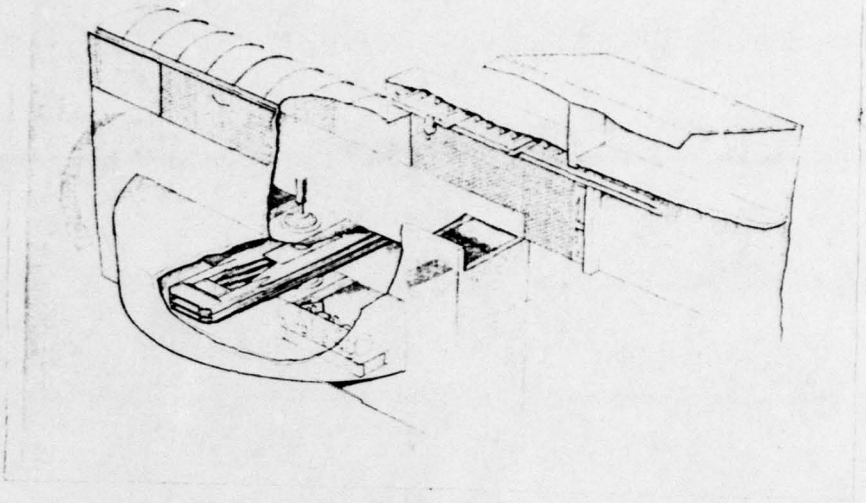

PLATE 1 - A sketch of the Cambridge centrifuge installation

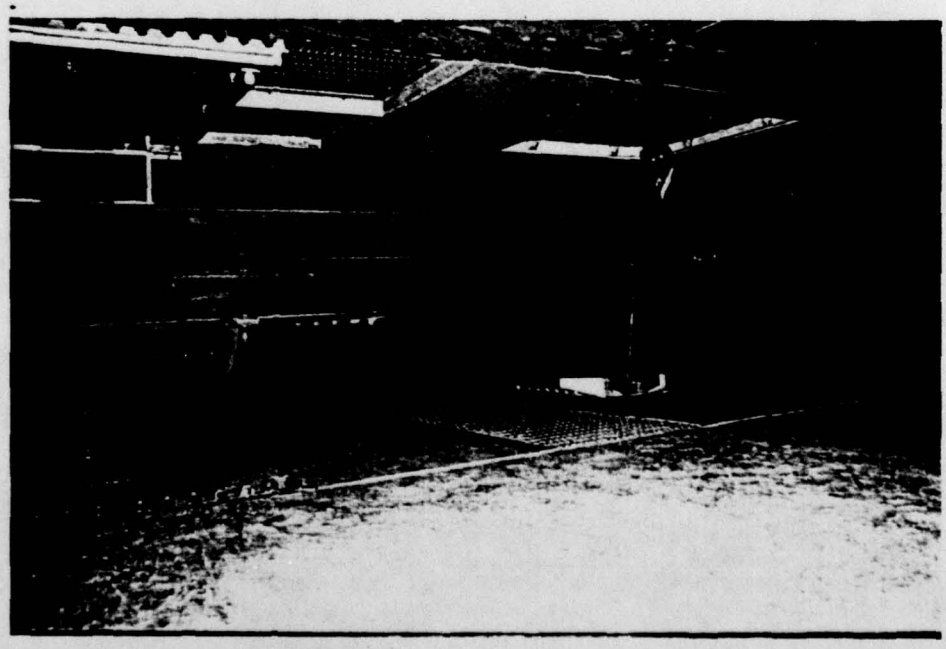

PLATE 2 - The centrifuge arm, underground

CHAPTER 4

INITIAL EXPERIMENTS ON DYNAMIC SOIL-STRUCTURE INTERACTION

4.1 INTRODUCTION

It was decided that the first use of the special centrifuge "earthquake apparatus" would be for the study of the soil-structure interaction of a model tower on a foundation of dry sand. As the focus of interest was the foundation interaction, the towers were simply designed as rigid bodies, and no attempt was made to model the flexibility of the structure - any structural motion would normally be superimposed onto the foundation motion.

This problem seemed suitable for initial investigation, as it appeared relatively straightforward theoretically, and the experimental results could be interpreted without too much difficulty and compared with the predicted values.

The motion of such a structure is dominated by "rocking" (as demonstrated later), and may be regarded as a simple one-degree-of-freedom dynamic system. The two important dynamic parameters of this soil-structure system are the natural frequency and damping, and it was clear that these parameters could be measured without the complication of an earthquake apparatus, simply by perturbing the tower and allowing it to undergo subsequent oscillation.

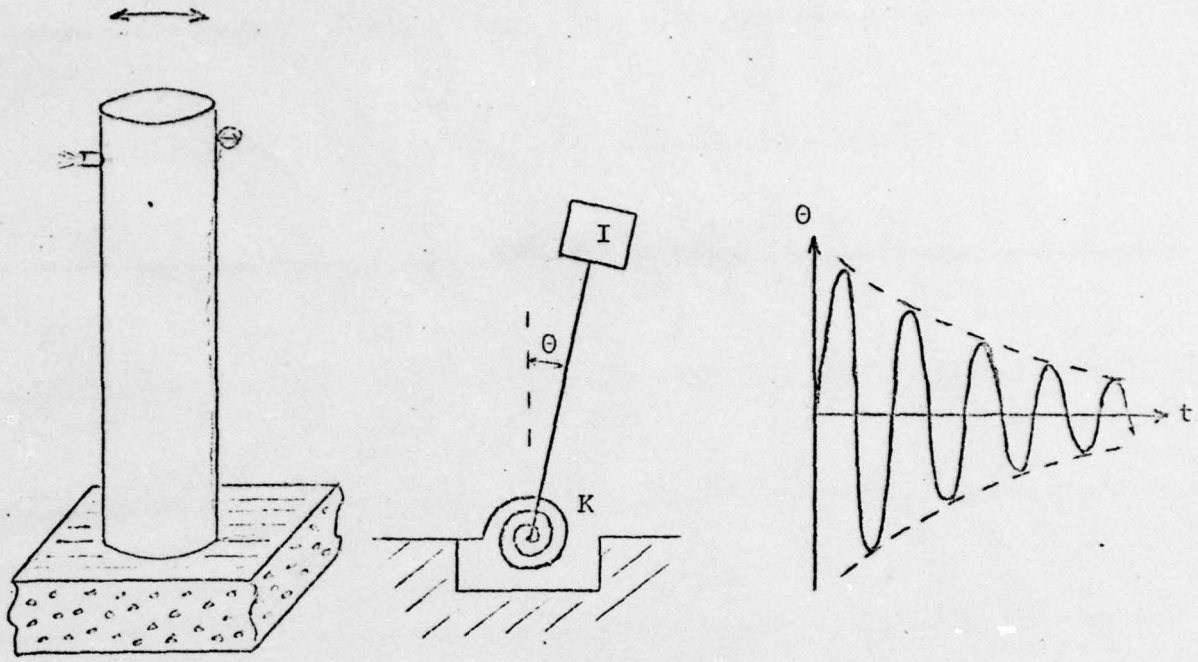

This perturbation took two forms. In the first instance a small explosive charge was detonated on one side of a tower top. It was also found that the towers executed small amplitude harmonic motion about their equilibrium position in response merely to the continuous buffeting of air inside the centrifuge chamber during steady running.

Plate 3 shows a general picture of the equipment. In this example, two towers are seen resting on a sand foundation, inside a circular container, which is bolted onto the swinging platform at the end of the centrifuge arm. This relatively simple arrangement enabled a substantial amount of quantitative investigation into this problem to be carried out.

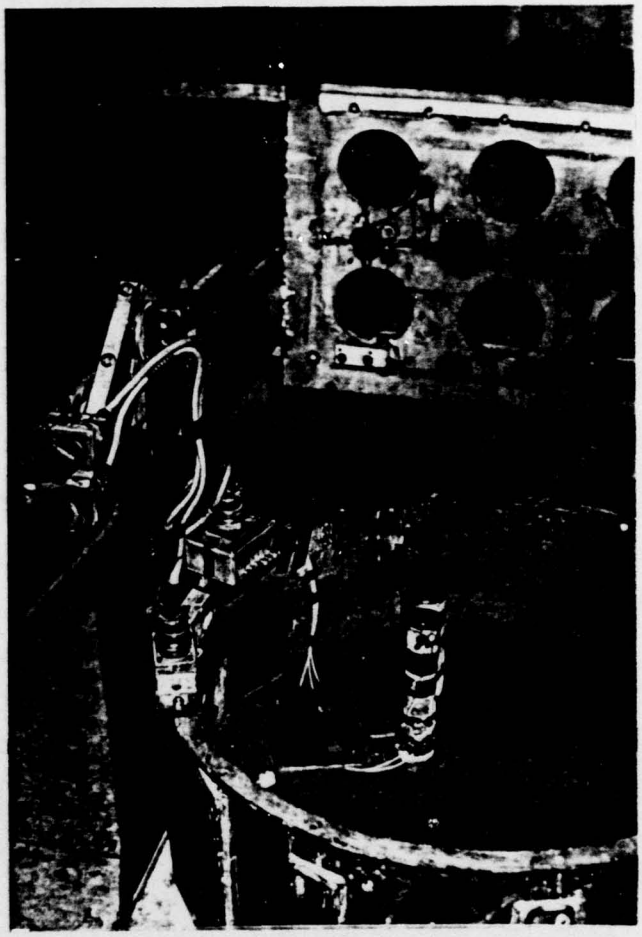

PLATE 3 - The container with a model tower, on the end of the centrifuge

4.2 EQUIPMENT DESCRIPTION

The model towers were constructed out of rigid steel tubing, about 250 mm high. Bases of different sizes and geometries could easily be fitted onto them, and extra mass could be bolted onto the tops to increase their moment of inertia if required. This moment of inertia was determined experimentally by hanging the towers from a bifilar suspension of known dimensions, and measuring the natural frequency of rotation. In this way, a fairly extensive variation of the important tower parameters could be undertaken, and they were chosen to correspond approximately with typical scaled values of mass, moment of inertia and foundation bearing stress, from real structures - although, of course, the structures themselves were modelled as being perfectly rigid.

An accelerometer was mounted on the top of each tower, in order to record its motion. The accelerometer outputs were passed through screened leads to specially constructed amplifiers inside the connector box, (shown in Plate 3 bolted onto the side of the container), and after amplification were then passed through the low-noise electrical slip rings to the exterior of the centrifuge. The signals were finally recorded on sensitized paper in an ultra-violet recording oscillograph. It was also possible to use integrating circuitry to change the acceleration signal into a velocity or displacement signal. Further details on the instrumentation are given in the later chapter entitled "Instrumentation", and in Appendix D.

The towers were placed inside the circular container, on a foundation of coarse sand, vibrated in layers to a uniform density. Once in position on the centrifuge arm, the whole assembly could be spun up to the desired centrifugal acceleration. Self-weight was always sufficient to keep the sand and the towers in position, and no cover of any kind was required. The television camera on the arm allowed constant visual monitoring of all tests. A videotape recorder enabled events to be stored and replayed, and photographs could be taken of single frames, if required.

Although the container was of a finite size, the boundary conditions were not regarded as important because the dimensions of the container were substantially greater than the dimensions of the tower base.

Whitman* (1972) has indicated that the existence of a rigid stratum under an elastic half-space has little effect on the behaviour of a surface foundation if the depth to the stratum is at least twice the width of the foundation, and this condition was observed in these tests.

Moreover, in these tests, the foundation moved primarily in rocking, and the deformation of the foundation soil was relatively localised compared with pure vertical or horizontal translation, so that the presence of the boundaries was, if anything, substantially less important than normally predicted by elastic theory.

---

* WHITMAN, R.V. (1972) "Analysis of soil-structure interaction - a state-of-the-art review" Proc. Symposium on Experimental and Theoretical Structural Dynamics, April 1972. Institute of Sound and Vibration Research, Southampton, U.K.

The sand used in these tests (and in all subsequent tests on dry sand) was Leighton-Buzzard 14/25 sand (the numbers denoting the passing and retaining British Standard sieve numbers respectively). a relatively uniform sand of medium angularity with a particle size between 0.6 mm and 1.2 mm.

The in-situ bulk density of the sand in the container, as deposited, was consistently about 1610 kg/m^3, corresponding to a voids ratio of about 0.65.

In order to perturb the towers with explosive, a short length of steel tube was welded onto the top of the tower. This tube was sleeved inside with plastic, and threaded down the middle by some high resistance electrical heating wire. A close-up of this arrangement is shown in Plate 4. Into this was placed about 20 mg of thermally sensitive explosive powder (in this case silver azide which was specially prepared in small quantities - brief details of the preparation are contained in Appendix C).

At the required instant, about 2 amps of current were passed through the resistance wire via the slip rings. This was sufficient to cause the wire to glow red-hot within a second, upon which detonation took place almost instantaneously. In general, the tower then executed oscillatory motion.

Video tape recorder pictures showed that the explosion itself occurred within two or three frames - or within about 0.1 seconds. A still photograph of such an explosion, seen on the television monitor, is shown in Plate 5.

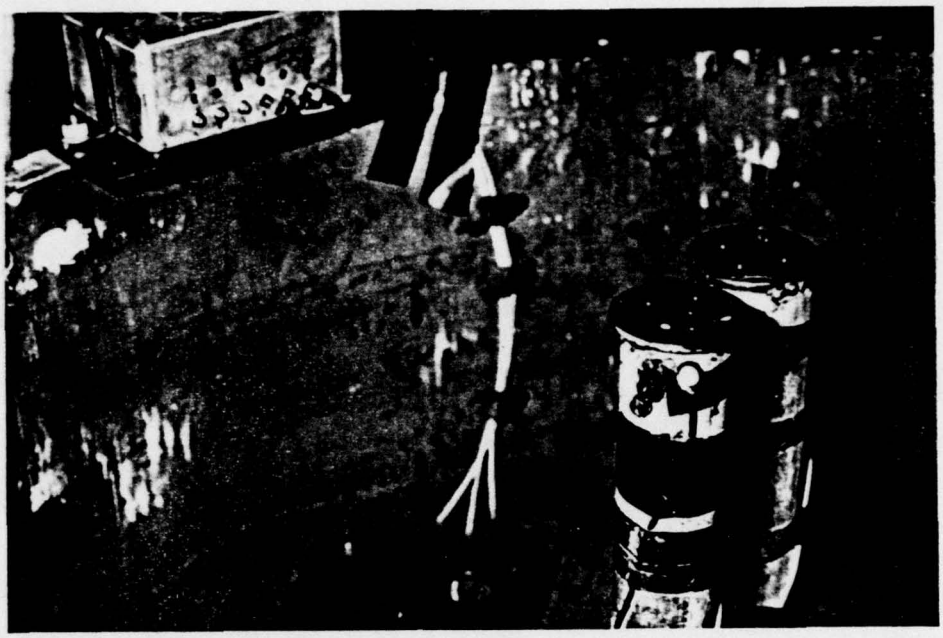

PLATE 4 - Detail of model tower

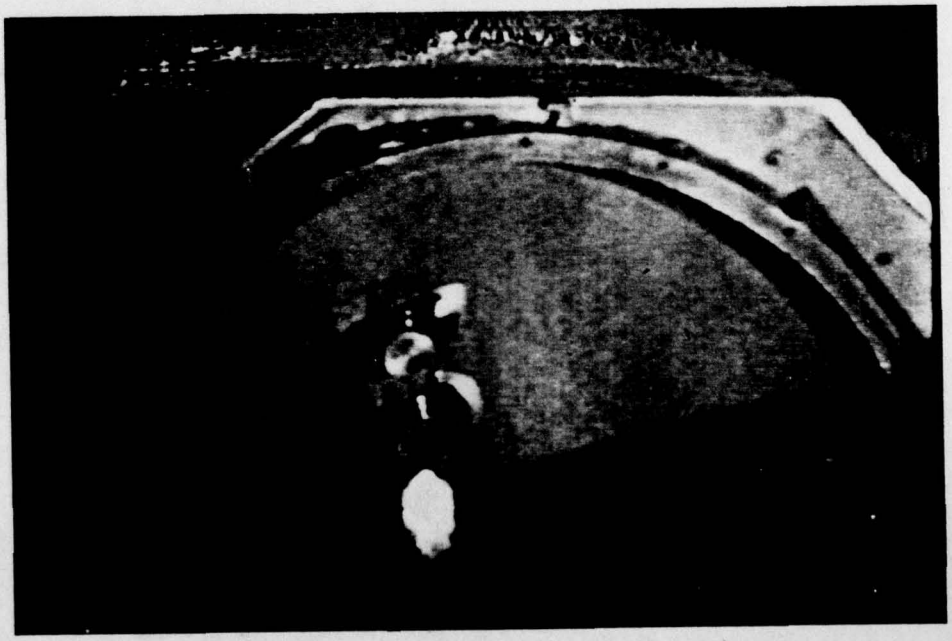

PLATE 5 - Television picture of charge detonation, from above

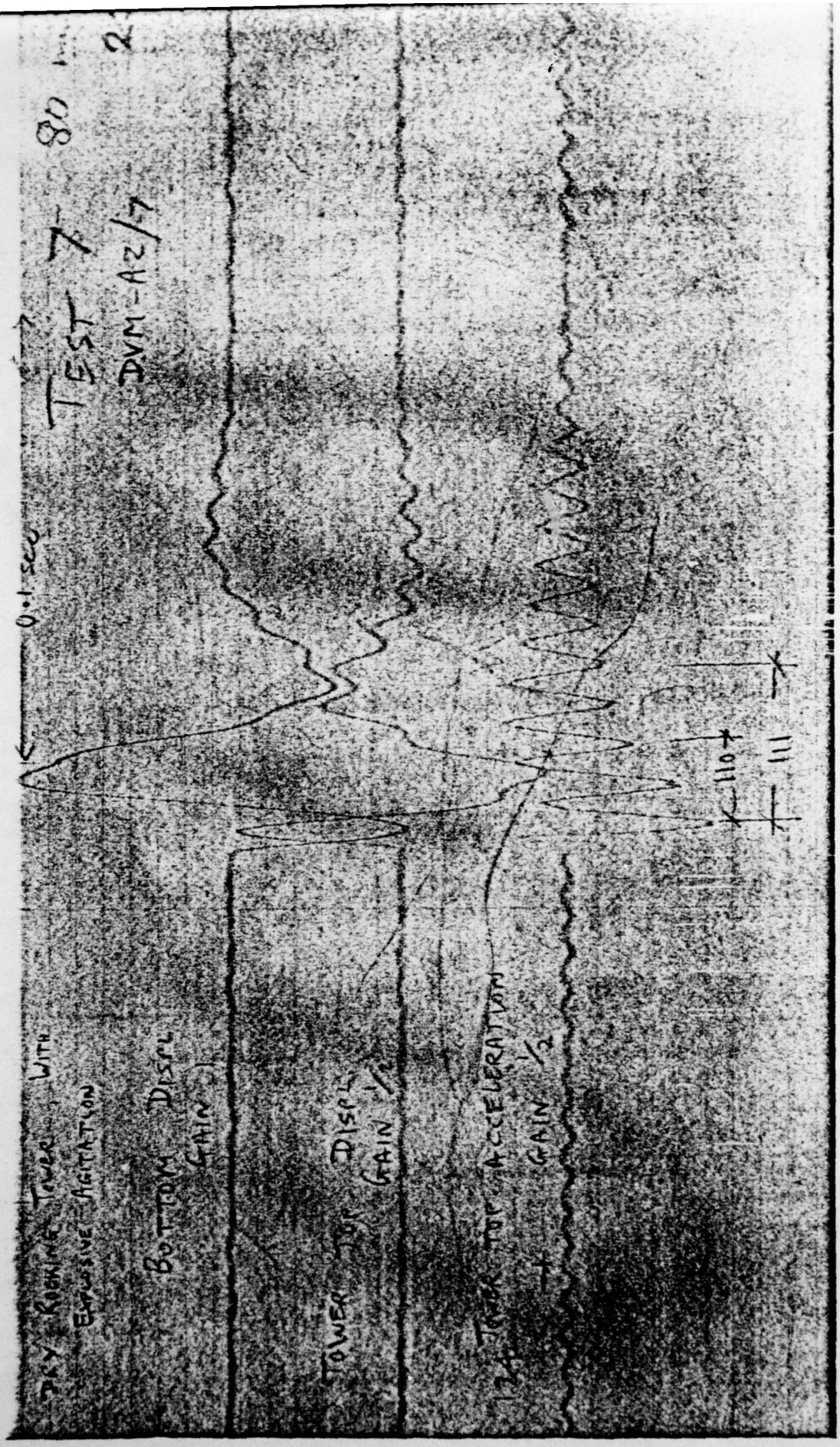

Figure 3 - Oscillatory decay of a tower (i) - original

4.3 TEST METHOD

Contrary to expectations, it was found that the easiest way of measuring the natural frequency of the system, was by recording the wind-induced vibration of the tower-foundation system. This motion was the natural oscillation of the soil structure system in response to random gusting and air turbulence inside the centrifuge chamber (not to be confused in any way with vortex shedding, the characteristic frequency of which is much lower, and the behaviour of which is very different).

Consequently, the resultant motion is stochiastic in nature - at times reinforcing to give large amplitudes of motion, and at other times cancelling to give periods of relative calm. This behaviour is illustrated in Figure 1, which reproduces the original accelerometer traces. Figure 2 is a tracing of these results, and the centrifugal modelling rules have been applied to give the equivalent prototype values.

As a result, tests were conducted as follows: two towers were placed, side-by-side, (only one of these equipped with an explosive charge), each with slightly different parameters so that the maximum amount of information could be extracted from each test. The package was spun up to speed fairly slowly, and records of the wind-induced oscillation taken at intermediate values of acceleration, so that the variation of natural frequency with acceleration could be easily measured. Then at a pre-determined acceleration, the explosive was detonated, and a trace of the subsequent behaviour taken, from which the damping at that modelling scale could be measured.

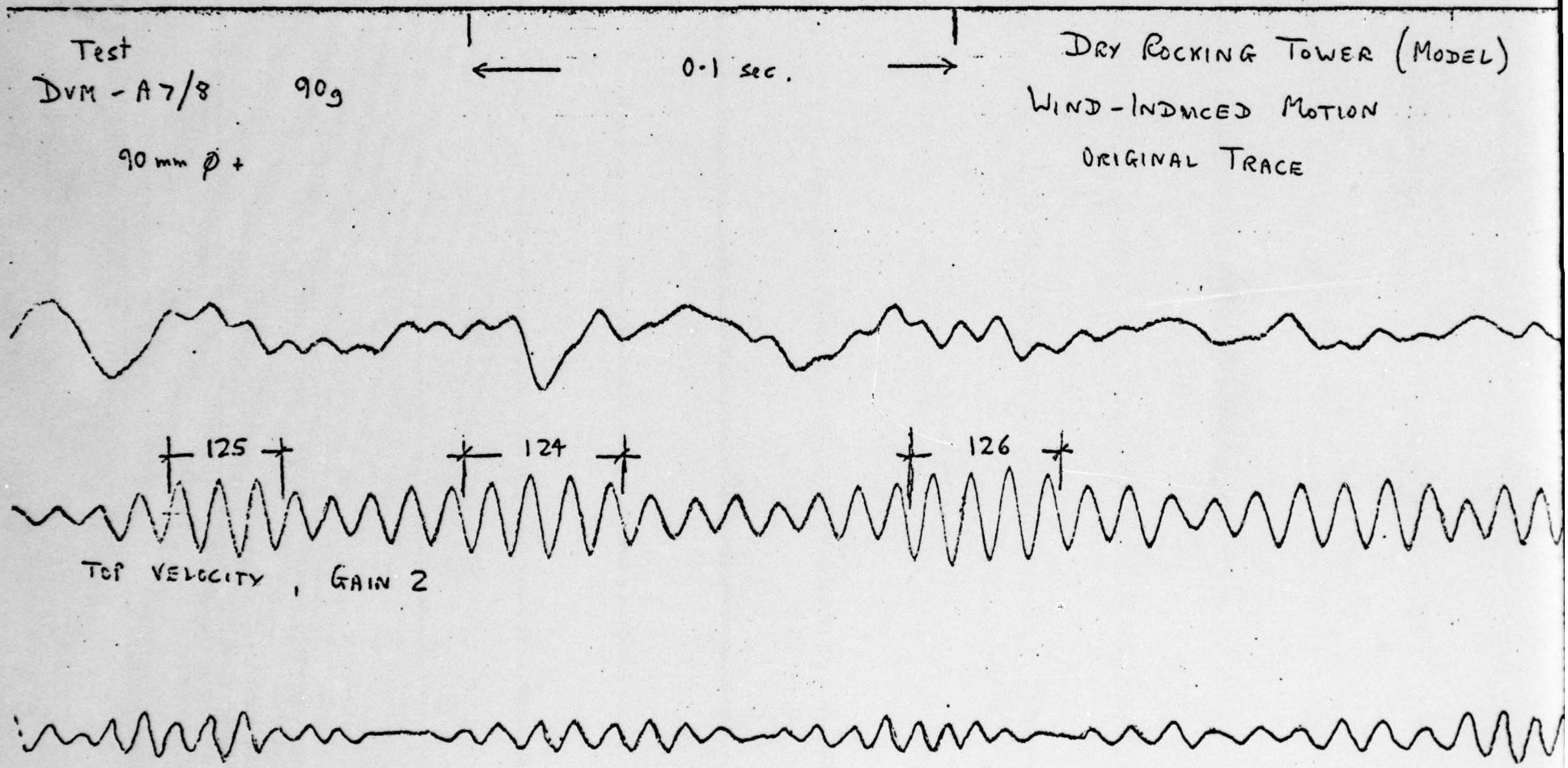

Figure 1 - Wind-induced oscillation of a tower - original

A7/8
(90g)

ROCKING TOWER, WIND-INDUCED MOTION, ON A FOUNDATION OF DRY SAND.

(Prototype values — Tower 23.5 m. high, 8.1 m. diameter base, Mass 1230 tonnes)

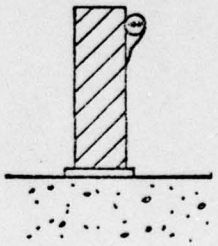

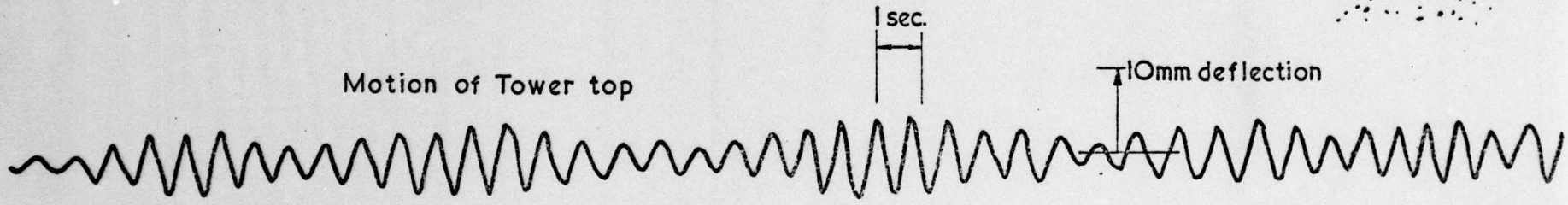

Natural frequency of approx. 1.39 Hz.

Figure 2 - Wind-induced oscillation of a tower - traced and converted to full scale

Measurements of the wind-induced oscillation (at a higher amplifier gain to allow for the different magnitude) were then taken after the detonation, and again at intermediate values of centrifugal acceleration on the way down.

In this way, it was possible to acquire data relatively quickly.

4.4 QUALITATIVE RESULTS

Figure 3 shows a typical trace from one of the experiments at the moment of explosive perturbation. The top two traces are double-integrated to give a displacement trace, and show large non-oscillatory movement for the first 50 milliseconds or so. These movements are emphasized by the nature of the double-integration process, each step of which essentially provides a gain inversely proportional to frequency. They occur as a result of the finite time of the explosion, and are not of great interest.

The oscillatory motion is visible most clearly in the bottom acceleration trace. This is shown alone for greater clarity in Fig. 4, and the modelling laws have been used to convert all values into equivalent prototype values. The frequency of oscillation (averaged over a number of cycles) is pencilled in at various points. This is measured by hand to an accuracy of about 1 % to 2 % (depending on the number of cycles counted).

A2/7
(25g)

ROCKING TOWER, EXPLOSIVE PERTURBATION, ON A FOUNDATION OF DRY SAND

(Prototype values — Tower 6.5 m. high, 2m. diameter base)

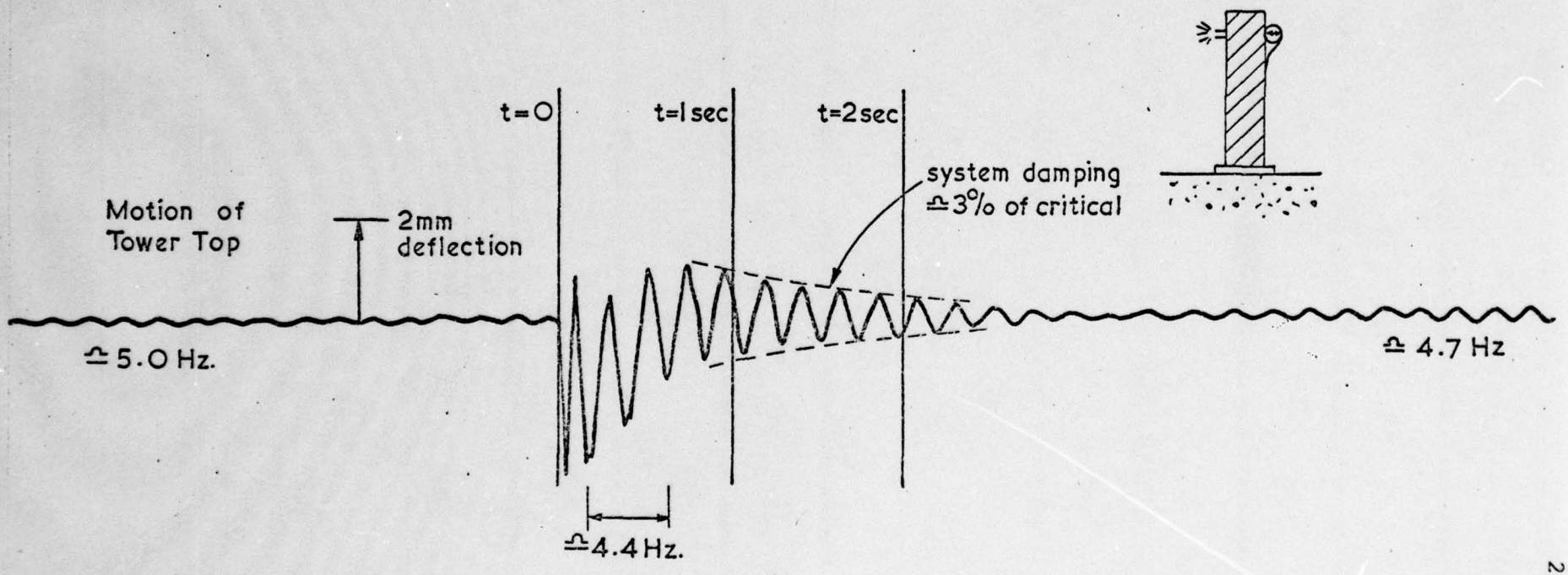

Figure 4 - Oscillatory decay of a tower (i) - traced and converted to full scale

Wind-induced oscillation could be seen before and after the event - at a considerably smaller magnitude than the explosive oscillation. During the much larger oscillation, the frequency visibly dropped (corresponding to "softening" of the foundation stiffness for large amplitudes of strain, as would be expected from resonant column tests on sand), and then rose as the amplitude of motion decreased. Eventually the tower lapsed back into wind-induced oscillation, although not at quite such a high frequency as before - presumably some long-term softening of the effective foundation stiffness occurred as a result of localised reduction of sand density under the base.

Although the amplitudes of strain as a result of explosive perturbation were sufficiently large to demonstrate strain-softening behaviour, wind-induced oscillations were of much lower magnitude, and could be considered too low for this effect to occur. This is discussed in Appendix H. Consequently in the analysis of wind-induced motion, no allowance need be made for strain-softening.

The system damping may be derived from the oscillatory decay following explosive perturbation, by measuring the amplitude a_o of one cycle followed by the amplitude a_n of another, 'n' cycles later. This uses what is known as the "logarithmic decrement" method, and in Figure 4 the damping ratio is about 3 %. Details of the method are given in section 6.1 .

In some experiments, two towers were placed close together, and only one of them perturbed by an explosive charge. The movement of both towers could be measured, and in this way the interaction between adjacent towers could be investigated.

CHAPTER 5

ANALYSIS OF TOWER OSCILLATIONS (WIND-INDUCED)

5.1 INTRODUCTION

A circular disc resting on an elastic axisymmetric foundation has four distinct degrees of freedom - vertical and horizontal translation, torsional and "rocking" rotation.

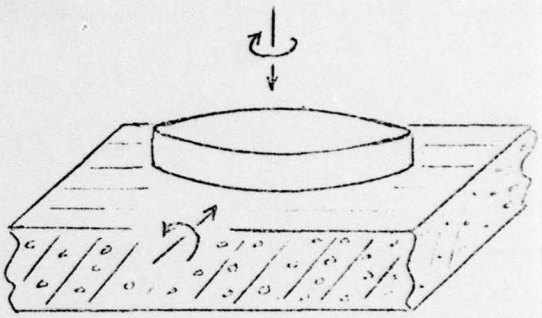

This investigation concerns itself only with "rocking" motion, which is the most important - as in any real structure the natural frequency of rocking is much lower than for other modes, and is consequently much more likely to be excited. Additionally, the level of damping associated with a structure of reasonable height in rocking, is far less than for other modes, and as a result the effect of resonance is much more marked.

"Rocking" motion is always associated theoretically with some horizontal translation - but if the natural frequency and damping of "rocking" is much less than horizontal translation, there will be virtually no interaction, and horizontal translation may effectively be ignored. Appendix E demonstrates that this is so in this case.

Consequently a rigid tower resting on an elastic foundation may be idealised as a spring-mass system of one degree of freedom, as illustrated. The natural frequency is given by $f_n = \frac{1}{2\pi}\sqrt{\frac{K}{I}}$ - - - - - - - - - (1)

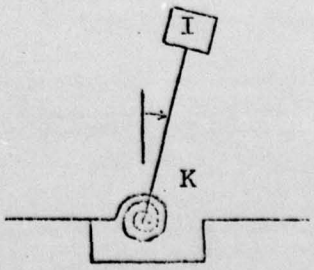

where I is the moment of inertia of the structure about its base, and K is the rotational spring stiffness of the foundation system.

5.2 INITIAL ANALYSIS OF NATURAL FREQUENCY

For a circular base of radius r resting on an infinite uniform elastic half-space with shear modulus G and Poisson's ratio ν, the rotational spring stiffness is given by

$$K = \frac{8Gr^2}{3(1-\nu)} \qquad (2)$$

as derived originally by Borowicka* (1963).

This spring stiffness may need to be modified for very high frequencies, at which the wavelength of shear waves becomes comparable to the base dimensions, but this is not the case here, as is shown in Appendix F. An alternative approach is simply to point out that typical values of the non-dimensional frequency parameter a_o that is used in the literature, e.g. in the book by Richart, Hall and Woods+ (1970), are less than 0.2, and that at such low values frequency effects are not significant. This approach is elaborated in Appendix F.

The effective elastic modulus G of dry sand is in turn, dependent on stress, and this dependence may be written

$$\left(\frac{G}{G_o}\right) = \left(\frac{p'}{p'_o}\right)^x \qquad (3)$$

---

* BOROWICKA, H. (1963) "Concerning eccentrically loaded rigid discs on an isotropic elastic foundation" Ingenieur-Archiv, 1:1-8 (in German).

+ RICHART, F. E.; HALL, J. R. and WOODS, R. D. (1970) "Vibrations of Soils and Foundations", Prentice-Hall,

where p' is the appropriate mean effective stress, and G_o and p'_o are constants used to make the equation dimensionless. The value of the index x is usually taken as 0.5 on the basis of resonant column tests by Hardin and Drnevich* (1972), and this is verified in due course.

Hardin and Drnevich found that for most sands at low strain amplitudes, the dynamic shear modulus $G \triangleq 10^5 \frac{(3-e)^2}{(1+e)} \sqrt{p'}$ (where all values are in S.I. units). Putting e = 0.65 for this vibrated sand, and writing the equation in the non-dimensional form $\frac{G}{G_o} = \sqrt{\frac{p'}{p'_o}}$, gives

$$\left(\frac{G_o}{\sqrt{p'_o}}\right) = 3.3 \times 10^5 \text{ Pa.}^{\frac{1}{2}} \qquad (4)$$

(1 Pa. ≡ 1 N/m^2)

Combining equations (1), (2), (3) and (4) with x = 0.5 gives

$$f_n = 172 \; r^{1.5} \; p'^{0.25} \; I^{-0.5} \qquad (5)$$

(in S.I. units only)

and in principle this should be sufficient to predict the natural frequency in rocking. However it still requires a value for the effective confining pressure p', and this in fact behaves in a very complex way.

---

* HARDIN, B. O. and DRNEVICH, V. P. (1972) "Shear modulus and damping in soils: design equations and curves", Proc. Am. Soc. of Civil Engineers, Vol. 98, SM7

5.3 FURTHER DISCUSSION OF THE ANALYSIS

It is possible to estimate the rocking frequency of a particular tower, simply by using an average value of the base pressure to predict the appropriate dynamic soil modulus.

Using the test data shown in Figure 1, for instance, the tower in that test had a mass of 1.693 kg, so that at 90 g the average vertical stress under the 90 mm diameter base was 235 kPa. Multiplying this by

$$\frac{1 + (\frac{2\nu}{1-\nu})}{3}$$

to allow for the reduction in the horizontal soil stresses, and putting $\nu = 0.25$, gives a mean pressure of 131 kPa. As the measured moment of inertia of the tower about its base was 4.3×10^{-2} kg.m^2, equation (5) predicts a natural frequency of 150 Hz.

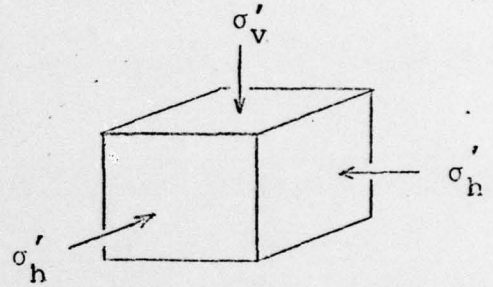

$$\triangleq \frac{\nu}{(1-\nu)}\,\sigma'_v$$

(The calculation could equally well have been done in terms of the equivalent full-size tower with properties scaled up according to the modelling laws. This would have resulted in a predicted natural frequency of $\frac{150\ \text{Hz}}{90} = 1.67$ Hz).

From Figure 1 the average measured natural frequency was 124 Hz, which is significantly lower than the predicted value of 150 Hz, and this trend was repeated consistently in other tests - all of which produced experimental values about 17 % less than the predicted results.

This result corresponds with what has been observed from full scale tests, such as those by Fry, reported in Richart and Whitman* (1967). These have shown the same sort of behaviour, with natural frequencies about 20 % less than predicted.

There are several reasons for this discrepancy.

Firstly it is possible that the values for the dynamic shear modulus published by Hardin and Drnevich (and represented by equation (4)) do not apply to this sand. Resonant column tests were, however, carried out on this sand by the Waterways Experiment Station, Vicksburg, U.S.A. These results are reported in Appendix G and, apart from the apparently quite normal degree of scatter, they agree acceptably with equation (4).

It is possible, but unlikely, that the magnitude of deformation was sufficient to reduce the effective elastic modulus of the sand. Hardin and Drnevich found that, for most sands, there was no significant softening behaviour for values of strain below about 2.5×10^{-5}, and that above this level gradual softening took place. Resonant column tests on this sand, reported on Figure 38, show no appreciable reduction of the shear modulus for shear strains below about 5×10^{-5}. Appendix H shows that wind-induced oscillation of the towers resulted in shear strains in the foundation material of the order of 1 to 3×10^{-5}, so that it is doubtful whether the effect of strain softening was significant.

---

* RICHART, F.E. and WHITMAN, R.V. (1967) "Comparison of footing vibration tests with theory", Proc. Am. Soc. of Civil Engineers, Vol.93, SM6.

It seems reasonable, therefore, to assume that the values recommended by Hardin and Drnevich from tests on many different sands, are applicable for these tests, and that there is some other reason for this discrepancy.

Secondly, in order to use equation (5), it is necessary to decide on an appropriate value of effective strsss. In the previous calculation, the average vertical stress directly under the foundation was used for this purpose. However, the actual stress distribution under such a base is, of course, very much more complex, as it varies with depth and with the radial distance from the centre line.

One common procedure is to use the elastic modulus corresponding to a "typical" point under the base. Whitman and Richart* (1967) recommend that a suitable point in this respect would be at one base radius below the edge of the circular base, and that the stress at this point be computed from elastic theory (including the self weight of the soil).

Real soils, however, behave in a very different fashion, as they are not elastic in their behaviour, and also cannot develop the very high edge pressures predicted by elastic theory. Furthermore, no distinction is usually made between "typical" points for vertical motion and rocking motion, although the soil deformation associated with vertical translation of the foundation is clearly more deep-seated that for rotation of the foundation. Consequently this type of procedure appears somewhat unsatisfactory.

---

* WHITMAN, R.V. and RICHART, F.E. (1967) "Design procedures for dynamically loaded foundations", Proc. Am. Soc. of Civil Engineers, Vol.93, SM6.

Thirdly the value for the rotational spring stiffness given in equation 2, clearly makes many assumptions that are not valid in practice - notably that the soil is linearly elastic, of infinite strength, and of uniform stiffness independent of confining pressure and depth.

The surface distribution of vertical stress for such a soil is shown by the solid line on the sketch. However, a more probable distribution of stress for a real inelastic soil is shown by the dotted line - and this falls to zero at the edges, where the soil must yield to be at equilibrium.

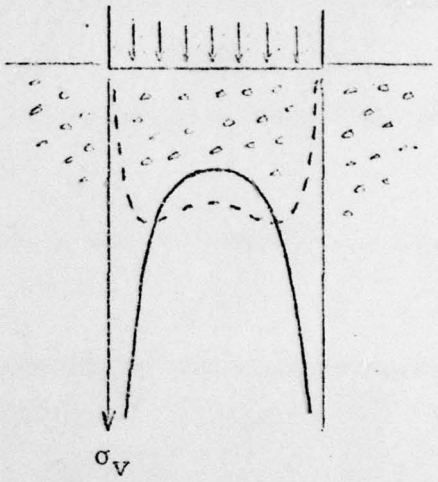

Clearly if the peak soil stresses predicted by elastic theory are not developed at the edges of the base, then the moment resistance provided by pressures at the extremities is severely reduced. Consequently the rotational foundation stiffness is reduced, and the natural frequency of the whole system will be less than that predicted from elastic theory. This difficulty has been recognised for some time, e.g. by Barkan* (1962).

---

*BARKAN, D.D. (1962) "Dynamics of Bases and Foundations" McGraw-Hill, New York, p.23, published in Russian 1948.

As far as vertical vibration is concerned, attempts have been made to consider other possible distributions of vertical stress under the foundation. Sung[+] (1953) gives results for a parabolic distribution of vertical stress. However this raises problems in turn as the foundation is now assumed flexible, the displacement varies across its diameter and some sort of "typical" value must be selected. In any case these results do not apply to rotational motion. No analytic solution that fully accounts for these difficulties is known to the author, and even a rigorous numerical analysis would be a complex undertaking.

It is clear therefore that there is no immediate substitute for the use of the elastic rotational spring stiffness, given in equation (2), but that it should be modified in some way to allow for the difficulties previously described. Whitman**(1972) for instance, suggests using a range of values between the full elastic spring stiffness, and half of this value. In view of all the previous uncertainties involving the soil stress, however, it seems most logical to the author, simply to consider some factor α of the average mean effective

---

+ SUNG , T.Y. (1953) "Vibrations in semi-infinite solids due to periodic surface loading" Symposium on Dynamic Testing of Soils, A.S.T.M. Special Technical Publication No. 156

** WHITMAN , R.V. (1972) "Analysis of soil-structure interaction - a state-of-the-art review", Proc. Symposium on Experimental and Theoretical Structural Dynamics, April 1972, Institute of Sound and Vibration Research, Southampton, U.K.

pressure under the foundation as being appropriate for the prediction of soil modulus, and to absorb all these effects into this single factor.

In fact, as will be seen, this value of α is relatively constant. It amounts to saying that predicted values of rocking frequency fit observed values if, for the purpose of linear elastic theory, the appropriate vertical stress under the base is assumed to be a factor α of the average vertical stress.

It is questionable whether greater sophistication is justified at present - either theoretically, or in practice, as the actual natural frequency is relatively insensitive to the precise assumptions that are made about the stress levels under the base (being proportional only to the fourth root of their value).

Adopting this approach, then, the appropriate value of vertical stress under a model structure of mass M, base radius r, at a pseudo-gravitational acceleration of ng, becomes $\alpha \left(\frac{Mng}{\pi r^2}\right)$

Making due allowance for the reduced horizontal soil stresses, the mean effective stress p′ is $\alpha \left(\frac{Mng}{\pi r^2}\right)\frac{\left(1 + \frac{2\nu}{(1-\nu)}\right)}{3}$

and writing $\nu = 0.25$ gives $p' = 0.177\ \alpha \left(\frac{Mng}{r^2}\right)$ (6)

Combining equations (1), (2), (3) and (6) gives in the most general form :-

$$f_n = 0.30\ (0.177\ g)^{\frac{x}{2}} \left[\frac{G_o}{p_o'^{\,x}}\right]^{0.5} \alpha^{\left(\frac{x}{2}\right)} \left[\frac{M^x}{I}\right]^{0.5} r^{\left(\frac{3}{2} - x\right)}\ n^{\frac{x}{2}} \qquad (7)$$

which describes how the theoretical natural frequency varies with :- (a) soil properties (b) the value of the factor α (c) the mass and moment of inertia of the tower. (d) the tower base radius (e) the centrifugal acceleration in gravities.

It should be pointed out in passing, that this last result in no way invalidates the centrifugal frequency modelling law, which states that $f \propto n$ for the same prototype size - rather than for the same model size, as here. If the same prototype was being modelled, at different modelling scales, then different models would be needed for each case, for which $M \propto n^3$, $I \propto n^{-5}$ and $r \propto n^{-1}$, so that the overall relation would become $f \propto n$, as expected, quite independently of the value of the index x (as indeed it should be).

This theoretical relationship was used to analyse the behaviour on dry sand of model towers of various kinds. The tests reported in the next four sections used five different models with circular bases resting on the surface, three different models with an embedded circular base, and four different models with square bases resting on the surface.

This represents a total of 13 different models, tabulated on page 46, and the natural frequency of each of these was measured at a variety of modelling scales between 1 and 100, and this measurement was usually repeated at least once. Some 250 individual data points are represented in this way, and they enable a very comprehensive experimental investigation to be made of the theoretical analysis.

5.4 EXPERIMENTAL VARIATION WITH CENTRIFUGE SPEED

In practice the centrifugal acceleration 'n' was the most easily varied of the parameters in equation (6), and it provided a quick check of Hardin and Drnevich's determination of x = 0.5. Figure 5 shows a graph of the measured variation of natural frequency with centrifuge acceleration, first for a tower with a 90 mm diameter base, and then for the same tower with a 65 mm diameter base - all other parameters remaining constant.

Values of natural frequency were measured from 1 g (by just hitting the tower when the centrifuge was at rest) up to 100g (by recording wind-induced oscillations). When plotted on a logarithmic graph, they fell on a line of slope 0.25, implying that $f_n \propto n^{0.25}$. This pattern was also followed by subsequent tests, and thus by reference to equation (6) which predicted that $f_n \propto n^{\frac{x}{2}}$, it is reasonable to conclude that x = 0.5.

Hardin and Drnevich's resonant column tests on sand in uniform torsional shear were thus confirmed by these tests, even though the test conditions were substantially different.

Using Hardin and Drnevich's values for the shear modulus and the index x , equation (7) reduces to

$$f_n = 195 \quad \alpha^{0.25} \quad \left(\frac{\sqrt{M}}{I}\right)^{0.5} \quad r \quad n^{0.25} \qquad (8)$$

(S.I. units throughout)

where any observed discrepancies may be allowed for by the factor α . It is possible to make a quick estimation of the value of α by noting that it is proportional to the fourth power of the observed natural frequency, and then referring

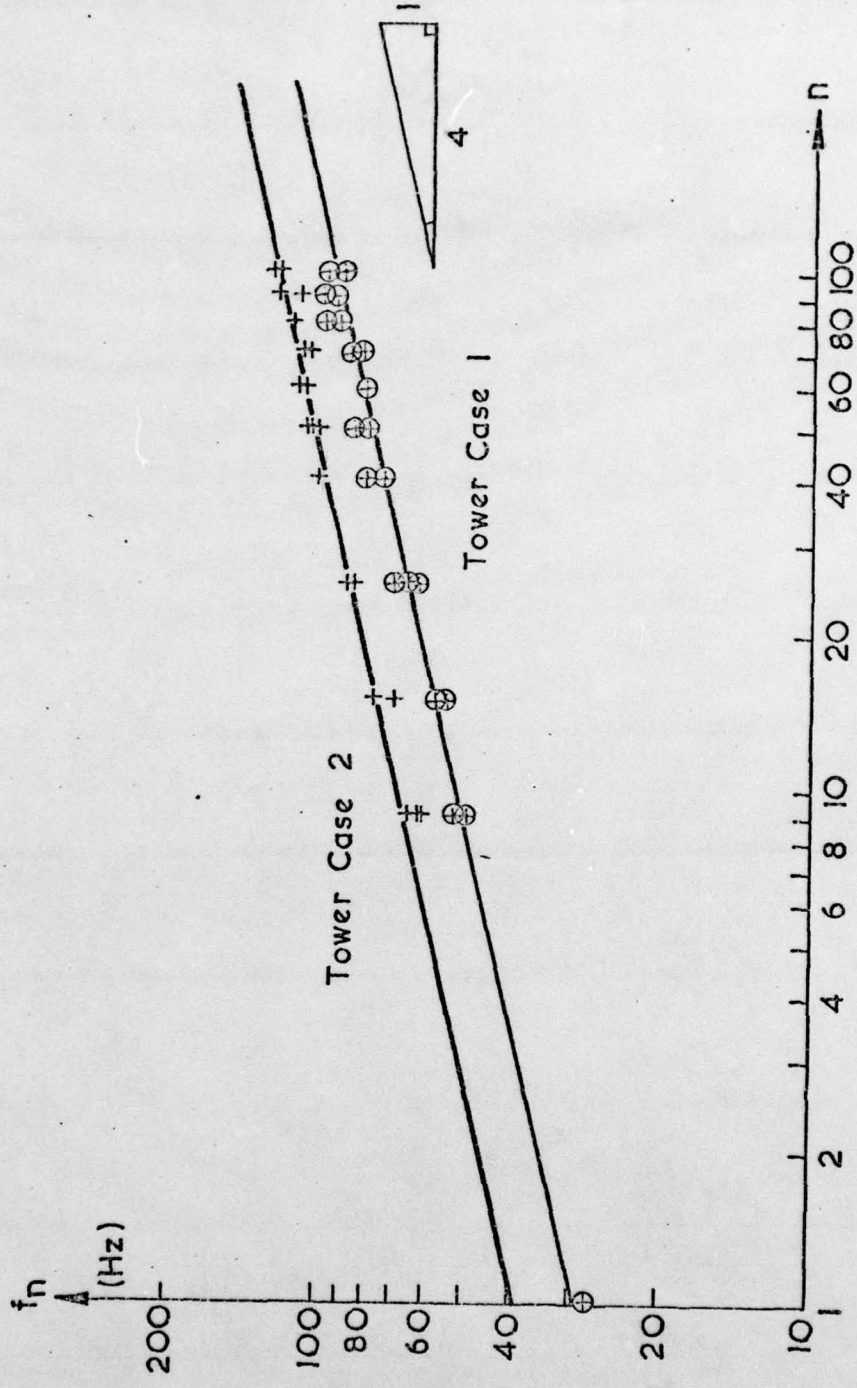

Figure 5 - Variation of natural frequency with acceleration (i)

to the earlier sample calculation made for the tower in Figure 1. As the observed frequency was 124 Hz., and the predicted frequency was 150 Hz. (effectively assuming $\alpha = 1$), then the value of α that correctly accounts for the observed result is

$$\left(\frac{124 \text{ Hz.}}{150 \text{ Hz.}}\right)^{4} \simeq 0.47$$

In fact, a value of 0.5 appears to be suitable for many different tests, presented subsequently in this chapter. The whole essence of these centrifuge model tests is that it was possible to do many more tests than could be envisaged with any program of full scale testing, and consequently it has been possible to produce a large amount of quantitative information on this particular problem.

Writing $\alpha \simeq 0.5$ then, equation (8) becomes simply

$$f_n = 163 \left(\frac{\sqrt{M}}{I}\right)^{0.5} r \, n^{0.25} \qquad (9)$$

(in S.I. units only)

where the natural frequency of a model tower is given as a function of the tower properties, the base radius and the modelling scale. This equation is the basis for subsequent analysis of the experimental results. It applies strictly only if the voids ratio of the sand was consistently 0.65. No attempt was made to conduct tests on different soil densities.

5.5 EXPERIMENTAL VARIATION WITH TOWER PROPERTIES

The experimental program tested various towers, in order to determine the validity of equation (9) for circular geometries, and to indicate whether current theory for other geometries, or for embedded foundations, was supported experimentally.

The major variation of natural frequency in each test was with n, the centrifugal acceleration in g's. Fig. 6 shows the values of two more such tests, plotted against n, for identical towers with a 90 mm and 65 mm diameter base - differing from Fig. 5, however, in that the moment of inertia of the towers had been significantly increased. Again, lines of slope 0.25 fit neatly onto the data points, confirming theoretical predictions. Since it appears, therefore, that the effect of centrifugal acceleration is well understood, and is in accordance with theory, it seems only logical to "remove" it as a variable in equation (9) by considering the intercept of the lines with a particular value of n - in this case unity.

Each of these experimental lines then reduces to a single point - the value of the natural frequency at 1 g. Measurements at different values of centrifugal acceleration serve only to define a more accurate value of this intercept.

These values were all measured using wind-induced oscillations of the towers, and they may be summarised in the following table:

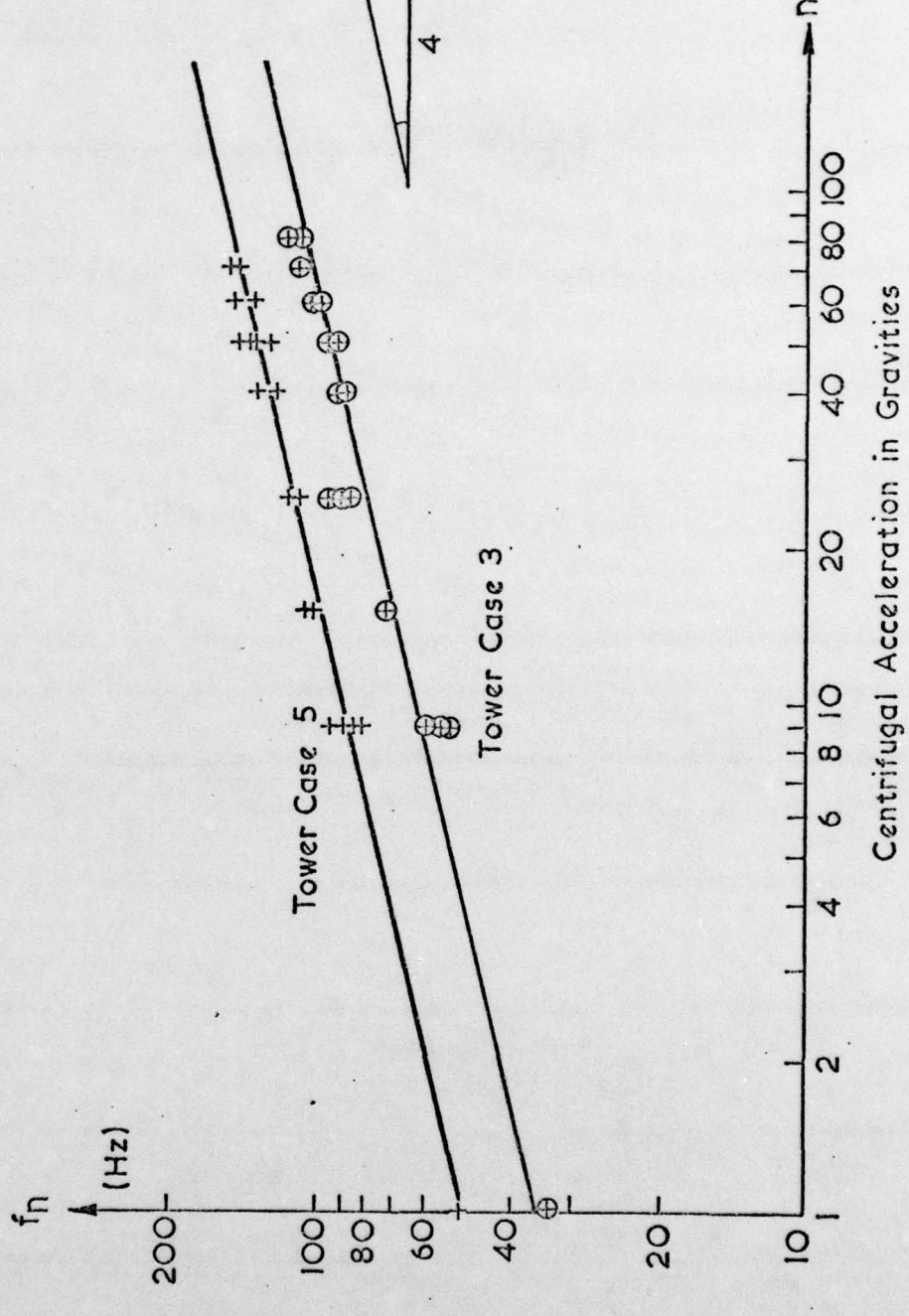

Figure 6 - Variation of natural frequency with acceleration (ii)

tower parameters

	M	I	r	measured f_n at 1g
	CIRCULAR BASES			
1.	1.693 kg	0.0430 kg.m^2	0.0325 m	29 Hz.
2.	"	"	0.045 "	39 "
3.	1.480 kg	0.0275 kg.m^2	0.0325 m	35 Hz
4.	"	"	0.04 "	42 "
5.	"	"	0.045 "	50 "
	CIRCULAR BASES - 20mm. EMBEDMENT			
6.	1.480 kg	0.0275 kg.m^2	0.0325 m	44 Hz
7.	"	"	0.04 "	52 "
8.	"	"	0.045 "	59 "
	SQUARE BASES			
9.	1.627 kg	0.0407 kg.m^2	0.03 m	33 Hz
10.	"	"	0.04 "	43 "
11.	1.414 kg	0.0275 kg.m^2	0.03 m	37 Hz
12.	"	"	0.035 "	44 "
13.	"	"	0.04 "	50 "

The next step in checking equation (9) is to verify that, for similar experiments, the natural frequency is indeed proportional to r (or, in the case of square bases, to the base semi-dimension).

Fig. 7 shows the variation of f_n with r for each of the five groups of experiments in which only r was varied. Since it was only practicable to vary r by a relatively small amount, the lines can hardly be said to be conclusive. However, in each case the group of points lie fairly well on lines of slope 1 - certainly there is no obvious discrepancy at this stage.

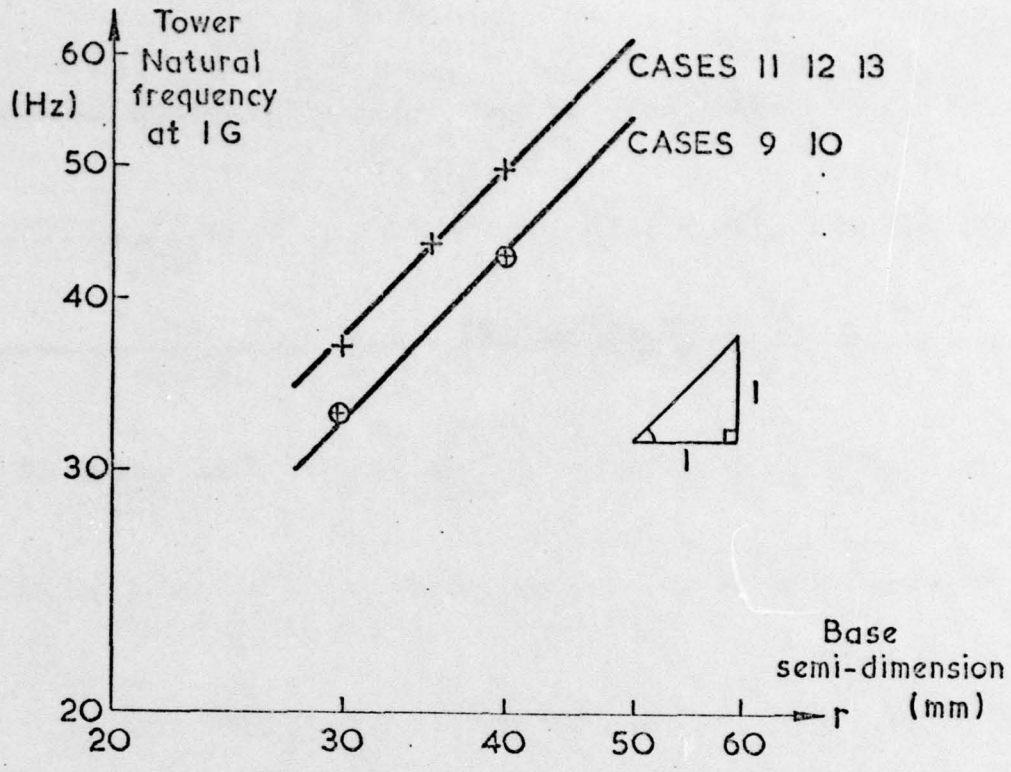

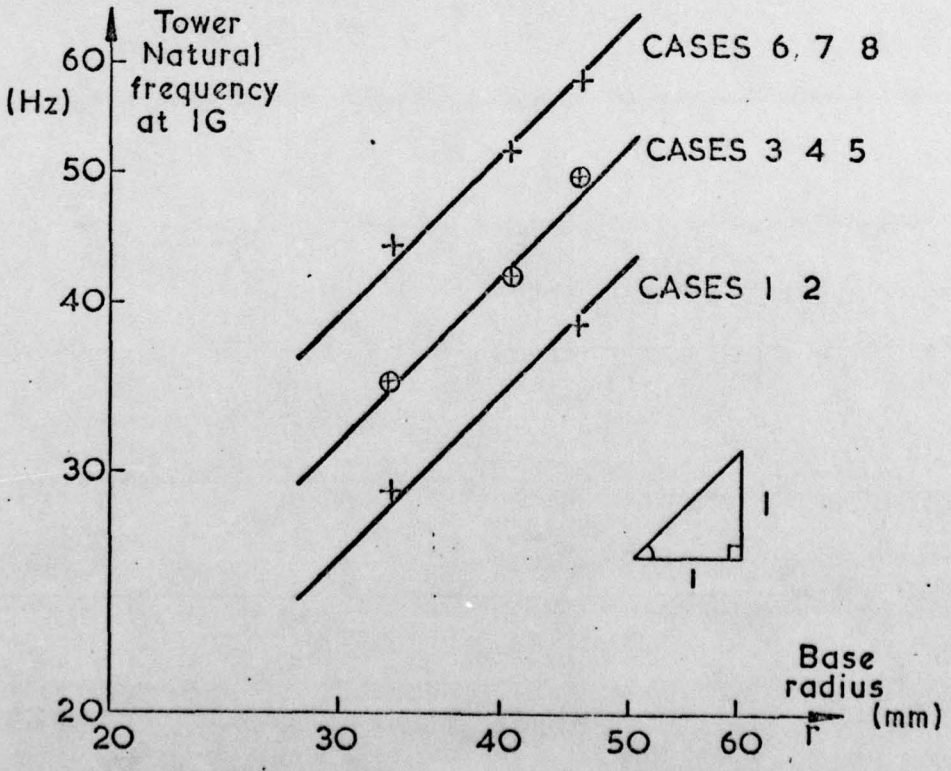

Figure 7 - Variation of natural frequency with base radius

It remains, then, to check that the variation of frequency with tower mass and moment of inertia is correctly predicted by equation (9).

For the experiments on circular bases, the following table compares the measured with predicted values, (using $\alpha = 0.5$ throughout, as assumed in equation (9)).

EXPERIMENT NO.	MEASURED f_n AT 1 g	PREDICTED f_n AT 1 g
1.	29 Hz.	29 Hz.
2.	39 "	40 "
3.	35 "	35 "
4.	42 "	43 "
5.	50 "	49 "

Agreement is good for each different experiment, and this also supports the assumption that α is constant and equal to 0.5.

5.6 EFFECT OF SQUARE FOUNDATIONS

Experiments 9 → 13 are concerned with square bases, and allowance must be made for the different geometry. If the base semi-diameter is c, then the spring stiffness is given by Gorbunov-Possadov and Serebranjanyi* (1961) as $\frac{4Gc^3}{(1-\nu)}$. The equivalent circular radius may be found by equating this spring stiffness to the spring stiffness for a circular

---

* GORBUNOV-POSSADOV, M. I. and SEREBRAJANYI, R. V. (1961) "Design of structures upon elastic foundations", Proc. 5th I.C.S.M.F.E. (Paris), Vol. 1

base from equation (2), $\frac{8Gr^3}{3(1-\nu)} \equiv \frac{4Gr^3}{(1-\nu)}$

so that the equivalent $r \equiv 1.14\ c$.

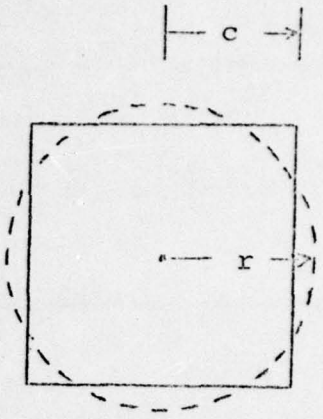

This result now enables equation (9) to predict the natural frequency of experiments with square bases. The measured and predicted values are compared below (again assuming $\alpha = 0.5$ throughout).

EXPERIMENT NO.	MEASURED f_n AT 1 g	PREDICTED f_n AT 1 g
9.	33 Hz	31 Hz
10.	43	42
11.	37	37
12.	44	43
13.	50	49

Agreement is generally good, although the measured natural frequencies seem to be consistently higher than predicted by a few per cent. It is doubtful whether this is significant, and, in general, these results support the assumption that α is constant and equal to 0.5.

5.7 EFFECT OF FOUNDATION EMBEDMENT

Experiments 6 → 8 concern foundations that were embedded by 20 mm. A theoretical analysis of embedment in an elastic medium, based on numerical computer techniques, is given by

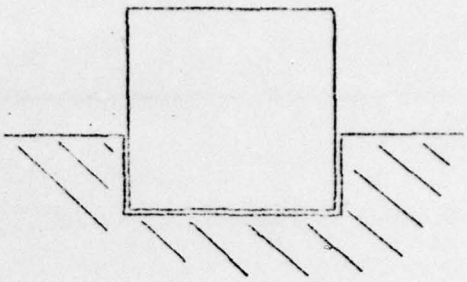

Urlich and Kuhlemeyer* (1973). It assumed full side contact of a circular footing.

Results are presented graphically in Fig. 10 of their paper, for the rocking displacement as a function of embedment and frequency (although the frequency effect is negligible in this case). An increase in rocking stiffness is predicted in each case, by factors of 2.16, 1.94 and 1.79 respectively, compared with the equivalent surface experiments 3 → 5.

Since the natural frequencies are proportional to the square root of the stiffness, they, in turn, should increase by factors of 1.47, 1.39 and 1.34. The predicted values are therefore given in the following table :-

EXPERIMENT NO.	MEASURED f_n AT 1 g	PREDICTED f_n AT 1 g
6.	44 Hz	51 Hz
7.	52	60
8.	59	66

In these tests, there was a significant discrepancy between theory and experiment, as the predicted frequencies were between 12% and 16% higher than the measured frequencies. It is the view of the author that this was primarily the result

---

* URLICH, E. M. and KUHLEMEYER, R. L. (1973) "Coupled rocking and lateral vibrations of embedded footings", Canadian Geotechnical Journal, May 1973

of the theoretical assumption of full side adhesion on the embedded base. This implied that there were large shear stresses along the edges of the foundation. However in practice the soil was unable to sustain these large stresses without yielding, and as a result the real rocking stiffness (and consequently the natural frequency) was less than predicted.

Similar results were found in full-scale tests by Stokoe and Richart* (1974), who found that the actual natural frequency of an embedded foundation was intermediate between the results predicted for embedment, and the result predicted for no embedment at all - depending also on the nature of the side contact.

The general trend of the experiments is quite clear, however, even though the theoretical analysis is imperfectly understood - the foundations were stiffened by embedment, although not by as much as would have been predicted by the assumption of full side friction.

5.8 CONCLUSION

On the basis of these centrifuge tests, the natural frequency of a variety of structures on dry sand appears to be satisfactorily predicted by a simple one-degree-of-freedom analysis, using equivalent elastic theory for the rotational stiffness of a circular foundation. This is summarised in equation (9), for a sand of voids ratio 0.65 and Poisson's ratio 0.25. The experiments also provided an indirect verification of the usual observation that the dynamic modulus

---

* STOKOE K.H. and RICHART F.E. (1974)"Dynamic response of embedded machine foundations" Proc. Am. Soc. of Civil Engineers, Vol.100, GT 4.

of sand is proportional to the square root of the confining pressure.

However, such a prediction requires an assumption as to what particular value of soil stress (and hence soil modulus) under the foundation is considered appropriate for such a calculation. The results of these tests suggest that a suitable empirical rule would be simply to use half the mean effective stress under the structure for the prediction of dynamic modulus. This rule applies strictly only for small amplitudes of motion in the rocking mode, for which strain softening does not occur. It allows for the inelastic behaviour and yielding of the sand under the foundation, which is particularily important in this mode.

The stiffness of square foundations appears to be adequately predicted by current elastic theory. Similarly, the embedment of a foundation is found to increase the rotational stiffness, as would be expected, but by less than predicted by theory. This is believed to be because the theoretical assumption of full side contact is not justified in practice.

These observations should apply equally to full-size foundations, and there is some full-scale evidence to support them.

In general, model behaviour corresponded with what would be expected from a full-size prototype, and gave quantitative overall support to the technique of centrifugal modelling.

CHAPTER 6

ADDITIONAL RESULTS FROM INITIAL EXPERIMENTS

6.1 DAMPING

The characteristic damping of the tower in Figure 4 was calculated using the "logarithmic decrement" method, applied to the oscillatory decay following explosive perturbation. If any particular cycle of amplitude a_o is followed 'n' cycles later by a cycle of amplitude a_n, then (for an equivalent linear elastic system) the proportion of critical damping is given by :-

$$c = \frac{\ln (a_o/a_n)}{2\pi n}$$

In this case, a value of 3 % was measured.

The behaviour of another model tower is shown in Figure 8, converted into prototype values in Figure 9, and this behaves in a similar fashion. The oscillatory decay is somewhat slower than in Figure 4, and the proportion of critical damping was measured on this occasion as about 2 %.

In principle, the damping can be predicted theoretically by adding that due to the dissipation of energy radiated away by elastic waves ("radiation" damping) to that due to internal deformation of the soil itself ("material" damping). However, in this case (and indeed for all rigid structures of reasonably

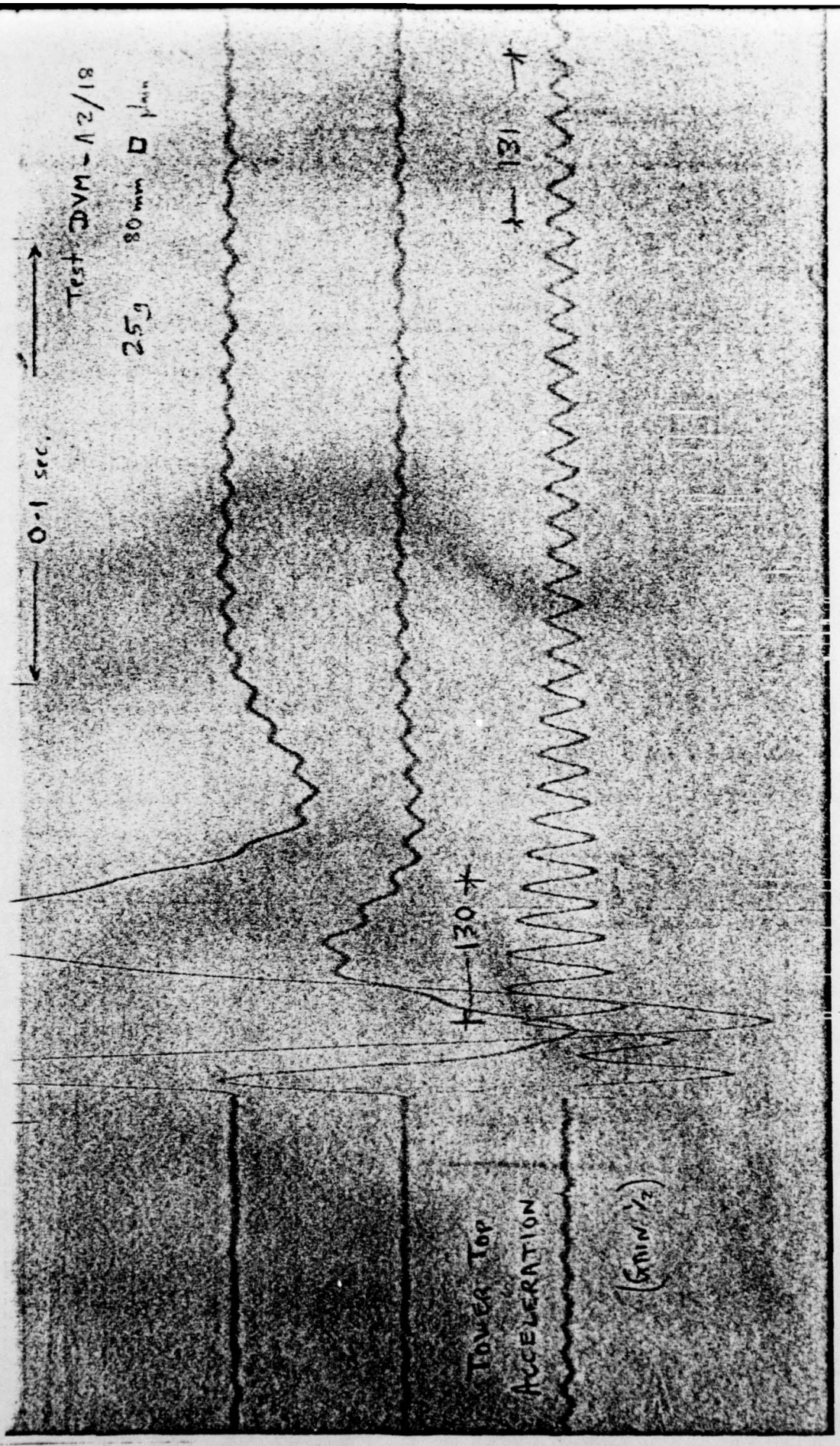

Figure 8 - Oscillatory decay of a tower (ii) - original

A2/18
(25g)

ROCKING TOWER, EXPLOSIVE PERTURBATION, ON A FOUNDATION OF DRY SAND

(Prototype values — Tower 6.5 m high, square base 2m x 2m.)

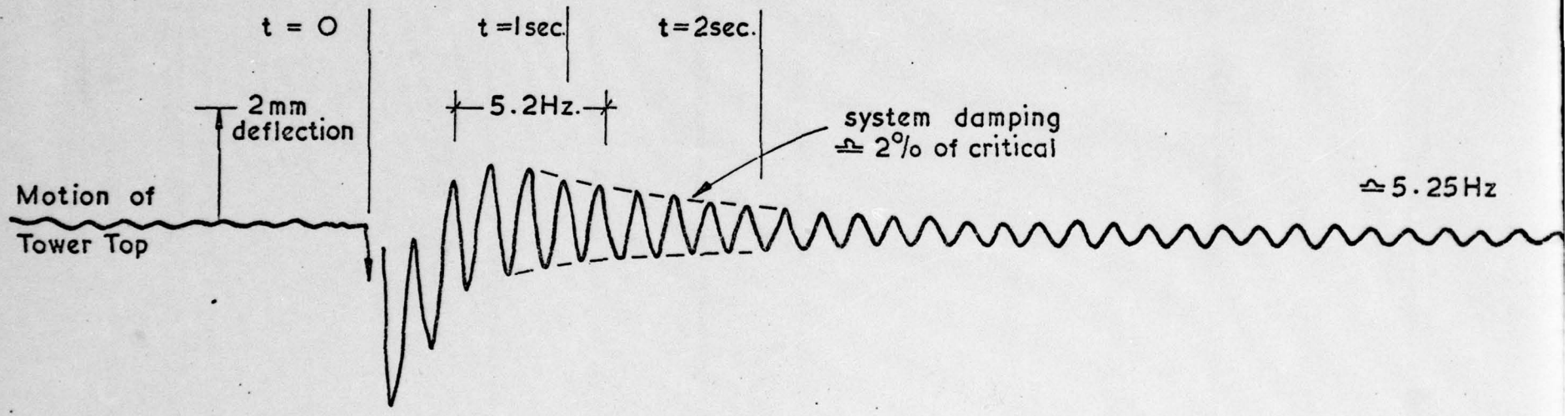

Figure 9 - Oscillatory decay of a tower (ii) - traced and converted to full scale

slender aspect ratio) the predicted radiation damping is extremely small. It is given theoretically by Hall* as

$$\frac{0.15}{(1+B)\sqrt{B}} \qquad \text{(as a proportion of critical damping)}$$

where $$B = \frac{3(1-\nu)\ I}{8\ \rho r^5}$$

Putting in values of base radius r = 0.04 m, tower moment of inertia I = 0.0275 kg.m^2, and soil density ρ = 1610 kg.m^{-3}, gives B = 47, and a damping factor of 0.05 %.

Consequently, the overall damping behaviour is dominated by the internal soil damping. This was measured experimentally from resonant column tests, reported in Appendix G, but these show considerable variation with strain and stress levels, depending also on whether the column excitation was longitudinal or torsional.

In practice it is only really possible to say that the material damping was found to be between 1 % and 6 % from resonant column tests (in general agreement with other tests on dry sands, e.g. those by Hardin+ (1965)), and that this agrees with values of between 1.5 % and 4.5 % observed for model foundations at resonance.

---

* HALL, J.R. (1967) "Coupled Rocking and Sliding Oscillations of Rigid Circular Footings" Proc. Intnl. Symp. on Wave Propagation and Dynamic Properties of Earth Materials, Albuquerque, U.S.A.

+ HARDIN, B.O. (1965) "The Nature of Damping in Soils" Proc. Am. Soc. of Civil Engineers, Vol.91, SM 1.

6.2 FOUNDATIONS ON CLAY

A brief investigation was made of the rocking of a tower on a base of kaolin "speswhite" clay, consolidated from slurry to ensure uniformity. The clay was fairly soft, with an undrained shear strength of about 30 kPa.

The same technique was used as before - the instrumented model tower was placed on the clay foundation and the centrifuge speed continuously increased. Records were taken at various centrifuge speeds of the wind-induced tower oscillation, and this provided values of the rocking natural frequency at different accelerations.

Figure 10 shows the variation of natural frequency with acceleration for identical towers, with base radii of 0.045 m, and 0.0325 m respectively. As no attempt was made to let the clay drain during the test, it might be assumed that it corresponded fairly well to the theoretical ideal of a uniform elastic half-space. Using the simple one-degree-of-freedom analysis, combining equations (1) and (2) and writing $\nu = 0.5$ for saturated soil, gives

$$f_n = 0.37 \sqrt{\frac{Gr^3}{I}} \qquad (10)$$

If the soil behaviour was entirely undrained, the soil modulus G should have remained substantially unchanged, and there should have been no appreciable variation of natural frequency with acceleration. Figure 10, however, shows some tendency for the natural frequency to increase initially, and then to level off at an approximately constant value, at higher values of centrifugal acceleration.

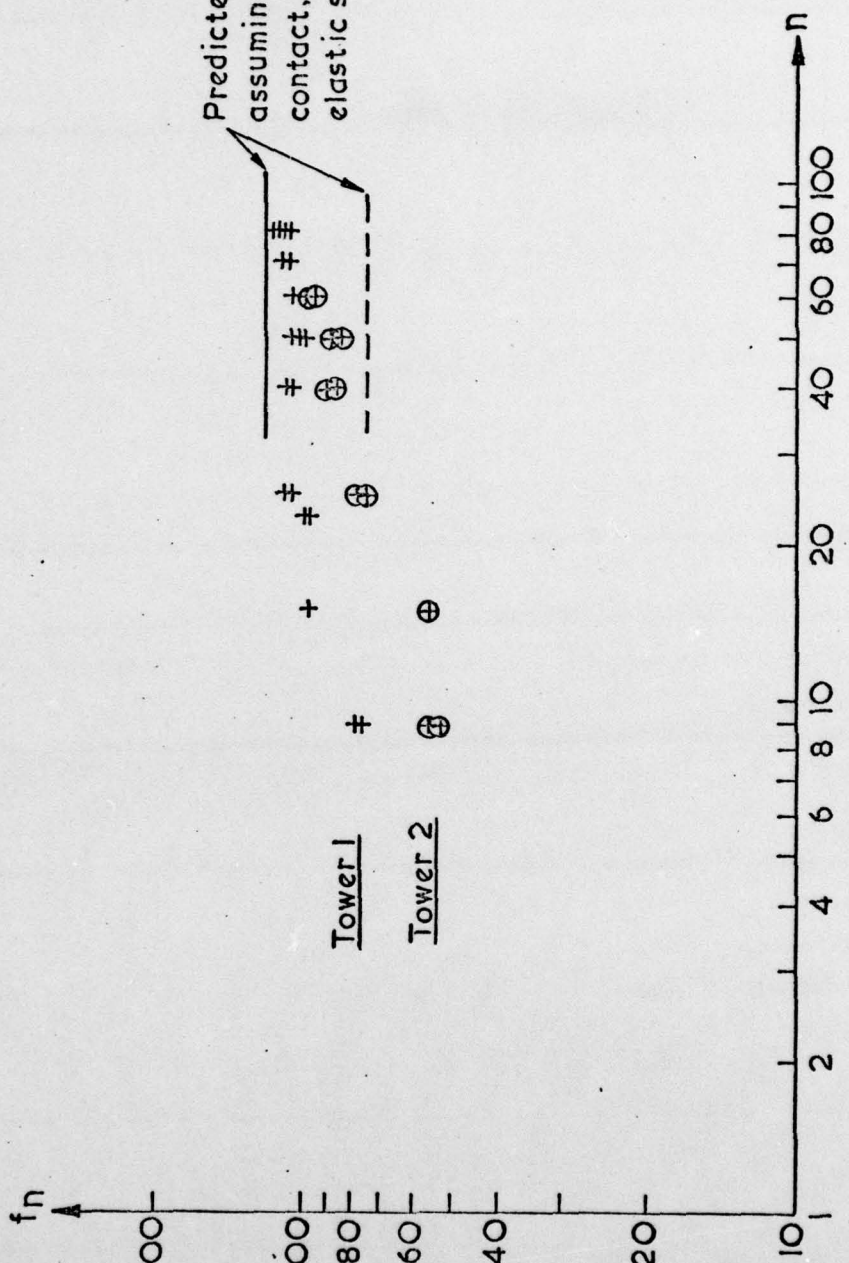

Figure 10 - Variation of natural frequency with acceleration - clay

It is likely that, to some extent, this was associated with the "bedding-down" of the base onto the clay, resulting in an increase in the effective base contact area, as the normal stress increased.

A value of the shear modulus of the clay was derived directly in each case, by measuring the velocity of a Rayleigh wave on the clay surface. This was done simply by timing a surface wave impulse between two accelerometers on the clay, attached to a twin-trace oscilloscope.

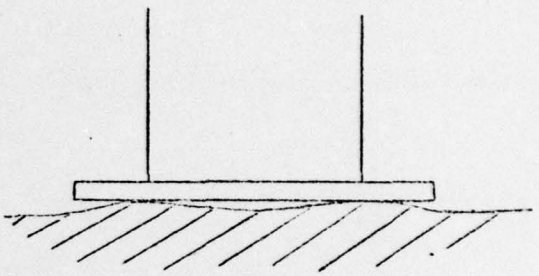

For saturated material ($\nu \triangleq 0.5$) the Rayleigh wave velocity is $0.95\sqrt{\frac{G}{\rho}}$. As the soil density was 2000 kg/m^3 and the measured Rayleigh wave velocity was 120 m/s, then the dynamic shear modulus G of this clay was approximately 32 MPa.

This enables a simple prediction of the natural frequency. Both towers had a moment of inertia of 0.0275 kg.m^2 about their base. For the tower with a base radius of 0.045 m, equation (10) predicts f_n = 120 Hz, and for the base radius of 0.0325 m, f_n = 74 Hz.

This agrees reasonably well with the range of values displayed in Fig. 10. It is not, in fact, possible to assume definitely that the clay is acting in either a purely undrained or drained fashion, as the coefficient of consolidation for kaolin clay is about 3×10^{-6} m^2/s, so that, for typical drainage paths, consolidation will start to take place within 10 seconds, and continue for at least 20 minutes or more.

A thorough investigation of soil-structure interaction on clay footings would require firstly that full base contact be ensured (perhaps by embedding it in Plaster of Paris), and secondly that the soil pore-pressures be allowed to reach equilibrium (which could be checked by letting the rocking frequency stabilise).

However, measurement of Rayleigh wave velocity is clearly a reasonably effective way of determining the dynamic elastic modulus of cohesive material, and, once again, a simple one-degree-of-freedom analysis of the type demonstrated, produces acceptable results.

6.3 STRUCTURE-STRUCTURE INTERACTION

There has been considerable interest recently in the effect of cross-coupling between adjacent structures, such as outlined in Lee and Wesley* (1973), and a few pilot model tests were attempted. Two towers were placed close to each other, separated by about one base radius, and the response of one tower to the explosive perturbation of the other, was monitored.

No elaborate study was performed of this phenomenon, but Figure 11 shows a typical original trace for two such towers on sand. This is traced for clarity in Fig. 12, where the values of frequency etc. have been converted into prototype values. The central trace shows the motion of the tower subjected to primary agitation, and its peak movement

---

* LEE AND WESLEY (1973) "Soil-structure interaction of nuclear reactor structures considering through soil coupling between adjacent structures" Nuclear Engineering and Design, Vol.24, North Holland Publishing Co., Amsterdam, Netherlands.

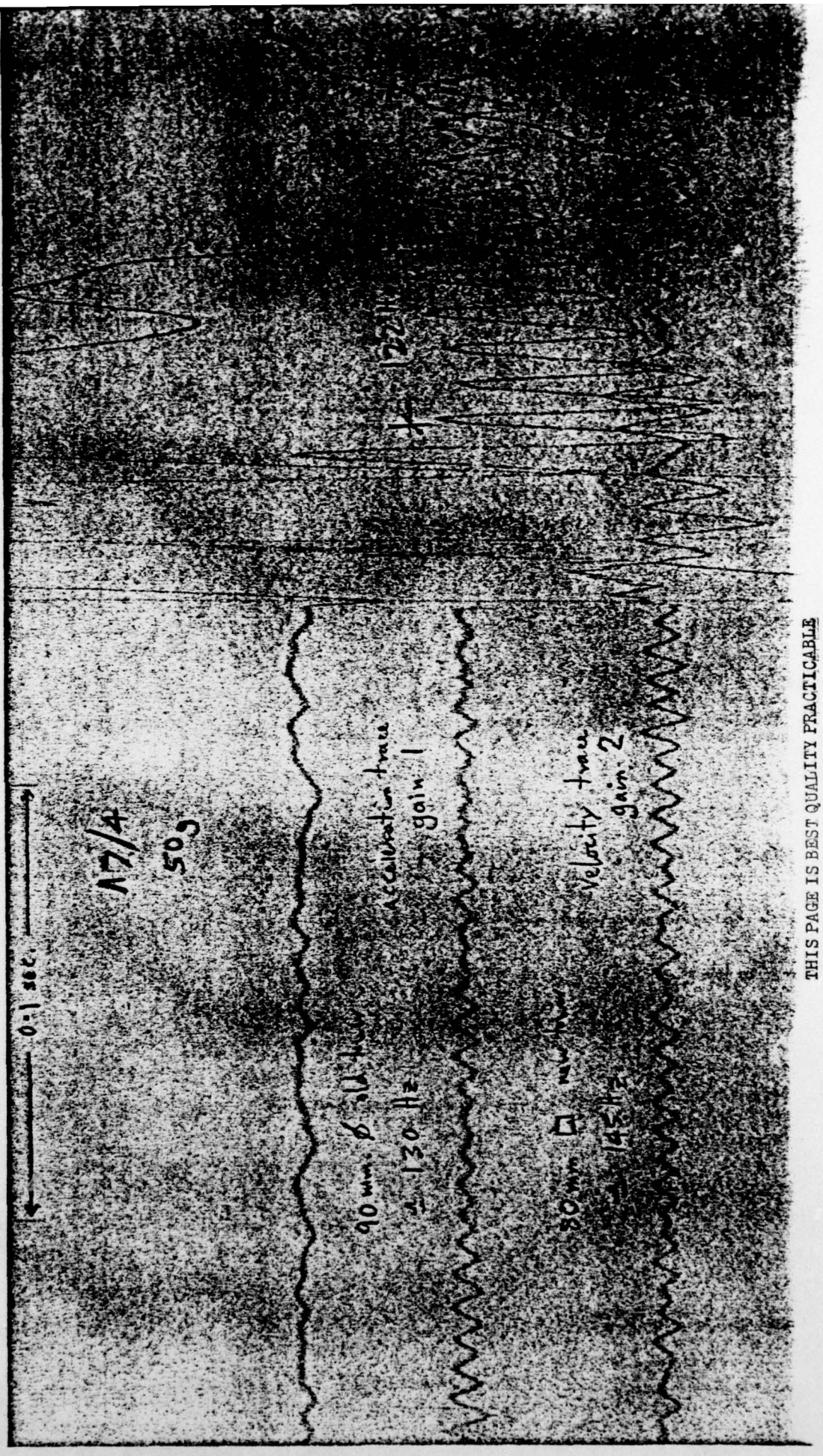

Figure 11 - Structure-structure interaction on sand (i) - original

DVM-A7/4
(50g)

STRUCTURE - STRUCTURE INTERACTION OF NEIGHBOURING TOWERS, ON DRY SAND.

(Prototype values – Tower 13 m. high, separated by 2m.)

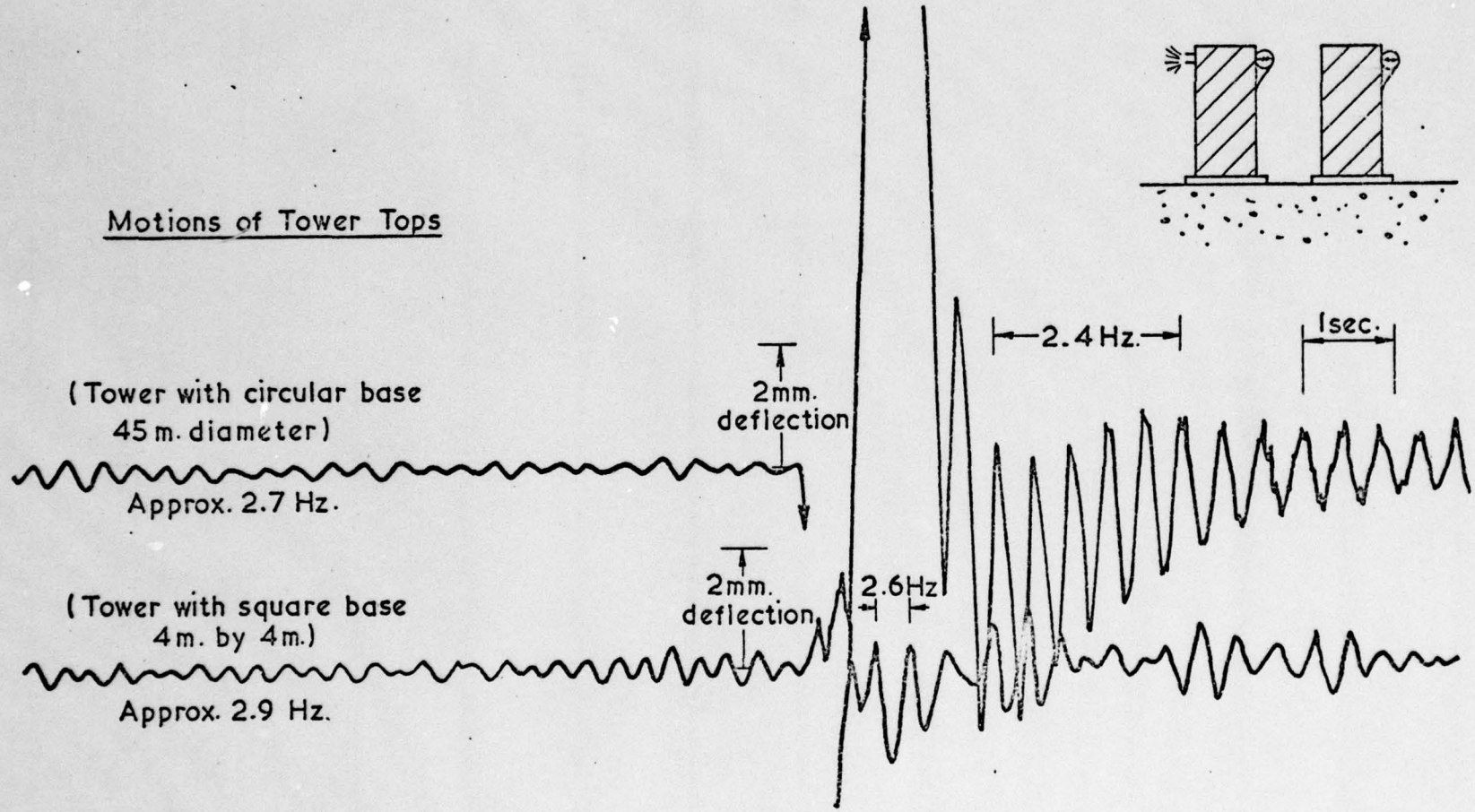

Figure 12 - Structure-structure interaction on sand (i) - traced and converted to full scale

corresponds to an angular rotation about the base of approximately 100 x 10^{-5} radians.

Beneath it is shown the motion of the "companion" tower, with a measured natural frequency about 10% higher, and it shows a peak rotation of about 12 x 10^{-5} radians. This particular example showed an unusually large amount of interaction.

Figure 13, again traced for clarity in Fig. 14, shows another similar case, where the "companion" tower on the bottom trace again had a measured natural frequency about 10% higher than the explosively perturbed tower, and yet on this occasion practically no interaction was visible at all (apart from some very small high-frequency "ringing" just visible on the lower trace). The instrumentation itself appeared not to be at fault, and the interactive motion of the lower trace was less than 1% of the primary trace.

Tests on clay however, demonstrated substantially more in the way of interaction, and one such is illustrated in Figure 15, again traced in Figure 16, where the motion of the secondary tower is roughly 10 to 15% of the motion of the primary tower. On this occasion the natural frequency of the towers, measured just before the explosion, differed by only one or two per cent - which may have contributed to the larger interaction.

Qualitatively it seems reasonable that interactive effects are more marked on clay than on sand foundations, as the energy transfer between adjacent foundations must take place via wave energy (in particular via Rayleigh waves), and a clay surface would seem better able to transmit surface

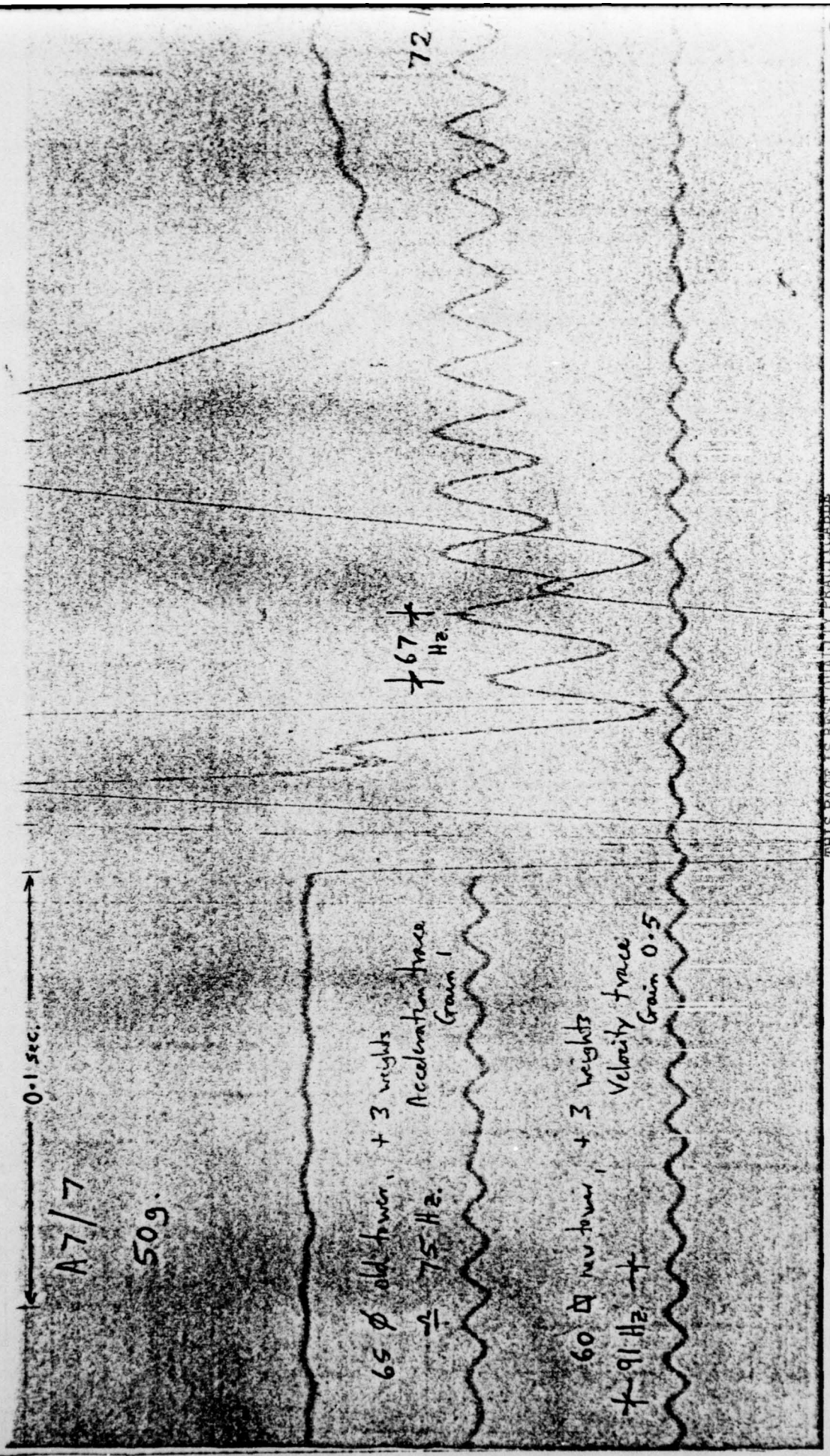

Figure 13 - Structure-structure interaction on sand (ii) - original

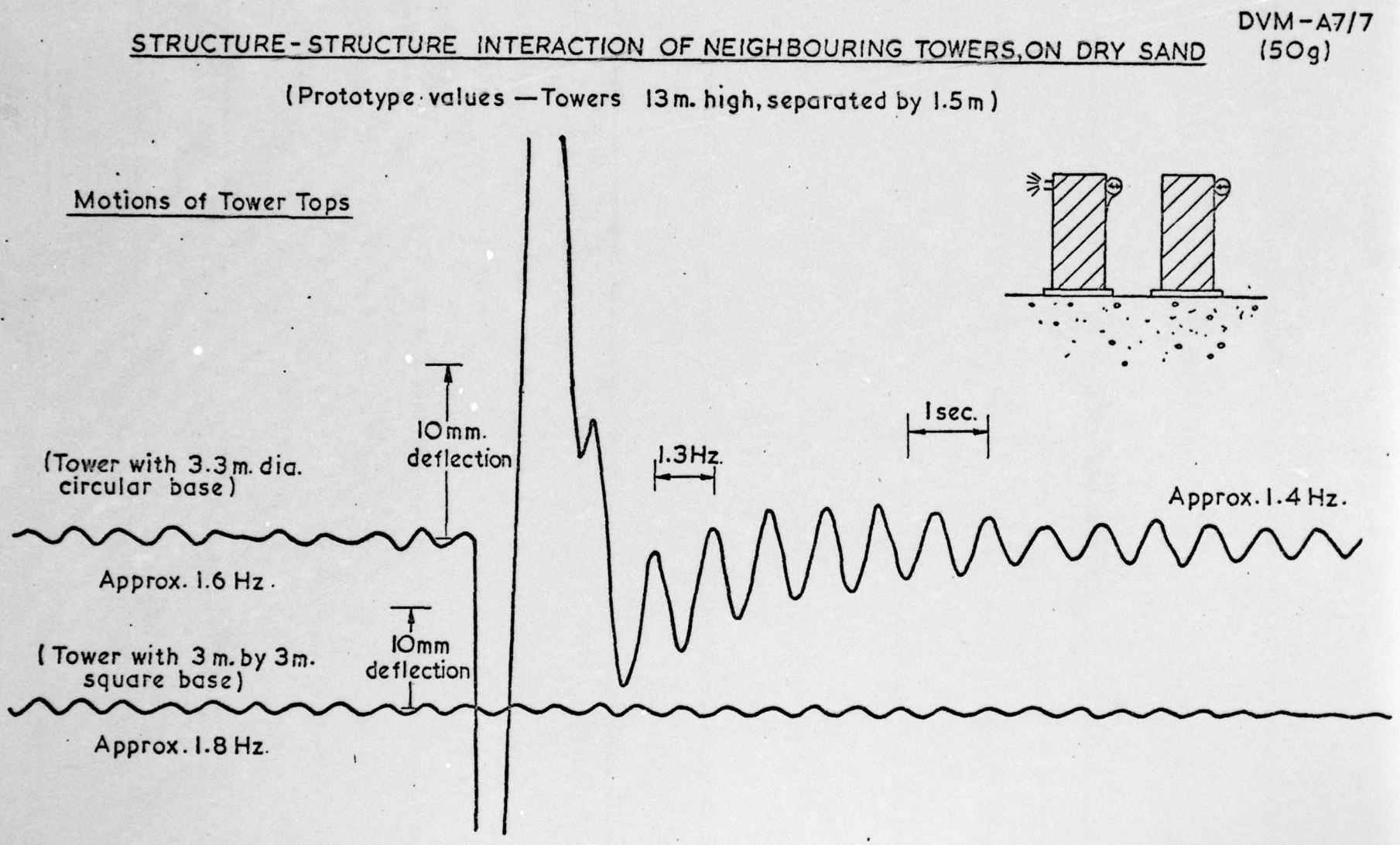

Figure 14 - Structure-structure interaction on sand (1.1) - traced and converted to full scale

Figure 15 - Structure-structure interaction on clay - original

DVM-A6/2
(25g)

STRUCTURE - STRUCTURE INTERACTION OF NEIGHBOURING TOWERS, ON CLAY.

(Prototype values — Towers 6.5 m. high, separated by 1.1 m.)

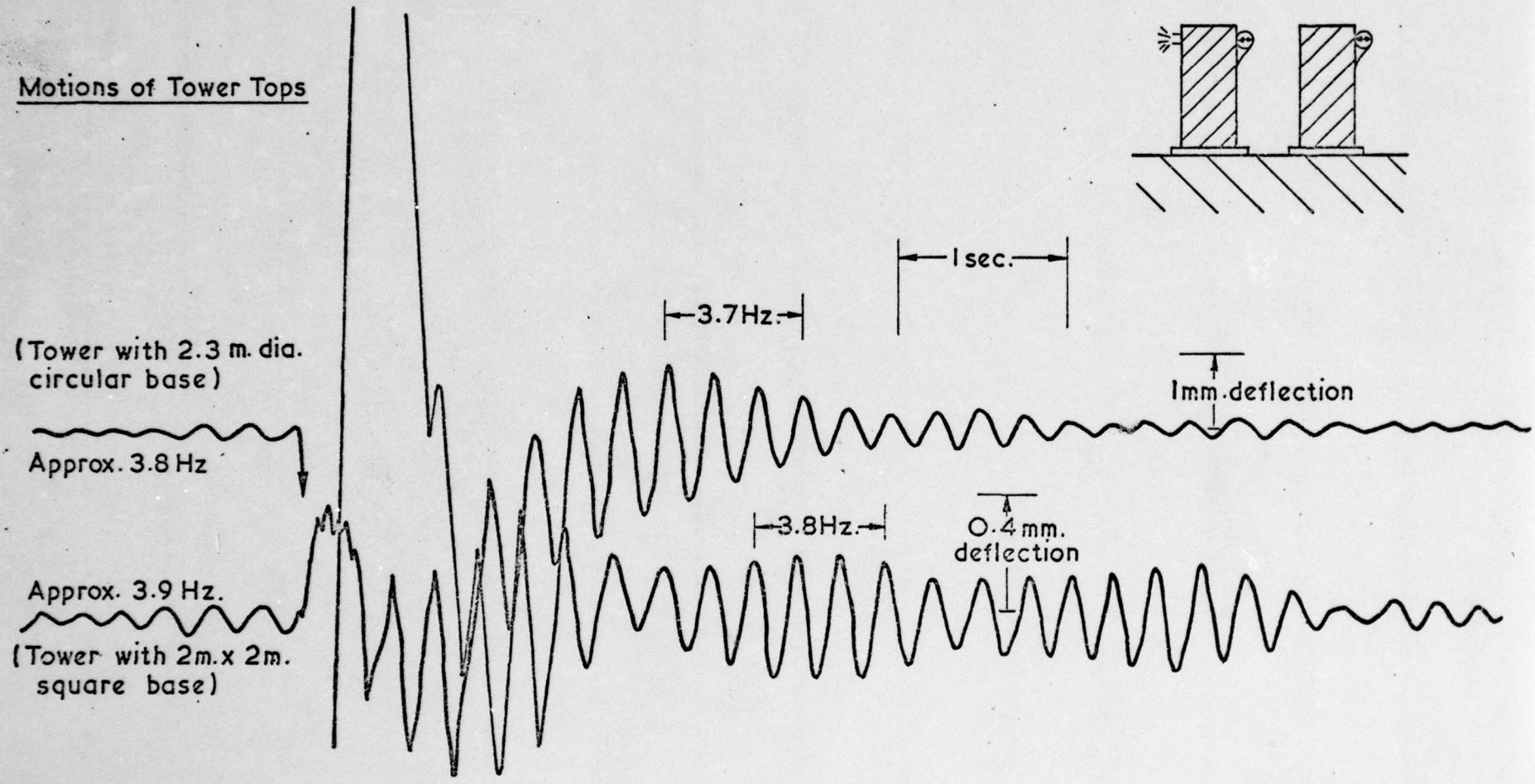

Figure 16 - Structure-structure interaction on clay - traced and converted to full scale

waves than a sand surface. The material damping associated with clay foundations is also usually less than for sand foundations.

Warburton, Richardson and Webster*(1971) have presented analytical work showing large amounts of cross-correlation between two discs on an elastic half-space separated by ten base radii. However, this considered only vertical perturbation of a disc (which would naturally tend to produce more radiation energy in the soil than rotational motion), and no intrinsic soil damping or non-linear behaviour was included in the analysis.

In general, on the basis of these very sketchy results, the interaction between neighbouring structures in "rocking" motion appears to be relatively important.

6.4 MODELLING AT DIFFERENT SCALES

Although it was not possible to verify the modelling laws by comparing the natural frequencies of model towers with the equivalent full-size structure, it was still possible to test the modelling laws by modelling the same prototype structure at different modelling scales, and checking that the predicted full-scale result coincided. This method of indirect verification of the modelling laws has been used for static tests, e.g. on model footings by Krebs Oveson+ (1975), but as

---

* WARBURTON, G. B.; RICHARDSON, J. P. and WEBSTER, J. J. (1971) "Forced vibrations of two masses on an elastic half-space", Journal of Applied Mechanics, Trans ASME, Series E, Vol. 38 No. 1

\+ KREBS OVESON N. (1975) "Centrifugal testing applied to bearing capacity problems of footings on sand", Geotechnique, p. 394.

far as the author is aware, has not been done for dynamic centrifuge tests.

This required the construction of geometrically similar towers, of different sizes. Three such towers were made in the ratio of 1:2:3, and they are shown in Plate 6, mounted on a sand base. Each of them was monitored with an accelerometer on the top, and when they were spun up to speed in the centrifuge, the natural frequencies of the towers were measured in the usual way, from wind-induced oscillations.

Figure 17 shows a composite record, made up of the wind-induced motions of the 150 mm high tower at 45 g, followed by the 300 mm high tower at 22 g, followed by the 450 mm high tower at 15 g. Under this set of circumstances, each tower is modelling the same full-size structure, of height about 6.7 m; and if the modelling laws are correct, the natural frequencies should be in the inverse ratio - i.e. 1:½:⅓, so that the full-size prototype frequency would be the same in each case.

This is in fact so, if the traces are examined. For the 0.15 m tower at 45 g, the predicted natural frequency for the 6.75 m high prototype is 105.5 Hz/45 = 2.34 Hz. Similarly, for the 0.3 m tower at 22 g, the predicted natural frequency for the 6.6 m high prototype is 51 Hz/22 = 2.32 Hz; and for the 0.45 m tower at 15 g, the predicted natural frequency for a 6.75 m high prototype is 35 Hz/15 = 2.33 Hz. These values are all within experimental error, and provide a valuable check on the modelling laws.

This can be shown graphically by plotting natural frequency linearly against modelling scale, in Figure 18. Now if F_n is

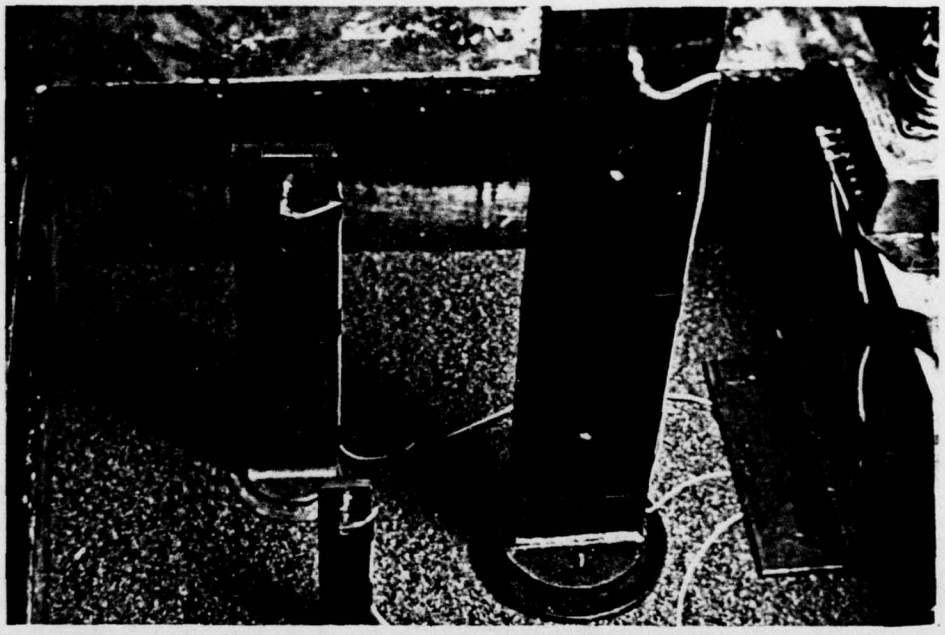

PLATE 6 - Geometrically similar model towers

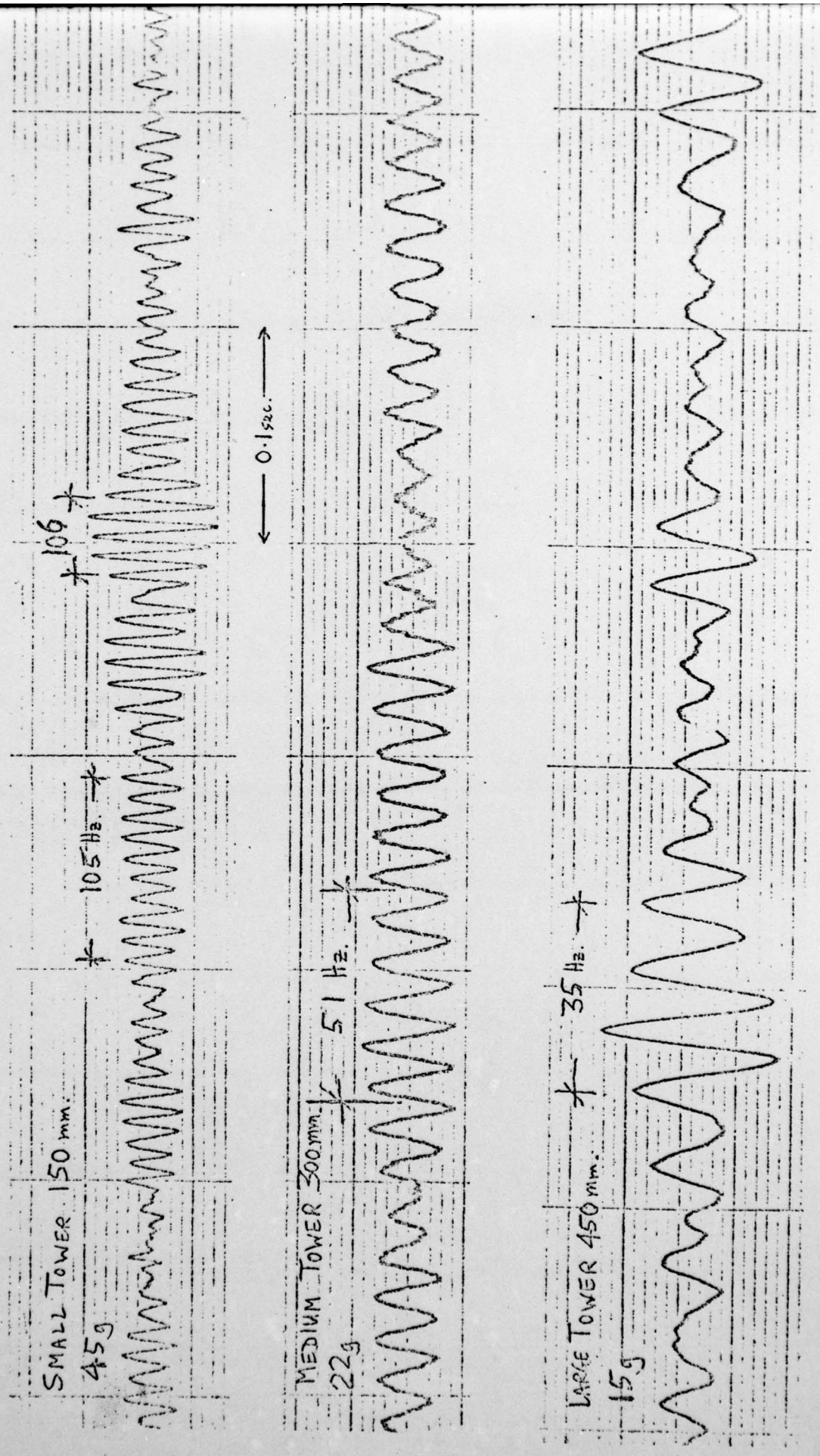

Figure 17 - Modelling at different scales - composite oscillatory trace (i)

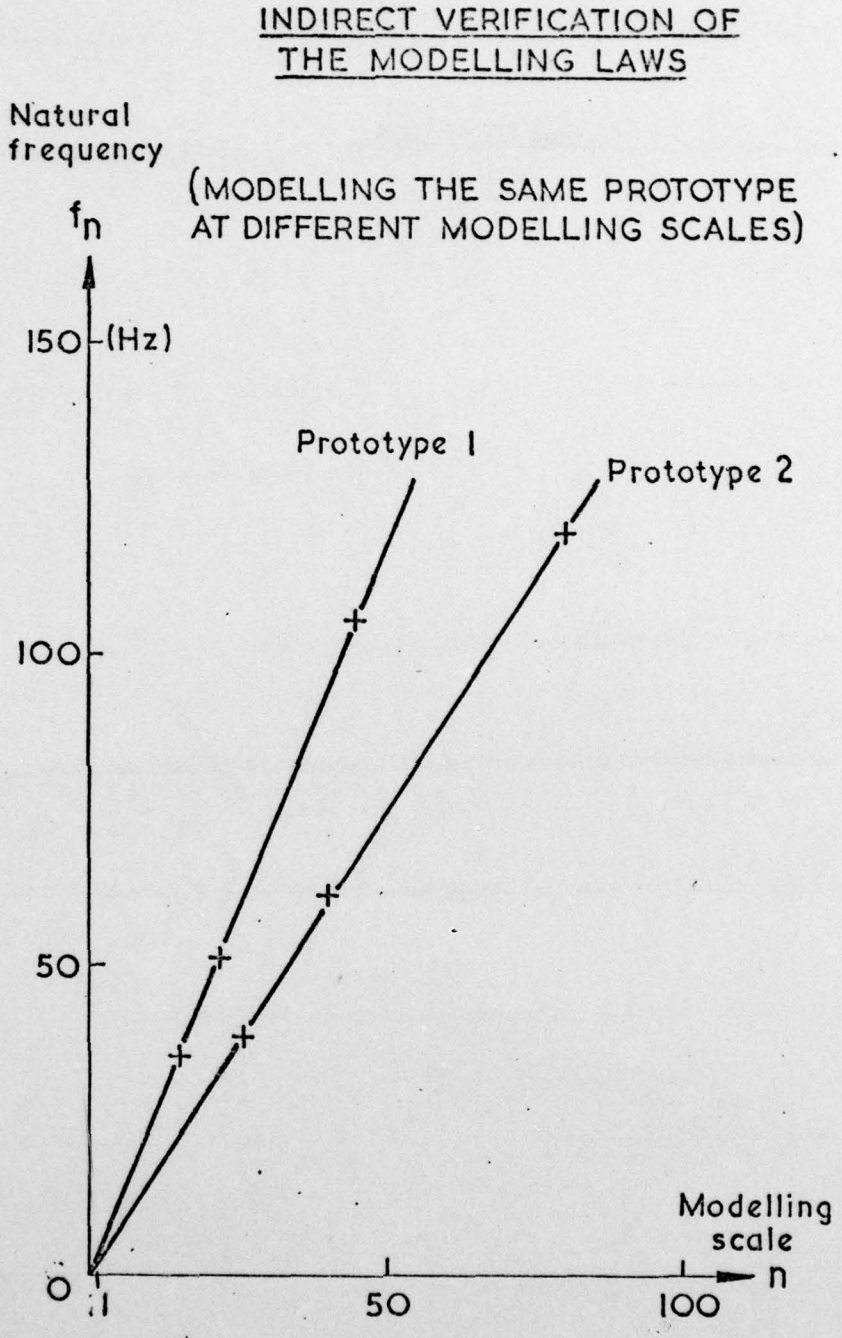

Figure 18 - Graph of natural frequency against modelling scale, for the same prototype

the natural frequency of a full-scale structure, i.e. at a modelling scale of 1, then at a modelling scale of n, the natural frequency of a model $f_n = F_n n$. Thus, if the natural frequencies of different models of the same prototype are graphed against the modelling scale, they should lie on a straight line through the origin, as F_n is constant. The only advantage of actually testing a full-size structure itself would be to provide a point at n = 1. Although desirable, this is not absolutely necessary for verifying the modelling laws.

Figure 19 shows another composite record for the same three towers, only this time at 26 g, 40 g and 80 g. The prototype height in each case was about 12 m, and the equivalent prototype frequencies were 1.48 Hz, 1.53 Hz, and 1.49 Hz.

These results are also graphed on Figure 18, and in both cases, a good straight line through the origin is obtained.

Some experimental error would be expected to arise, simply because the towers were not in fact perfectly geometrically similar - firstly because of the presence of identically sized accelerometers (which were clearly not geometrically similar), and secondly because the proximity of the sides and bottom of the container was roughly the same in all cases, so that the boundary conditions were not scaled in correct proportion in each case. However, the effects of these experimental difficulties appear to be small.

It is possible to conclude, therefore, that centrifugal modelling laws may be checked without requiring a full-size experiment - and in this case the particular technique of modelling at different scales has provided strong support for the dynamic modelling laws.

12 M. HIGH PROTOTYPE, MODELLED AT SCALES OF 80, 40, AND 26

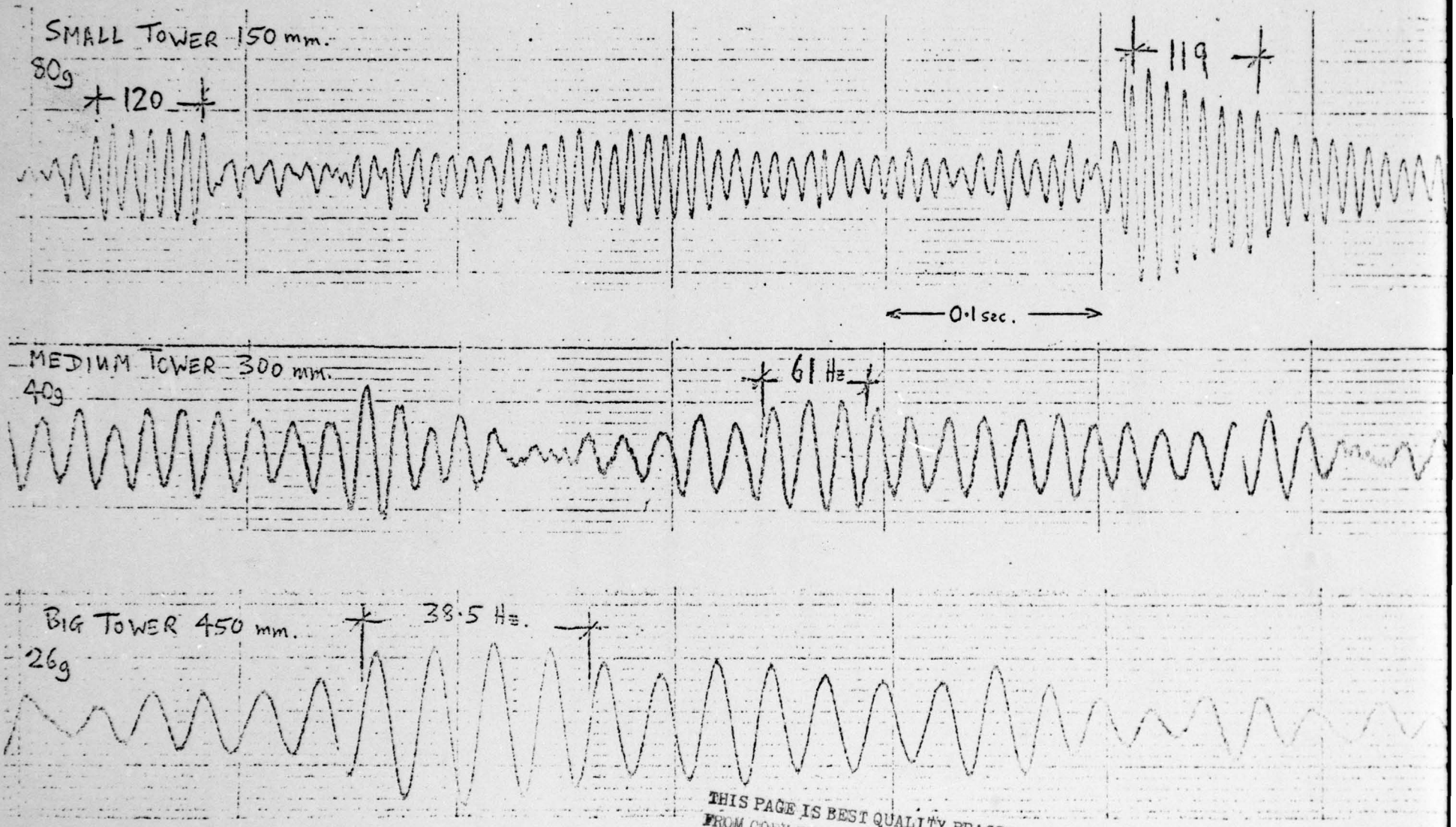

Figure 19 - Modelling at different scales - composite oscillatory trace (ii)

CHAPTER 7

THE APPARATUS USED FOR MODELLING EARTHQUAKES

7.1 INTRODUCTION

For engineering purposes it is generally assumed that earthquake damage to engineering structures arises from the horizontal shear deformation of soil, as a result of the vertical propagation of a shear wave from underlying bedrock.

In practice, behaviour is more complex than this, as waves of many kinds are generated in an earthquake, by the slipping of tectonic fault lines. As areas of high earthquake intensity are usually close to a fault line, in relation to the length of the fault line itself, such an area will be traversed by waves travelling in different directions from each part of a fault, so that an earthquake record may vary significantly between locations separated by only a few hundred yards.

However, all motions can be resolved vertically and horizontally, and since most civil engineering structures (designed primarily for vertical load) have enough vertical static strength in reserve to cope with dynamic effects, it is normally horizontal motions that cause concern. Similarily liquefaction failures in dams and embankments occur primarily as a result of horizontal movements.

Consequently the special package constructed to model earthquake behaviour on the centrifuge, was designed to produce horizontal motion only. It may conveniently be described as a shaking table on the centrifuge, and is sketched schematically in Figure 20.

7.2 DESIGN PARAMETERS

Considerations of cost ruled out a variable-frequency agitation system for the design, and, therefore, a mechanical spring system was used to provide the horizontal forces required.

The dynamic parameters of the package were a shaking frequency of 61 Hz (which was constant) and a maximum acceleration of 20 g (corresponding to an amplitude of movement of 1.3 mm). The full-scale values implied by the modelling laws depend on the particular centrifugal modelling scale chosen, and are outlined in the following table:-

	Centrifugal acceleration		
	25 g	50 g	80 g
Full-scale frequency (constant)	2.4 Hz	1.2 Hz	0.76 Hz
Full-scale amplitude (max.)	33 mm	65 mm	105 mm
Full-scale acceleration (max.) (as a proportion of vertical acceleration)	80 %	40 %	25 %

These values correspond to typical field values of earth-

quake motion.

The package was designed to contain a maximum soil mass of 120 kg in a plan area of 500 mm by 565 mm. At 80 g this corresponded to a prototype soil mass of approximately 61,000 tonnes, and a sample area of 1,800 square metres.

7.3 PRINCIPLES OF OPERATION

A primary consideration in the design of the apparatus was that the oscillating forces needed to produce the acceleration of the soil model and its container did not react onto to the arm of the centrifuge. Since the soil and its associated packaging had a total mass of around 250 kg, a horizontal acceleration of 18 g required horizontal forces of the order of 4.5 tonnes force. It was felt that this might damage the centrifuge bearings, and in any case large forces in this direction might interfere with the operation of the swinging platform.

A "reaction mass" was consequently provided, attached to the main package by relatively stiff leaf springs, and the primary oscillation took place between this and the main package. The main package was in turn flexibly suspended from hanging strips.

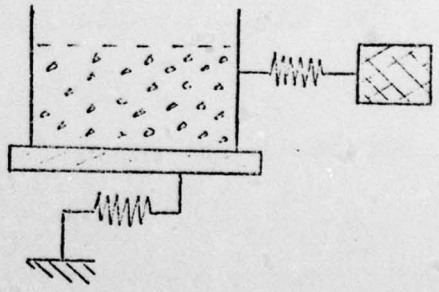

These had a high capacity for vertical load, together with a very low value of lateral stiffness, and effectively isolated the whole system from the centrifuge arm, transmitting only a small fraction of the dynamic forces. Theory indicated an

isolation factor of about 20, and this was supported experimentally. Another advantage of hanging strips over other forms of isolating systems (e.g. rubber bearing pads) was that they were flexible in one direction only - so that horizontal movement of the container could take place without any associated twisting or rocking motion.

Dynamic agitation of the soil and its container took place by jacking the reaction mass away from the container, and releasing it at the desired point in time. The subsequent relative motion provided the model earthquake agitation. The frequency of vibration was determined by the relation of the reaction mass to the spring stiffness. The dynamic energy was effectively stored in these springs, which had to be designed simultaneously to produce vibration at the desired frequency, and to withstand the dynamic forces safely.

The dynamic motion was parallel to the axis of rotation of the centrifuge, in order to avoid Coriolis accelerations that might be produced from velocities in any other direction.

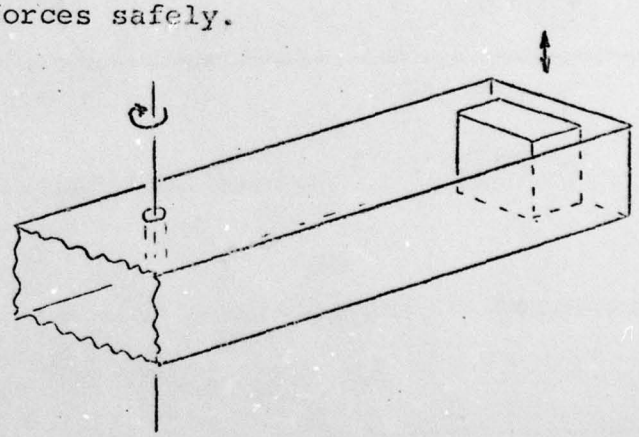

7.4 FURTHER DESCRIPTION

A diagrammatic representation of the apparatus is shown in Figure 20.

The soil container 5/. was supported on an underlying decking 8/. that was suspended by flexible strips 2/. These hung from hollow towers 9/. which carried the total weight onto the centrifuge swinging platform. The entire assembly could then

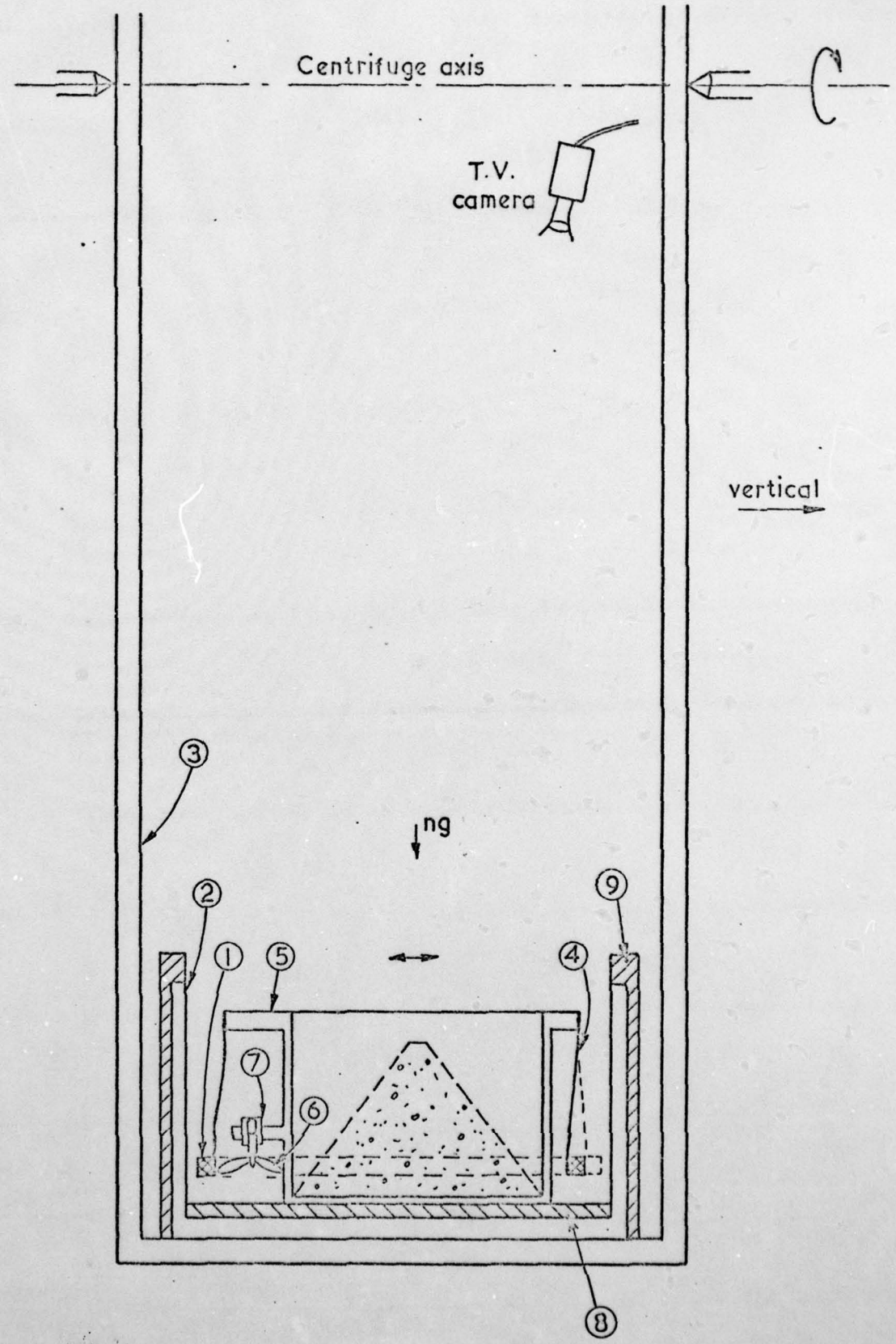

Figure 20 - Diagrammatic representation of apparatus for modelling earthquakes

AD-A083 972 CAMBRIDGE UNIV (ENGLAND) DEPT OF CIVIL ENGINEERING F/G 8/13
CENTRIFUGAL MODELLING OF SOIL STRUCTURES. PART II. THE CENTRIFU--ETC(U)
JUN 79 D V MORRIS, A N SCHOFIELD DA-ERO-76-G-040
UNCLASSIFIED NL

2 OF 3
AD
A083972

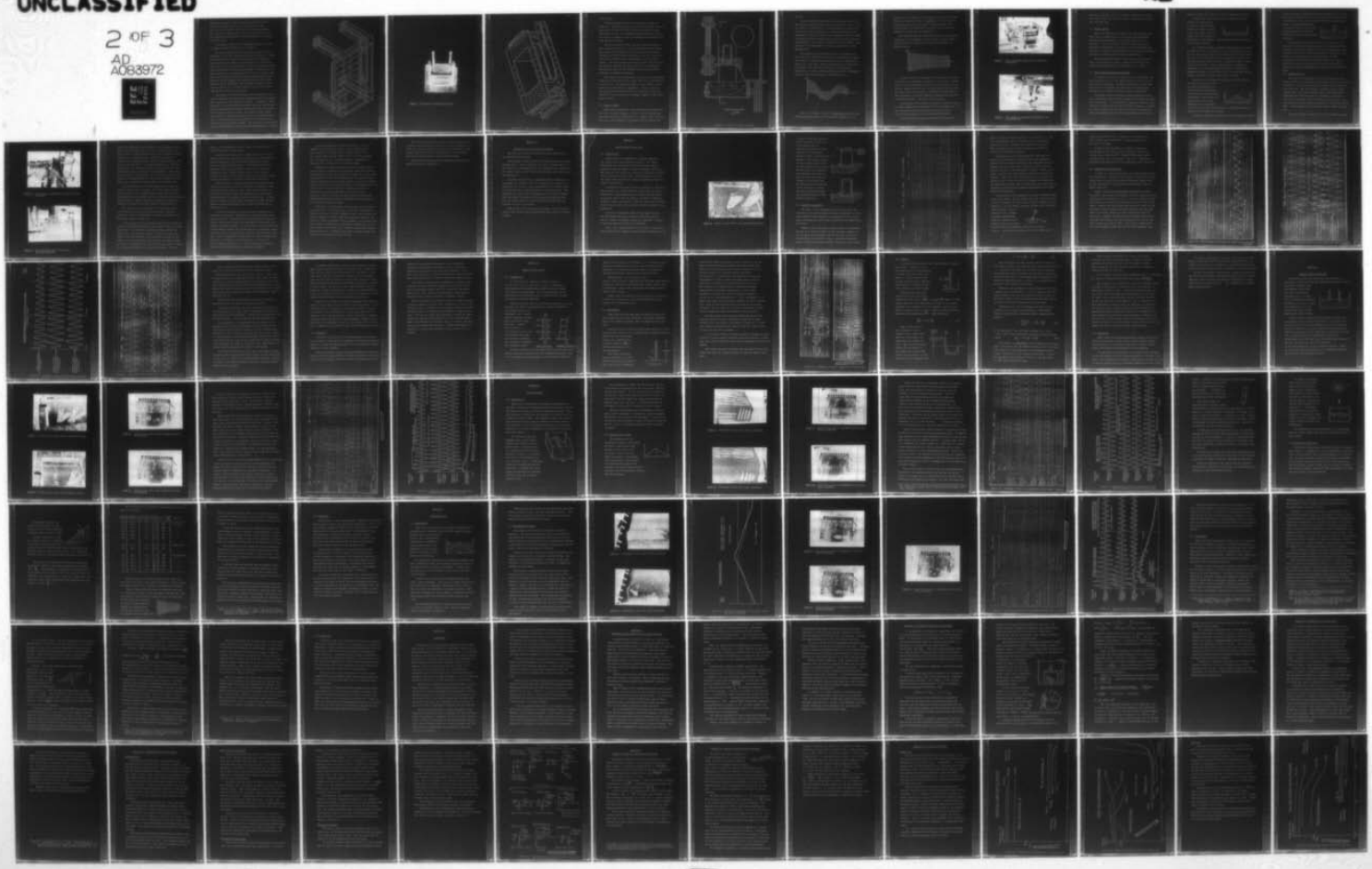


NC

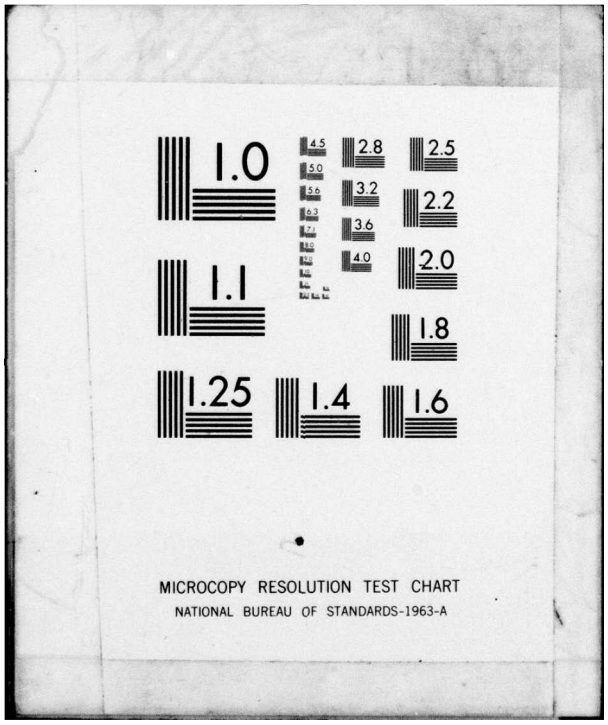
1.0
1.1
1.25
1.4
1.6
1.8
2.0
2.2
2.5
2.8
3.2
3.6
4.0
4.5
5.0
5.6
6.3
MICROCOPY RESOLUTION TEST CHART
NATIONAL BUREAU OF STANDARDS-1963-A

swing into position as the centrifuge started to revolve. The ribbed decking together with the flexible strips and the towers, formed a self-contained assembly labelled the "suspension system", onto which the soil container and the associated superstructure could be bolted, as a separate structural unit.

An isometric sketch of the "suspension system" is shown in Figure 21, and a picture of it in Plate 7.

The primary dynamic motion took place between the soil container 5/. and the circumferential reaction mass 1/. These were connected on each side by six multiple leaf springs, that could deflect sideways in double bending in the manner illustrated, and that also served to support the counterweight. The specifications required these springs to deflect by 6 mm when subjected to a horizontal dynamic force of 4 tonnes, and they were constructed from heat treated chromium alloy steel. This part of the package was constructed mainly out of aluminium alloy for lightness, and an isometric sketch of it is shown in Figure 22. It simply bolted on top of the "suspension system" referred to previously.

The system was activated before a test by bolting a temporary attachment onto the box and jacking against the reaction mass, causing the leaf springs to deflect. A system of catch pieces 6/. was then placed into position by hand, and the temporary jacking pressure slowly released until the spring force was transferred onto the catch. The catch was then jammed into position, and held the inertia mass in a deflected position - the magnitude of which depended on the thickness of a steel insert in the catch assembly. In this way it was possible to vary the magnitude of the horizontal acceleration in a fairly

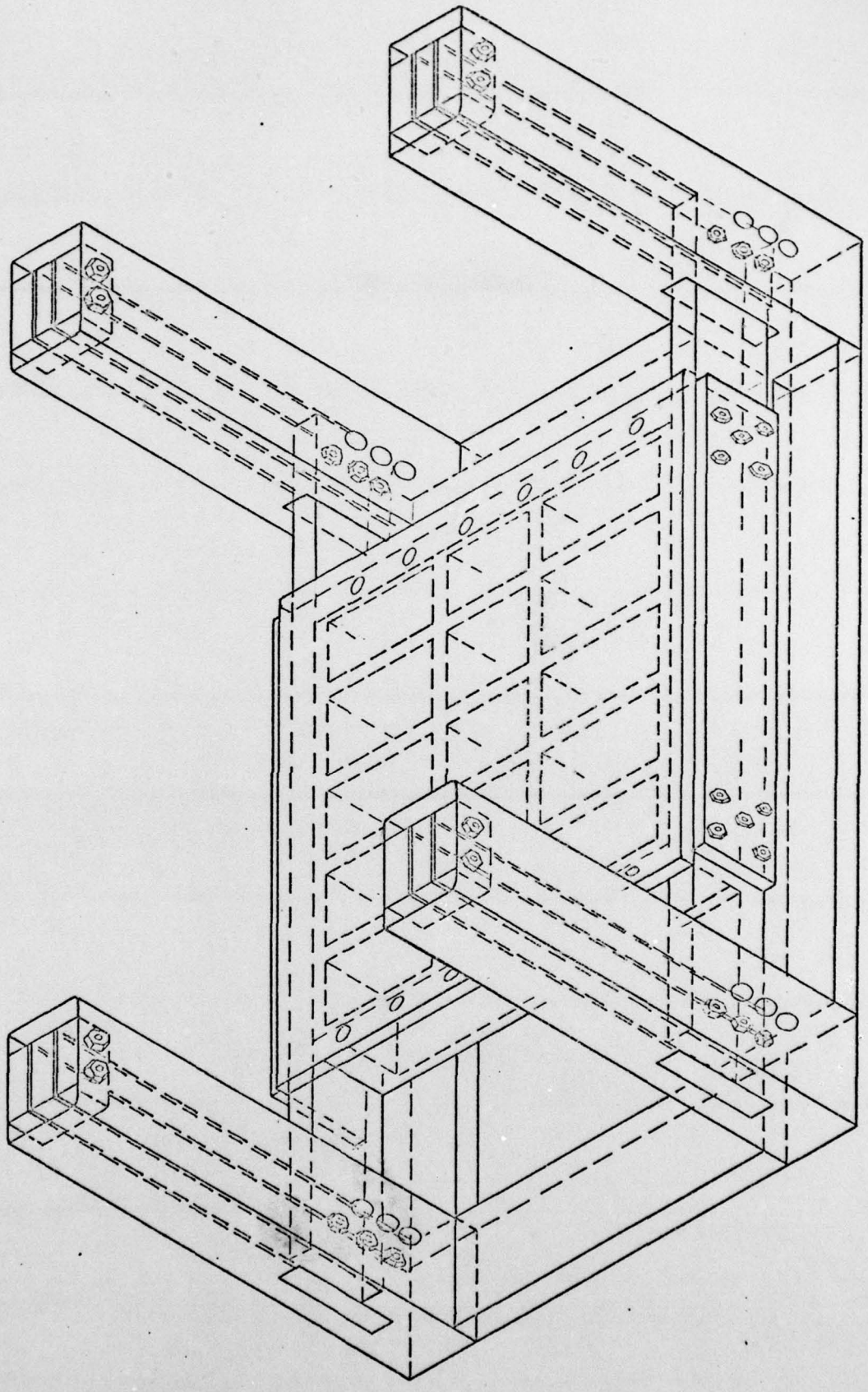

Figure 21 - Isometric sketch of "suspension system"

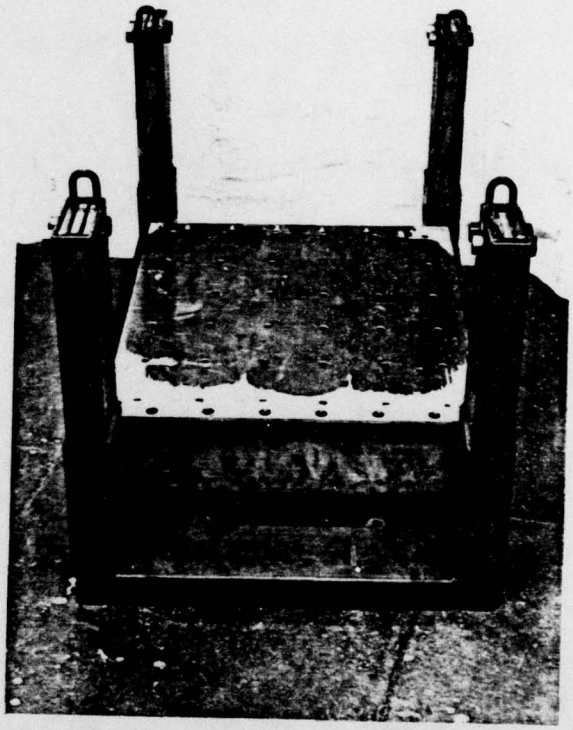

PLATE 7 - Photograph of"suspension system"

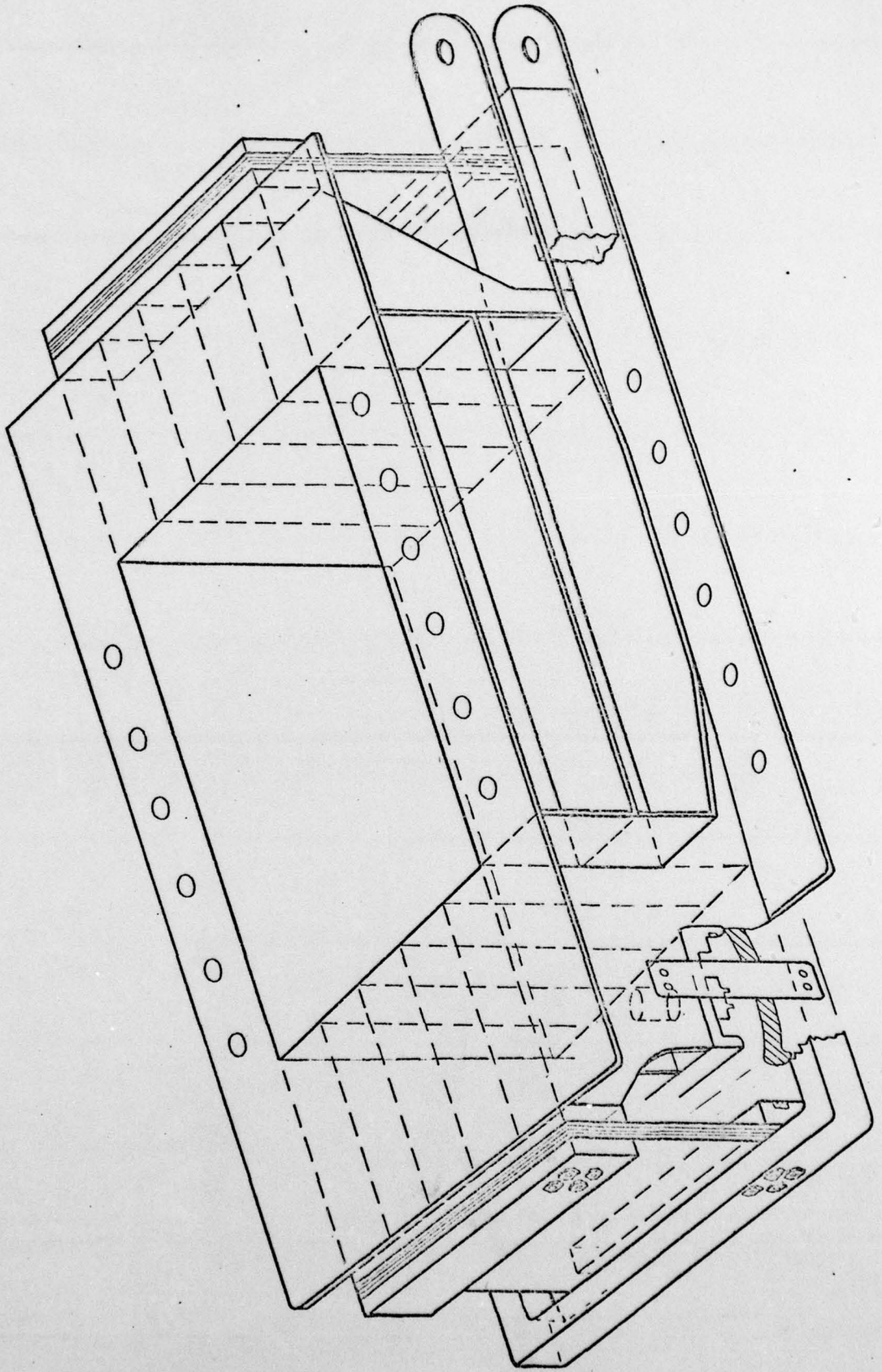

Figure 22 - Isometric sketch of soil container

crude fashion.

A detail drawing of the catch mechanism is shown in Figure 23. Above the catch itself were five minature jacks 7/. which were fed with oil from a nitrogen accumulator bottle mounted on the box, via a solenoid operated hydraulic valve. Just prior to running a test the accumulator was charged with high pressure nitrogen.

The whole system was then spun up in the centrifuge in this "energised" position. At the predetermined centrifugal acceleration the solenoid valve was electrically actuated, allowing oil under nitrogen pressure to flow via a manifold to the five minature jacks, which pushed the catch "over-centre". The catch pieces would "snap through" and fall with considerable velocity into the collecting tray underneath. The reaction mass and the deflected leaf springs would be released, to vibrate as intended.

This method (and in particular the action of the solenoid valve) has functioned reliably under centrifugal accelerations of up to 80 g. The whole apparatus, and its design, is described in greater detail in Appendix I. The mass of the entire apparatus was about 380 kg, so that with a full soil payload of 120 kg, the total centrifuge loading was 50 tonnes force at 100 g.

7.5 DYNAMIC MOTION

After being "triggered", the entire system oscillated at the characteristic frequency of 61 Hz. The maximum package acceleration of 20 g corresponded to a motion of the container of 1.3 mm, and a motion in "anti-phase" of the inertia mass

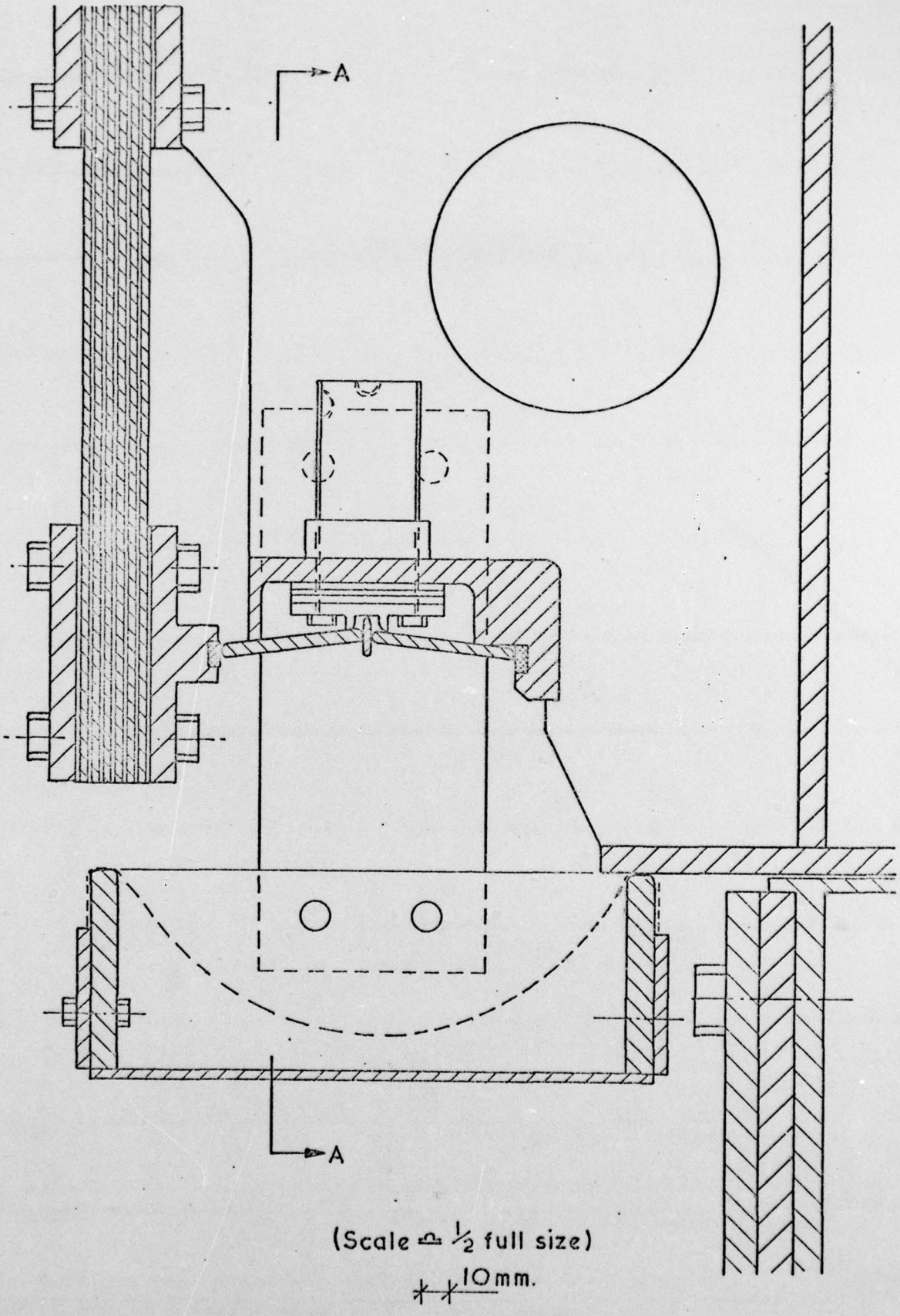

Figure 23 - Detail of catch mechanism

of 5 mm.

It was considered reasonable to assume that the soil in the container moved uniformly with the container itself. This was indicated theoretically as the wavelength of shear waves in the soil at this frequency was very much longer than the dimensions of the soil sample, and consequently the soil would be expected to move uniformly and in phase with the container (see Appendix J for a typical calculation of this kind). This assumption was subsequently verified in practice (see "Dry Embankments").

The complete path traced out by the soil container in free space also involved the motion of the underlying suspension system at its own (but much lower) natural frequency of about 9 Hz. This was a result of the position of the centre of gravity of the system not being the same before the oscillation, as after, and the overall horizontal "earthquake" motion of the soil container is sketched below :-

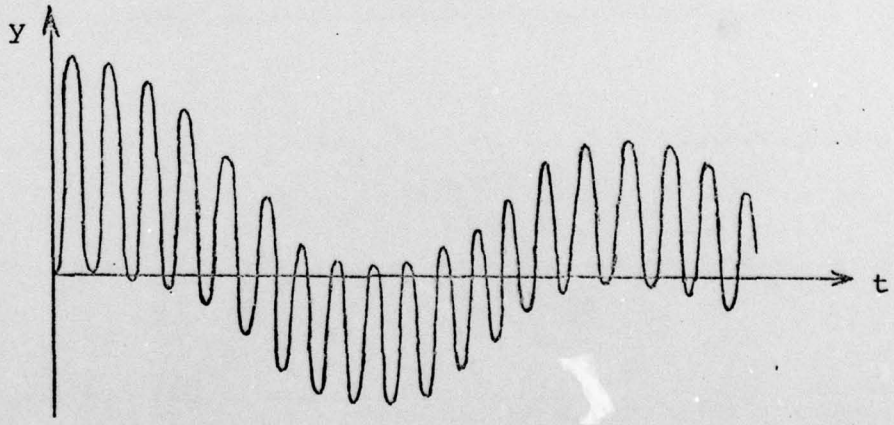

This is, of course, a graph of <u>displacement</u> against time. The <u>acceleration</u> caused by any particular component is in

proportion to the square of its frequency, so that the effect of the low frequency motion was $\left(\frac{9\ Hz}{61\ Hz}\right)^2$ or about 2% of the high frequency motion, and could be safely ignored. The accelerometers and associated electronics were in any case designed to filter out low frequencies.

The resulting lateral acceleration of the soil container (simulating the "earthquake" acceleration) was thus a sine wave decaying very slowly in an exponential fashion, as sketched below.

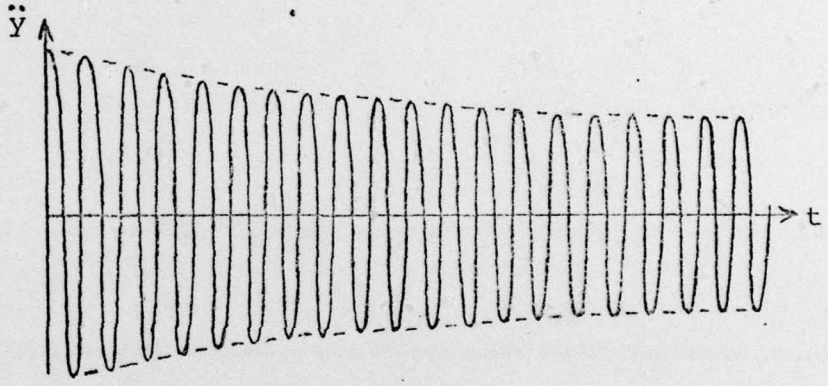

A major concern in the design of the apparatus, was that the decay be as prolonged as possible, and this was a further reason for using hardened steel for the leaf springs, as the material damping would be low. It was found in practice that the "half-life" of the decay was between 50 and 100 cycles, corresponding to a material damping of between 0.1% and 0.2% of critical damping - which was indeed very low.

A photograph of the complete apparatus is shown in Plate 8, fully assembled but not mounted on the centrifuge arm. In the foreground may be seen the high pressure nitrogen accumulator connected to the solenoid-operated valve.

Plate 9 shows the apparatus mounted on the swinging

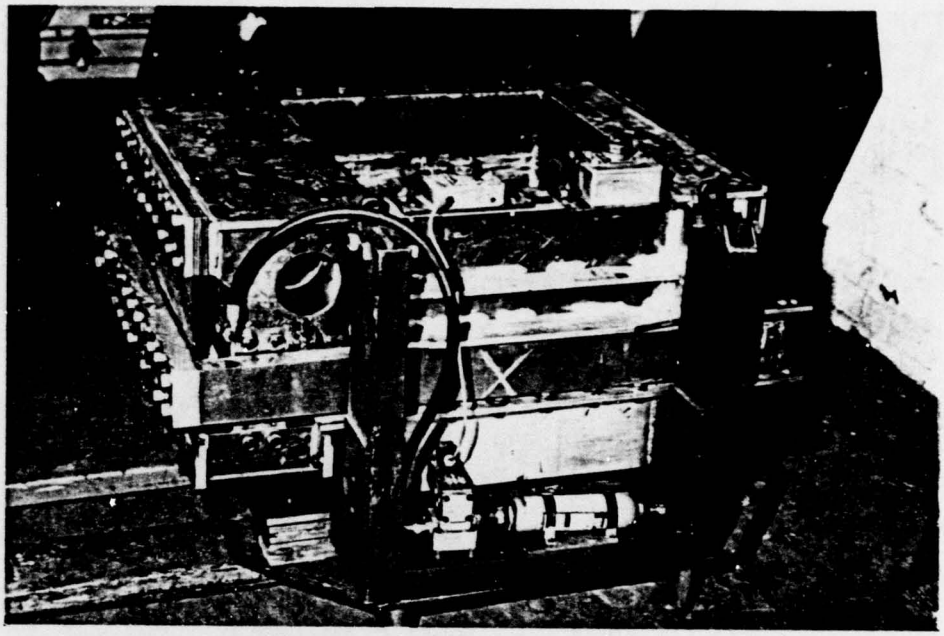

PLATE 8 - Fully assembled apparatus for modelling earthquakes

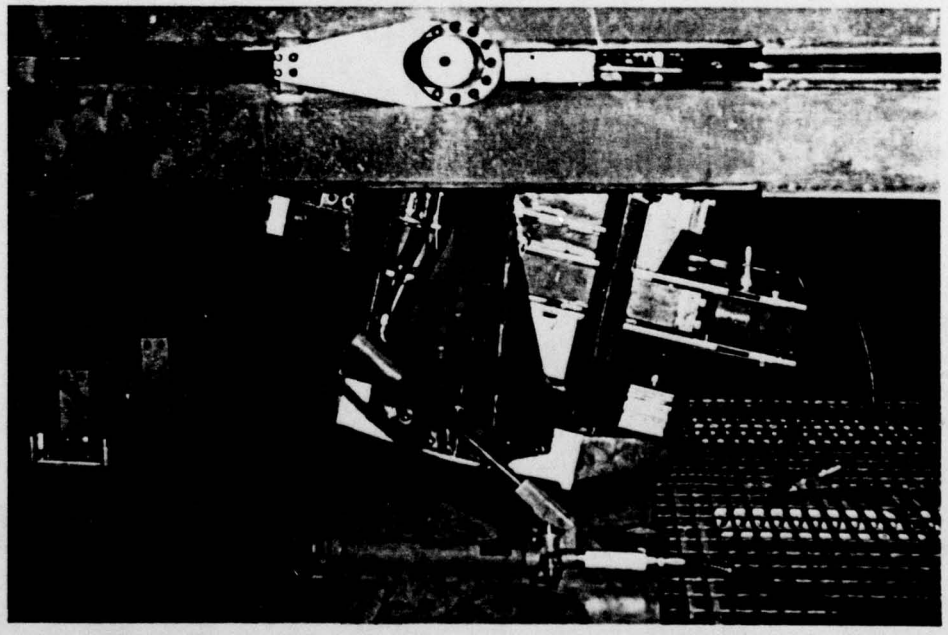

PLATE 9 - The earthquake apparatus installed on the centrifuge arm

centrifuge platform. To it is attached the temporary attachment against which the reaction mass is jacked by the portable jacks and hand pump.

7.6 SAFETY TESTING

Before the apparatus was used on the centrifuge for the first time, an exhaustive set of stressing and performance calculations were prepared. It was then tested in the laboratory. The catch loading and firing operations were performed and monitored; the apparatus jacked internally and externally to simulate centrifugal stresses, and the stiffnesses measured and compared with theoretical predictions.

It was then proof tested at full capacity on the centrifuge, in this case up to 100 g. Normal operation was subsequently restricted to 80% of this value - i.e. 80 g.

7.7 SOIL CONTAINER BOUNDARY CONDITIONS

In modelling of any kind, whether on the centrifuge, computer modelling, or at 1 g, proper attention must be paid to the boundary conditions. In dynamic experiments of the type described in this thesis, the soil mass is conventionally idealised as an infinite horizontal stratum of material.

At present the soil container consists simply of a box with rigid walls, and no special attempt has been made to model this idealisation. It is possible to imagine a side wall constructed to deform "just as the soil does". However, it would be a major undertaking, as such a wall would be required to deform dynamically with the soil and simultaneously withstand

changing lateral soil pressures without significant movement.

A simpler but less efficient way of modelling such an infinite stratum would be to keep the "aspect ratio" of the soil sample very low, so that the sample is flat enough that the presence of end effects is unimportant. This would unfortunately require a very large container.

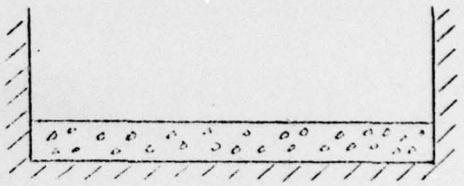

It is doubtful however, whether such sophistication would be justified with this apparatus, as the dimensions of the box are not large enough that any non-uniform dynamic deformations of the soil will take place at the frequencies involved, and the soil will move more or less as a rigid body, with or without such precautions. This is demonstrated in Appendix J. Furthermore, any real prototype will have its own peculiar boundary conditions in real life, and it is these that must be modelled correctly if model tests are to be valid.

Considering an embankment founded on rock, for instance, the boundary conditions will be correctly modelled if it is constructed free-standing on the bottom of the container, as sketched. This is the condition chosen for all the embankment tests reported in this thesis, and sand was glued onto the container bottom to ensure full frictional soil contact.

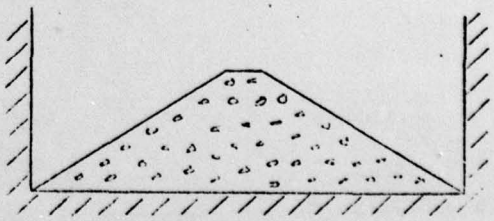

Similarly, the rocking behaviour of a tall structure results

in only localised deformation under the foundation, and it has been shown in Section 4.2 that the presence of a rigid stratum is unimportant if it is at a depth of more than two base diameters. Thus merely providing an adequate volume of soil underneath the foundation would be sufficient to model the behaviour correctly.

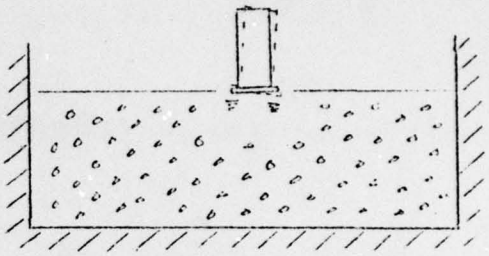

All the experiments conducted with this apparatus fall into one of these two categories, and it is believed that the measures outlined were adequate at the model frequencies used. At higher frequencies additional precautions might have to be taken if the box dimensions became comparable to the wavelength of shear waves in the soil. However all these problems are best dealt with on an "ad hoc" basis, and in practice an adequate approximation to reality can usually be made.

7.8 INSTRUMENTATION

Two types of transducers were used - minature accelerometers (referred to previously) and minature pore water pressure transducers. Both of these were very small, with a volume of less than 1 cc. The pore pressure transducers were already waterproofed, and on the occasions when it was necessary to waterproof the accelerometers (for embedment in saturated material for instance), this was done by smearing them - and most particularly the screw-on connectors - with silicone jelly glue. A photograph of one of each of these is shown in Plate 10.

The pore pressure transducers were of the diaphragm type,

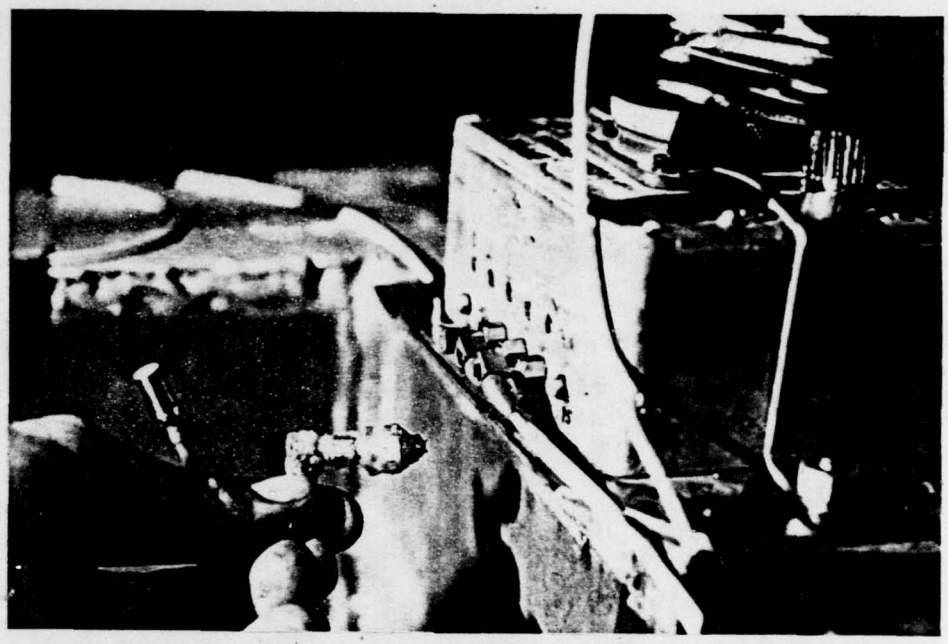

PLATE 10 - A miniature accelerometer and pore pressure transducer

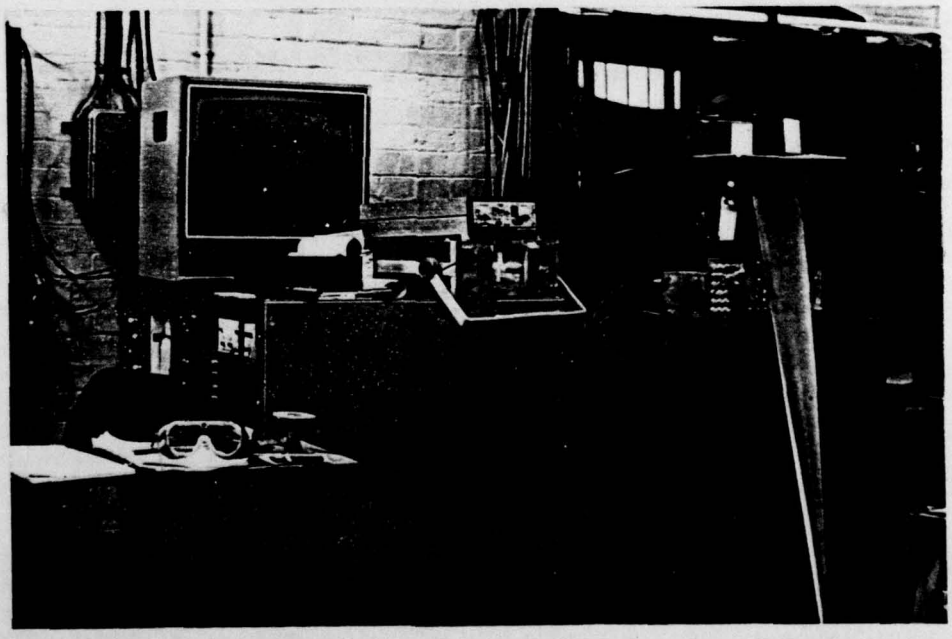

PLATE 11 - The centrifuge signal console and recording equipment

purchased commercially, and employed a semi-conductor strain gauge bridge diffused into the rear of a silicon diaphragm of high stiffness. When properly de-aired the frequency response appeared to be extremely high - the rate of increase of pressure that could be measured with the standard porous stone was at least 10^{10} $Pa.s^{-1}$ - and their sensitivity to acceleration was low - at any rate if they were aligned so that such accelerations lay in the plane of the diaphragm. These transducers required a power supply, and this was provided from the junction box shown in Plate 10, via a 5-pin lockable DIN plug which also connected the output leads to the junction box.

The accelerometers were of the piezo-electric type and needed no power supply. However, the output current capacity was effectively zero, as these devices essentially produce a pure charge, and their output had to be taken via low-capacitance screened leads to special amplifiers immediately inside the junction box, before the signals could be passed very far.

The junction box was connected via a multipin connector to the electrical slip rings, and each channel eventually terminated outside the centrifuge, in sockets at the back of the console, shown in Plate 11.

It was necessary to use balanced signal lines in order to minimise electrical interference (particularly from the centrifuge motor). The soldered connectors and wires inside the junction box, and most particularly the amplifier circuitry inside, were not protected in any particular way against the effects of high acceleration, and survived continuous running up to 100 g - although there had originally been plans to embed the electronic components in a supporting medium. From the

console, it was possible to supply power as required, and to record the output of each channel.

Initially each channel was recorded directly on a multi-channel ultra-violet recording oscillograph, via intermediate current amplifiers, and this produced simultaneous signal traces on light-sensitized paper. This system worked satisfactorily, but it was necessary to make a fairly accurate estimation of the expected output levels in the course of a test, in order to avoid either exceeding the available range of the oscillograph or producing insufficient deflection.

Later, however, a multi-channel frequency-modulated tape recorder was acquired, and this enabled the recording of many more simultaneous channels, which could then be replayed at leisure at different speeds and output levels on the recording oscillograph to produce a suitable visual trace. In principle it would also be possible subsequently to digitise each signal for computer analysis, but in this case there was no reason to do so.

It was also possible to pass each signal through one or two steps of electronic integration, via specially built electronic circuitry. Originally this was motivated by a desire to convert acceleration traces into displacement traces,which were thought to be more "useful". In fact, there was little advantage in this respect, except that integration of an alternating signal acted as a useful low pass filter to remove high-frequency "ringing", as such integration is equivalent to a gain inversely proportional to frequency. All circuitry was a.c.-coupled to prevent integration of any d.c. signal components building up indefinitely and saturating the electronic equipment.

Excessive integration of signals results in an over-emphasis of low-frequency signals, and, in general, the best compromise was found to be a velocity trace. This is, in fact, true for most dynamic work, as it can be shown that the magnitude of a velocity signal is independent of frequency for a wave spectrum of uniform energy.

Calibration of the transducers and of the entire associated electronic circuitry was carried out most satisfactorily all together "in situ" by recording the output to a known stimulus directly onto the oscillograph paper. The accelerometers could be attached to a very simple device that gave an acceleration of precisely 1 g at the electrical mains frequency of 50 Hz, and the pore pressure transducers could be calibrated by moving them up and down through a known distance in a measuring cylinder of water, and this could be subsequently checked by measuring the rise of the static water pressure as the centrifuge spun up to speed.

Ultimately all measurements were recorded on ultra-violet recording paper. The ultra-violet traces were "developed" by exposing the paper to light, although it had to be treated with care as exposure to direct sunlight, or premature exposure, was liable to result in complete loss of contrast. Up to about five traces could be comfortably accommodated, side-by-side, on one roll of paper, and exposed rolls could be stored effectively in light-proof boxes - although traces start to fade of their own accord over the course of a year or two.

All tests were monitored visually with the closed circuit television camera mounted on the centre of the centrifuge. A video tape recorder allowed all events to be recorded for subsequent playback, either at normal speed or in slow motion, and still pictures could be taken of single frames.

Detailed specifications of the transducers and the electronics are given in Appendix D.

CHAPTER 8

INTRODUCTION TO EARTHQUAKE EXPERIMENTS

Two distinct classes of experiments were performed with the "earthquake" apparatus.

The response of model towers on a sand foundation was investigated first. This is, perhaps, not such a serious problem as the stability of embankments, but was considered more appropriate for initial tests, as the modelling requirements were relatively straightforward.

Secondly, the behaviour of model embankments subjected to earthquakes was studied. This is a problem of great practical importance, but fraught with difficulties both in current analytic treatment and in performing precise centrifuge tests. Consequently, the intent was to demonstrate in the first instance that centrifugal modelling of this problem was possible, and that the results agreed at least qualitatively with what is believed to occur in the field.

Both of these test series were performed, firstly with dry coarse sand, and then with saturated fine sand, and are discussed in turn.

CHAPTER 9

ROCKING TOWERS ON DRY SAND

9.1 INTRODUCTION

These tests were conducted in a similar fashion to the rocking tower tests described earlier. Two towers were placed on a sand base, that had previously been deposited in vibrated layers to ensure reasonable uniformity. The motion of the towers was monitored by miniature accelerometers screwed into their tops. The only purpose of using two towers simultaneously was simply to produce two sets of output from each test.

A picture of the towers is shown in Plate 12. Accelerometer outputs were led by flexible coaxial leads to the amplifier box. Steel plates could be bolted onto the towers to increase their moment of inertia, and bases of different diameters could be screwed on. Sand was glued onto the bottom of the bases to ensure full friction between the base and the foundation.

Originally cylindrical towers of the types used for the preliminary tests were used, but these were seen on the T.V. monitor to undergo a permanent "twisting" - always in the same direction during the earthquake.

Such a tower rocking parallel to the axis of rotation of the centrifuge will generate a second order twisting force, as

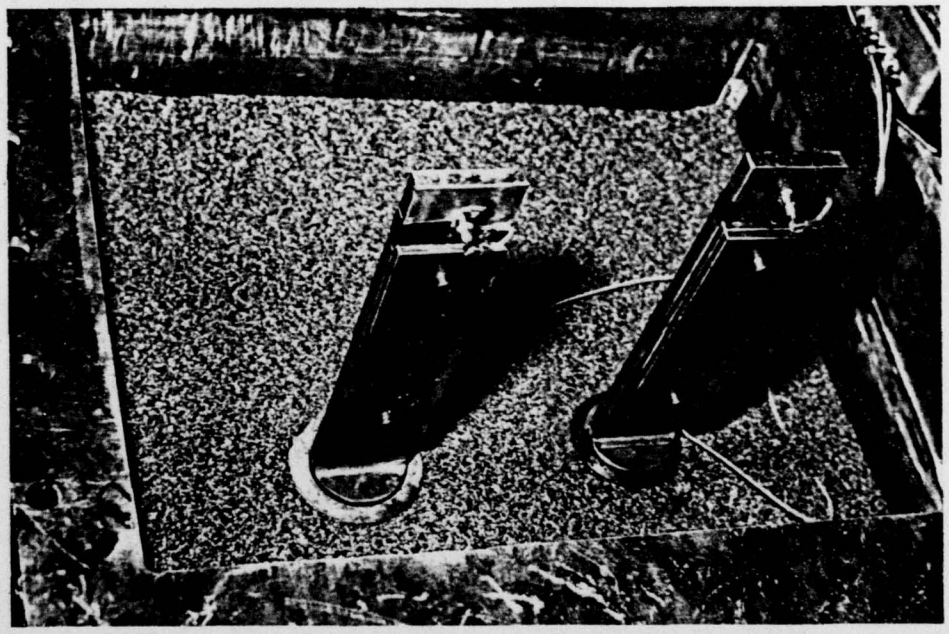

PLATE 12 - Towers on dry sand in the earthquake apparatus

a result of Coriolis acceleration on elements off the axis of the tower. This is analysed in Appendix B, which indicates that the effect should be small, and should only produce an oscillatory torque. It is not clear why there was a large unidirectional rotation, but the effect was eliminated by redesigning the towers so that they were thin and rectangular, as sketched, and by glueing sand to the bottom of the detachable bases, so that full frictional contact was ensured between the soil and the foundation.

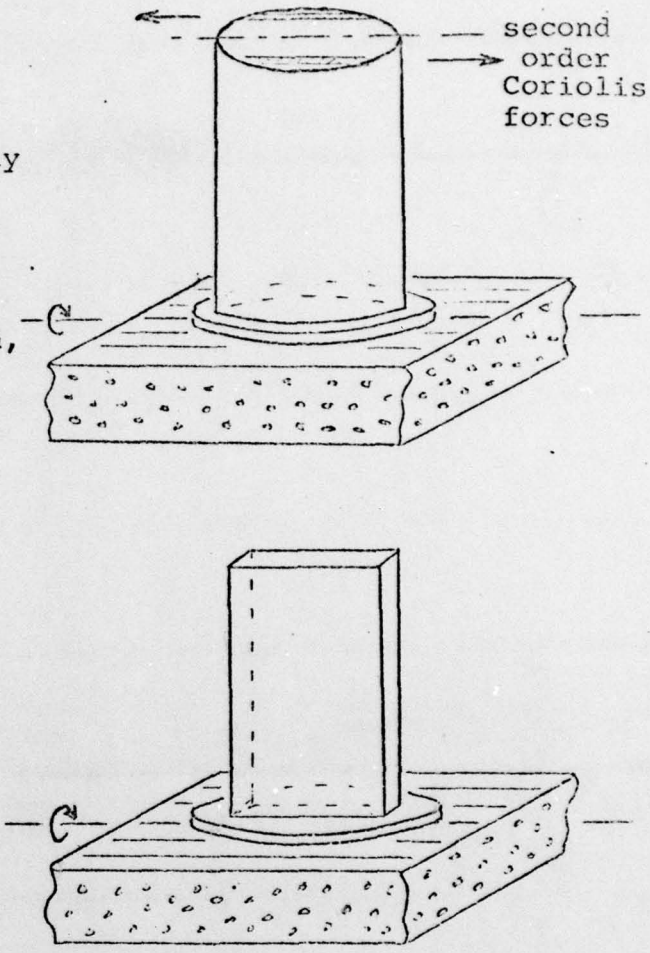

9.2 EARTHQUAKE RESONANCE

The object of the experiment was to try to detect any resonance of the tower-foundation system in response to earthquake motion of the foundation, and generally to see if the motion conformed with what would be expected from simple dynamic theory.

Figure 24 shows the actual record of such an experiment. The top trace shows the motion of the container (assumed to be the motion of the ground), and the next two traces show the motion of the top of two towers. Now the wind-induced motion of these towers was recorded, just prior to the earth-

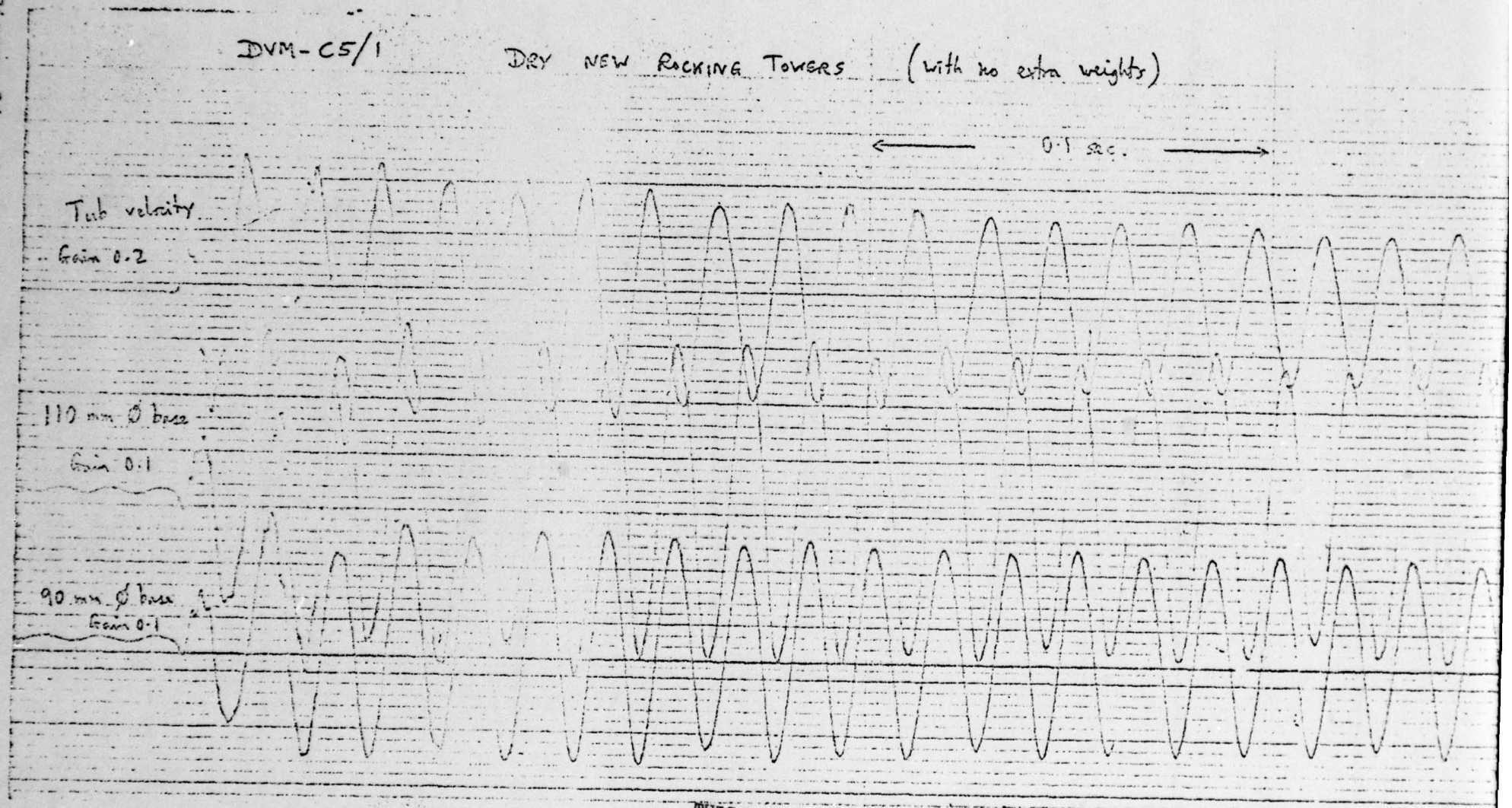

Figure 24 - Earthquake record of rocking towers on dry sand

quake, and their natural frequencies were measured as 77 and 73 Hz respectively, which was higher than the earthquake frequency of 60 Hz, although any strain-softening would tend to reduce the tower natural frequency, bringing it closer to the earthquake frequency.

The amplitude of the centre trace is larger than the lower one, even though it represents the tower apparently further from the resonant condition. The amplitude of motion depends not only on how close a particular tower is to resonance, but also on the magnitude of damping - which is not known, and will vary from towers of different mass and base diameter. Thus, it is not very productive to try and gauge whether or not a tower is close to resonance, by considering the amplitude of motion, and it would appear more promising to concentrate on measuring the phase relationship of the tower motion with the ground.

It is initially not necessary to go into the dynamic equations in any depth. One can simply note that a structure with a natural frequency well above the earthquake frequency should behave in a "stiff" fashion, and move in-phase with the earthquake movement - while a structure with a natural frequency substantially below the earthquake frequency should be relatively "isolated" from the earthquake, moving out-of-phase with it. Intermediate structures will show a phase lag of

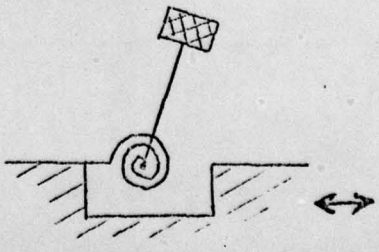

between 0^{o} and 180^{o}, while a structure at resonance will show a phase lag of around 90^{o} - largely independent of the value of damping.

On this basis, therefore, the towers in Figure 24 (which appear to be slightly above resonance) should show a phase lag of less than 90^{o}. However, both towers appear to show a phase lag of much more - about 135^{o}. Similar experiments were performed and this unexplained result persisted.

9.3 ABOVE AND BELOW RESONANCE

In order to resolve the problem, two very different towers were constructed - designed to have natural frequencies substantially above and below the earthquake frequency respectively, so that the behaviour of each tower would "bracket" the resonant condition.

Figure 25 shows the wind-induced oscillation of these two towers, just before an earthquake at 60 Hz, and their natural frequencies were measured as 150 Hz. and 48 Hz..Figure 26 shows the behaviour of towers at the beginning of such a model earthquake. Normally one would expect the tower with a high natural frequency to move in-phase with the earthquake, and the tower with a low natural frequency to move out-of-phase with the earthquake. However, the record shows that <u>both</u> towers moved initially out-of-phase with the ground motion (or at any rate with a phase lag of about 170^{o}). This would be expected for the "low frequency" tower, but not the "high frequency" one.

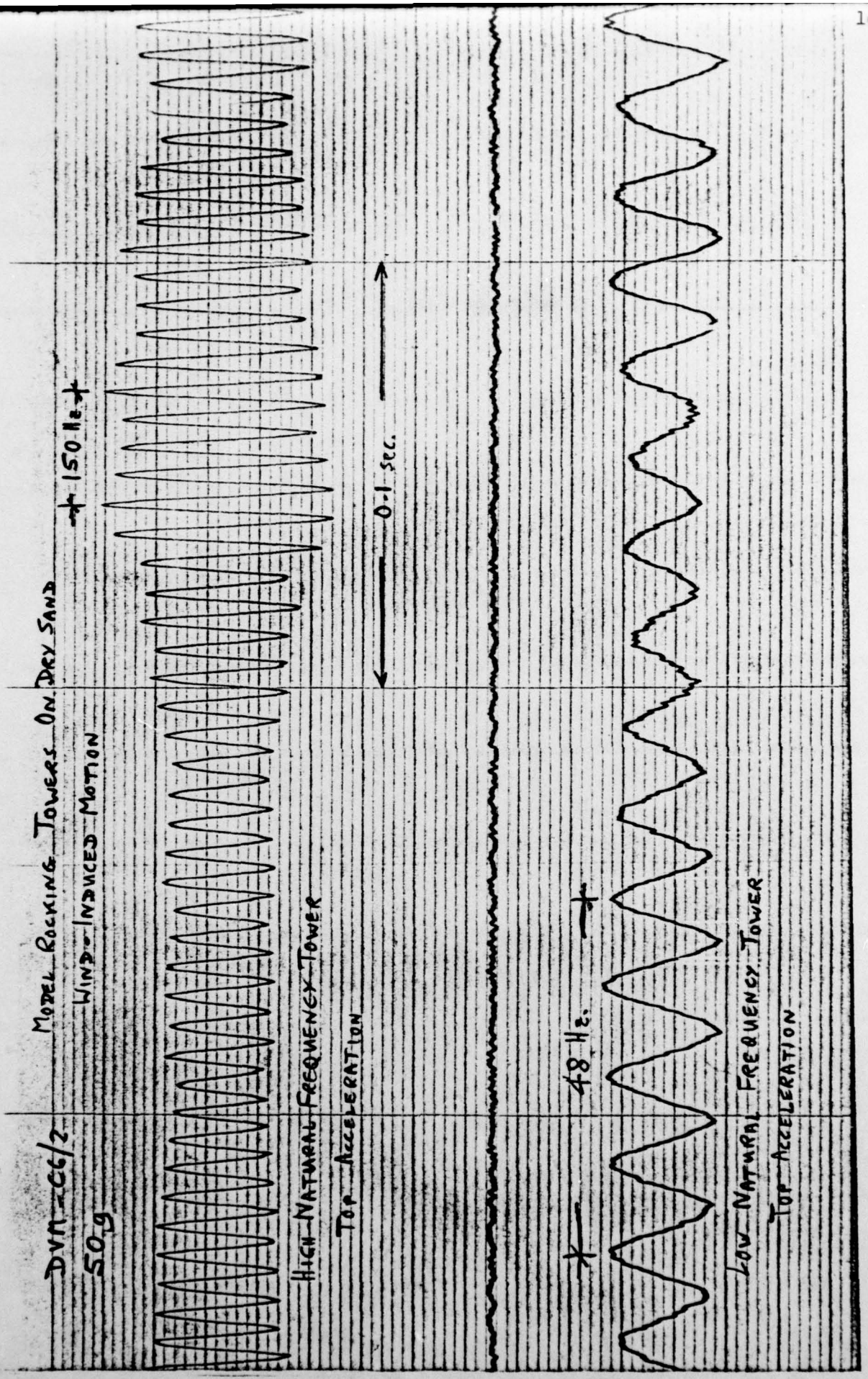

Figure 25 - Wind-induced oscillations of towers above and below resonance

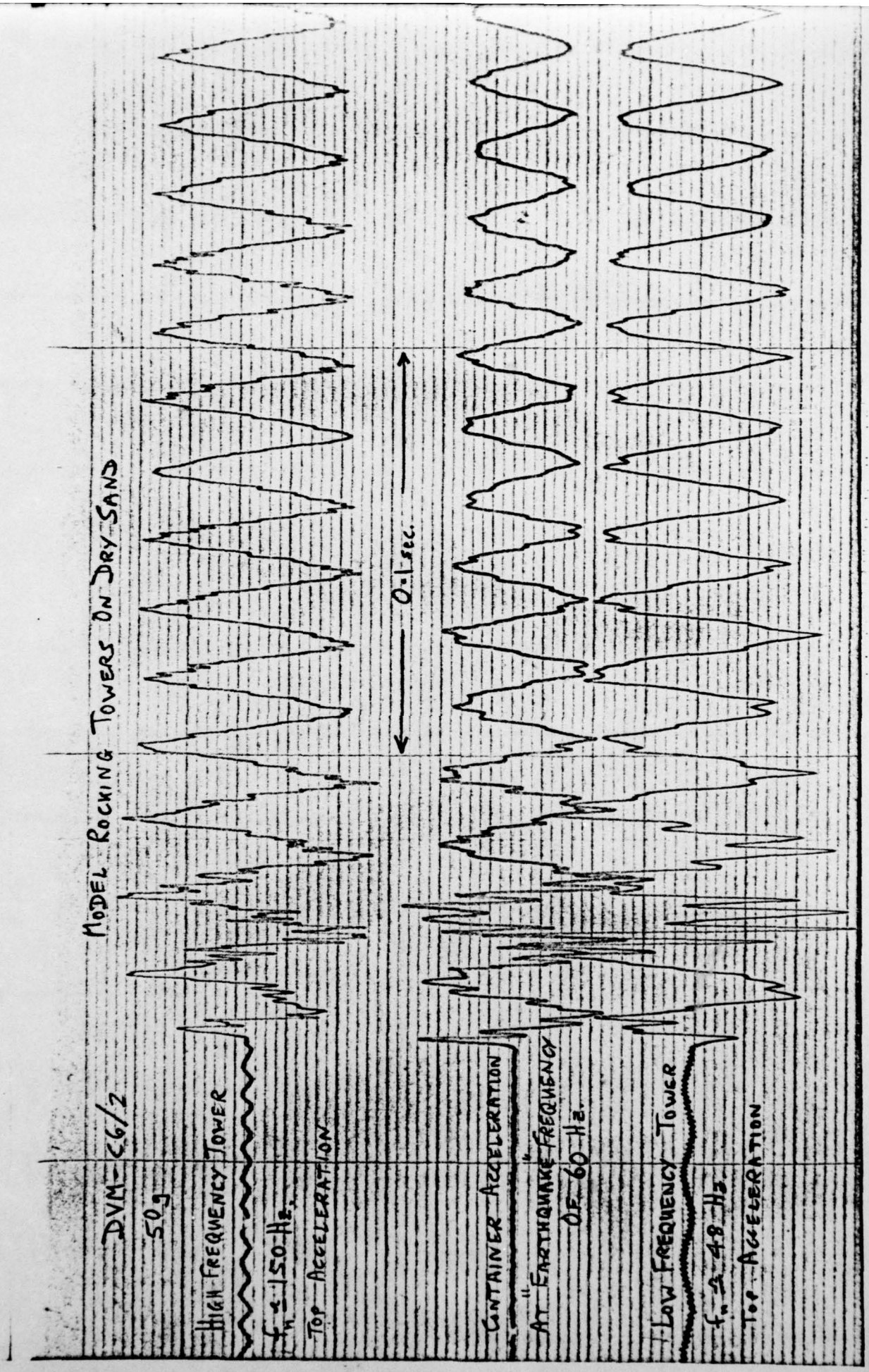

Figure 26 - Earthquake record of towers above and below resonance - original

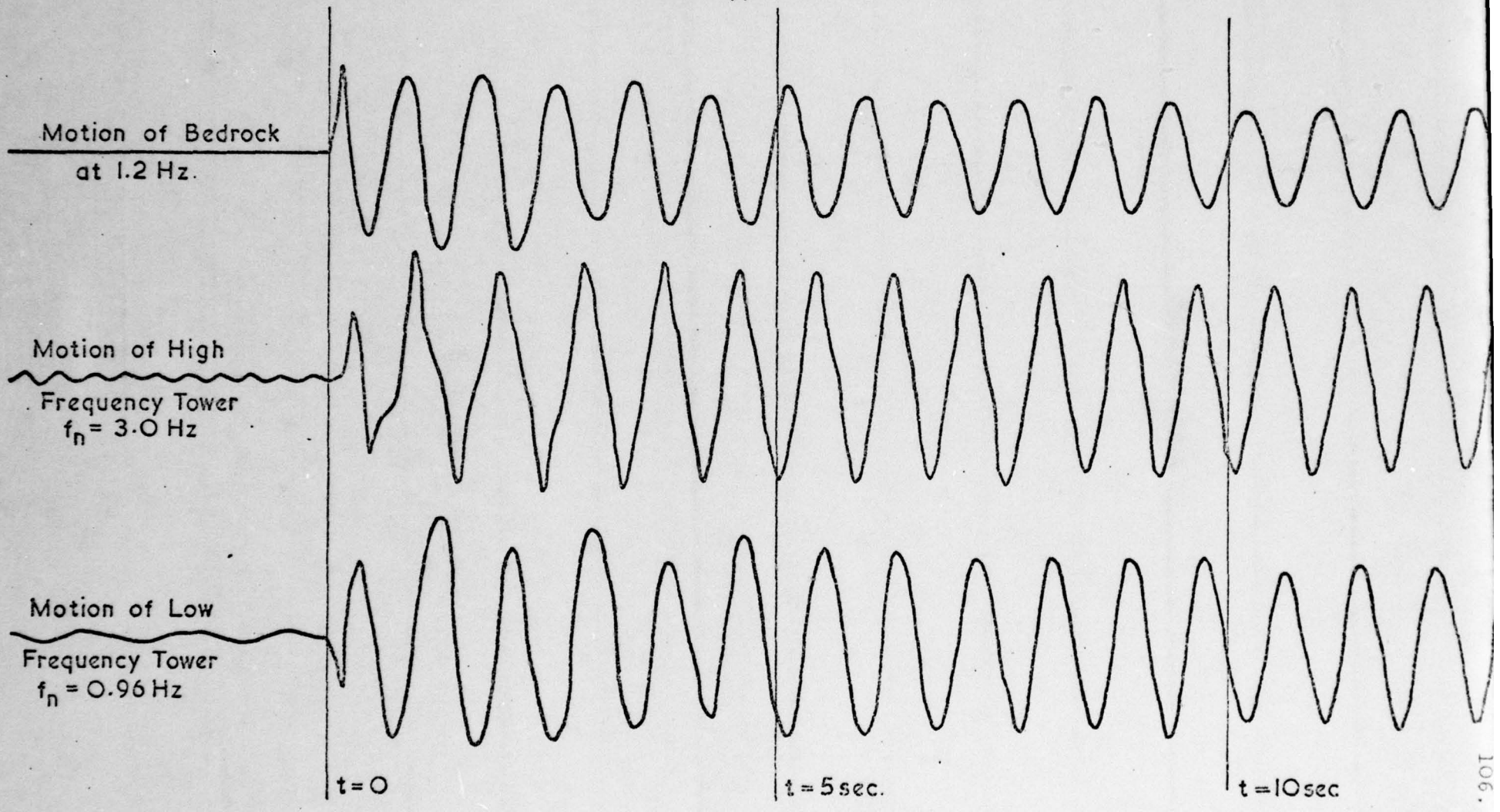

Figure 27 - Earthquake record of towers above and below resonance - traced and converted to full-scale

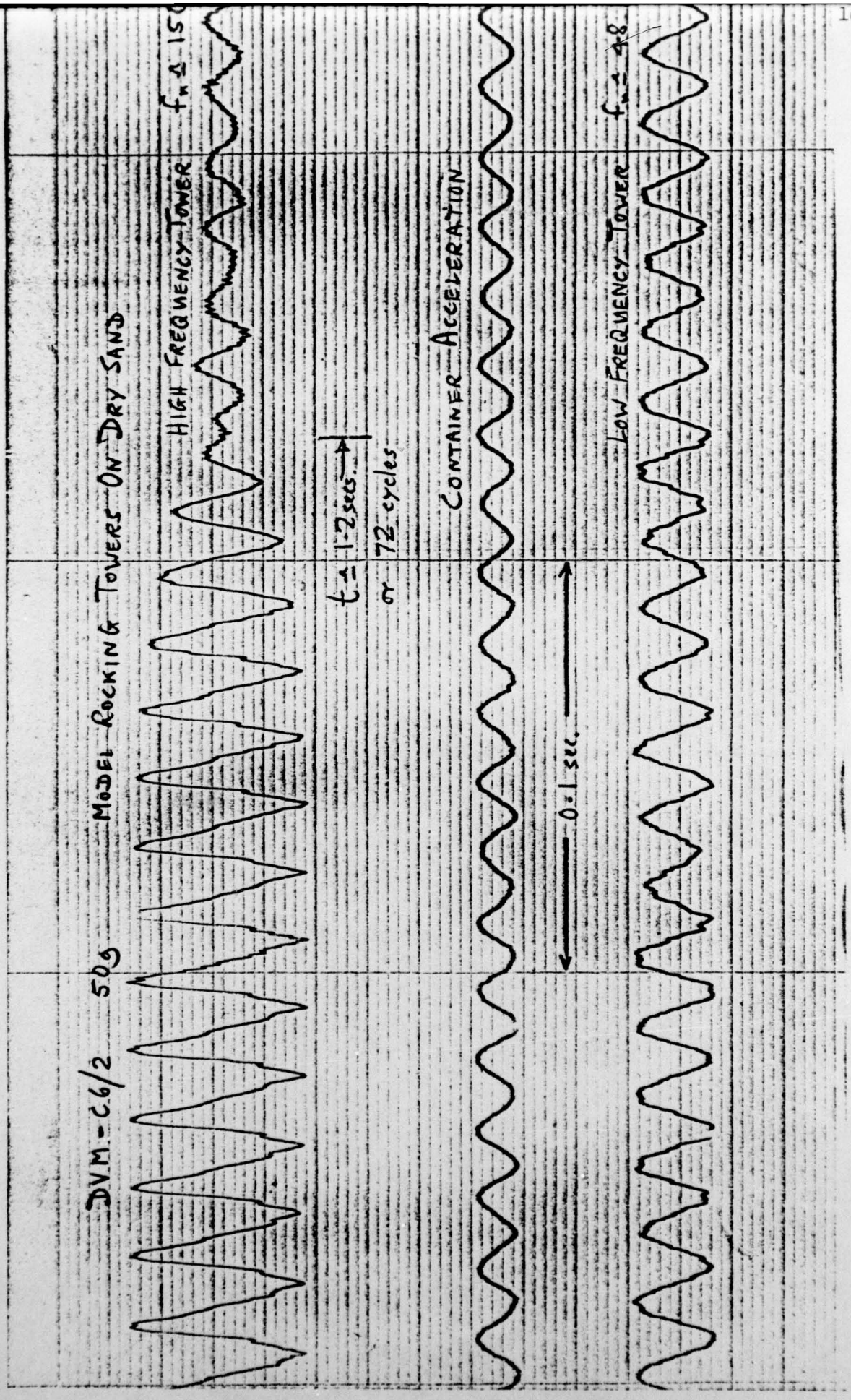

Figure 28 - Last portion of the earthquake record of towers above and below resonance

Fig. 27 shows the same record, but traced to give a fair copy, and with all values converted into prototype values.

Close examination of the entire record, however, shows that towards the end of the earthquake motion (after about 70 cycles) the phase lag of the "high frequency" tower gradually decreased, until becoming almost in-phase with the earthquake motion, shortly before cessation of motion, while the "low-frequency" tower continued to move with a phase lag of about 170^{o} as expected. This is shown in Fig. 28.

Similar behaviour also seemed to occur for the towers in Figure 24 at the very end of the record (not shown).

It appears, therefore, that after many cycles of movement, the phase behaviour of these towers corresponds more closely to what elementary theory predicts - although not for the initial part of the earthquake. It is not obvious why this should be so.

It is unlikely to be simply the initial response of the dynamic system to such a perturbation (i.e. that part of the theoretical solution usually referred to as the "complementary function") as this would be associated with the natural frequency of the appropriate tower-foundation system, which in the case of the "high-frequency" tower would be almost three times the earthquake frequency, and there is no sign of this. Additionally any initial response would die out within 5 to 10 cycles.

It is also unlikely to be due to very large dynamic damping resulting from the large foundation movement, as this would tend, in all cases, to reduce the expected dynamic phase lag - whereas in Figure 26 the "high frequency" tower had a very much greater phase lag than expected.

A possible explanation is that the strain-softening taking place under the base of a tower is so great, that a foundation that may initially be "above resonance", in fact softens to become "below resonance" during the majority of the earthquake - until the end, when it hardens to become "above resonance" again. This would explain the observed behaviour qualitatively, although it would require (in the case of the "high frequency" tower in Figure 26) a drop in frequency by a factor of 3, corresponding to a drop in stiffness by a factor of 9, and it is difficult to visualise strain-softening of this magnitude taking place.

Figure 28 also shows an interesting phenomenon that has been noticed in many tests on rocking towers, both wet and dry. During the course of the earthquake, a tower would continue to rock at a relatively uniform magnitude for a long time, until all of a sudden it would stop oscillating, within a few cycles. Normally, one would expect this motion to decay gradually, roughly in proportion to the earthquake motion, but this appears not to be the case. No immediate explanation of this curious phenomenon is known.

9.4 CONCLUSION

At present, this portion of the experimental work can only be concluded by saying that the response of a structure-foundation system to a model earthquake appears to be very much more complex than was at first supposed.

Tests attempting to detect the resonant behaviour of towers by monitoring the phase difference between the motion of the tower top and the earthquake, failed to show the expected phase lag of

around 90°, even though measurements of small-amplitude wind-induced oscillations indicated that the tower natural frequencies were close to the earthquake frequency. Even a tower that clearly had a natural frequency well above the earthquake frequency moved out of phase with the earthquake motion.

In general, all the towers, irrespective of whether they were above or below resonance, appeared to move out of phase with the earthquake motion, until the very end of the earthquake record, when, after 50 or more cycles, their behaviour reverted to what would be expected from dynamic theory.

Short of assuming an inordinate amount of strain softening, it must be assumed at present that the behaviour of such a soil structure system in response to an earthquake seems to be highly non-linear and is not adequately described by a simple dynamic model. This may be because the amplitudes of strain for these experiments were very much larger than in the previous experiments on wind-induced oscillations, and, as a result, much more plastic soil deformation took place. Further investigation is required if a proper understanding of this problem is to be reached.

CHAPTER 10

TOWERS "FALLING OVER"

10.1 INTRODUCTION

In many cases of practical foundation design, it may be difficult by conventional means to demomstrate satisfactorily that a particular structure will not simply "fall over" in an earthquake. This is particularly so for relatively stiff structures, where a "quasi-static" analysis is normally considered justified.

Clearly structures that are deliberately designed to be very flexible, are able in large measure to "isolate" themselves from ground motion in an earthquake, and a "quasi-static" analysis is inadequate to describe their behaviour. However many structures are relatively stiff, and are designed with sufficient lateral stiffening and strength to withstand the earthquake forces.

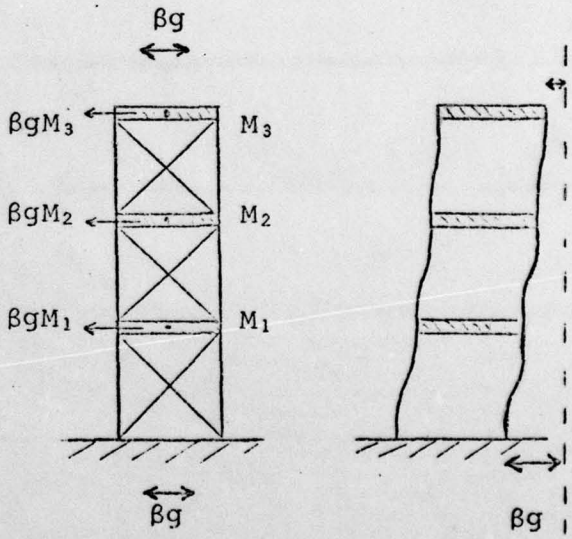

Stiff structure Flexible structure

If such a structure is sufficiently stiff that the intrinsic natural frequency is greater than the earthquake frequency, then it is reasonable to compute forces in the structure itself by a

"quasi-static" analysis, as sketched - i.e. by assuming that the entire structure moves in phase with and with the same amplitude as the horizontal ground motion, and inserting appropriate horizontal forces at the centres of mass.

Unfortunately, such an analysis often implies that the entire structure will fall over (particularly structures with raft or pad foundations) unless further work is undertaken - such as the installation of tension piles to combat uplift forces.

Common sense indicates that such structures are unlikely to fall over in practice, and some centrifuge tests were carried out to demonstrate this.

10.2 EXPERIMENTS

These tests used the same towers pictured in Plate 10, with relatively small base dimensions, and simply subjected them to the largest earthquake that the apparatus could produce.

Considering such a tower, of height 300mm and with a 70 mm diameter base affixed to it, a "quasi static" analysis would indicate that the tower would tip over at a horizontal acceleration equal to $\frac{70}{300}$ of vertical acceleration, or a "23% earthquake".

This tower was placed in the centrifuge, on a sand foundation at 20 g, and subjected to the lateral "earthquake"

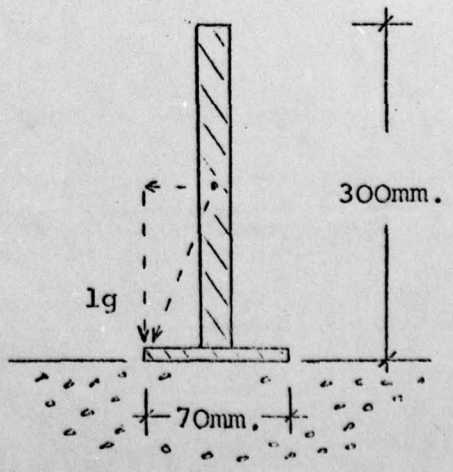

acceleration shown on the upper trace in Figure 29. On the basis of the quasi-static analysis, the tower should have fallen over if the lateral acceleration exceeded 4.7 g, although in practice it remained upright throughout the whole test. In this case, the acceleration record was "unsmoothed" in order to reveal transient peaks in the acceleration, in addition to the underlying 60 Hz motion - the "quasi-static" method makes no distinction between accelerations at different frequencies, so this seems reasonable - and the peak lateral acceleration shown is as high as 32 g (corresponding to a " 160 % earthquake "), or about seven times the acceleration predicted to cause "falling over". Even if the transient peaks are ignored, the maximum "smoothed" value is about 20 g (a "100 % earthquake"), which is still about four times the predicted critical value.

A total of four such tests were conducted, and in each case the values of lateral acceleration predicted to cause "tipping over" are marked on the traces in Figure 29. In each case, lateral accelerations of several times this value failed to cause any noticeable movement.

It is clear, therefore, that"quasi-static" analyses are inappropriate in this respect, and that real structures are, in fact, much less likely to fall over than would be supposed by using this method.

Intuitively this must be because the earthquake motion takes place "too fast" for a tower actually "to have the time to fall over".

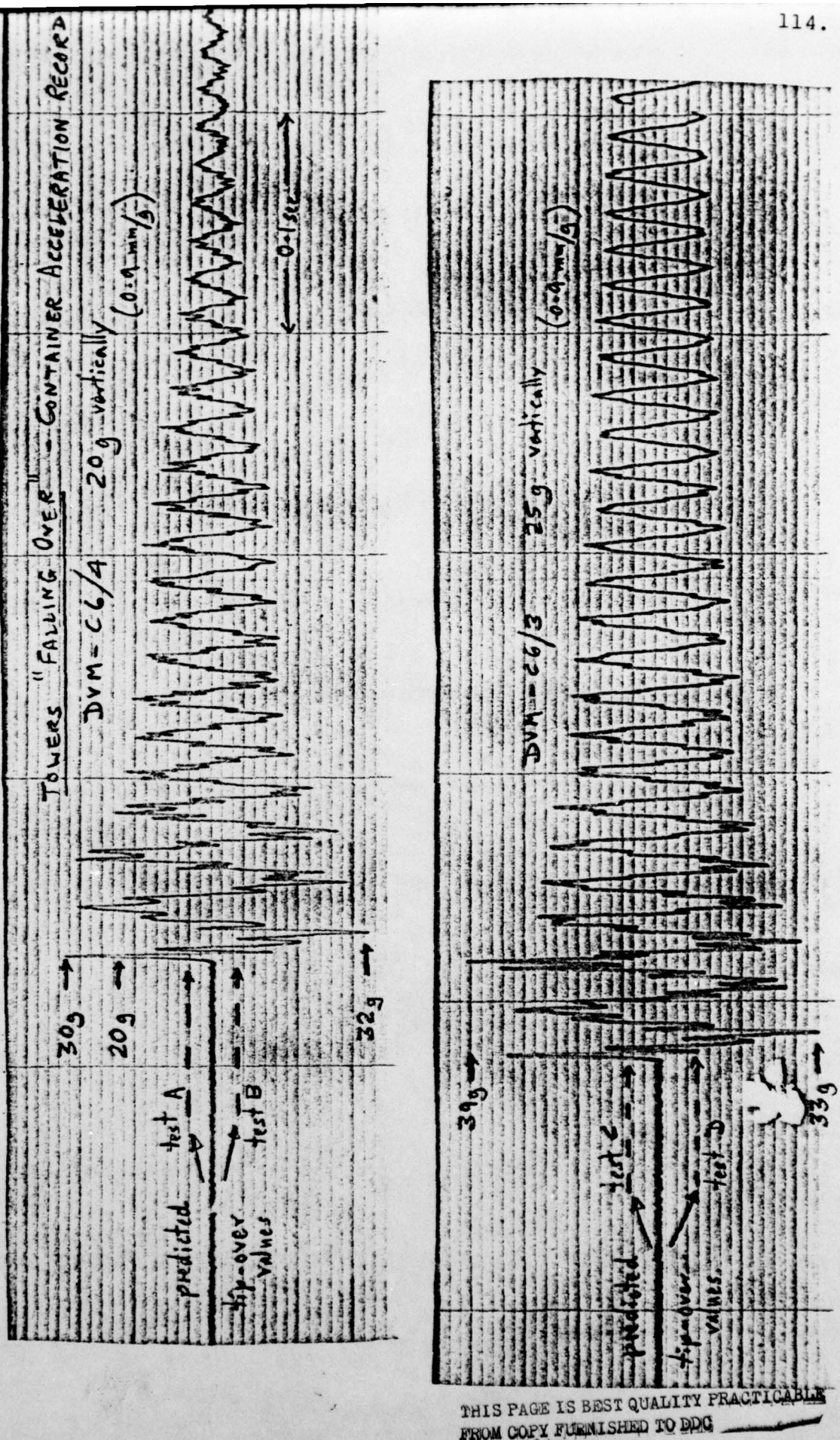

Figure 29 - Earthquake records, trying to tip towers over

10.3 ANALYSIS

It is possible to produce some simple theory to analyse this effect. Consider a tower of uniform vertical cross-section, of height h and with a base diameter d. It will start to tip up when the equivalent earthquake acceleration βg, exceeds the critical value of $\beta_o g$ (where $\beta_o = \frac{d}{h}$).

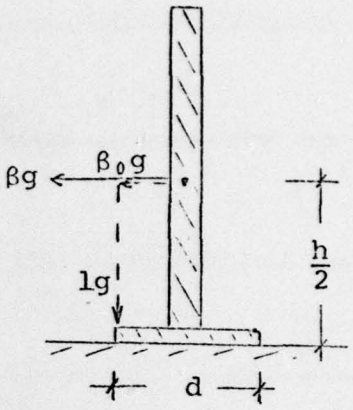

Taking moments about the corner of the base about which tipping will take place, $I(\frac{d^2\theta}{dt^2}) = (\beta g - \beta_o g)\ \frac{Mh}{2}$, where θ is the angular rotation of the tower about its edge, M is its mass (assumed to be concentrated at its midpoint), and I is its moment of inertia about its edge - which in this case can be assumed to be approximately $\frac{Mh^2}{3}$. This then gives

$$\frac{d^2\theta}{dt^2} = (\beta - \beta_o)\ \frac{3g}{2h} \qquad (10)$$

Now, if the shape of the earthquake motion is assumed to be a square wave, then for a half-cycle, integrating twice between t=0 and $t = \frac{1}{2f}$, which corresponds roughly to the integral of the shaded area in the neighbouring sketch (where f is the frequency of the waveform) gives

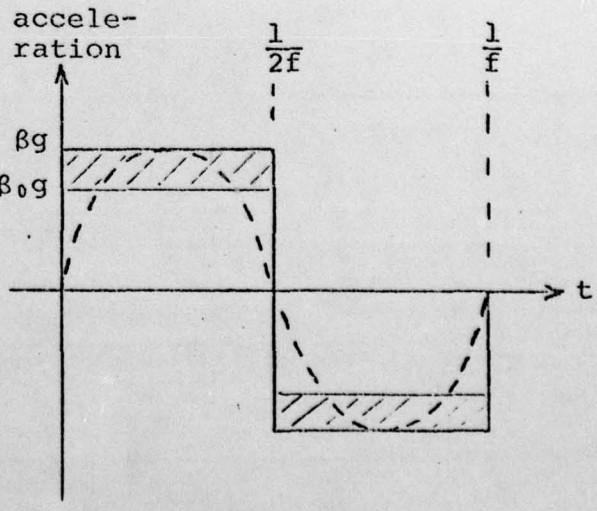

$$\theta = (\beta-\beta_o)\left(\frac{3g}{2h}\right) \tfrac{1}{2} \left(\frac{1}{2f}\right)^2 \qquad (11)$$

This represents the angle through which the tower will tilt, after a single half-cycle of square wave acceleration βg .

In fact, on average, the first half of this movement will simply be taking up movement in the opposite direction on the previous cycle (if the square wave is symmetrical and builds up slowly from zero), so that for a steady-state oscillation, this figure may be halved.

Moreover, the assumption of the earthquake motion being a square wave is conservative. If it is assumed to be sinusoidal instead, then from the previous sketch the value of the double integral would be substantially decreased and the net deflection would be approximately halved again.

Altogether then, for an earthquake building up sinusoidally in a few cycles with frequency f, the maximum "angle of tip" of such a structure would be approximately given by

$$\theta \simeq \frac{3g(\beta-\beta_o)}{16hf^2}\left(1 - \frac{\beta_o}{\beta}\right) \times\left(\frac{1}{4}\right) \qquad (12)$$

If the amplitude of the earthquake movement is a , then $\beta g = a(2\pi f)^2$, from fundamental mechanics, and eliminating f gives

$$\theta_{max.} \simeq 1.85 \left(\frac{a}{h}\right)\left(1- \frac{\beta_o}{\beta}\right) \qquad (13)$$

This formula is <u>independent</u> of the frequency of the earthquake, and implies that the maximum "angle of tilt" is a function primarily of the amplitude of the earthquake motion, largely irrespective of the maximum acceleration - as even for extremely large earthquakes where $\beta >> \beta_o$, the factor $\left(1 - \frac{\beta_o}{\beta}\right)$ merely approaches unity.

High frequency earthquakes of a given acceleration naturally have only small amplitudes of movement and this confirms the intuitive feeling that the higher an earthquake frequency, the less likelihood there is of a structure "having the time" to tip over.

If a structure is to fall over completely, then θ must exceed $\frac{d}{h}$, and the earthquake displacement must exceed $\frac{0.54\ d}{(1 - \beta_o/\beta)}$.

This implies that no matter how strong an earthquake may be, in order to "knock over" a stiff structure, the amplitude of motion must exceed one half of the base diameter, which in the case of the centrifuge model tests would be of the order of 40 mm - even though the actual dynamic movements realised in practice were only of the order of 1 mm. In the case of a real foundation of diameter 30 m, for instance, an amplitude of over 15 m would be required and this would correspond to a peak-to-peak motion of over 30 m, which is far larger than is ever observed in practice for real earthquakes. Although it is obvious that at these levels of motion, structures will be in danger of falling over, this analysis implies that this will only happen when these levels are reached, and not before.

10.4 CONCLUSION

These tests have provided experimental support for the intuitive feeling that a simple "quasi-static" analysis greatly over-estimates the likelihood of "tip-over" of towers taking place, particularly for earthquakes of high frequency.

Consideration of the dynamics of the problem show why this is so, and indicate that the important parameter in causing "tip-over" is the amplitude of earthquake displacement, and that the value of lateral acceleration is of secondary importance in this respect.

In practice, long before "tip-over" would occur, the whole problem would become non-linear, bearing stresses would be exceeded at the edges of the foundations, and severe damage would have already been caused to both the foundation and the structure.

However, the dynamic analysis gives a general indication of the major factors involved, and both the analysis and the centrifuge model tests show that the problem of "tip-over" of structures is not as serious as may be supposed from a simple quasi-static analysis.

CHAPTER 11

ROCKING TOWERS ON WET SAND

Some brief qualitative tests were done on towers on a foundation of saturated fine sand, deposited relatively loosely. The towers themselves were instrumented in the usual way, with accelerometers attached on top. In addition a miniature pore-pressure transducer was buried in the sand underneath one of the towers, and a model earthquake was let off as before.

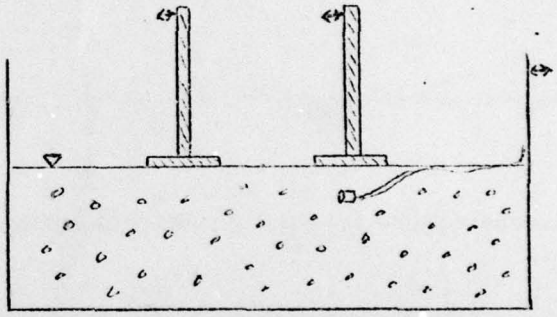

Plates 13 and 14 show such a test before and after the "earthquake". The displacement amplitude of earthquake motion was only about 2% of the base diameter, but on this occasion one of the towers fell over as a result of the generation of excess pore pressures in the foundation of saturated fine sand This is commonly known as"liquefaction" failure. Not surprisingly it was the tower with the smaller base diameter of the two, that fell over, and it was possible to see this immediately via the television monitor. Plates 15 and 16 show still photographs of the videotape record before and after the foundation collapse.

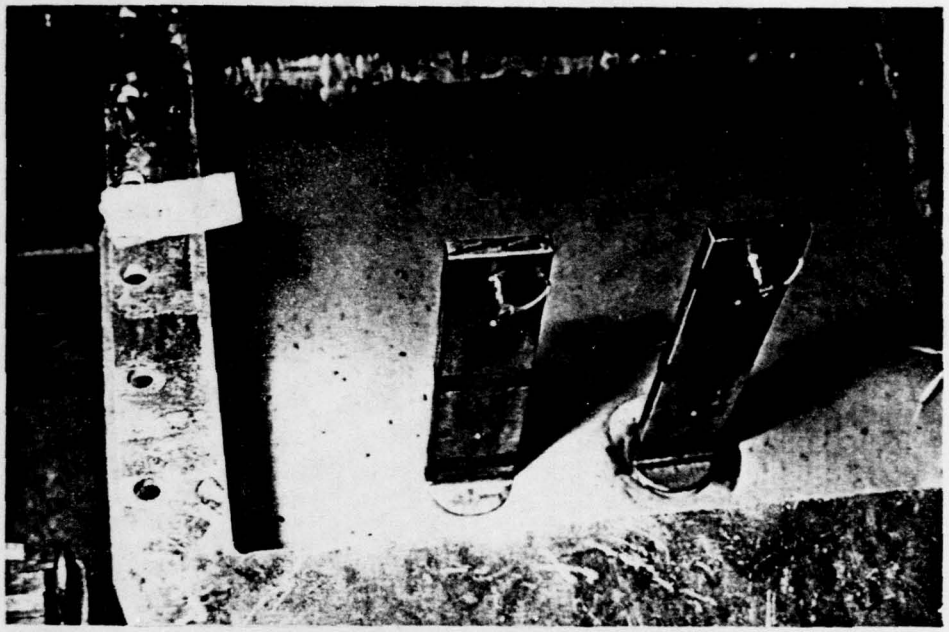

PLATE 13 - Towers on wet sand, before foundation failure

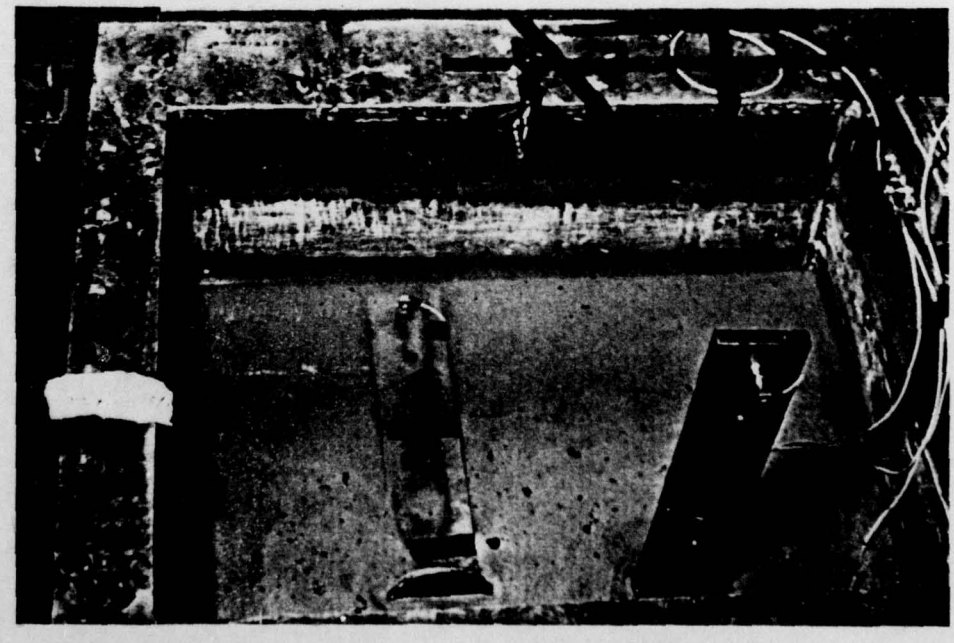

PLATE 14 - Towers on wet sand, after foundation failure

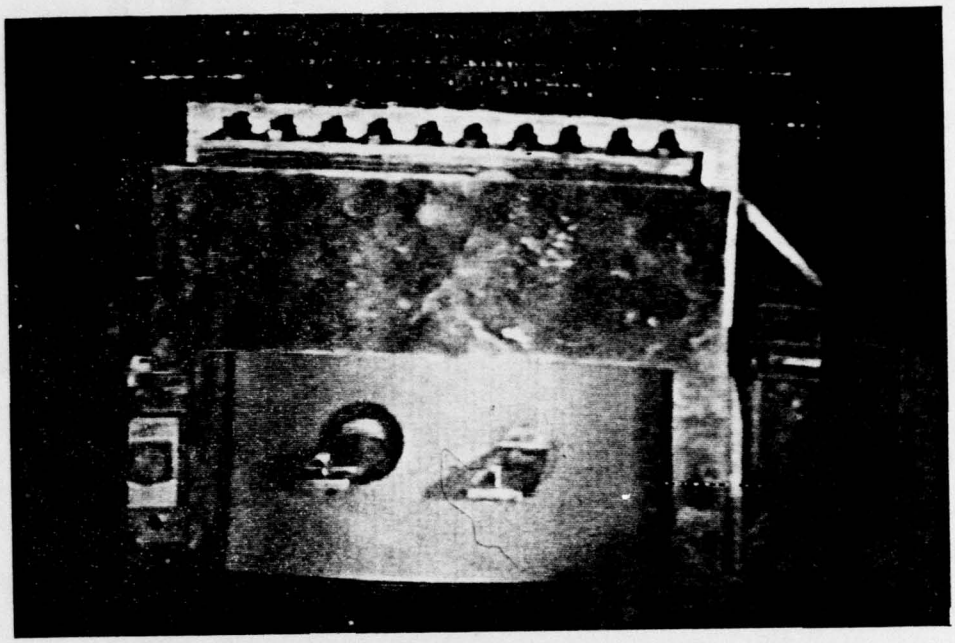

PLATE 15 - Towers on wet sand, before foundation failure, on television

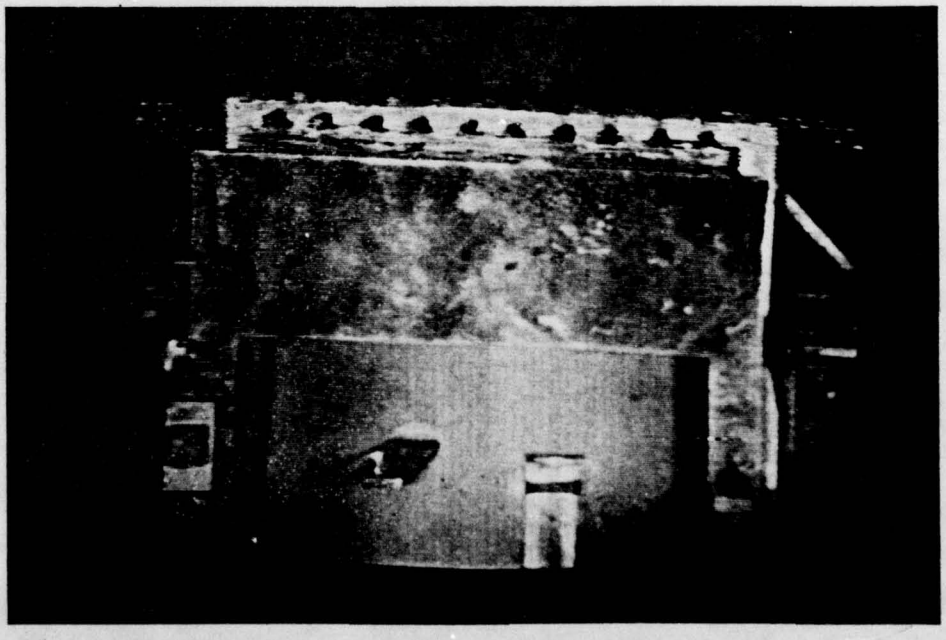

PLATE 16 - Towers on wet sand, after foundation failure, on television

Figure 30 shows the instrumented record of another test. The "earthquake" motion and the motion of the two towers are displayed in the top three traces. Of particular interest, however, is the bottom trace - the pore pressures recorded under the base of the first tower, which are positive downwards in the original.

These traces have been redrawn more clearly in Figure 31 (with the polarity of the pore-pressure trace reversed) and the sharp rise in pore-pressure under the tower base is shown. This pressure then decays rapidly, and subsequently cycles as the tower rocks and exerts cyclic stresses on the foundation. The long term drop in pore pressure is believed to be the result of the pressure transducer "floating" upwards through the fine sand, during the period of "liquefaction", by the equivalent of about 1 metre in full scale dimensions, and subsequently being subjected to a reduced static head of water. On this particular test, full foundation failure did not occur, although the second tower tilted backwards by about 10^{o}.

These tests were of course largely qualitative as any analysis of the pore pressure build-up under the sand foundation was beyond the scope of this thesis. However, observation of the general pattern of behaviour was valuable nevertheless - it clearly demonstrated the pore pressure behaviour in these circumstances, and showed that foundation failure could occur as a result. It is encouraging to see that the instrumentation operated satisfactorily, and that the modelling technique appears quite able to deal with problems of this nature.

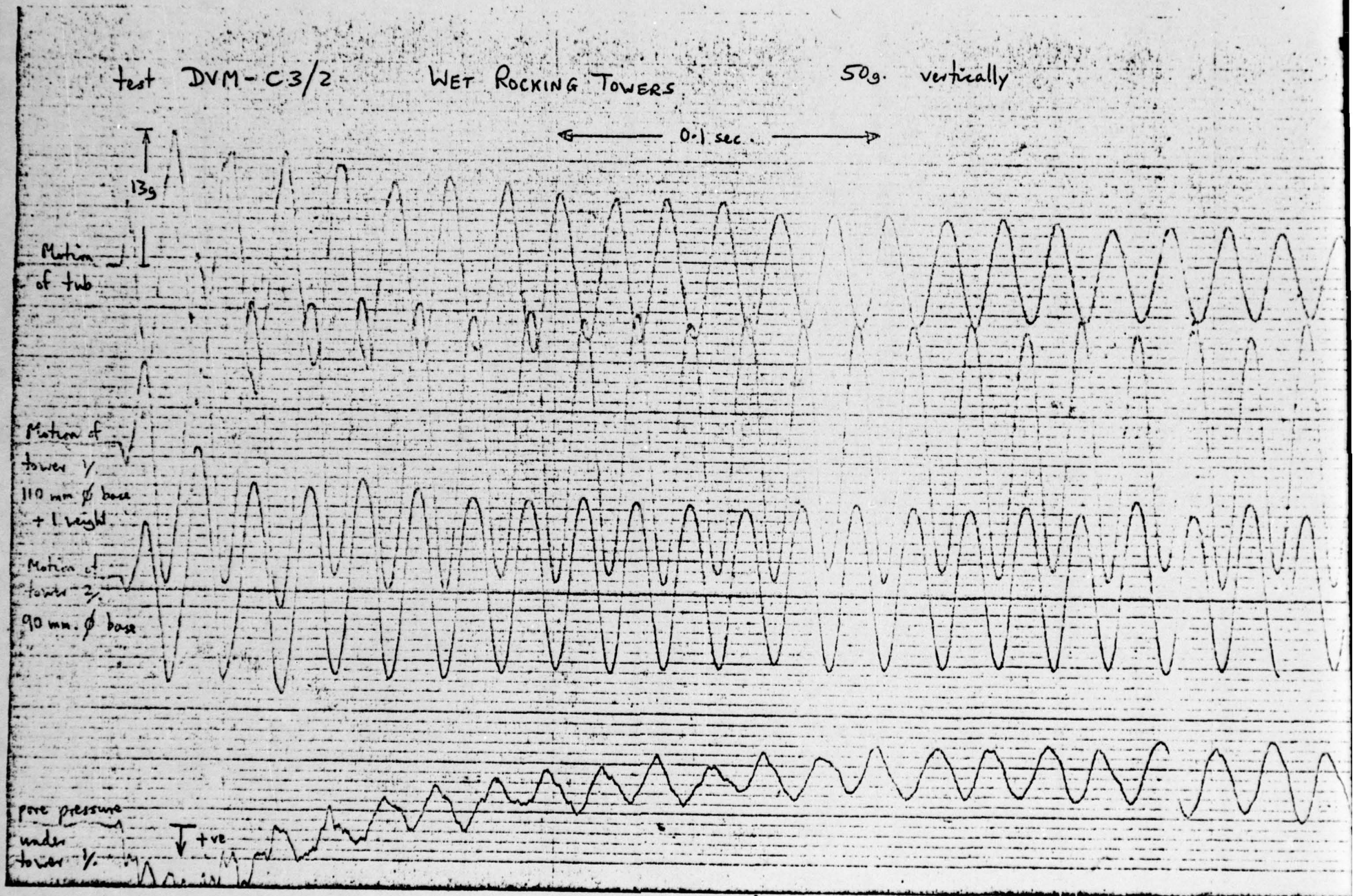

Figure 30 - Earthquake record of towers on wet sand - original

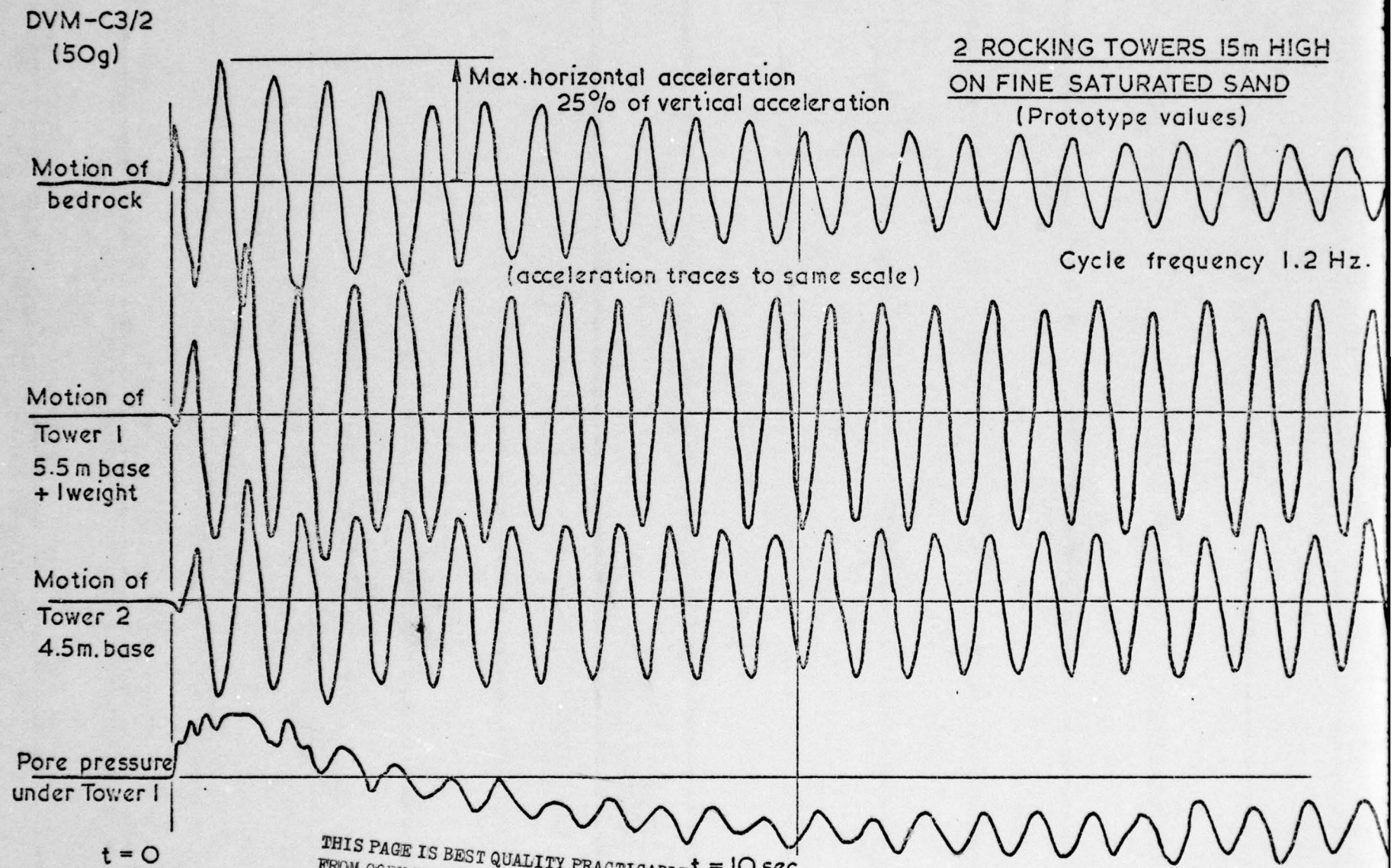

Figure 31 - Earthquake record of towers on wet sand - traced and converted to full scale

CHAPTER 12

DRY EMBANKMENTS

12.1 INTRODUCTION

These tests investigated the response of embankments of dry sand. Coarse 14/25 Leighton-Buzzard sand was used, and this was deposited by hand to the desired embankment profile. Sand was glued onto the bottom of the container, to ensure full frictional sand contact there. The embankment slopes were led down onto the bottom of the container without substantial contact with the sides, so that the boundary conditions at the bottom simulated a full-scale embankment on a foundation of solid bedrock, for instance.

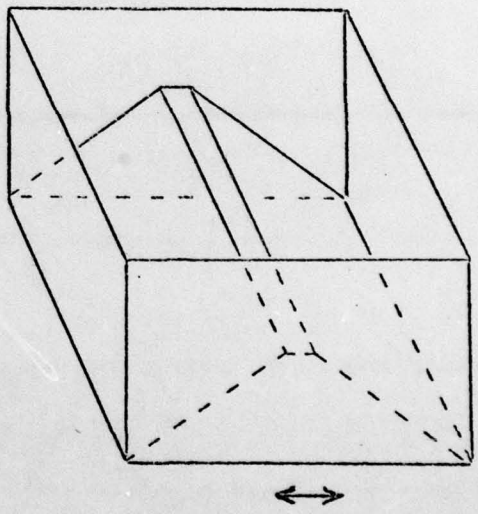

The surfaces of the embankments were lightly spray painted with vertical and horizontal lines, so that the slip of a slope could easily be seen on the T.V. monitor. In general, each side of the embankment was at a different slope, so that more information could be gained from each test. A typical test would produce slipping of the top layer of sand on one side or other - sometimes both.

It was possible to relate the occurrence of slip to the horizontal acceleration and the slope angle, and this is described shortly. It was also possible, by observing the vertical lines on the slope with the T.V. monitor, to check that slip did indeed occur along the direction of maximum slope, and the paths of the sand grains did not appear to be curved in any way by Coriolis forces.

Plates 17 and 18 show such an embankment before and after a model earthquake. In this case, surface slippage took place on both sides of the embankment. Plates 19 and 20 show the same embankment as seen from directly above, on the T.V. monitor, immediately before and after the model earthquake.

12.2 INSTRUMENTED RESULTS

The embankment was instrumented as shown in the sketch. Miniature accelerometers were embedded in the sand at various depths - one at the top, middle and bottom of the embankment respectively. These accurately followed the motion of the material, and could be compared with the motion of an accelerometer screwed into the container.

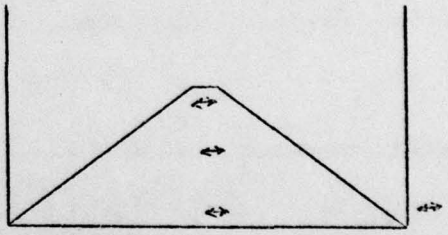

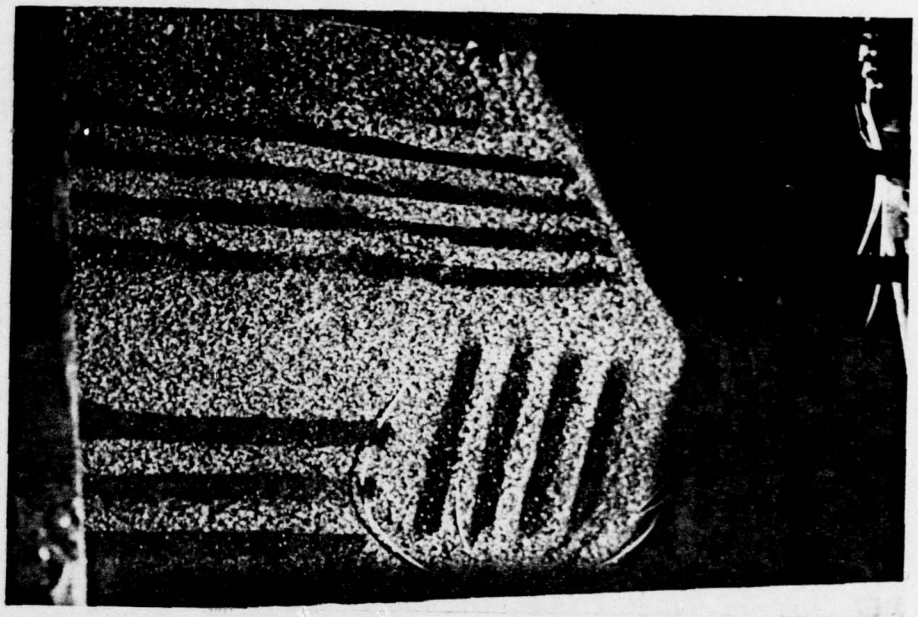

PLATE 17 - Embankment of dry sand, before earthquake

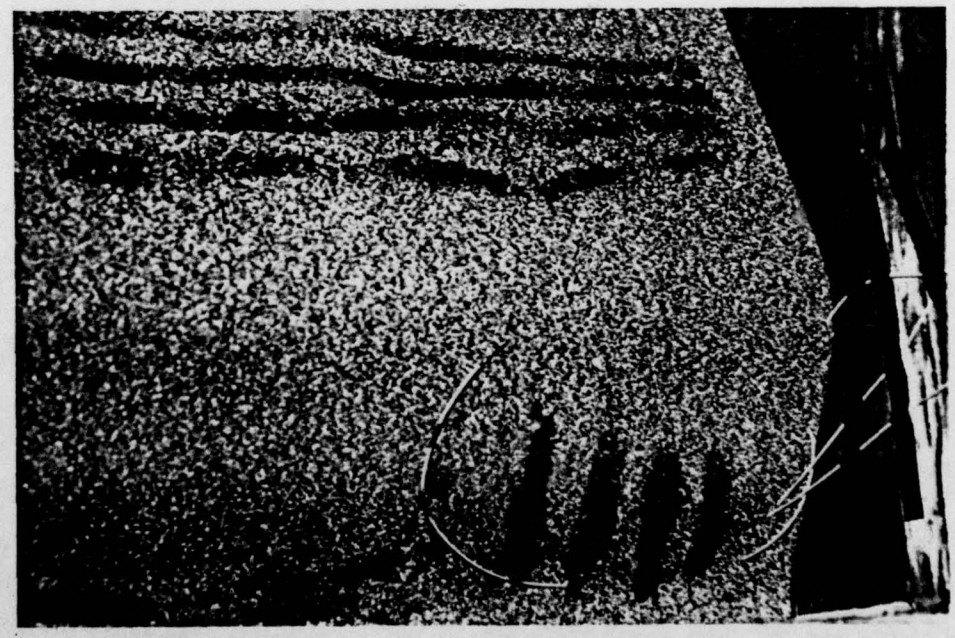

PLATE 18 - Embankment of dry sand, after earthquake

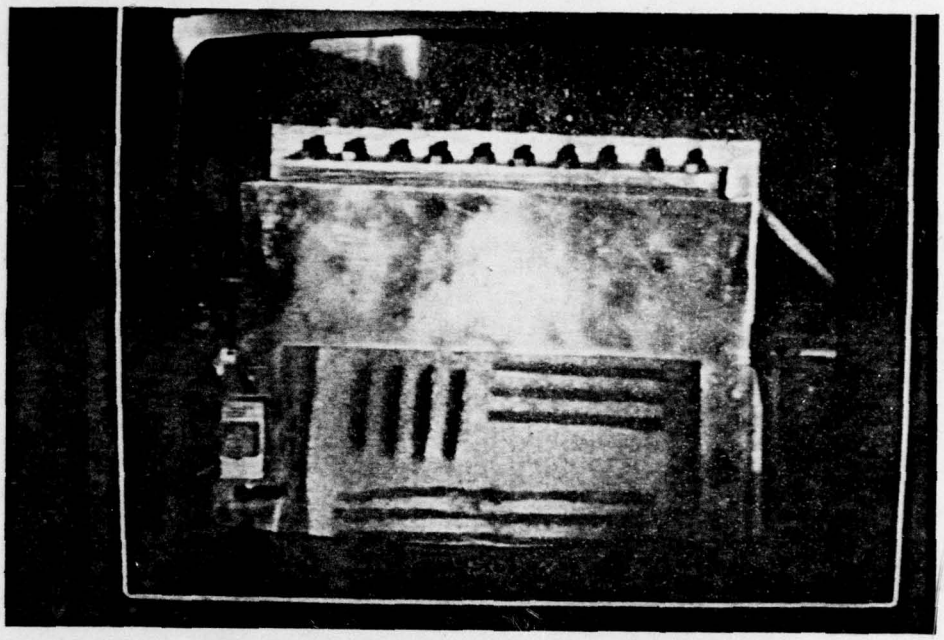

PLATE 19 - Television picture of embankment of dry sand, before earthquake

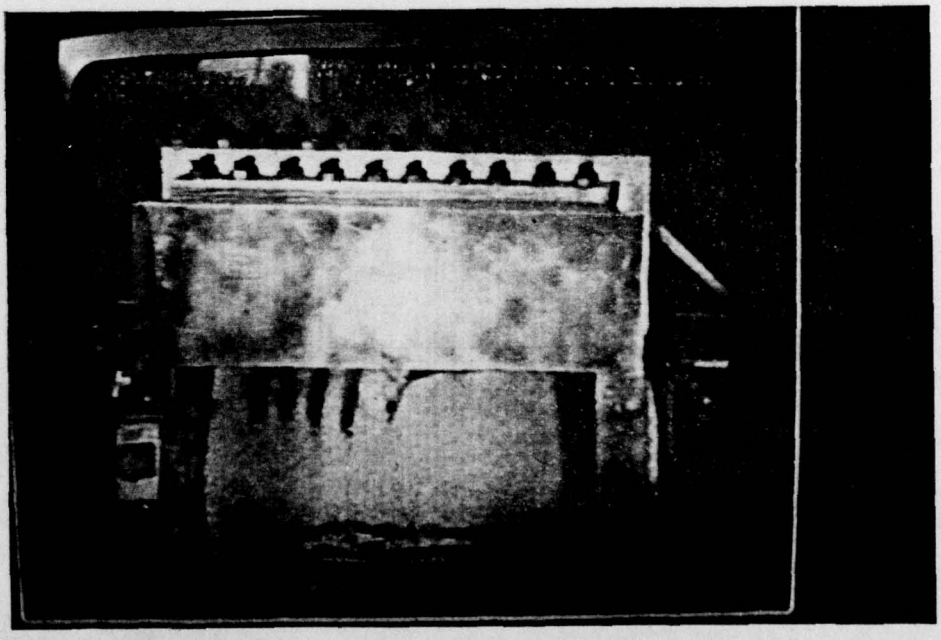

PLATE 20 - Television picture of embankment of dry sand, after earthquake

Figure 32 shows the accelerometer outputs of a typical test, traced on ultra-violet recording paper to the same scale (the accelerometer direction in the top trace was reversed, so that the signal was inverted). This top trace shows the acceleration record of the container (which may be regarded as the "bedrock" acceleration), and has a peak initial value of 12 g horizontally. As this test was carried out at 80 g centrifugal acceleration, this corresponds to an earthquake acceleration equal to 15 % of gravity. Similarly, as the actual height of the model embankment was 150 mm, the height of the equivalent full-size embankment was 12 m, and the model earthquake frequency of 61 Hz corresponded to a full-size frequency of 0.75 Hz.

Figure 33 shows these results converted to prototype values in this way (and with the polarity correction made). It appears that the motion of the whole embankment was more or less uniform, and in phase with the bedrock movement. In other words, the entire embankment was moving roughly as a rigid body, in response to the earthquake motion. This was expected, as the lowest natural frequency of such a prototype embankment - considered as a"shear beam" - was estimated at about 2.5 Hz, (see Appendix J for details of this calculation), and this was well above the agitating frequency of 0.75 Hz. Consequently, it would behave in a "stiff" fashion.

As a result, there is little in the way of "dynamic amplification" of the embankment motion between the top and the bottom of the embankment, as might otherwise be expected from theoretical wave propagation analysis, e.g. for the Patoka Dam*

*U.S. Army, W.E.S. (1974) "One dimensional wave propagation analysis, Patoka Dam, Indiana" W.E.S., Vicksburg, Mississippi, USA, Paper S-74-26.

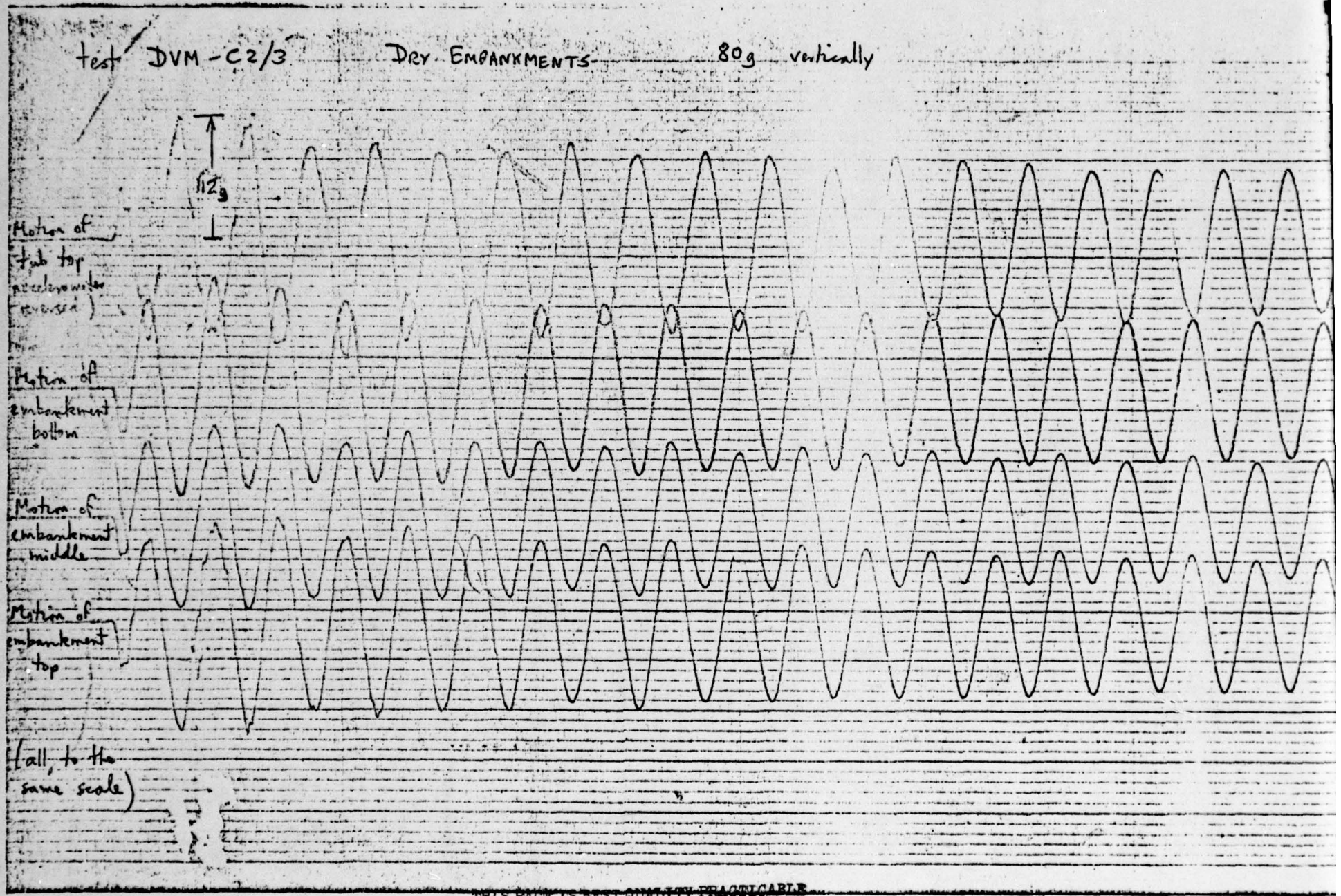

Figure 32 - Earthquake record of an embankment of dry sand - original

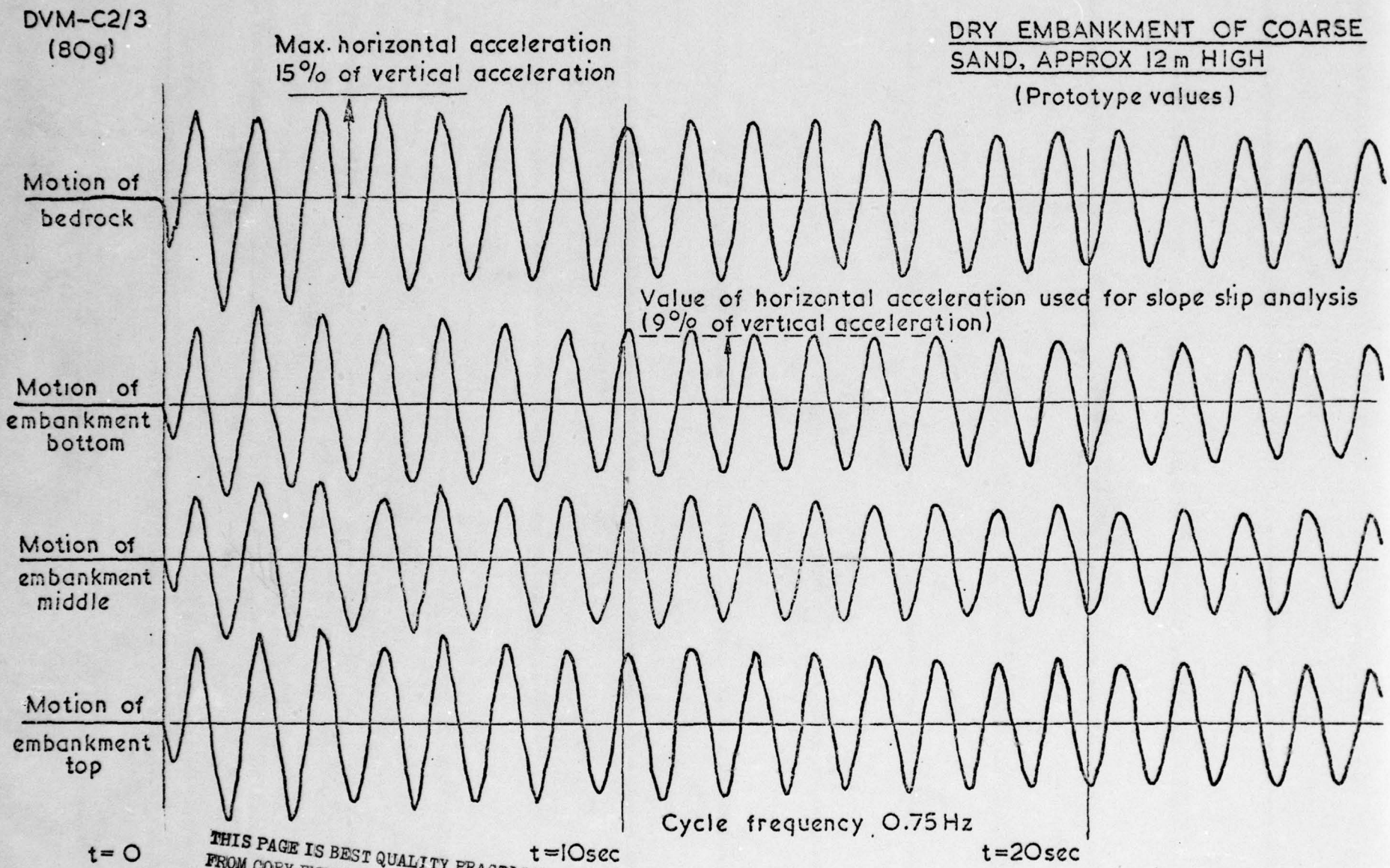

Figure 33 - Earthquake record of an embankment of dry sand - traced and converted to full-scale

(1974). In order to investigate such "dynamic amplification" (which is predicted theoretically and is of considerable interest in earthquake analysis) it would be necessary to excite the embankment at or near resonance.

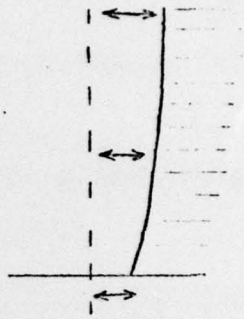

This would require an apparatus that was either capable of containing a substantially larger embankment, or of oscillating at a higher frequency (an increase of a factor of at least 4 would be necessary). In addition, in order to detect resonant conditions precisely, it would be desirable to have a continuously variable oscillating frequency - and this is not possible with the present apparatus.

On examining the original record again, it is perhaps possible to notice a slight phase lag between the base motion and the top of the embankment. A much more pronounced phase lag would be produced (it is believed) near resonance, but for these conditions a phase lag of only a few degrees would be predicted.

Although these results were relatively straightforward, it is nevertheless interesting to note that in this case the predictions of simple theory were confirmed by experiment.

There was originally some concern that the miniature accelerometers, embedded in sand, might not accurately follow the motion of the surrounding material.

In theory, an accelerometer would follow the soil motion if the natural frequency of the accelerometer mass embedded in the surrounding medium (considered as an elastic support) substantially exceeded the frequency of the soil motion. A relatively straightforward calculation, presented in Appendix K, demonstrates that this condition was easily satisfied for these accelerometers.

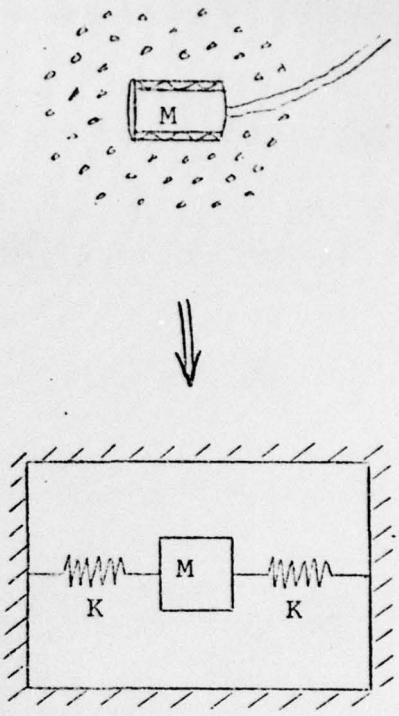

The experimental results also appear to be consistent, and, as a result, there seems to be no cause for concern in this respect.

12.3 ANALYSIS OF SLOPE SLIP

As mentioned previously, a particular slope on an embankment would, as a consequence of a model earthquake, either display a small amount of slip, a large slippage, or no slip at all. The slip in question would consist mainly of movement of the surface layer of sand, and not of deep seated slip. Not surprisingly, steeper slopes were more prone to slippage than shallower slopes, and larger model earthquakes were similarly more likely to cause movement.

This may be analysed very simply, by considering the equilibrium of a sand grain subjected to dynamic forces on such a slope.

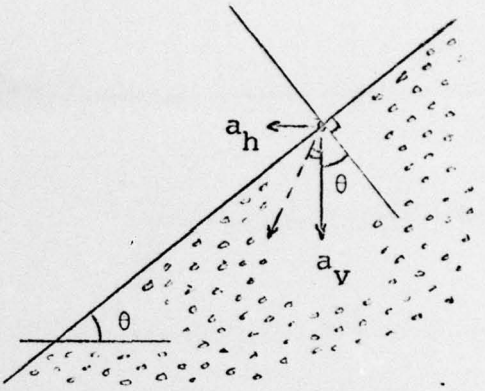

If such a sand grain, lying on a slope of angle θ, is subjected to a purely vertical acceleration a_v due to gravity, then the angle made by the net force on the grain with the normal to the surface is θ. Slip would normally occur if this angle exceeded the angle of friction ϕ'.

The presence of an additional horizontal acceleration a_h downhill, results in this angle increasing by an amount $\tan^{-1}\left(\frac{a_h}{a_v}\right)$. The procedure of considering an equivalent horizontal acceleration is valid in this case, as it has been established that the embankment is acting as a rigid body. Consequently, under these circumstances, the condition for slip becomes $\theta + \tan^{-1}\left(\frac{a_h}{a_v}\right) > \phi'$.

This prediction can be checked by tabulating the observed results as follows :-

Slope Angle θ	Vertical Acceleration a_v	Horizontal Acceleration a_h	$(\frac{a_h}{a_v})$	$\theta+\tan^{-1}(\frac{a_h}{a_v})$	Result
15^o	80 g	4 g	5 %	18^o	no slip
22^o	80 g	5 g	6 %	$25\frac{1}{2}^o$	"
22^o	80 g	7 g	9 %	27^o	"
25^o	80 g	4 g	5 %	28^o	"
22^o	50 g	6 g	12 %	29^o	"
22^o	25 g	5 g	20 %	33^o	small slip
22^o	25 g	6 g	24 %	35^o	"
33^o	80 g	5 g	6 %	$36\frac{1}{2}^o$	slip observed
33^o	80 g	7 g	9 %	38^o	"
33^o	50 g	6 g	12 %	40^o	"
33^o	25 g	5 g	20 %	44^o	"
33^o	25 g	6 g	24 %	46^o	"

Since the angle of internal friction ϕ' for this sand was around 35^o, based on the angle of repose of a static slope, the results appear to be consistent with elementary analysis.

However, because the horizontal acceleration consisted of an exponential decay, it was necessary to decide what value of horizontal acceleration was appropriate for the analysis. If the initial peak value of horizontal acceleration was chosen, then inconsistent results were obtained. It was necessary to use instead the

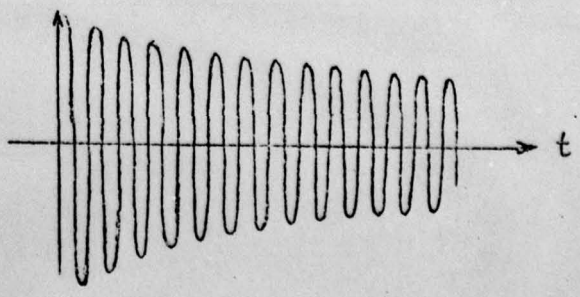

value of acceleration after about 7 or 8 cycles of motion - i.e. after the high transient values of initial acceleration had died away and more uniform motion had been maintained over a number of cycles.

It was also better to use the acceleration output from accelerometers actually embedded in the embankment, as these did not usually produce such high initial peaks as accelerometers that were rigidly attached to the container. Figure 33 shows the appropriate value used in the analysis of that test.

This approach was rather empirical, but the fundamental observation was simply that an initial peak value of horizontal acceleration was not enough to cause real slip - and that only a sustained vibration could properly be considered in such an analysis.

A similar effect was found by Seed and Goodman* (1964) from tests on shaking tables. Noticeable deflections only occurred when the amplitude of the horizontal acceleration substantially exceeded the minimum value required for initial movement.

More accurate experimental results would be possible with a centrifuge apparatus that could produce a steady earthquake motion which could be slowly increased in amplitude until slip took place. However, accepting the equipment limitations, the results obtained do make sense - they satisfy the fundamental physical laws, and the experimental method appears to be viable.

---

* SEED, H. B. and GOODMAN, R. F. (1964) "Earthquake stability of slopes of cohesionless soils", Proc. Am. Soc. of Civil Engineers, Vol. 90, SM6

12.4 CONCLUSION

The behaviour of dry sand embankments subjected to horizontal motion appears to have been modelled satisfactorily. Slip of the sand surface occurred in certain cases, depending on the slope angle and the "earthquake magnitude". The incidence of slip correlated with a simple quasi-static analysis, if peak initial values of horizontal acceleration were ignored, and the value after about seven cycles of motion used instead - which was generally about 75 % of the peak motion.

Accelerometers embedded in the sand appeared to give a faithful record of the soil motion, and indicated that, at this frequency of excitation, the embankments behaved almost as rigid bodies, with only a very slight phase lag visible between the top and bottom, in accordance with elementary dynamic theory, as the natural frequency of the embankment was well above that of the model "earthquake".

It was not possible to investigate the resonant behaviour of the embankment with this apparatus. This would require a substantial increase in either the model earthquake frequency or in the dimensions of the apparatus, and preferably also the ability to change the earthquake frequency in flight, so that resonance could be accurately detected. This is not practical with the present equipment.

CHAPTER 13

WET EMBANKMENTS

13.1 INTRODUCTION

These tests investigated the response of embankments of saturated sand. They were made with fine 120/200 Leighton-Buzzard sand, placed loosely by hand, and instrumented by accelerometers embedded in the top and bottom of the embankment, and by a pore-pressure transducer in the base of the embankment.

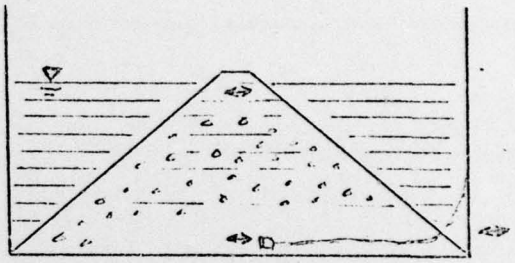

The embankment remained mostly submerged throughout the test, although the crest was allowed to stand just proud of the water surface, as shown in the sketch. In this way it was possible to see the movement of the crest on the television monitor.

Plates 21 and 22 show such an embankment before and after a model earthquake. The crest was lightly sprayed with matt black paint to highlight any movement, and a line of vertical straws was inserted to show slope movement. After the model earthquake the crest slumped, scattering the covering of spray paint, and the straws tilted away from the crest.

The embankment profile was crudely measured by tracing it against the plastic backing sheet. This is reproduced "before" and "after" in Figure 34.

Television pictures during the test showed the embankment splitting down the crest, and then spreading laterally. This can be seen on Plates 23, 24 and 25, which are still photographs of the television monitor screen.

13.2 INSTRUMENTED RESULTS

The original record from the same test is shown in Figure 35. The top trace shows the motion of the container (the direction of the accelerometer being reversed in this case), followed by the motions of the accelerometers embedded in the bottom and top of the embankment respectively, and the lowest trace is the pore pressure response.

Figure 36 shows the same record traced and separated for clarity, and converted to full-size prototype values. The height of the embankment becomes 7.5 metres, and the peak horizontal acceleration is 0.36 g at 1.2 Hz - corresponding usefully to real values.

The pressure transducer response shows how the pore-pressure built up cyclically over the first three or four cycles of earthquake motion, and then slowly died away. The embankment bottom moved more or less identically with the bedrock. However, the top of the embankment was subjected to a greatly reduced earthquake motion, during the period of liquefaction, which appeared to isolate the top from the dynamic motion of the bottom. After appreciable dissipation of these pore-pressures however, the top then gradually reverted to moving together with the rest of the embankment.

This effect of "dynamic isolation" has been postulated theoretically, and it is clearly demonstrated by these experiments.

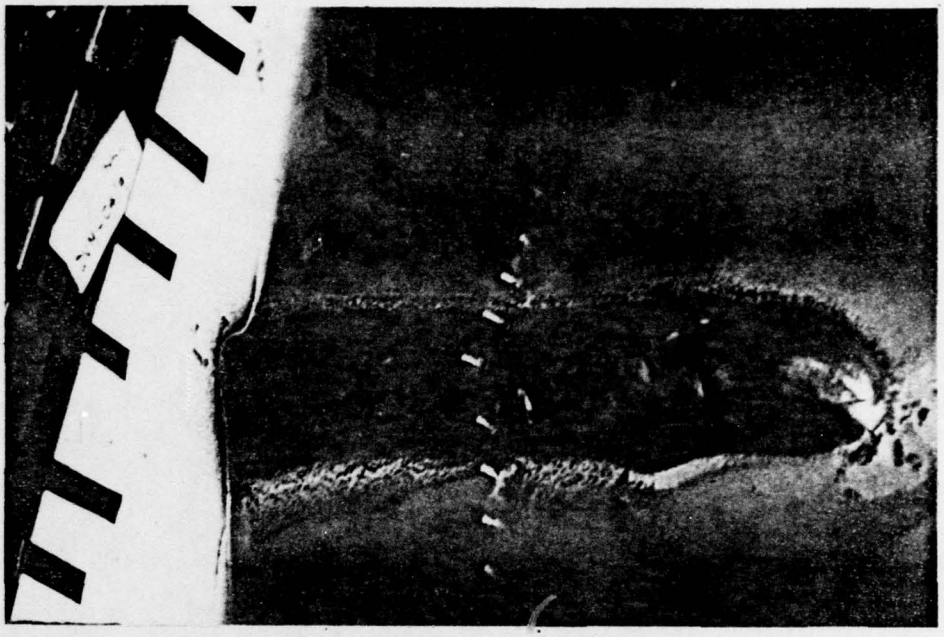

PLATE 21 - Embankment of wet sand, before earthquake

PLATE 22 - Embankment of wet sand, after earthquake

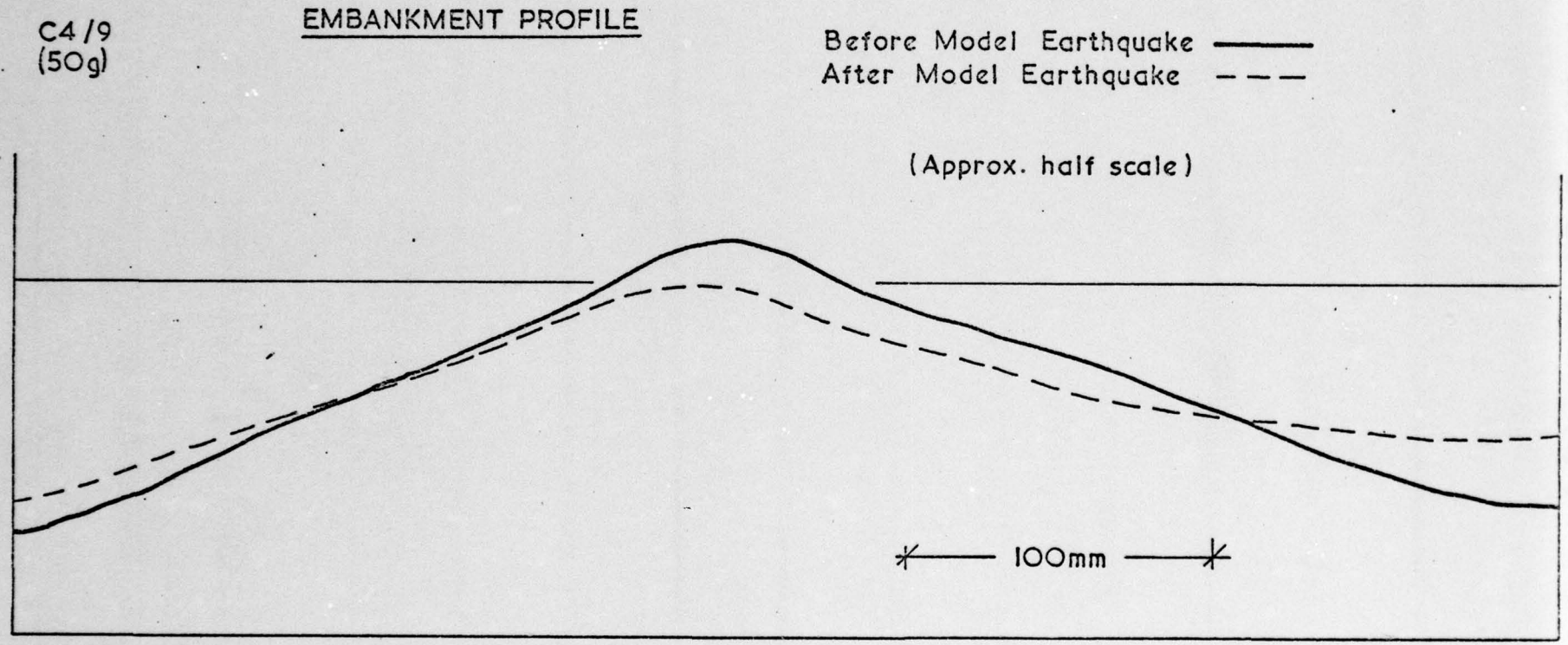

Figure 34 - Profile of embankment of wet sand, before and after earthquake

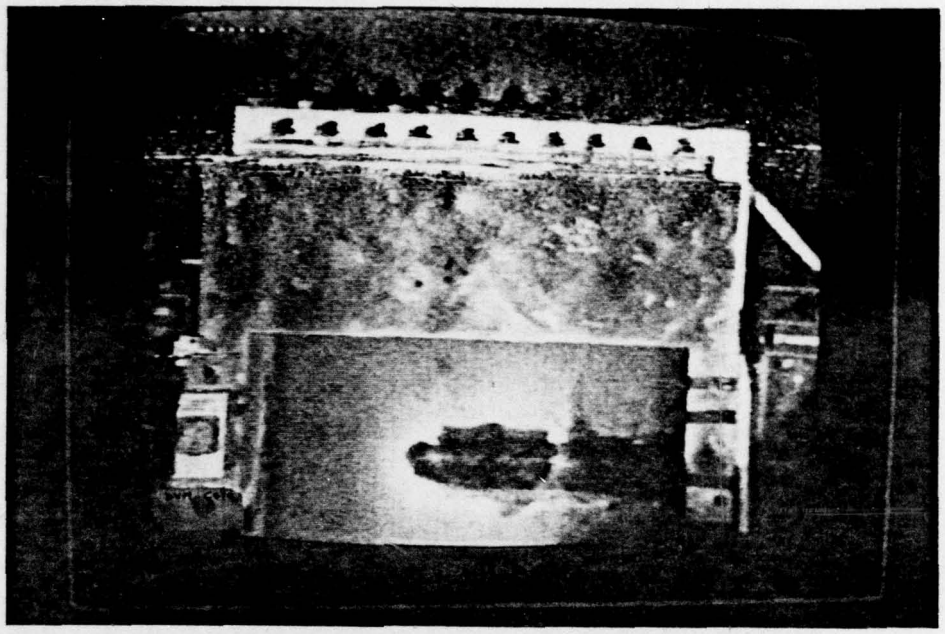

PLATE 23 - Television picture of embankment of wet sand, before earthquake

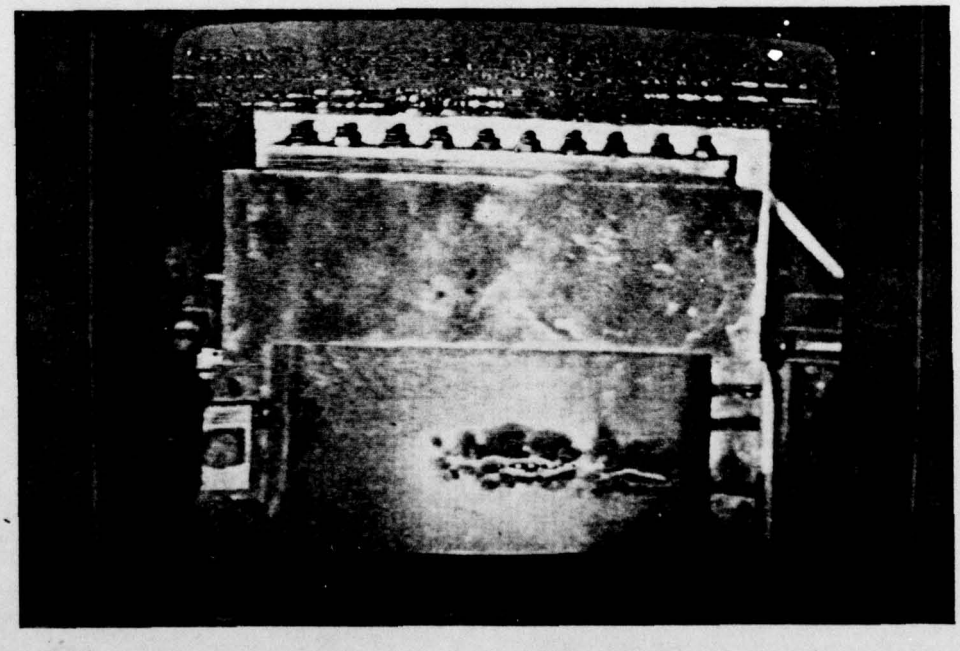

PLATE 24 - Television picture of embankment of wet sand, during earthquake

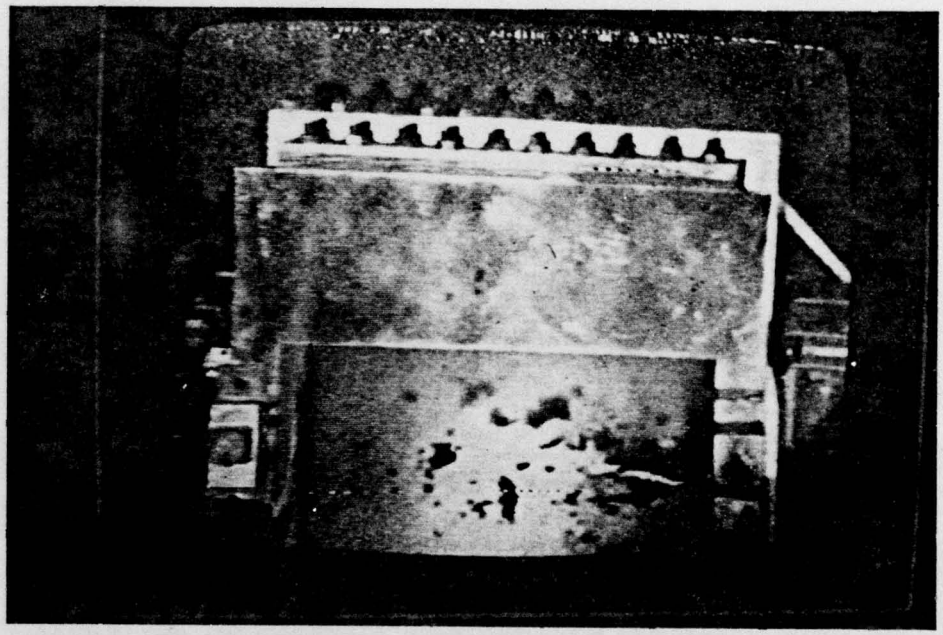

PLATE 25 - Television picture of embankment of wet sand, after earthquake

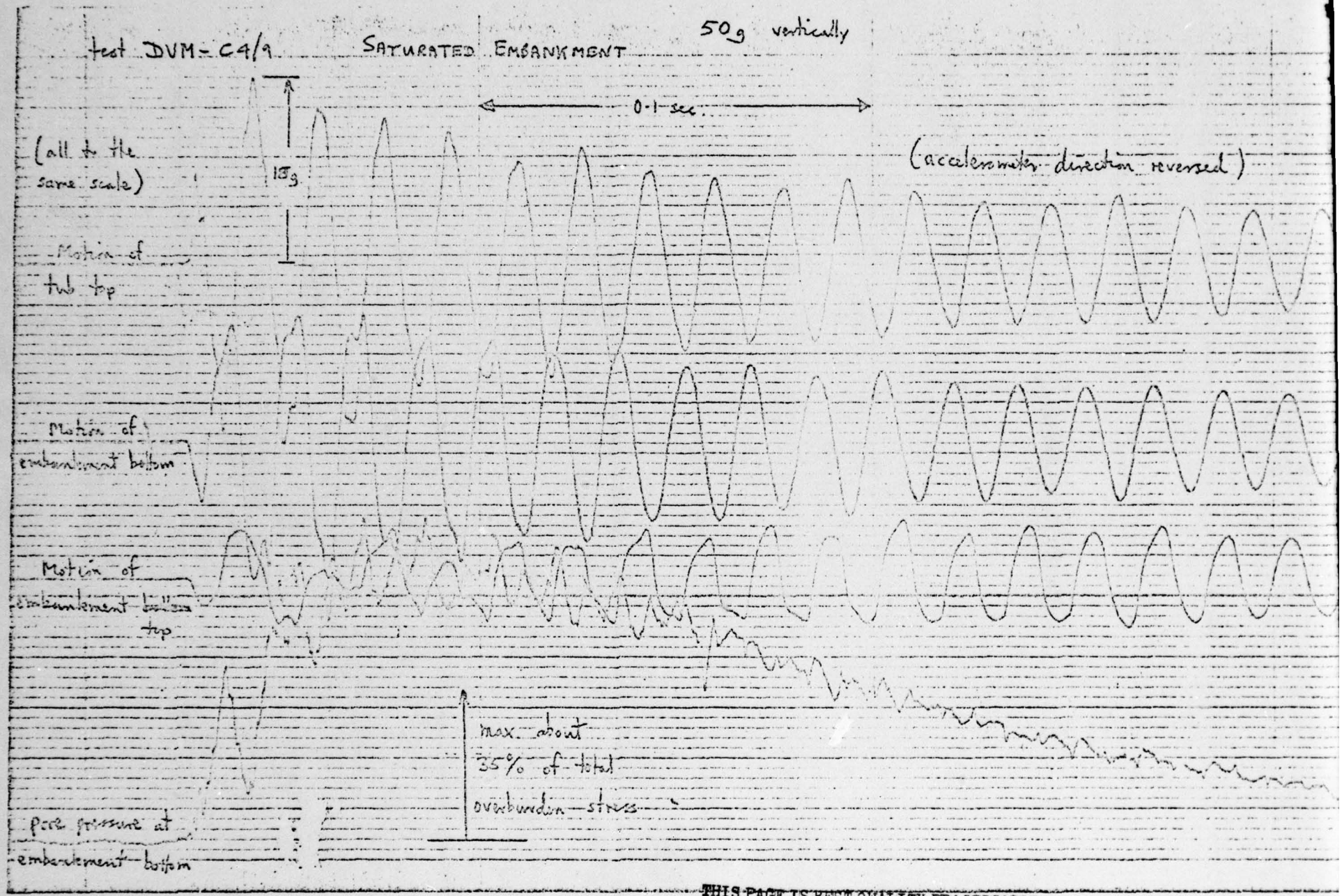

Figure 35 - Earthquake record of an embankment of wet sand - original

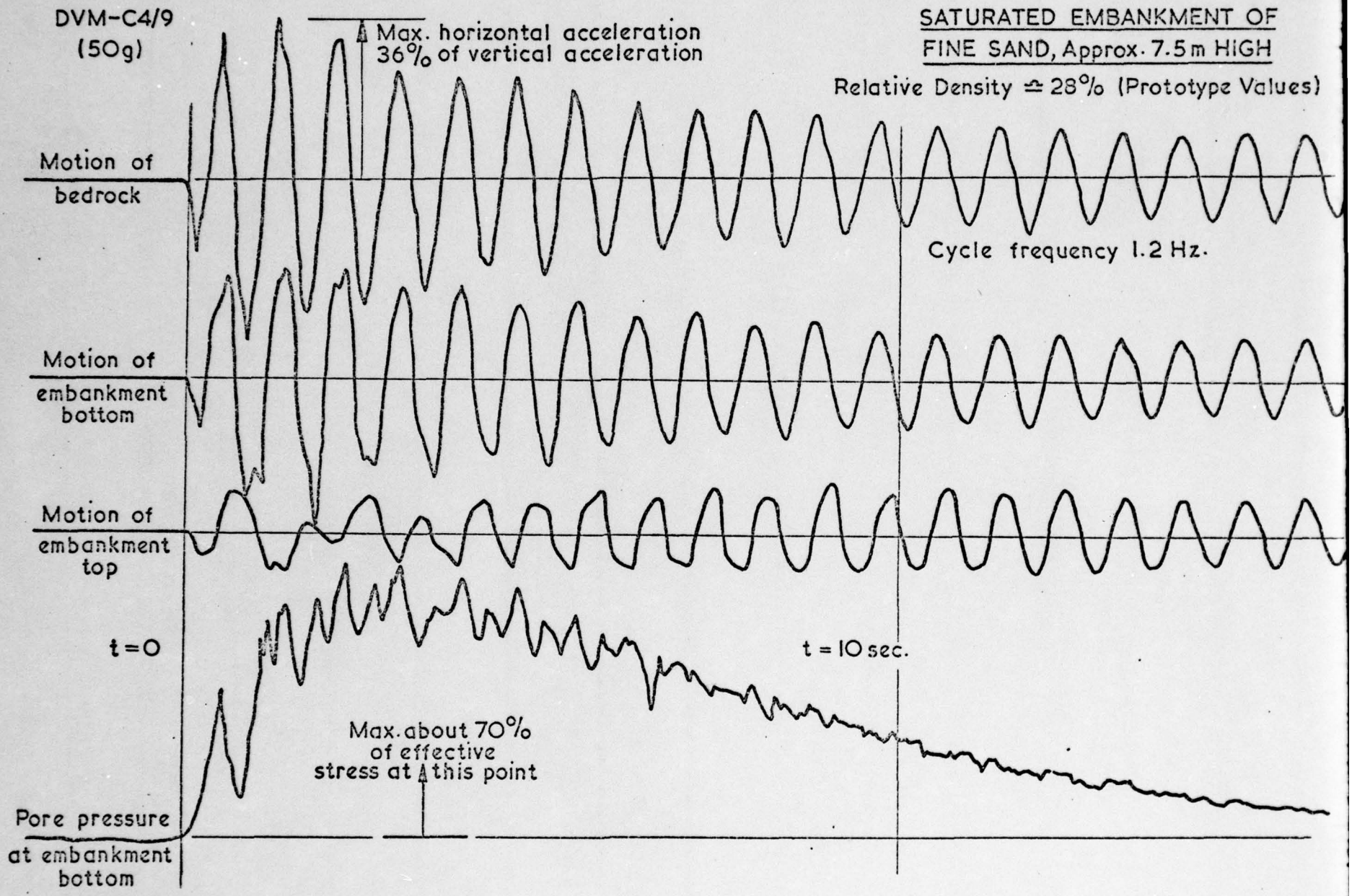

Figure 36 - Earthquake record of an embankment of wet sand - traced and converted to full-scale

The maximum magnitude of the excess pore-pressure at the base of the embankment was about 30% of the total overburden stress at that point, or about 60% of the effective stress. This implies that the soil strength fell to about 40% of its value at this point, prior to the earthquake, and it is therefore not surprising that the embankment failed by "liquefaction", in a manner similar to full scale reports, e.g. by Seed and Idriss*.

13.3 DISCUSSION

These tests have demonstrated clearly that it is possible to model the earthquake behaviour of saturated embankments on the centrifuge, that it is possible to instrument such a model successfully, and that the results correspond with what is known about full-scale behaviour. However, at this stage these particular experiments must still be regarded as largely qualitative for the following reasons.

Firstly, it was only possible to make an approximate estimate of the in-situ density of the fine sand, because of the irregular shape of the model embankment. In practice, the density was estimated as 1860 kg/m^3 simply by attempting to reproduce the method of deposition in a measuring cylinder. Before any accurate tests could be performed it would be necessary to make a more precise measurement of the in-situ soil density. Ideally such a measurement should be made on the centrifuge

---

* SEED, H. B. and IDRISS, I. M. (1967) "Analysis of soil liquefaction - Niigata earthquakes", Proc. Am. Soc. of Civil Engineers, Vol. 93, SM3

immediately prior to the test, so that any consolidation of the embankment material under centrifugal acceleration would be automatically taken into account.

Secondly, it is not clear whether the embankment, which was simply deposited by hand, was sufficiently uniform to enable a valid comparison to be made between a theoretical prediction and experimental measurements. It has been postulated e.g. by Seed* (1968), that the presence of pockets of loose material acting as stress concentrations may prematurely initiate liquefaction in an otherwise uniform stratum of material. Now it may be that a non-uniform embankment is in fact more representative of a true prototype than an unrealistic assumption of complete uniformity. However accurate tests will require a method of deposition that can produce an embankment of a specified and known degree of uniformity.

These problems are equally relevant to the collection of full scale practical data, as there are similar difficulties in measuring the in-situ density and uniformity of material in the field.

Once these two conditions are satisfied, it will be possible to make a theoretical comparison between a centrifuge model test and a computer analysis of dynamic liquefaction, as reported for instance by Seed, Idriss, Lee and Makdisi+ (1975). Any scaling anomalies resulting from different scaling laws for dynamic failure and pore pressure dissipation, can be accomodated by suitably modifying the soil properties in the numerical model, as outlined subsequently in this discussion.

---

* SEED, H. B. (1968) "Landslides during earthquakes due to soil liquefaction", Proc. Am. Soc. of Civil Engineers, Vol. 94, SM5, Terzaghi lecture

\+ SEED, H. B.; IDRISS, I. M.; LEE, K. L. and MAKDISI, F. I. (1975) "Dynamic analysis of the slide in the Lower San Fernando Dam during the earthquake of February 9th, 1971", Proc. Am. Soc. of Civil Engineers, Vol. 101, GT9

If, on the other hand, a full size prototype is to be modelled, and the expected rate of pore pressure dissipation is not either very fast or very slow - in other words where the rate of pore pressure dissipation interacted with the time taken for failure to occur - then the third condition is that careful thought must be given to the relationship of model measurements to full-scale values.

Consider a full scale embankment of characteristic dimension H, at 1 g. From the constant acceleration formulae it will fail in a time proportional to $\sqrt{\frac{H}{g}}$. If it is constructed of material with a coefficient of consolidation C_v then drainage will take place in a time proportional to $\frac{H^2}{C_v}$. Thus, if these two values are comparable and the interaction between them is important, the ratio between these two factors, $\left(\frac{C_v}{\sqrt{gH^3}}\right)$, must be the same in an accurate model as in the full scale structure.

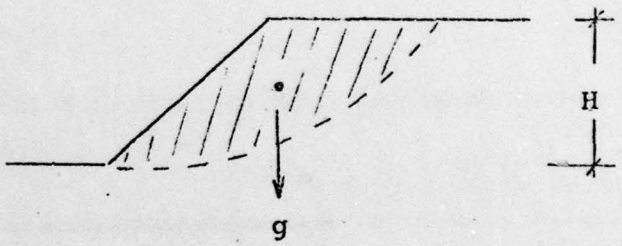

In such a situation, if a centrifuge model were simply made of the same material at a scale of 1:100, and tested at 100 g, then this ratio would be increased by a factor of 100. In other words, the pore pressure would dissipate 100 times too fast (relative to the time taken for slip to occur) than in the full scale soil structure, and it is doubtful whether a "liquefaction failure" would be correctly modelled if this effect was important.

The answer to this particular dilemma must be to abandon the original concept of using only the field material in the soil model, and instead to allow the soil properties to be modified. In this case this would require a soil with a coefficient of consolidation reduced in proportion to the modelling scale.

For such a centrifuge model, the dimensionless group $\left(\frac{C_v}{\sqrt{gH^3}}\right)$ would then become $\frac{C_{v/n}}{\sqrt{ng\ (\frac{H}{n})^3}} \equiv \frac{C_v}{\sqrt{gH^3}}$, and would be unchanged. Such reduction of the coefficient of consolidation can be accomplished most easily in practice by reducing the permeability of the model material - either by increasing the viscosity of the pore fluid, or by using a soil with a smaller grain size.

It would still be necessary to make sure that the relevant properties of the original soil were preserved. The shear strength and/or frictional properties would have to be the same, but most importantly the tendency of the soil to generate excess pore pressures in response to cyclic shear stresses must also be modelled correctly. This latter condition might be verified by comparing cyclic triaxial test data on the two materials, perhaps in accordance with the procedure recommended by Seed and Peacock* (1971).

On the basis of this approach then, the test that was performed at 50 g, on material with a coefficient of consolidation of about 1.5 m^2/s, can be regarded as corresponding to the full scale "liquefaction" behaviour of an embankment of similar material but with a coefficient of consolidation equal to 75 m^2/s.

---

* SEED, H.B. and PEACOCK, W.H. (1971) "Test procedures for measuring soil liquefaction characteristics", Proc. Am. Soc. of Civil Engineers, Vol. 97, SM8

There are precedents for this philosophy in other fields - coastal hydraulics for instance, where models are often made of crushed bakelite instead of coastal sand, to study harbour erosion. This procedure is described by Ippen* (1966) for instance. In these areas any theoretical analysis would be unrealistically complex, and resort must be made to a model - and although harbours themselves are not in fact constructed from crushed bakelite, study of the relevant transport phenomena has shown that these are modelled correctly if such an artificial material is used in the models.

Lest it is imagined that other model techniques are any better in this respect, it is instructive to note that if a similar model test, using the original field material, was performed at 1 g (not using a centrifuge), then the ratio between the failure time and the drainage time would be increased by a factor of 1000, compared to the full scale soil structure. The problem would thus be 10 times more acute than for a centrifuge model, and this calculation also demonstrates why it is difficult to observe liquefaction failures in laboratory models.

---

* IPPEN, A.T. (1966) "Estuary and Coastline Hydrodynamics" McGraw-Hill, New York, Chapter 17

13.4 CONCLUSION

It has been shown how "liquefaction" failures in saturated soil due to earthquake motion may be modelled on a geotechnical centrifuge. Model embankments of fine sand failed by splitting of the crest followed by lateral spreading and substantial crest settlement. Instrumentation by minature accelerometers and pore pressure transducers embedded in the soil showed that the top of the embankment was isolated from the ground motion in this period, while cyclic generation of large excess pore pressures took place in the body of the embankment.

There are still certain difficulties to which careful attention must be paid before these results may be accurately related to a full size prototype, but it is shown how these may be resolved.

Ultimately the justification for developing these modelling techniques is not just that of economy, but simply that adequate repeatable high quality test data concerning earthquake behaviour is not available in any other way - either in order to produce empirical recommendations directly, or to compare with the great variety of conflicting analyses that are used at present and that remain largely unvalidated.

CHAPTER 14

CONCLUSION

On the basis of the experiments reported in this thesis, there appears to be no obstacle to modelling a large range of dynamic phenomena on a geotechnical centrifuge. It is possible to measure both dynamic motion and rapid pore pressure changes accurately with existing instrumentation. This technique enables higher quality testing of physical models of soil problems, than by using conventional soil models in the laboratory at an acceleration of 1 g . In particular, earthquakes have have been modelled using newly developed equipment, and this is of special interest as it is, in general, extremely difficult to do such experiments at full scale.

Initial tests, modelling the rocking of towers on a circular foundation in a straightforward fashion, have demonstrated that a simple one-degree-of-freedom dynamic analysis appeared to predict the stiffness of the soil-structure interface successfully, once certain assumptions were made about the stress state under the foundation, and on the basis of observed results an appropriate empirical rule was proposed.

The predicted stiffnesses of square foundations were supported experimentally, but it appeared that the stiffening effect of embedding a foundation was over-estimated theoretically. Indirect verification of the modelling laws was possible using different models of the same prototype, and some observations were made about the magnitude of structure-structure interaction.

A new apparatus for modelling earthquake behaviour on a centrifuge has been constructed, and has functioned successfully. Experiments on the behaviour of dry embankments and of structures on dry sand, in response to a simulated earthquake perturbation, have yielded interesting quantitative results - in the first case supporting straightforward analytical techniques, while in the second case showing that the real behaviour was very much more complex than initially imagined.

Similar experiments were performed using saturated fine sand, and these displayed all the characteristics normally associated with earthquake behaviour - in particular the generation of substantial excess pore pressures in the soil, followed by loss of strength and large-scale failure of the soil.

There are some problems associated with the centrifugal modelling of saturated soils, and these tests require further development before specific full size soil structures may be modelled in this way. However, it is shown that these problems may be solved, and in general the difficulties associated with apparatus design and construction, and with instrumentation, have been overcome.

It may be concluded simply that it is possible to use a geotechnical centrifuge for accurate physical models of dynamic phenomena and earthquake behaviour in soil mechanics, as has been demonstrated in this thesis, and there is every propect that further refinement of the technique may make it a useful regular tool in dynamic, as well as static, soil mechanics.

APPENDIX A

FUNDAMENTAL EQUIVALENCE OF CENTRIFUGAL MODELLING

As pointed out in section 2.1, there is a one-to-one correspondence between points in a full-scale prototype and geometrically similar points in a centrifuge model of indentical material. If the soil is regarded as a continuum with the same properties in both model and prototype, there seems intuitively to be no immediate way that an element of soil can distinguish whether it is in one or the other. Not only are the values of stress and strain the same, but so too are values of stress and strain gradient, using transformed dimensions in each case.

However it was shown in section 2.3 that the rate of pore water seepage, for instance, obeys a modelling law that is different from that derived from fundamental modelling considerations.

This is because such a problem deals with three absolute dimensions - the overall size of the structure, the soil grain size and the molecular size of the pore fluid. In a centrifuge the overall size is reduced to model size, and the ratio between the grain and pore fluid sizes is kept constant so that the bulk material properties remain the same.

If it were possible to scale down not only the model, but also the grain size and the pore fluid molecular size, then in principle such equivalence would be complete, and it really would be impossible for a hypothetical observer on a centrifuge model to tell that he was not on the full size structure. The logic of this is supported by noting that if this were to

happen, then the coefficient of consolidation C_v would be reduced by a factor n (the modelling scale), and thus by reference to section 2.3 the consolidation time would be reduced by n in a centrifuge model - just like dynamic time - and the exceptions referred to in section 2.3 would no longer exist.

That C_v would be neatly reduced by n in this way, can be shown in one of two ways. It may be regarded as sufficient just to note from a dimensional argument that C_v has dimensions of m^2s^{-1}, and since the dimensions of length and time are both reduced by a factor of n in a centrifuge model, so therefore is C_v .

Alternatively a physical argument may be used. The permeability of a soil of grain size d is found experimentally to be proportional to $\sqrt{d}$, for the same pore fluid. However a reduction in the size of the pore fluid molecules will increase the pore fluid viscosity which is given from kinetic theory as proportional to $\frac{\sqrt{R_o T(MW)}}{N_a \rho r^2}$. Now Avogadro's number N_a , the ideal gas constant R_o , the absolute temperature T and the bulk density ρ will all be constant if the molecular size r is decreased. However the molecular weight (MW) will be proportional to r^3 . Therefore the net viscosity will be proportional to $1/\sqrt{r}$. Each of these factors will reduce the net permeability by a factor of $\sqrt{n}$, so that together, the permeability will be decreased by a factor n - and so too will the coefficient of consolidation.

The important parameter of soil strength would remain unchanged, as the ratio of grain size to pore fluid is constant.

However the entire argument is academic of course, as

the molecular size cannot easily be scaled in the manner indicated, and the real soil and pore fluid must be used if the bulk properties of the soil (i.e. the strength, stiffness and compressibility etc.) are to be modelled correctly.

It is as a result of these fundamental dimensions that these exceptions to the general modelling laws exist. Phenomena such as seepage and diffusion depend on the ratio between the material size and the absolute model dimensions, which is not the same in a centrifuge model as in the full size prototype.

There are other exceptions. Creep induced strain, for instance, will take place at exactly the same rate in a prototype as in a centrifuge model of indentical material. This is because the rate of creep is dependent on the dislocation spacing in the material concerned. If this dislocation spacing was itself scaled down in the model material in proportion to the modelling scale, then the time taken for a given amount of creep to take place would be similarly reduced, in accordance with the normal modelling laws.

In summary, if it were possible to scale down every aspect of a centrifuge model, right down to the molecular level, the the equivalence between such a model and the real prototype would be exact. As this is not possible, there are certain exceptions to the modelling laws, and these must usually be considered on an "ad hoc" basis.

APPENDIX B - EFFECTS OF CORIOLIS ACCELERATIONS

It is convenient to consider the centrifuge tip velocity V as the parameter most representative of centrifuge performance. If the height of a centrifuge model is restricted to 10% of the centrifuge radius R, then this corresponds at a velocity V to an equivalent prototype height of $(0.1\,R)\ (V^2/R) \times \frac{1}{g} = \frac{V^2}{10g}$. Thus the maximum prototype height is a function only of the centrifuge tip velocity, which is in turn limited only by the material properties and design of the centrifuge itself, and not by the absolute radius of the centrifuge.

For the installation at Cambridge, the maximum velocity is about 80 m/s.

If motion takes place with a velocity V in the plane of the centrifuge itself, then it will give rise to a Coriolis acceleration of magnitude $2\Omega v$ where $\Omega = V/R$ is the angular velocity of the centrifuge. If this is limited to 10% of the centrifugal acceleration, then

$$2(V/R)v \leq 0.1\ V^2/R \quad , \quad \text{or} \quad v \leq V/20 \quad .$$

This implies that if the velocities in any dynamic experiment are less than about 5% of the centrifuge tip velocity, then the effects of Coriolis acceleration will be small. Since peak earthquake particle velocities very rarely exceed 1 m/s, this would certainly seem to be the case for most earthquake experiments.

In the case of the earthquake experiments reported in this thesis, the peak earthquake velocity was only 0.5 m/s, and in a direction not subject to Coriolis effects, so that only

second order motions would be affected in this way. The results reported in Chapter 12 supported this, as the tests showed that sand particles rolling down a slope did so directly down the line of greatest slope, without any observable deviations due to Coriolis forces.

The Coriolis effects that arise in a cylindrical rocking tower are rather more complex. Considering such a tower of height h, radius a, and density ρ, rocking about its base at the natural frequency of the soil-structure system in the direction indicated by the rotational vector $\dot{\theta}$ in the sketch. In this orientation the effect of Coriolis acceleration will be small for a "slender" tower, but will still affect a point off the centreline of the tower, as indicated by the position vector $\underset{\sim}{r}$ in the accompanying sketch.

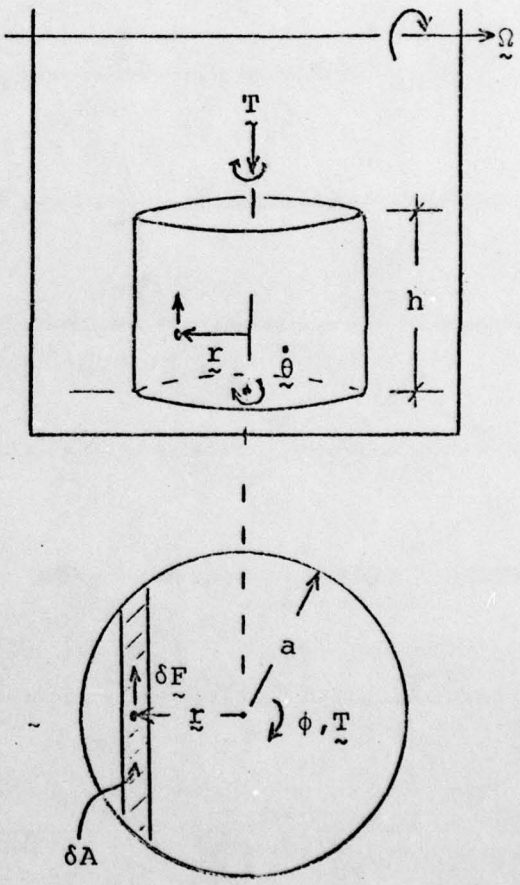

If the rotational velocity vector of the tower is $\dot{\theta}$ about its base as a result of this rocking motion, then the component of velocity of the point in the plane of the centrifuge is $\dot{\underset{\sim}{\theta}} \times \underset{\sim}{r}$. Then the Coriolis acceleration becomes $2\underset{\sim}{\Omega} \times (\dot{\underset{\sim}{\theta}} \times \underset{\sim}{r}) = 2\dot{\underset{\sim}{\theta}}(\underset{\sim}{\Omega}.\underset{\sim}{r}) - 2\underset{\sim}{r}(\underset{\sim}{\Omega}.\dot{\underset{\sim}{\theta}})$ and the second term is zero as the vectors $\underset{\sim}{\Omega}$ and $\dot{\underset{\sim}{\theta}}$ are perpendicular.

Carefully taking account of the direction of this acceleration, the net result on the cylindrical model is to

produce a torque $\underset{\sim}{T} = \int_{-a}^{a} \delta\underset{\sim}{F} \times r = \int_{-a}^{a} (h\rho dA)(2\dot{\theta}.\Omega r) r =$

$2\rho h \dot{\theta} \Omega \int_{-a}^{a} dA\, y^2$ in the direction shown. The integral is simply the second moment of area of the circular cross-section about its centre line, and is equal to $\frac{\pi a^4}{4}$. Thus the magnitude of the torque T is $\frac{\pi}{2} \rho h \dot{\theta} \Omega a^4$, fluctuating in accordance with the natural rocking frequency of the tower w_n, so that $|\dot{\theta}| = w_n \theta$.

Since the natural frequency of torsional vibration is much higher than the rocking frequency, for a tower of any appreciable height, the angle of rotation ϕ in torsion in response to the torque T may be estimated quasi-statically by writing $\phi = \frac{T}{16\ Ga^3/3}$, where the denominator is the static torsional stiffness of a circular foundation on an elastic half-space of shear modulus G.

Combining this with the previous expression for T gives $\frac{\phi}{\theta} = (\frac{3\pi\ \rho ha}{32\ G})\ w_n \Omega$. However the rocking frequency of the tower w_n is given by:

$$w_n^2 = \frac{\text{base stiffness of tower in rocking}}{\text{moment of inertia of tower in rocking}} = \frac{8Ga^3/3(1-\nu)}{Mh^2/3} =$$

$$= \frac{8\ Ga}{(1-\nu)\pi\rho h^3} \quad . \text{ Eliminating G then gives:}$$

$$\frac{\phi}{\theta} = \frac{\Omega}{w_n} \left(\frac{3}{4(1-\nu)}\right) \left(\frac{a}{h}\right)^2 \quad .$$

For the experiments reported in this thesis, $\frac{a}{h} \simeq 0.16$ for the towers, the rotational frequency of the centrifuge Ω was about 13 radians/sec., and the circular rocking frequency of the model towers was of the order of $2\pi \times 100$ Hz $\simeq 600$ radians/sec. Therefore this analysis implies that the dynamic torsional rotation ϕ caused by second-order Coriolis forces

should only be 0.05% of the associated rocking rotation θ, and this is clearly small.

It is surprising therefore that it was reported in Chapter 9 that such a cylindrical tower was seen not only to undergo a torsional rotation in response to earthquake perturbation, but actually a uni-directional rotation (for which there is no explanation using this model). This phenomenon disappeared when thin rectangular towers with a low second moment of area were used, but it nevertheless remains a mystery why it should have occurred when the preceding analysis predicts that Coriolis effects should be negligible.

However the theoretical indications are in general that Coriolis effects are small and a function mainly of the centrifuge tip velocity. In all respects except that just mentioned, the existence of substantial Coriolis forces has not been observed experimentally.

APPENDIX C - PREPARATION OF SILVER AZIDE

For certain experiments previously described, it was necessary to use a small quantity of explosive that could be easily detonated. Detonating caps available commercially were simply too powerful for these requirements and would also have required the use of an officially approved explosives store. Consequently small quantities of silver azide powder were manufactured specially, as this material could easily be thermally ignited by means of an electrical resistance wire, but was insensitive to mechanical shock and could be handled safely. A quantity of about 10 milligrams was generally found to be sufficient for each miniature explosion, as the energy release is about 2 Joules per milligram.

Silver Azide AgN_3 decomposes slowly to nitrogen and silver in response to light or to temperatures above 250° C. It will explode violently at a temperature of 340° C when pure, but the presence of impurities "sensitizes" the material and can reduce the explosion temperature to 270° C.

Although silver azide is itself not readily available, it may easily be prepared by precipitation, by combining solutions of sodium azide and silver nitrate, both of which are readily available. If about 13 milligrams of sodium azide and 34 milligrams of silver nitrate are combined in this fashion, a white cloudy precipitate of about 30 milligrams of silver azide will be formed. This can be collected either by filtering through filter paper, or by centrifuging in a test tube centrifuge, which produces a denser deposit of material and was found to be preferable. The solid may then be dried and stored in a light proof container.

By commercial standards the quantity of detonating explosive involved was very small, but in the interests of safety the silver azide was only prepared immediately prior to a set of tests, in suitable amounts, and kept in a locked box. The detonating circuits were short circuited until just before detonation to eliminate any spurious electrical currents, the explosive was handled wearing safety glasses, and was only introduced into the detonation chamber immediately before the experiment. Details involving normal safety procedures are available from explosive manufacturers.

Further information on the chemistry of silver azide may be found in the paper by Gray and Waddington*(1957).

---

* GRAY, P. and WADDINGTON, T. C. (1957) "Thermal decomposition of silver azide and its sensitisation by artificial lattice defects", Proc. Royal Society, Series A, Vol. 241

APPENDIX D - INSTRUMENTATION SPECIFICATIONS

ACCELEROMETERS

The miniature piezo-electric accelerometers were purchased from D.J.Birchall Ltd., Mildenhall, Suffolk, U.K., and were denoted as model A/23/T. The mass of each was 4 grams, and the external dimensions exclusive of the microdot connector were 9.5mm × 9.5mm × 7.2mm. The case was of stainless steel, with seams that were sealed with electron beam welding, and hence the only source of possible water leakage was at the microdot connector. It was found that smearing the completed connection with silicone jelly glue produced an adequate seal. The devices were constructed with a small length of integral threaded stud, for easy fastening to rigid surfaces, where necessary.

The nominal charge sensitivity was 3 pC/g, and, with an internal capacitance of 550 pF excluding the signal lines, this corresponded to a voltage sensitivity of about 5.5 mV/g. The output signal was passed along waterproof p.t.f.e. insulated coaxial cable, with an additional capacitance of 100 pF. per metre length, which correspondingly reduced the overall voltage output, and so it was advantageous to keep these output cables very short. The signal was subsequently amplified as described shortly.

The maximum rated continuous acceleration was 1000 g, and the maximum sensitivity to out-of-plane accelerations was 3% of the sensitivity along the axis. The frequency response was flat to around 30,000 Hz. Each device was individually calibrated and the net cost was around £90.

PORE PRESSURE TRANSDUCERS

These were manufactured by Druck Ltd., Groby, Leicestershire, U.K., and were approximately 0.3 gram in weight and about 5mm in diameter and 10mm long. Four separate p.t.f.e. insulated wires were permanently attached via a waterproof connection. Excitation of 10 volts d.c. max. was applied to two of these wires, and the output was provided between the other two - the silicon strain gauge bridge being totally internal and self-contained.

The device used was linear to 350 kPa., with a 300% overload capacity, and a sensitivity of about 0.05 mV/kPa. per volt of power supply. This corresponded to a maximum output of about 0.15 volts, with an output impedance of around 1000 ohms. They were thermally compensated, and the thermal zero shift was quoted as 80 μV per degree Centigrade, or less. The acceleration sensitivity was about 5 μV per g perpendicular to the plane of the sensing diaphragm (and much less in the other directions).

Before use the porous tips had to be deaired - either by boiling in water, or preferably by immersion in water under a vacuum. Ceramic tips of various kinds could be supplied, but it was found that with the standard porous stone the measurable rate of increase of pressure was as high as 10^7 kPa/s. Each device was individually calibrated by the manufacturer, and the net cost was about £150.

ACCELEROMETER AMPLIFIERS

These devices were fabricated inexpensively in the laboratory, and were mounted inside the "junction box". A circuit

diagram of the design is shown in Figure 37.

The first part of the circuit used a field effect transistor as a voltage follower, to lower the impedance of the accelerometer output signal without amplifying it. This was necessary because the piezo-electric accelerometers produced essentially a pure charge at zero current capacity, and a normal amplifier circuit would have required an appreciable current input. The value R of the earth resistor was chosen to give a frequency response that "rolled off" below a frequency of about 25 Hz., according to the formula $f = \frac{1}{2\pi RC}$, where C is the capacitance of the accelerometer and leads. In this way, any spurious low-frequency motions were automatically filtered out.

The signal was then amplified by a factor of 100 by passing it through a conventional amplifier, a.c. coupled to the previous output, as shown in Figure 37, and the signal then passed to the multipin connector on the top of the junction box. Six channels of each circuit were constructed in parallel, and the power supply of ± 15 volts was provided externally. The net output of the accelerometers after amplification was about 0.5 volts per g.

INTEGRATING NETWORK

This device could be used either during a test or at a later stage, to electronically integrate and filter any desired a.c. signal either once or twice, after the signal had been passed out of the centrifuge via the slip rings.

Six parallel channels were constructed in a self-contained box, in such a way that a signal from the centrifuge could be

plugged into each channel. It was first passed through a low pass filter, attenuating frequencies above 1500 Hz., so that any spurious transients in the acceleration trace would be eliminated, and this filtered acceleration signal could be recorded directly from a suitable output plug.

The signal was then passed through a high pass filter, "rolling off" below about 22 Hz., in order to eliminate any d.c. component, and then passed through an integrating amplifier. This is equivalent to an amplifier with gain inversely proportional to frequency (except at low frequencies because of the high pass filter), and the circuit constants were chosen in such a way that at 60 Hz (which was the model earthquake frequency) the gain was unity. This velocity signal could be recorded from a suitable output plug.

This procedure was then repeated once more, enabling a displacement signal to be finally recorded, if desired.

This device was also inexpensively fabricated in the laboratory, and an external power supply of ± 15 volts supplied. The relevant circuit diagram is shown in Figure 37.

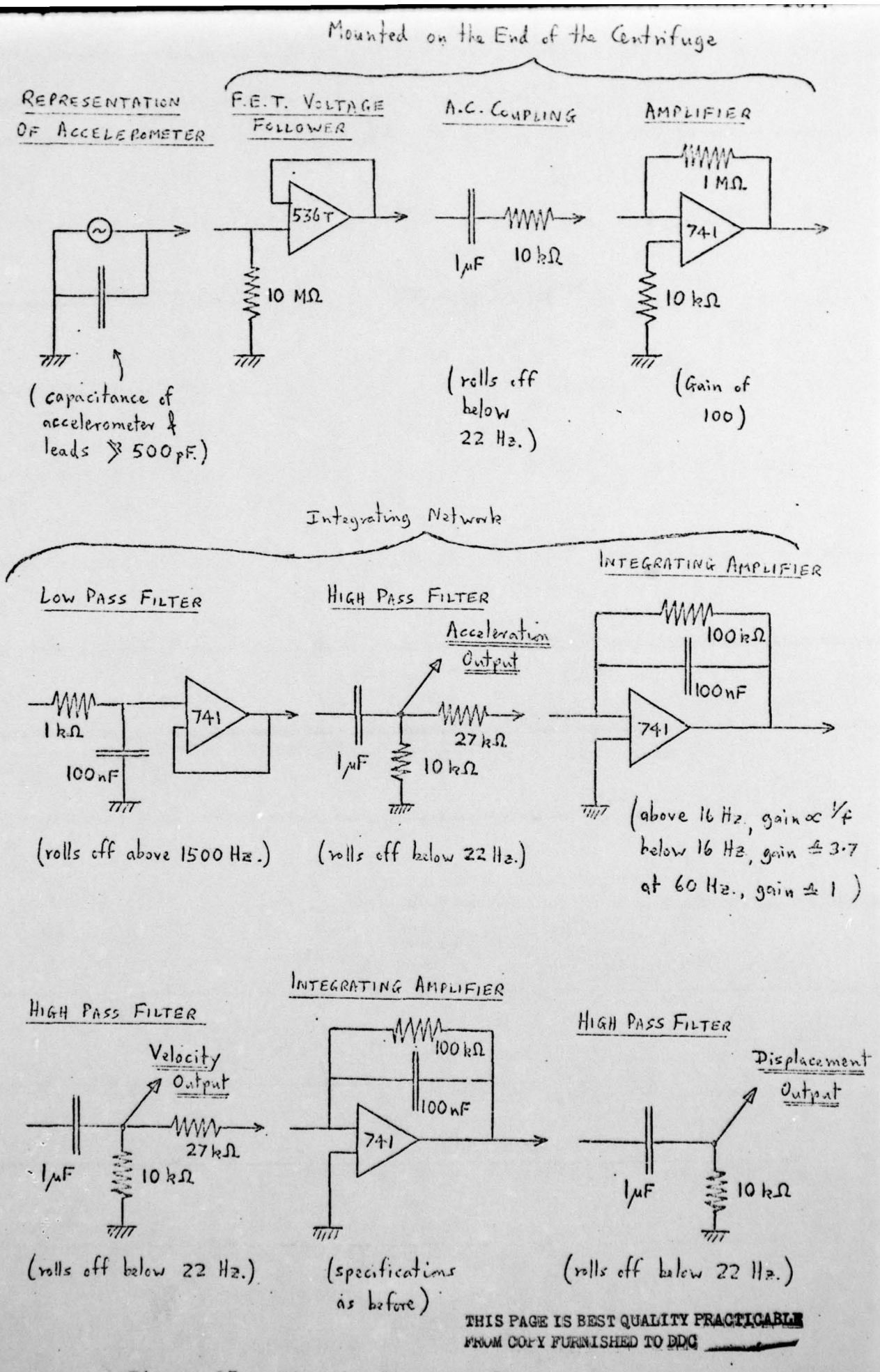

Figure 37 - Circuit diagrams for accelerometer preamplifiers and integrating circuitry

APPENDIX E

NATURAL FREQUENCY OF HORIZONTAL TRANSLATION

The spring constant for horizontal translation of a rigid circular footing of radius r on an elastic half-space of shear modulus G, is given by Bycroft*(1956) as $\frac{32(1-\nu)Gr}{7-8\nu}$. For a structure of mass M and moment of inertia I, the natural frequency of horizontal motion will be $\frac{1}{2\pi}\sqrt{\frac{(4.8\ G\nu)}{M}}$, assuming Poisson's ratio $\nu \simeq 0.25$.

Now equation (3) in section 5.3 gives the natural frequency of rocking as $0.30\sqrt{\frac{Gr^3}{I}}$, and dividing one by the other, the ratio between the two frequencies is $\frac{1.16}{r}\sqrt{\frac{I}{M}}$.

If the structure is of approximately uniform cross section and height h, then $I \simeq Mh^2/3$, and this ratio becomes $0.7\ h/r$. For the models tested here, $h \simeq 0.25m$ and $r \simeq 0.04m$, implying that the natural frequency of horizontal translation is about 4.4 times larger than that for rocking, and that this value depends primarily on the "aspect ratio" of the structure.

Since typical values of rocking frequency were measured as about 100 Hz., values for horizontal translation would have been about 450 Hz., and the two frequencies would be quite distinct and there would be little likelihood of confusion or of interaction.

---

* BYCROFT G.N.(1956) "Forced vibrations of a rigid circular plate on a semi-infinite elastic space and on an elastic stratum" Trans.Royal Society, Series A, Vol.248.

APPENDIX F - USE OF THE STATIC SPRING STIFFNESS

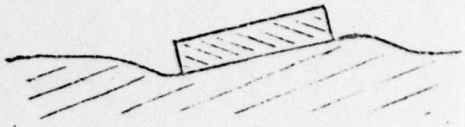

To predict the natural frequency of a rocking foundation on an elastic half-space, the rotational spring stiffness in response to a static torque is usually used. This is clearly an accurate approximation at low frequencies, but must be modified at very high frequencies when the wavelength of waves radiated into the soil decreases and becomes comparable with the diameter of the foundation. This is because the body waves radiated by one side of the foundation will start to interfere with those from the other side. It is necessary to demonstrate that this is not the case here.

The shear wavelength is given by $\lambda = V/f$ from elementary wave mechanics, and the shear wave velocity by $V = \sqrt{\frac{G}{\rho}}$, where ρ is the material density and f is the frequency. The dynamic shear modulus G under a model tower foundation was estimated in section 5.4 as 118 MPa., so that for a density of 1600 kg/m^3, the wave velocity was approximately 270 m/s. This value is relatively insensitive to the particular tower properties, as it is proportional only to the square root of the shear modulus.

As the maximum observed natural frequency of a rocking tower in the tests described was about 150 Hz., the minimum value of wavelength will therefore have been about 1.8 metres. Since the maximum base dimension was 0.09 metres, or only $1/20$ of the wavelength, it is clear that the static spring stiffness will have been quite adequate in these calculations.

An alternative approach is to consider the non-dimensional

frequency parameter a_o used in the literature, notably in the book by Richart, Hall and Woods (1970). This is defined as $a_o = \frac{r\omega}{V}$, where r is the base radius, ω is the circular frequency and V is the shear wave velocity. For values of a_o less than about 0.3, the static spring stiffness may be used. In this case, from the values used previously, $r = 0.045$m, $w = 2\pi \times 150$ Hz., and $V = 270$ m/s, so that $a_o = 0.16$, and the condition is not violated.

This is actually an equivalent analysis, as the factor $a_o = \frac{r(2\pi f)}{V}$, and, writing $V = f\lambda$ for the wave speed, $a_o = 2\pi(r/\lambda)$, showing that the factor a_o is proportional to the ratio between the base radius and the shear wavelength. In other words, if a_o is high, the base dimension is of similar size or larger than the shear wavelength, and the static spring stiffness must be modified, as pointed out earlier.

APPENDIX G - SAND SPECIFICATIONS

COARSE SAND

All tests on dry soil used the same coarse sand. This was Leighton Buzzard 14/25 sand (the numbers denoting the passing and retaining British Standard sieves respectively) - a relatively uniform sand of medium angularity with a particle size between 0.6mm and 1.2mm. This was always deposited by vibration and the resultant density was consistently about 1610 kg/m^3, measured in-situ, corresponding to a voids ratio of about 0.65. The angle of friction of this sand is usually taken as around 35^o from static tests.

Dynamic properties of this sand were measured in a resonant column apparatus, at the Waterways Experiment Station, Vicksburg, U.S.A. Values of the dynamic shear modulus and Young's modulus are plotted in Figure 38 for different values of confining pressure and shear strain. At lower values of confining pressure (similar to those encountered in the model tests) the shear modulus corresponds closely to the empirical relation suggested by Hardin and Drnevich and discussed in Section 5.4, while at higher values it appears to diverge somewhat. However the results were adjudged to be acceptable on the basis of considerable experience in conducting these tests.

In a similar fashion Figure 39 shows values of damping from both longitudinal and torsional excitation, at various values of confining pressure and shear strain.

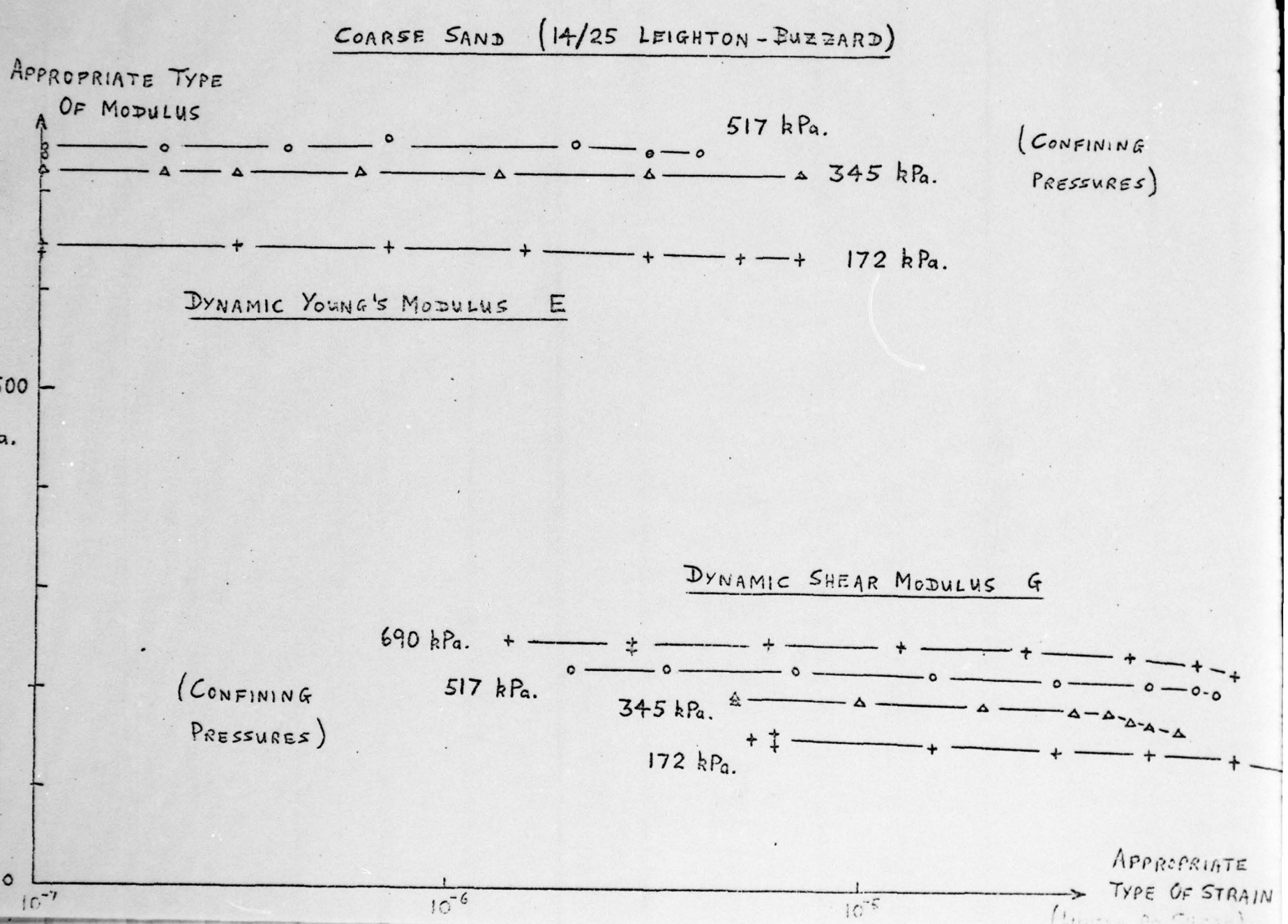

Figure 38 - Experimental dynamic moduli for coarse sand

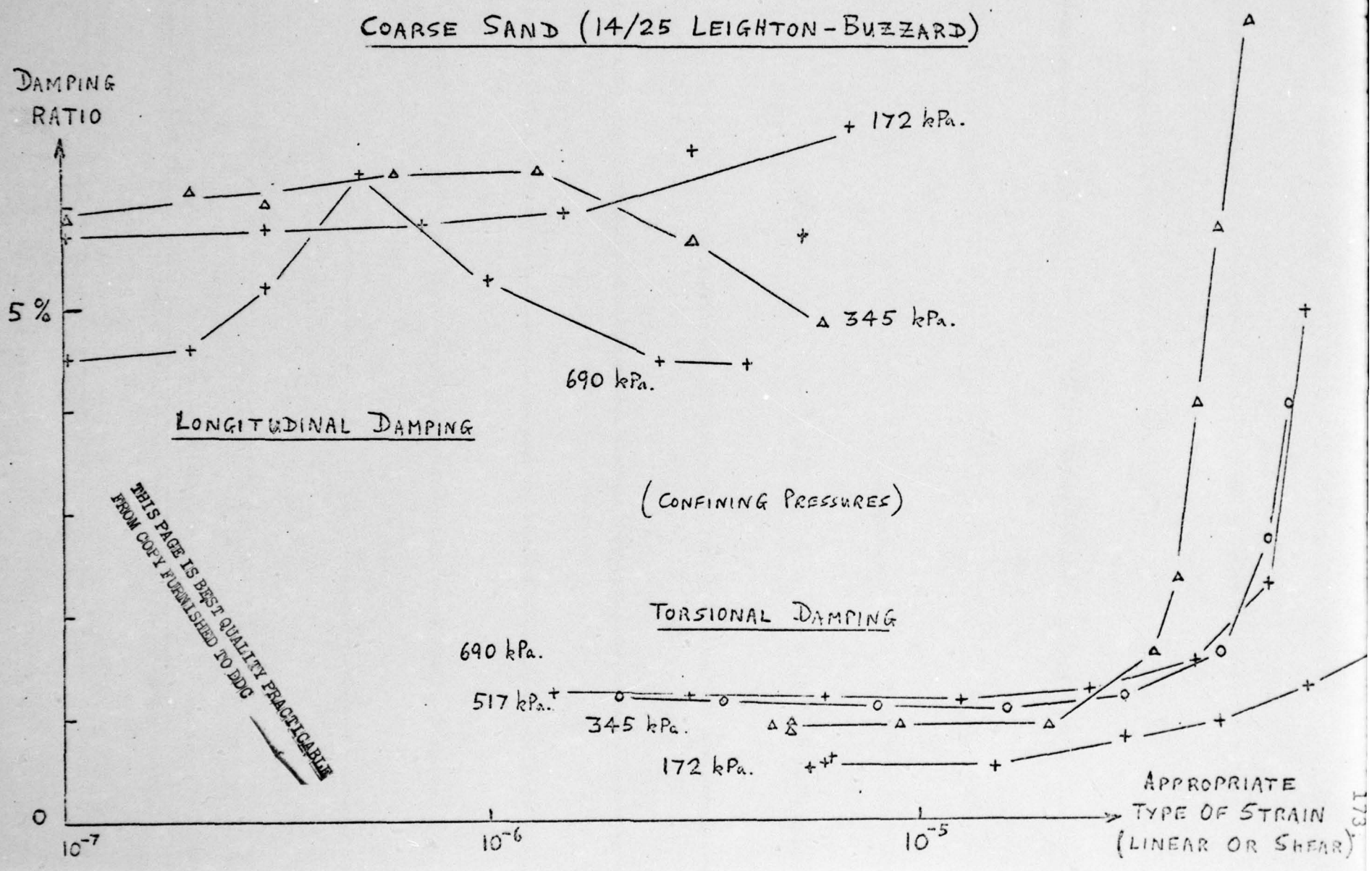

Figure 39 - Experimental damping values for coarse sand

FINE SAND

All tests on saturated soil used the same fine sand. This was Leighton-Buzzard 120/200 sand - a uniform sand with a particle size between 0.07mm and 0.13mm.

"Maximum" and "minimum" densities for this sand were measured as 2000 kg/m^3 and 1815 kg/m^3 respectively, when saturated, corresponding to voids ratios of 0.65 and 1.025. For the wet embankment tests, the in-situ density was estimated as 1860 kg/m^3 by attempting to reproduce the method of deposition in a measuring cylinder, corresponding to an in-situ voids ratio of about 0.92. Consequently the "relative density" of the sand in the wet embankment on the basis of voids ratio was about 28%.

The permeability of the fine sand was about 2×10^{-4} m/s, and at a pressure of 75 kPa the coefficient of volume compressibility was measured as about 1.5×10^{-8} Pa^{-1}, so that the coefficient of consolidation was roughly 1.5 m^2/s. These are representative figures for fine sand, as also are the values of dynamic shear modulus.

The dynamic properties of this sand were also measured in the same way as for the coarse sand, and are presented in Figures 40 and 41 for further reference, although they are not used in the course of this thesis.

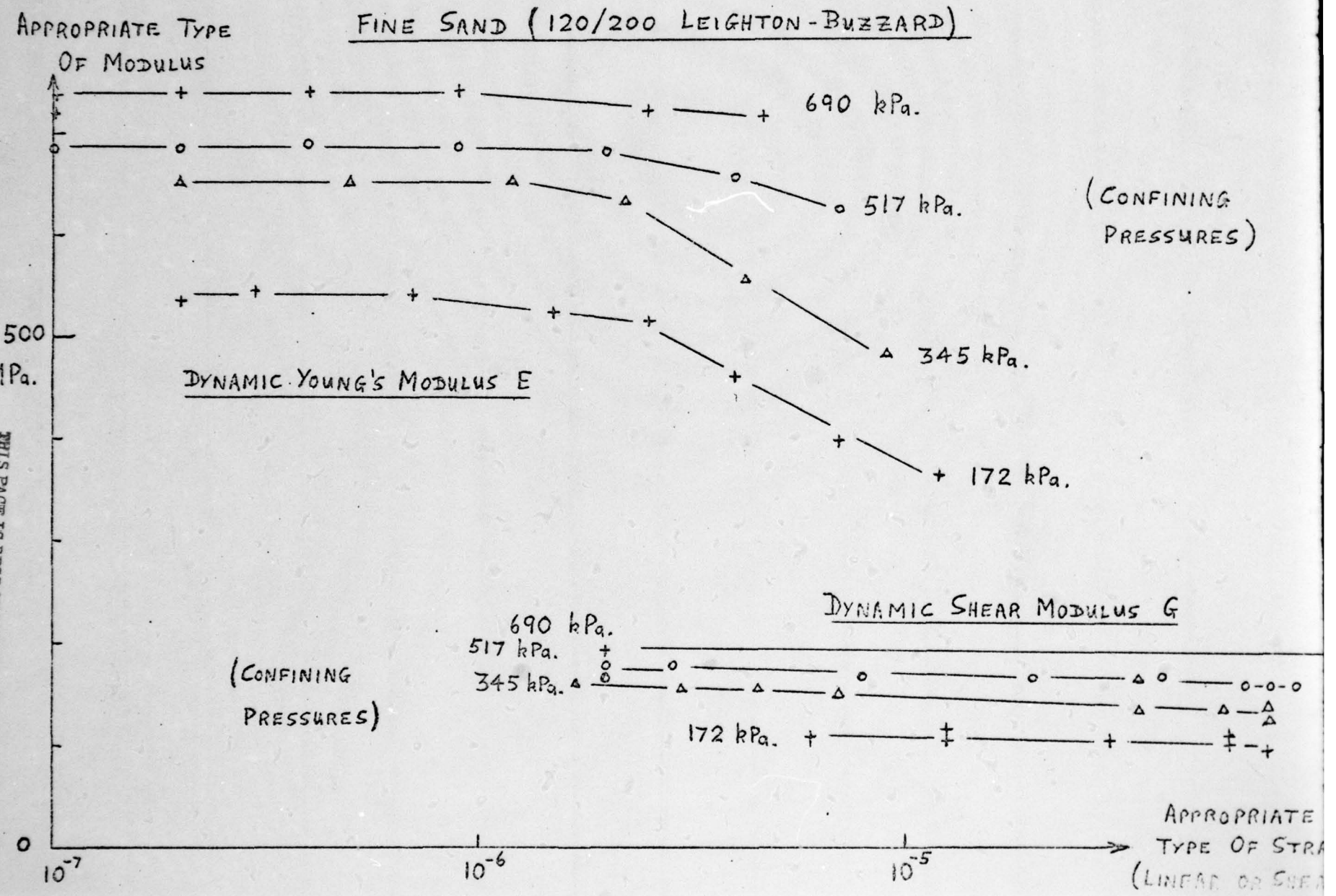

Figure 40 - Experimental dynamic moduli for fine sand

AD-A083 972 CAMBRIDGE UNIV (ENGLAND) DEPT OF CIVIL ENGINEERING F/G 8/13
CENTRIFUGAL MODELLING OF SOIL STRUCTURES. PART II. THE CENTRIFU--ETC(U)
JUN 79 D V MORRIS, A N SCHOFIELD DA-ERO-76-G-040
NL

UNCLASSIFIED

3 OF 3
AD
A083972

END
DATE
FILMED
6-80
DTIC

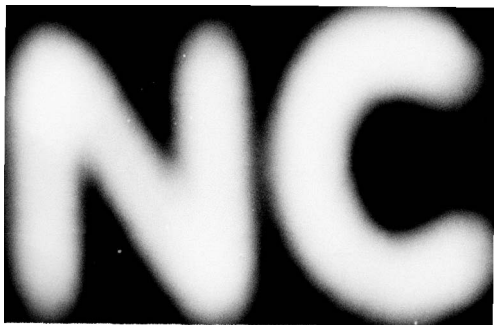
NC

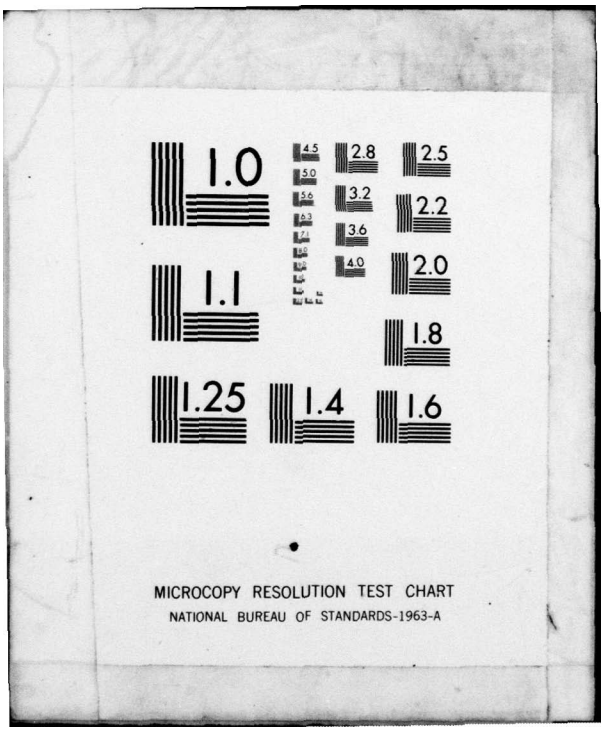
1.0
1.1
1.25
1.4
1.6
1.8
2.0
2.2
2.5
2.8
3.2
3.6
4.0
4.5
5.0
5.6
6.3
7.1
8.0
9.0
MICROCOPY RESOLUTION TEST CHART
NATIONAL BUREAU OF STANDARDS-1963-A

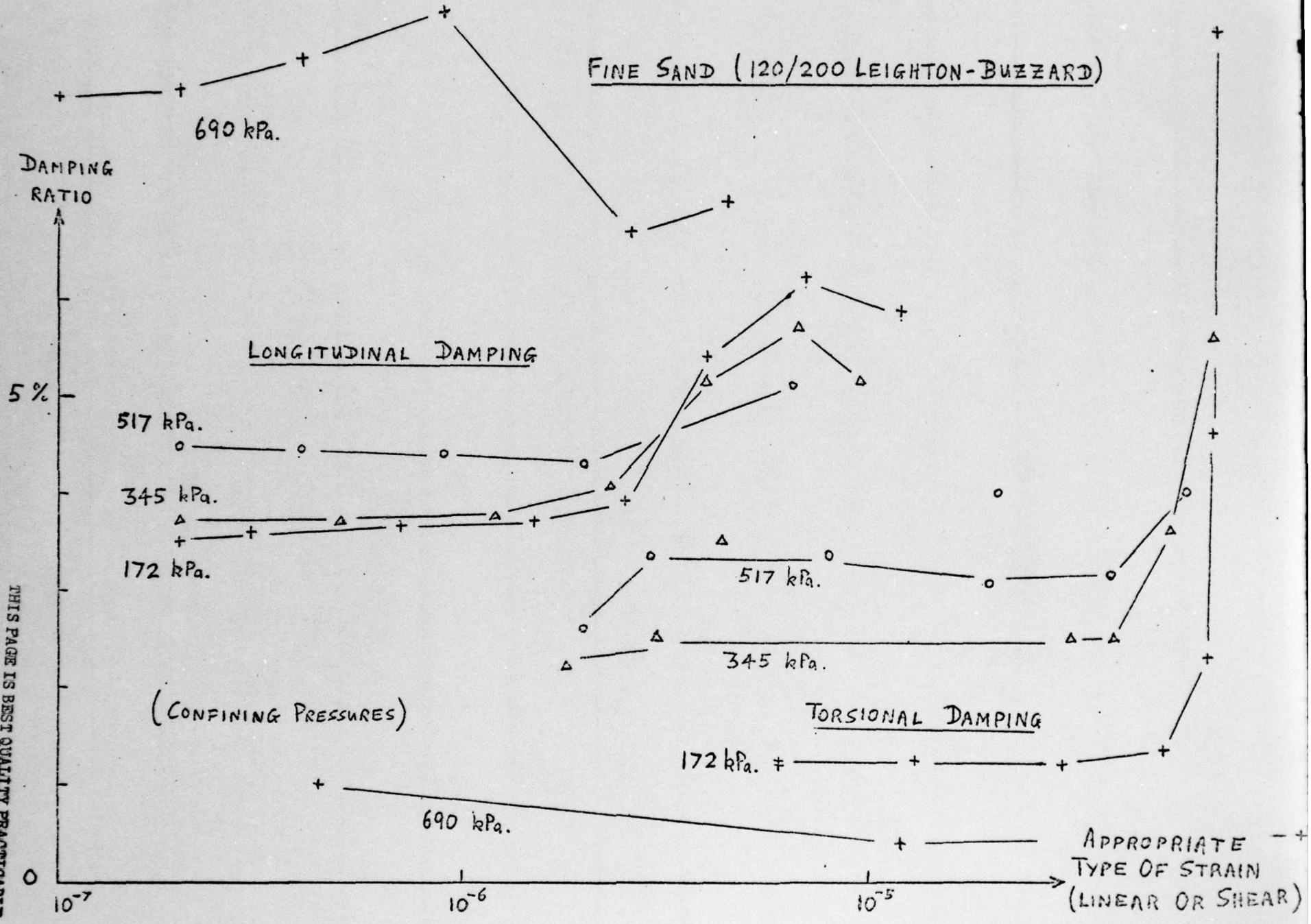

Figure 41 - Experimental damping values for fine sand

APPENDIX H - FOUNDATION STRAIN MAGNITUDES

In order to estimate the magnitude of shear strain under a rotating foundation, consider elements of soil underneath the foundation, deforming as shown in the sketch. The shear strain of the soil mass is then simply equal to the angular rotation of the structure and its base.

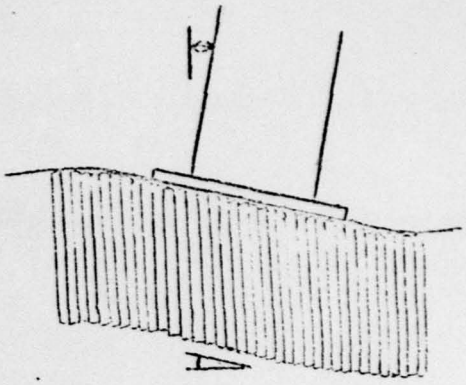

In order to make a rough estimate of this quantity, Figure 4 shows the motion of a tower top in terms of full size prototype values. This shows a typical wind-induced amplitude of about 0.1mm, and as the tower is 6.5m high this corresponds to an angular rotation (and shear strain) of 1.5×10^{-5}. As noted in Section 5.4 it has been found that there is no appreciable strain-softening for strains below about 2.5×10^{-5} and this enables the analysis of tower motion to ignore strain softening.

However it is clear that explosive perturbation, for instance, causes oscillatory movement of the order of 1mm, corresponding to a cyclic strain amplitude of 15×10^{-5}, and the effect of the resultant strain-softening can be seen by the slight reduction in the natural frequency at that point.

APPENDIX I - DETAILS OF EARTHQUAKE APPARATUS

SUSPENSION SYSTEM

As outlined in Chapter 7, the apparatus consisted of a lower portion, dubbed the "suspension system" and illustrated in Figure 21 and Plate 7. This was relatively self-contained, and its main function was to carry the weight of the apparatus as a whole, but in a flexible fashion, so that horizontal motion could take place freely.

This "suspension system" consisted of a welded aluminium grillage, supported on each side by two side beams of heat treated alloy steel via 38 high tensile friction grip bolts. These beams were suspended at their ends by thin suspension strips of high strength steel, hanging inside vertical steel rectangular hollow sections, to which they were bolted at the top. These rectangular hollow sections were welded together in a frame which located them correctly, and which could be bolted straight onto the centrifuge swinging platform.

As far as possible bolted connections were used, in conjunction with high tensile friction grip bolts torqued to their proof stress. This allowed relative ease of assembly, and at the same time resulted in connections that were very strong and stiff, without forming stress concentrations that might otherwise lead to fatigue failure. Plans of this part of the apparatus are shown in Figures 42 to 44. The load carrying capacity was tested with hydraulic loading machines, subjecting it to vertical loads of up to 80 tonnes force.

The use of hanging strips was an important design feature as they combined great flexibility in the single horizontal direction with stiffness against overall rotation, and with a

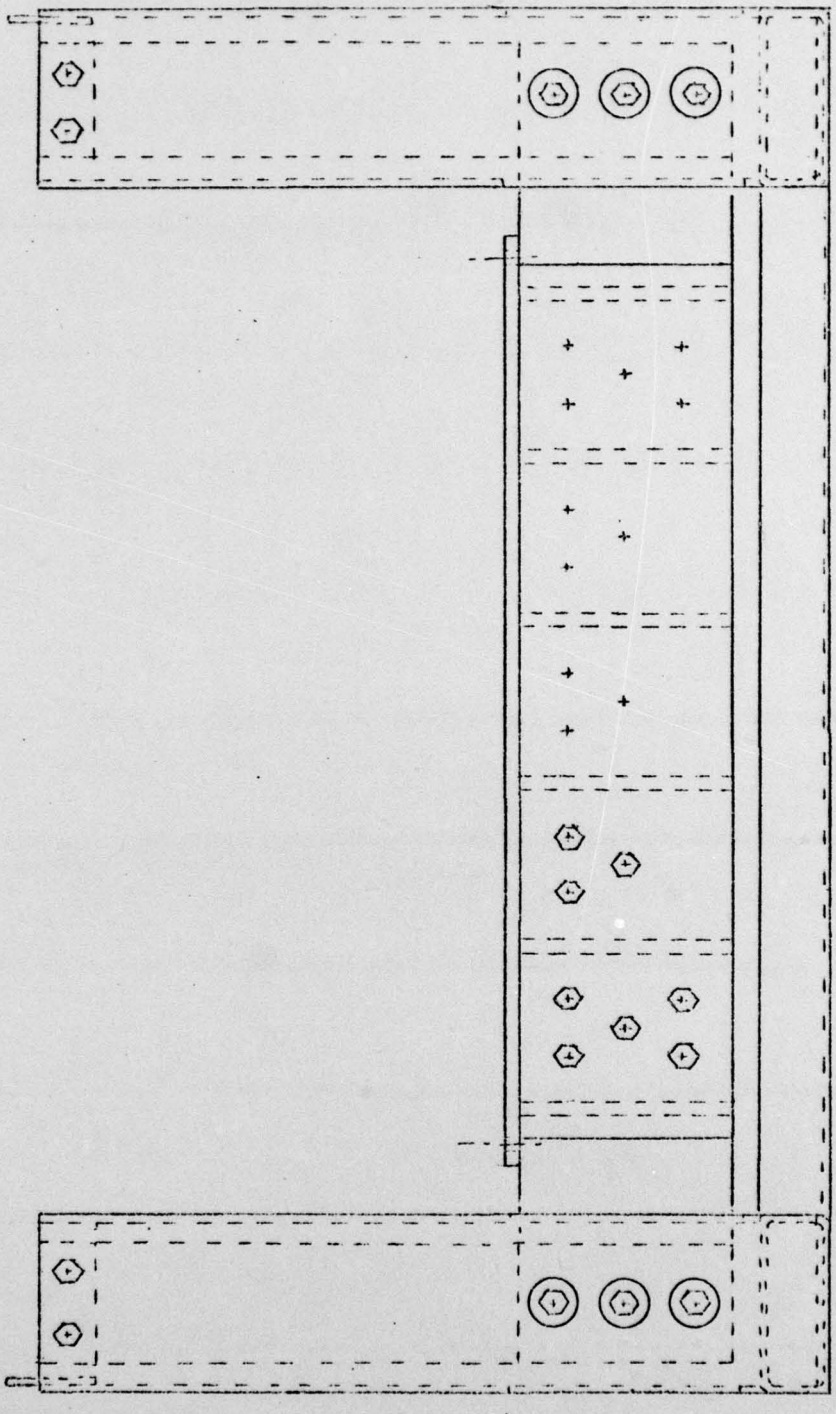

Figure 42 - Elevation of suspension system

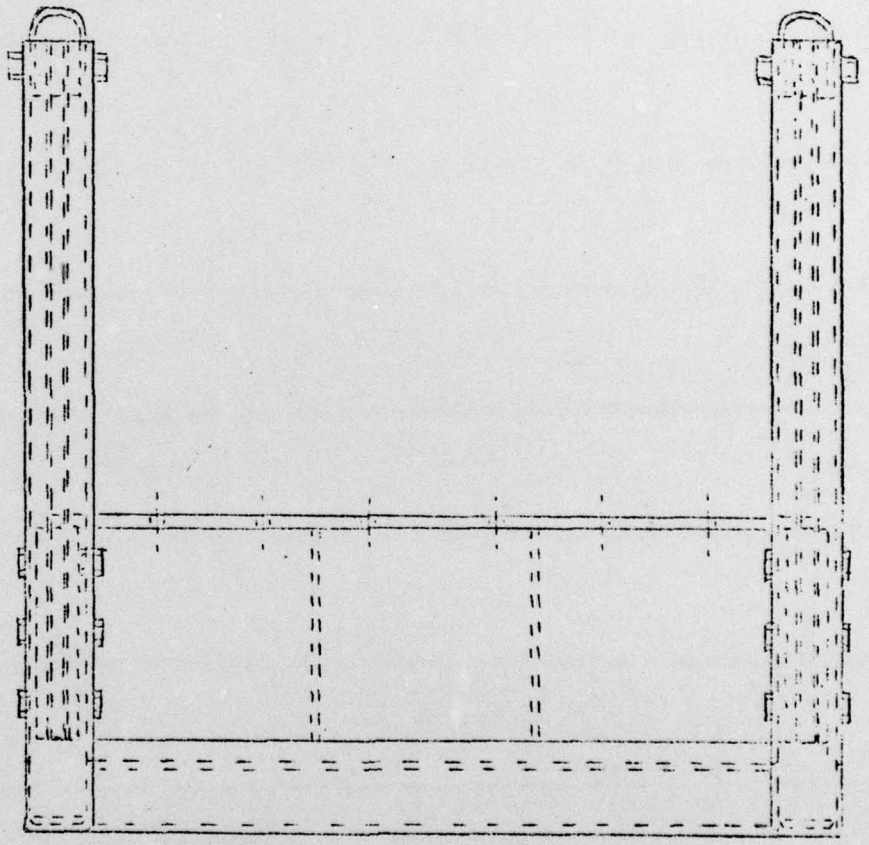

END ELEVATION OF SUSPENSION SYSTEM

(SCALE ± 1/5 FULL SIZE)

10 MM.

Figure 43 - End elevation of suspension system

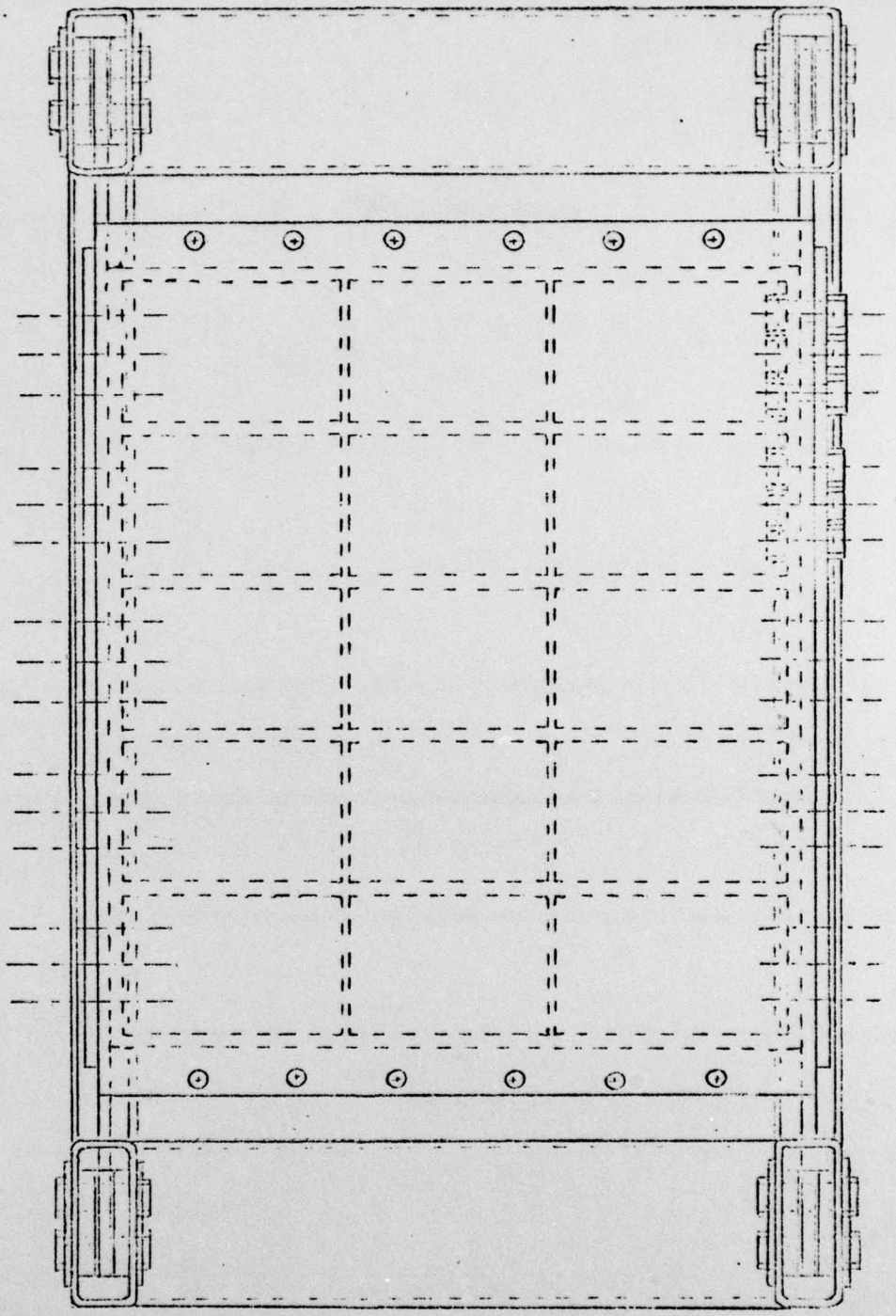

PLAN OF SUSPENSION SYSTEM (SCALE ≈ 1/5 FULL SIZE) 10 mm.

Figure 44 - Plan of suspension system

large carrying capacity vertically.

Considering the performance of such a hanging strip of thickness t, breadth b, length ℓ, and Young's Modulus E, then its stiffness in double bending is $Eb(t/\ell)^3$. However, added to this is the "pendulum stiffness" of W/ℓ, when the strip is carrying a weight W. This "pendulum stiffness" is significant at the large values of acceleration in the centrifuge, and is very insensitive to anything except the length of the hanging strip.

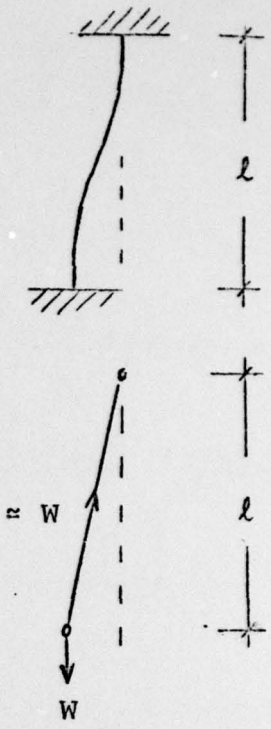

The length of the hanging strip was dimensioned on the basis of this "pendulum stiffness", to give the required amount of horizontal flexibility, and hence dynamic isolation. The strip thickness was then determined so that the bending stiffness was only a small fraction of the "pendulum stiffness". Lastly the breadth of the strip was dimensioned so as to give a sufficiently large load carrying capacity.

MAIN CONTAINER AND SPRINGS

This is shown in an isometric sketch in Figure 22, and served to contain the soil sample while simultaneously subjecting it to the desired horizontal movement. The container was of welded aluminium for lightness, and the base of this was bolted to the top of the grillage on the "suspension system". Plans of this part of the apparatus are shown in Figures 45 to 48.

In order to sustain the soil pressure the box was ribbed on all sides - the ribbing in the long direction being horizontal

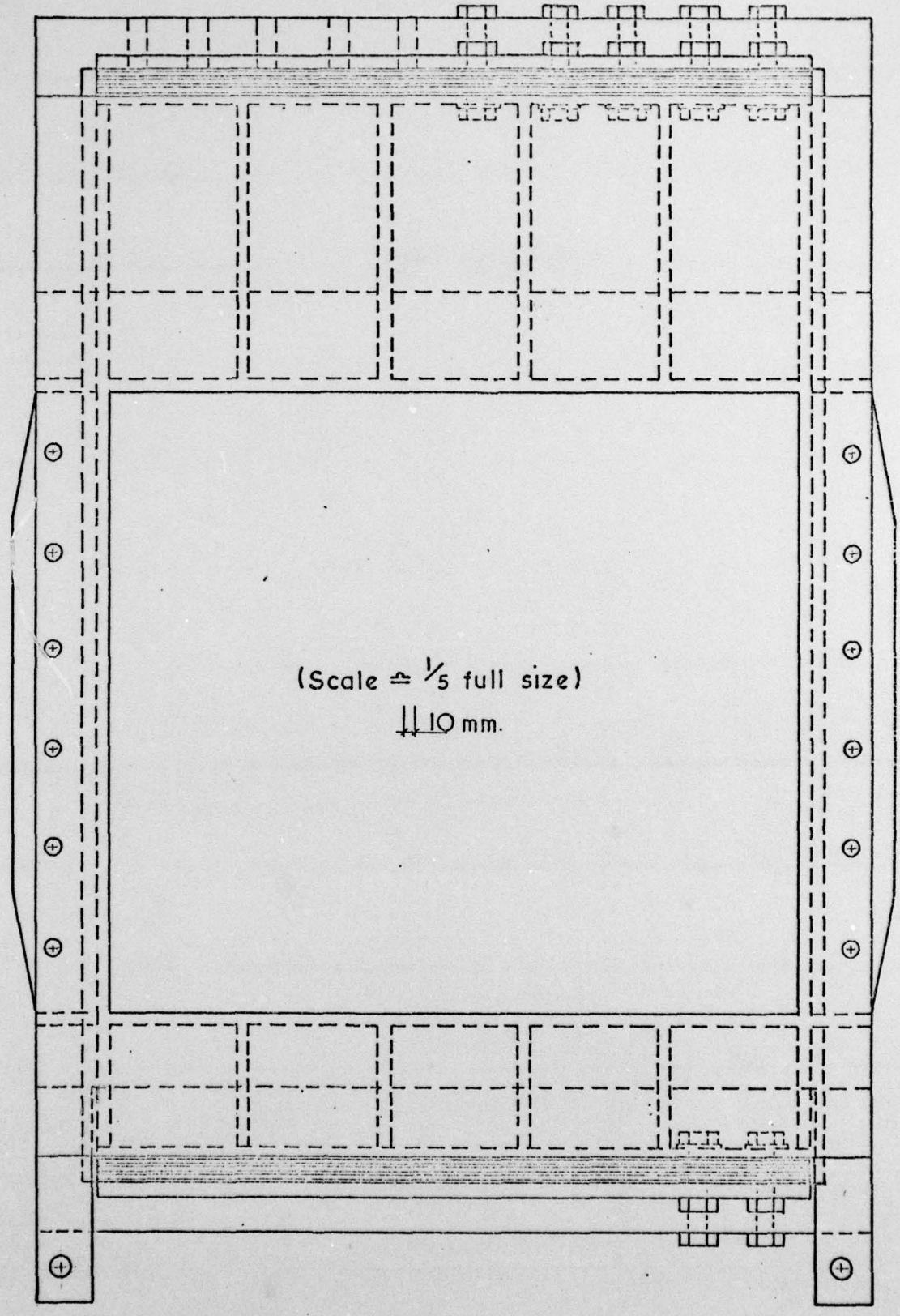

Figure 45 - Tub plan

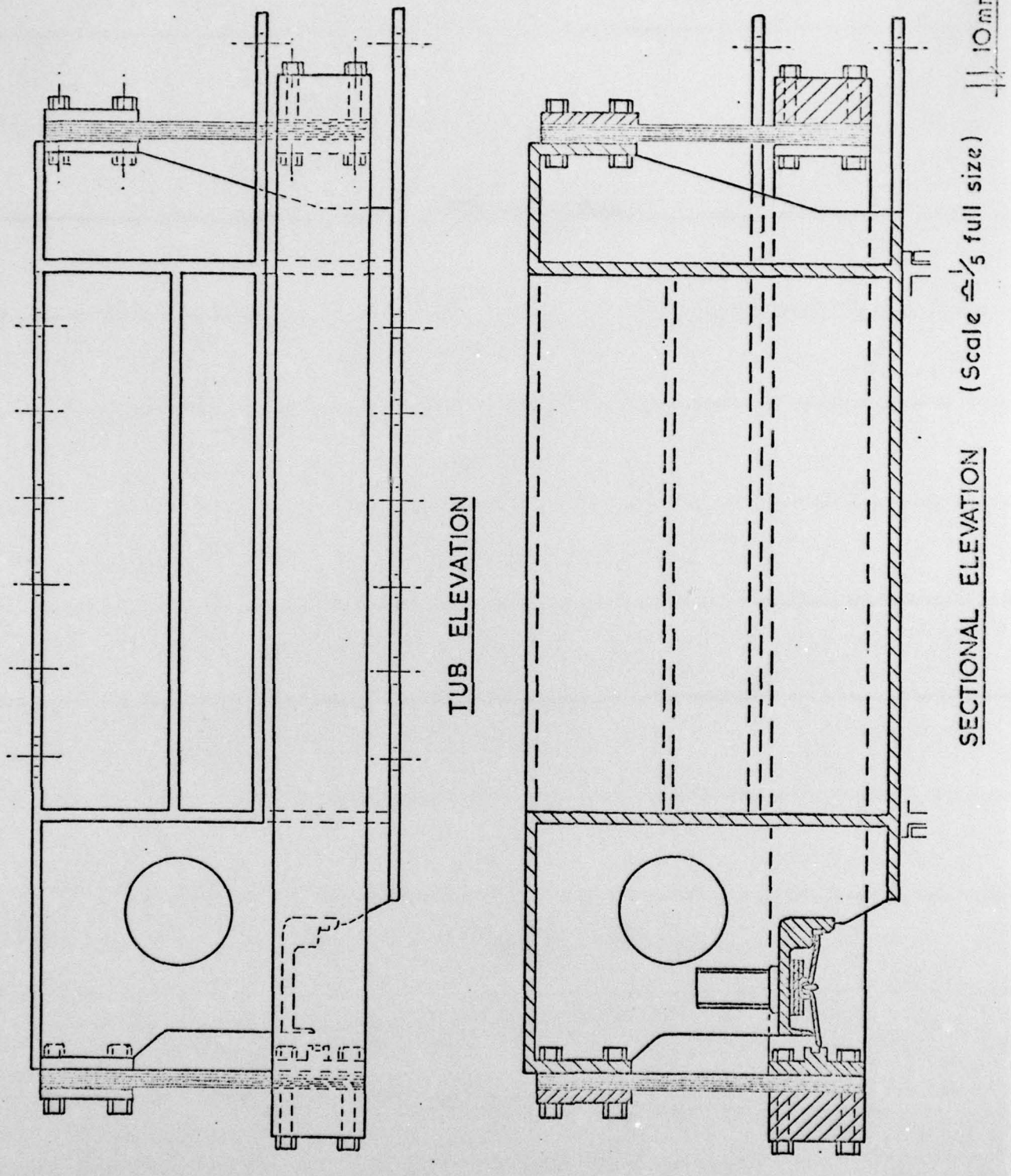

Figure 46 - Tub elevation and sectional elevation

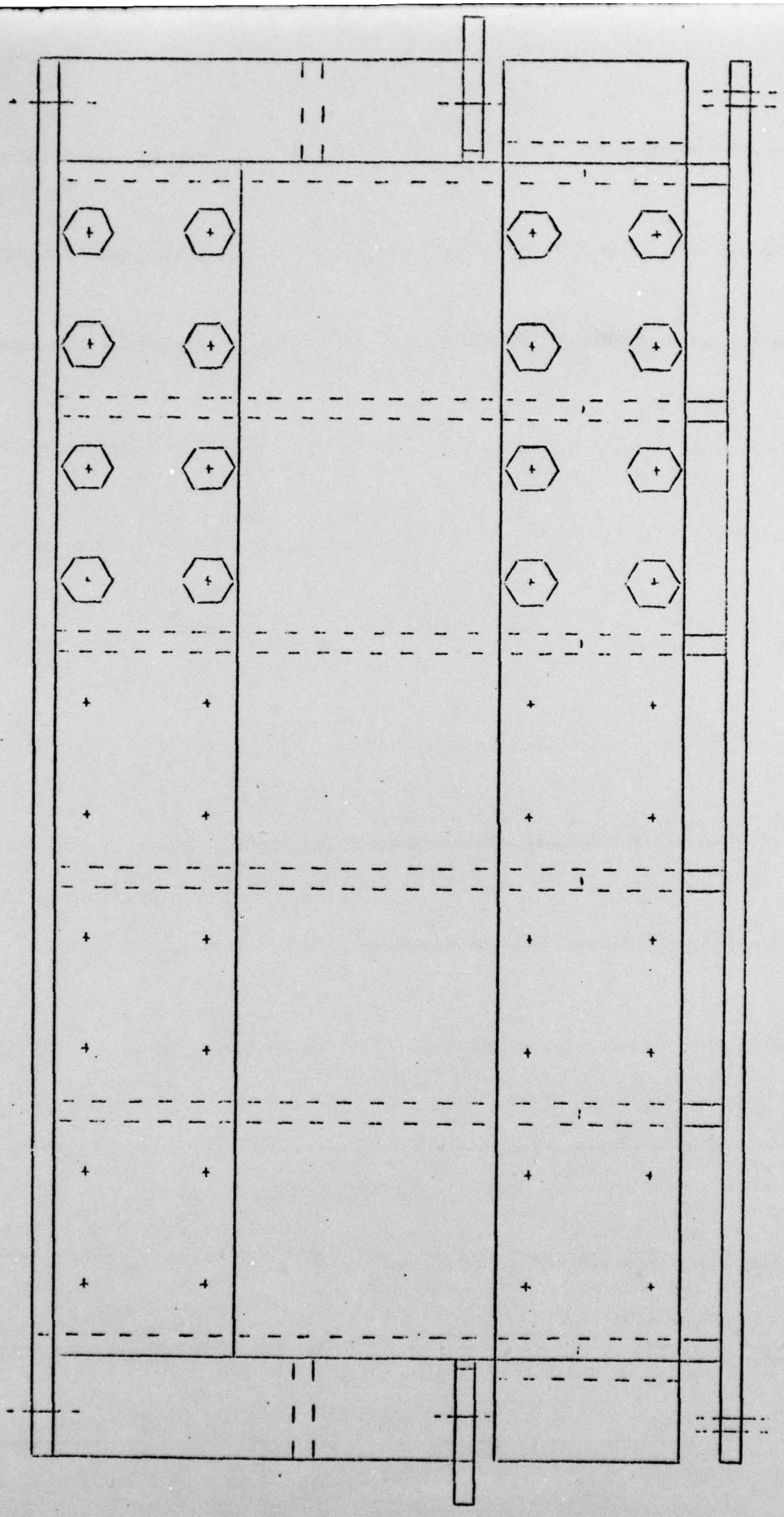

TUB END ELEVATION (SCALE 1/3 FULL SIZE)

10 mm.

Figure 47 - Tub end elevation

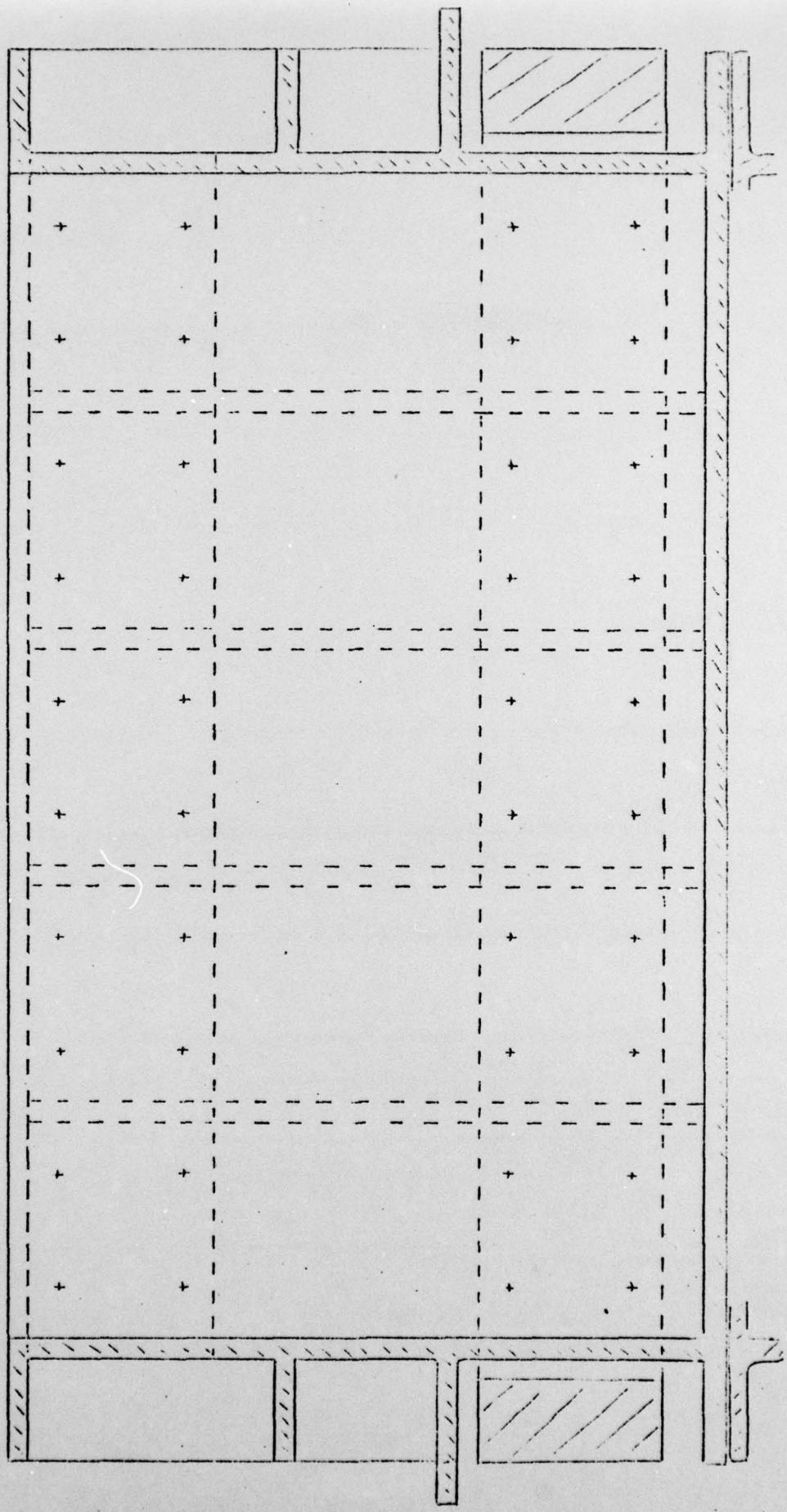

TUB SECTIONAL END ELEVATION (SCALE 2 1/3 FULL SIZE) 10 MM.

Figure 48 - Tub sectional end elevation

to allow the circumferential inertia mass to pass through, and the ribbing on the other two sides being vertical to take the bending moment from the leaf springs attached to those ends of the box.

The temporary jacking attachment was bolted onto extensions of two of the ribs on each of the long sides.

The main springs were thin plates of hardened spring steel, which were clamped together by fully torqued high tensile bolts, so that they acted in double bending. This allowed the circumferential inertia mass to move in horizontal translation, without any significant bending moments in the member connecting each end, and this could therefore simply be bolted on.

At their other end, the leaf springs were bolted onto a faced portion of the tub ribbing. This ribbing not only supported the weight of the leaf springs and the circumferential mass, but had to withstand a considerable bending moment due to the jacking force. Consequently the welding between the tub ribbing and the facing plate was of full depth and full strength, whereas in most other places fillet welding was sufficient. Circular holes were cut in the ribbing at one end for ease of assembly of the catch mechanism described shortly.

A number of considerations governed the design of the leaf springs. First of all their overall stiffness K was roughly determined by noting that the deflection of springs in response to the required horizontal earthquake force F, must be of the order of 5 to 10mm. if the mechanical

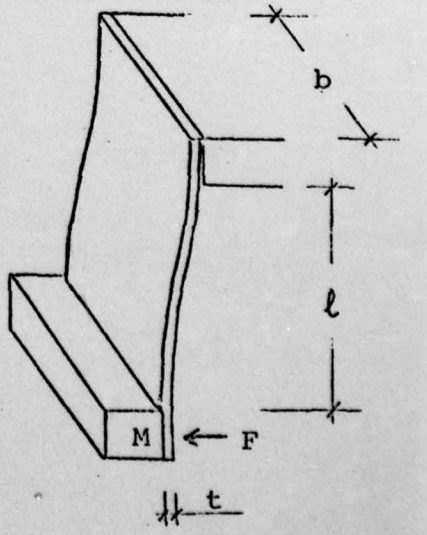

catch mechanism was to operate satisfactorily.

This then determined what value of inertia mass was needed in order to produce the model earthquake frequency required. Fortunately this value was not either too high or too low to be practicable.

The springs were also required to withstand the bending moments caused by the force F. If the bending stress was limited to σ, then this implied that $\frac{3F\ell}{bt^2} \leq \sigma$. Since the stiffness $K = \frac{Ebt^3}{\ell^3}$ was specified, then this condition became $\ell^2/t \leq \frac{3FE}{K\sigma}$. This allowed a limited choice of values of the spring thickness t and the length ℓ, although for practical reasons the length had to be between about 100mm and 400mm. However this implied rather large values of the breadth b, which was another reason for using multiple leaf springs. In all, twelve such leaf springs were used in tandem, and this was equivalent to a single spring of breadth twelve times that of the box.

In working out the frequency of vibration of this system more exactly, it was necessary to include part of the mass of the springs together with the mass of the inertia mass, and also to allow for the finite mass of the box. The appropriate dynamic parameters are shown in the sketch, and the net frequency of vibration of the two masses M_1 and M_2 together is given by $\frac{1}{2\pi}\sqrt{\frac{K}{M_1} + \frac{K}{M_2}}$.

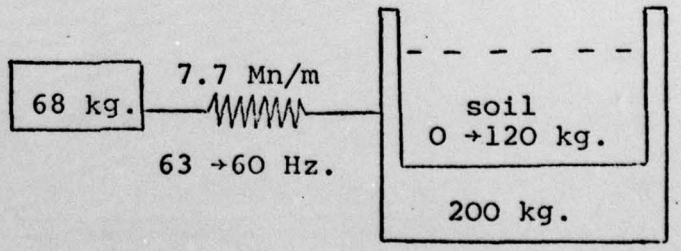

The stiffness K was measured experimentally by static jacking of the springs, and the predicted natural frequency

corresponded with what was observed.

In fact there was also a noticeable second mode of vibration, which involved the motion of opposite ends of the inertia mass, out-of-plane relative to each other, but held together by the connecting member, in the fashion indicated in the sketch. This manifested itself as an additional modal frequency of about 350 Hz., but was not very prominent and was usually ignored.

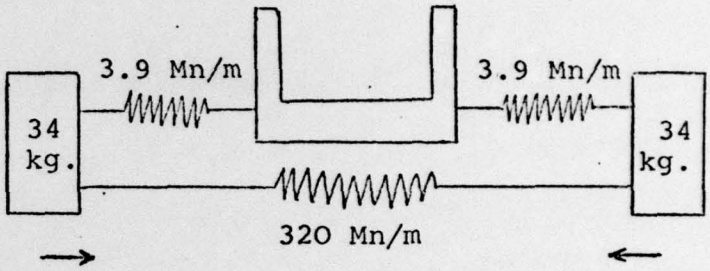

This part of the apparatus was of course asymmetric in design, and extra weights were always bolted onto the centrifuge swinging platform before a test, to bring the centre of gravity of the whole package close to the centre line of the swinging platforms, so that these could swing up as designed, when the centrifuge was started.

CATCH

A detail of the catch design is shown in Figures 49 and 50. As indicated in section 7.4, after temporary jacking out of the inertia mass, the three pieces of hardened steel were placed in the position shown, bearing on hardened steel pads set into the inertia mass and the main container. They were positioned by hand, flush against the machined receptacle, the geometry of which defined their orientation. In principle this geometry could have been changed by inserting extra packing pieces in the location shown, but it was found that a catch inclination of about 9^{o} to the horizontal gave sufficient

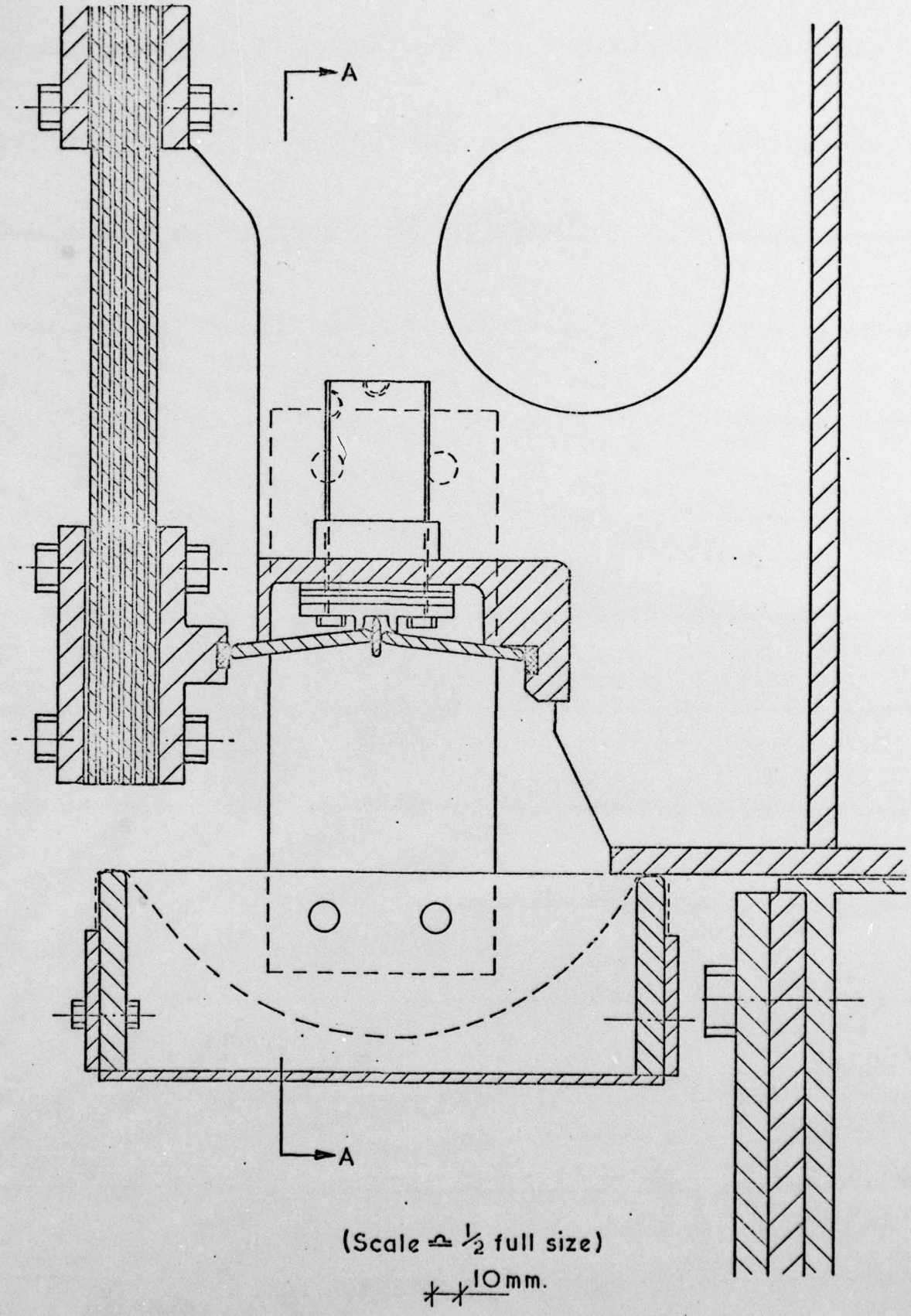

Figure 49 - Detail of catch mechanism

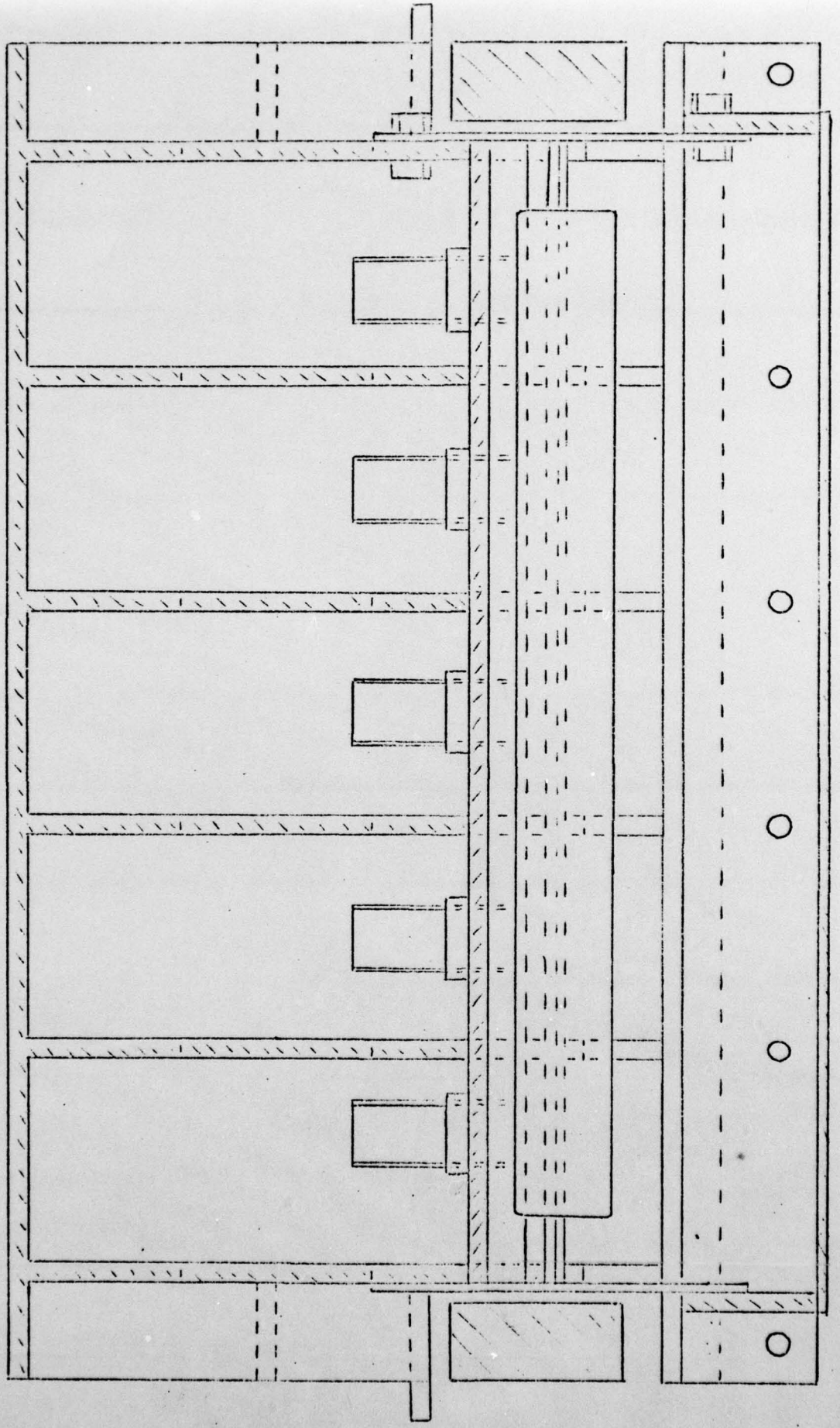

ELEVATION OF CATCH MECHANISM - SECTION ON A-A (SCALE = 1/3 FULL SIZE)

Figure 50 - Elevation of catch mechanism

"over-centre" stability to the arrangement, without any likelihood of the catch simply slipping off the bearing pads at the ends.

The five miniature jacks that pushed the catch pieces "over-centre" can be seen in the elevation in Figure 50. They were supplied with pressurised oil via a manifold, and it can be shown that under a constant jack pressure, the "snap through" is fully unstable all the way, so that the reaction mass is released very quickly.

The catch pieces were sized roughly to withstand the compressive forces without yielding or buckling, but in practice these stresses were low. Of much more concern were the contact stresses at the bearing pads, in particular the peak shear stress underneath the contact point. This is given by $0.127\sqrt{\frac{PE}{br}}$ in Timoshenko and Goodier* (1951), where P is the normal force, the length of the contact is b, the contact radius is r, and the Young's modulus of the material is E. As a result the ends of the catches were radiused to 5mm. Using a small catch piece between the two large pieces, also reduced the contact stress that would have occurred had they touched directly, as well as making the whole assembly more stable under compression. The thickness of this centre piece could be varied, to alter the magnitude of the dynamic forces in a crude fashion.

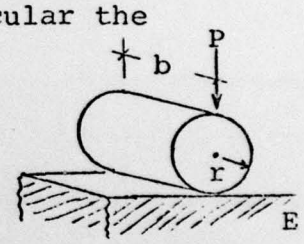

After installation of the catch, the collecting tray was put into position underneath, and this consisted of nylon

---

* TIMOSHENKO, S.P. and GOODIER, J.N. (1951) "Theory of Elasticity", McGraw-Hill Book Co., New York

webbing, hanging across an aluminium base, in order to absorb the considerable kinetic energy of the ejected catch pieces.

A source of concern was that it was possible in principle for the catch to release itself under its own weight, as indicated in the sketch. This was most likely at high values of centrifugal acceleration, and with a small "earthquake" force to hold the catch in position, and this did in fact happen once. By and large however, experiments at high values of centrifugal accelerations required correspondingly high values of horizontal force, so that this phenomenon was seldom a problem in practice.

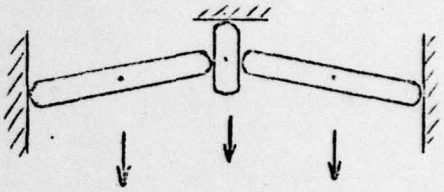

HYDRAULIC SYSTEM

This is sketched in Figure 51, and shows the way that high pressure nitrogen was stored prior to a test in a hydraulic accumulator mounted on the apparatus. It was separated from the oil by a flexible rubber membrane, capped with a small steel dome to prevent possible extrusion of the rubber membrane out of the accumulator.

This was in turn connected to an electrically operated soleroid valve, which, at the chosen moment, was opened to release oil under pressure to the miniature jacks. The pressure required to fire the catch for the highest value of horizontal force was about 3.5 MN/m^2 - roughly in agreement with what was predicted theoretically - but in order to allow for the pressure drop in the accumulator as the gas expanded adiabatically, a

HYDRAULIC SYSTEM

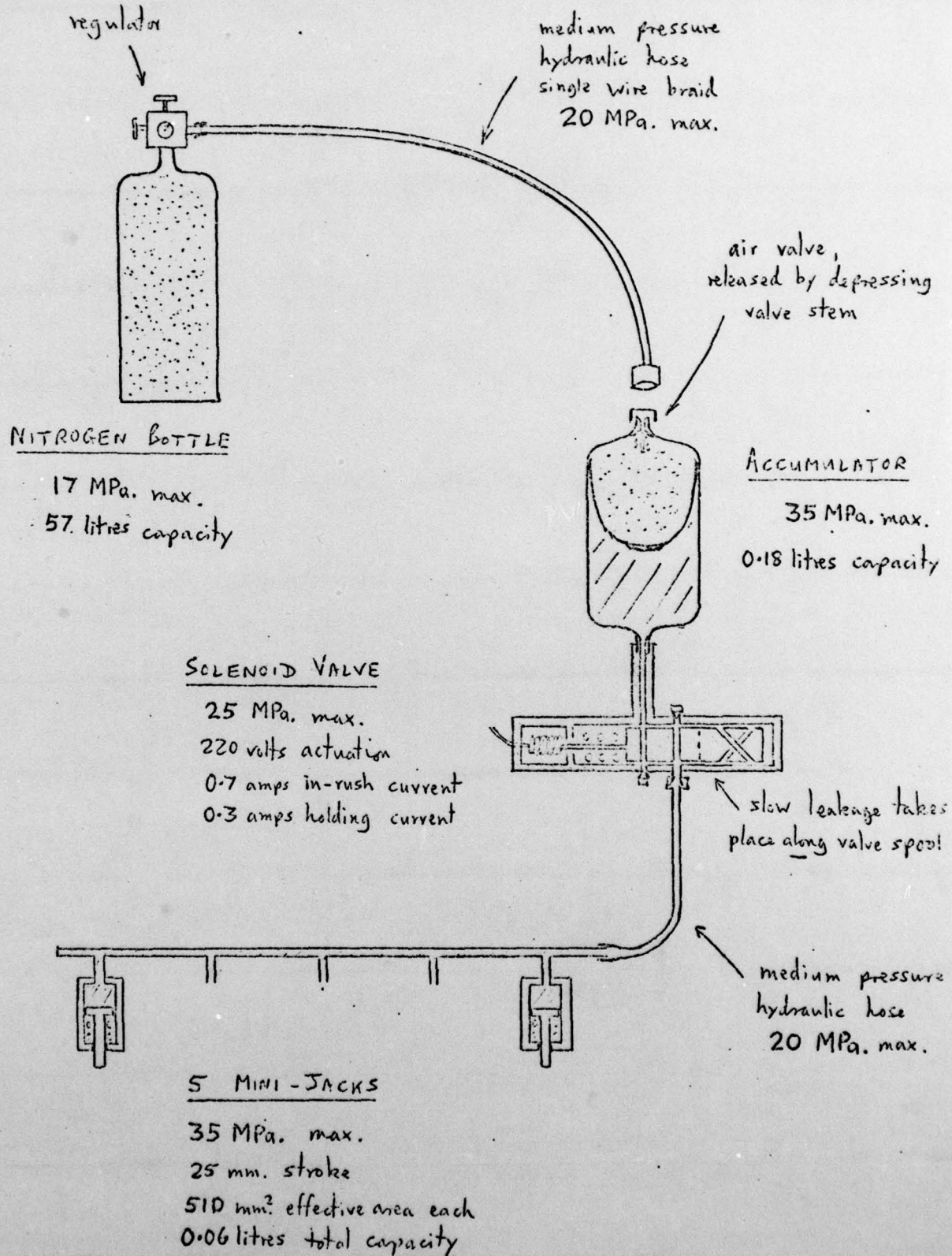

Figure 51 - Diagram of hydraulic system

precharge pressure of about 5 MN/m^2 was used to give reliable results.

The oil capacity of the little miniature jacks was small, so that only a small accumulator was needed. This accumulator was roughly half-filled with oil when the hydraulic system was first assembled, and the whole system then sealed, so that no more oil had to be added. After an experiment, the compressed nitrogen was released from the accumulator bladder by depressing the valve stem. The solenoid valve was then opened again, and this allowed the miniature jacks to retract under the force of their own built-in return springs, and the oil inside them was returned to the accumulator.

The return springs on the miniature jacks were strong enough to hold their pistons up against self-weight forces in the centrifuge. However the solenoid valve was of the spool type, and this did not seal perfectly along the spool, so that there was a slow leakage of fluid to the miniature jacks when the accumulator was pressurised, and this might have eventually caused the catch to fire prematurely. However this was no problem if there was a reasonable clearance between the jacks and the topmost catch piece, and if the accumulator was only charged with gas a short time before the experiment, so that little of this leakage could take place.

APPENDIX J - RIGID BODY MOTION OF SAND

If a column of soil is subjected to a lateral vibration at its base, there is the possibility of standing waves being set up at high freqencies of agitation. For frequencies that are sufficiently low, this will not occur and the soil will behave as a rigid body moving in phase with the base motion.

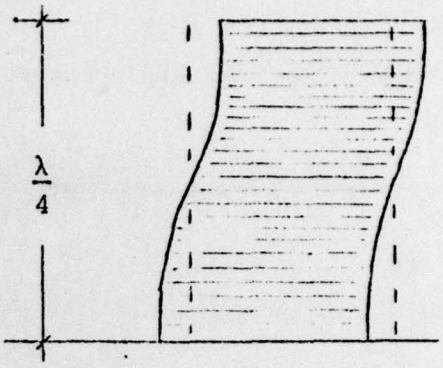

The lowest non-trivial standing wave is sketched above, with an "antinode" at top and bottom, and these standing waves will occur when the height of the soil column is equal to one half the wavelength λ of the wave being propagated through the soil, or multiples thereof. Now if the velocity of the vertical shear wave is V, and the frequency of generation f, then from elementary wave mechanics $\lambda = V/f$.

The shear wave velocity is given by $V = \sqrt{\frac{G}{\rho}}$ where ρ is the soil density, and the dynamic shear modulus G may be estimated using the relation by Hardin and Drnevich (1972) mentioned in Chapter 5.2, where $G \simeq 3.3 \times 10^5 \sqrt{p'}$ in S.I. units, for dense sand where $e \simeq 0.65$. Estimating the confining pressure p' under 0.1m. of sand say, at 50g, it will be about $0.1m \times 1600\ kg/m^3 \times 50 \times 9.81\ m/s^2 \simeq 8 \times 10^4$ Pa., and therefore $G \simeq 9 \times 10^7$ Pa., and $V \simeq 240$ m/s. This value is relatively insensitive to any inaccuracies in this derivation, as it is proportional only to the fourth root of the confining pressure.

Thus at the model earthquake frequency of 60 Hz., the appropriate wavelength is 4m. Since the maximum lateral

dimensions of the container is 0.5m., or $\frac{1}{8}$ of a wavelength, it is clear that one would normally expect the soil in the container to move uniformly and in phase at this frequency.

The maximum height of a model embankment in the container was about 0.2 or $\frac{1}{20}$ of a wavelength. Any "resonance" of the embankment as a result of standing waves would not occur until either the height of the embankment or the agitating frequency was increased by a factor of 10, so that the height approached half a wavelength, or more, as shown earlier.

In summary, then, for the range of model dimensions and frequencies used in this project, the soil may be assumed to move as a rigid body, "quasi-static" analysis of slope movement is generally valid, and no significant resonance or dynamic amplification effects would normally take place.

APPENDIX K - ACCELEROMETER EMBEDMENT

If a miniature accelerometer embedded in a soil mass is to faithfully follow the motion of the soil, then the natural frequency of the accelerometer supported by the surrounding soil, must be substantially higher than the frequency of soil motion.

This requires an assessment of the stiffness of the soil mass surrounding the accelerometer, and this may be estimated by assuming that it is divided into two infinite elastic half-spaces, as shown, which deform independently of each other. This is a conservative assumption and the problem becomes equivalent to two adjacent footings in tandem - one compressing the soil and the other acting to relieve compression. Then the combined stiffness is just twice the stiffness of a single circular footing in vertical translation on an infinite elastic half-space, derived originally by Timcshenko and Goodier*(1951), and is $2(\frac{4\ Gr}{1-\nu})$ where G and ν is the equivalent elastic modulus and Poisson's ratio of the soil respectively, and r is the footing radius.

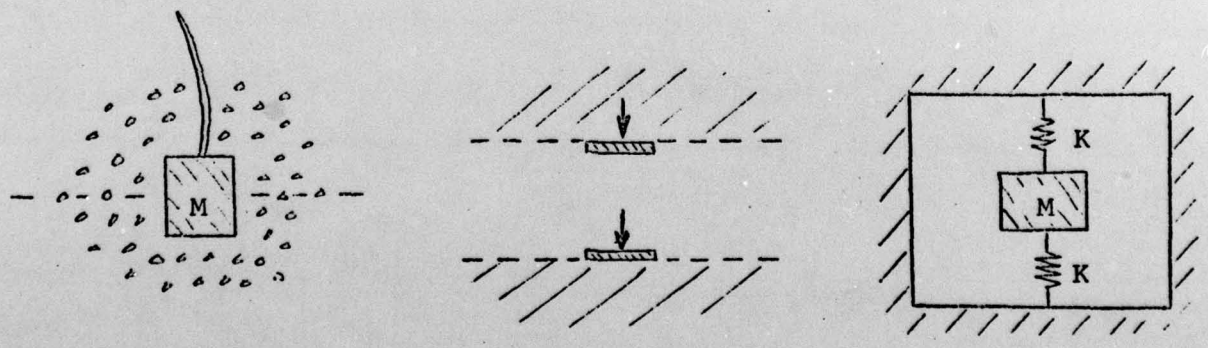

*TIMOSHENKO, S.P. and GOODIER, J.N. (1951) "Theory of Elasticity", McGraw Hill Book Co., New York.

The natural frequency of the system is then given by

$$\frac{1}{2\pi}\sqrt{\frac{2K}{M}} = \frac{1}{2\pi}\sqrt{\frac{8\,Gr}{(1-\nu)M}}$$

where the mass of the accelerometer is 0.004 kg., its radius is 0.005m, and Poisson's ratio for dry sand is assumed to be about 0.25. The dynamic shear modulus G of the soil may be estimated using the relation by Hardin and Drnevich (1972) mentioned in Chapter 5.2, where $G \simeq 3.3 \times 10^5 \sqrt{p'}$ in S.I. units, for dense sand where $e \simeq 0.65$. Making a conservative estimate of the confining pressure p', under 0.05m of soil, say, at 25g, it will be about
$0.05 \times 1600\ kg/m^3 \times 25 \times 9.81\ m/s^2 \simeq 2 \times 10^4$ Pa. and therefore $G \simeq 4.5 \times 10^7$ Pa.

Using these values the natural frequency of the accelerometer embedded in the soil will be about 4000 Hz., which is substantially above the model earthquake frequency of 60 Hz. This value is relatively insensitive to any inaccuracies in the derivation, as it is proportional only to the square root of the stiffness function, and the fourth root of the confining pressure.

Thus it is possible to state fairly categorically that under the sort of experiments described in this thesis, these accelerometers will follow the motion of sand when embedded in it, up to a frequency of at least 1000 Hz.

REFERENCES

BARKAN , D.D. (1962) "Dynamics of Bases and Foundations" McGraw-Hill, New York, p.23, published in Russian 1948

BASSETT, R. H. (1973) "Centrifugal model tests of embankments on soft alluvial foundations", Proc. 8th I.C.S.M.F.E. (Moscow), Vol. 2.2

BOROWICKA, H. (1963) "Concerning eccentrically loaded rigid discs on an isotropic elastic foundation", Ingenieur-Archiv, 1:1-8 (in German)

BYCROFT, G. N. (1956) "Forced vibrations of a rigid circular plate on a semi-infinite elastic space and on an elastic stratum", Trans. Royal Society, Series A, Vol. 248

GORBUNOV-POSSADOV, M. I. and SEREBRAJANYI, R. V. (1961) "Design of structures upon elastic foundations", Proc. 5th I.C.S.M.F.E. (Paris), Vol. 1

GRAY, P. and WADDINGTON, T. C. (1957) "Thermal decomposition of silver azide and its sensitisation by artificial lattice defects", Proc. Royal Society, Series A, Vol. 241

HALL, J. R. (1967) "Coupled rocking and sliding oscillations of rigid circular footings", Proc. Intnl. Symp. on Wave Propagation and Dynamic Properties of Earth Materials, Albuquerque, U.S.A.

HARDIN, B. O. (1965) "The nature of damping in soils", Proc. Am. Soc. of Civil Engineers, Vol. 91, SM1

HARDIN, B. O. and DRNEVICH, V. P. (1972) "Shear modulus and damping in soils: design equations and curves", Proc. Am. Soc. of Civil Engineers, Vol. 98, SM7

IPPEN, A.T. (1966) "Estuary and Coastline Hydrodynamics" McGraw-Hill, New York

KREBS OVESON, N. (1975) "Centrifugal testing applied to bearing capacity problems of footings on sand", Geotechnique, p. 394

LEE and WESLEY (1973) "Soil-structure interaction of nuclear reactor structures considering through soil coupling between adjacent structures", Nuclear Engineering and Design, Vol. 24, North Holland Publishing Co., Amsterdam

LYNDON, A. and SCHOFIELD, A. N. (1978) "Centrifugal model tests of the Lodalen landslide", Canadian Geotechnical Journal, February 1978

POKROVSKY, G. I. (1933) "On the use of a centrifuge in the study of models of soil structures", Zeitschrift für Technische Physik, Vol. 14, No. 4 (in German)

RICHART, F. E.; HALL, J. R. and WOODS, R. D. (1970) "Vibrations of Soils and Foundations", Prentice-Hall

RICHART, F. E. and WHITMAN, R. V. (1967) "Comparison of footing vibration tests with theory", Proc. Am. Soc. of Civil Engineers, Vol. 93, SM6

ROWE, P. W.; CRAIG, W. H. and PROCTOR, D. C. (1977) "Dynamically loaded centrifugal model foundations", Proc. 9th I.C.S.M.F.E. (Tokyo)

SCHOFIELD, A. N. (1978) "Use of centrifugal model testing to assess slope stability", Canadian Geotechnical Journal, February 1978

SEED, H. B. (1968) "Landslides during earthquakes due to soil liquefaction", Proc. Am. Soc. of Civil Engineers, Vol. 94, SM5, Terzaghi lecture

SEED, H. B. and GOODMAN, R. F. (1964) "Earthquake stability of slopes of cohesionless soils", Proc. Am. Soc. of Civil Engineers, Vol. 90, SM6

SEED, H. B. and IDRISS, I. M. (1967) "Analysis of soil liquefaction - Niigata earthquakes", Proc. Am. Soc. of Civil Engineers, Vol. 93, SM3

SEED, H. B.; IDRISS, I. M.; LEE, K. L. and MAKDISI, F. I. (1975) "Dynamic analysis of the slide in the Lower San Fernando Dam during the earthquake of February 9th, 1971", Proc. Am. Soc. of Civil Engineers, Vol. 101, GT9

SEED, H. B. and PEACOCK, W. H. (1971) "Test procedures for measuring soil liquefaction characteristics", Proc. Am. Soc. of Civil Engineers, Vol. 97, SM8

SILVER M.L. and SEED H.B. (1971)"Volume changes in sands during cyclic loading", Proc. Am. Soc. of Civil Engineers, Vol. 97, SM9

STOKOE K.H. and RICHART F.E. (1974)"Dynamic response of embedded machine foundations", Proc. Am. Soc. of Civil Engineers, Vol. 100, GT4

SUNG , T.Y. (1953) "Vibrations in semi-infinite solids due to periodic surface loading" Symposium on Dynamic Testing of Soils, A.S.T.M. Special Technical Publication No. 156

TIMOSHENKO, S. P. and GOODIER, J. N. (1951) "Theory of Elasticity", McGraw Hill Book Co., New York

URLICH, E. M. and KUHLEMEYER, R. L. (1973) "Coupled rocking and lateral vibrations of embedded footings", Canadian Geotechnical Journal, May 1973

U. S. ARMY, W. E. S. (1974) "One-dimensional wave propagation analysis. Patoka Dam, Indiana", W.E.S., Vicksburg, Mississippi, U.S.A., Paper S-74-26

WARBURTON, G. B.; RICHARDSON, J. P. and WEBSTER, J. J. (1971) "Forced vibrations of two masses on an elastic half-space", Journal of Applied Mechanics, Trans ASME, Series E, Vol. 38 No. 1

WHITMAN, R. V. (1972) "Analysis of soil-structure interaction - a state-of-the-art review", Proc. Symposium on Experimental and Theoretical Structural Dynamics, April 1972, Institute of Sound and Vibration Research, Southampton, U.K.

WHITMAN, R. V. and RICHART, F. E. (1967) "Design procedures for dynamically loaded foundations", Proc. Am. Soc. of Civil Engineers, Vol. 93, SM6

LIST OF SYMBOLS USED

a - amplitude of oscillation, also external structure radius

a_h - horizontal acceleration

a_v - vertical acceleration

a_o - amplitude of initial cycle, also non-dimensional frequency parameter

a_n - amplitude after n cycles

A - area

b - breadth of metal strips, also contact length

c - damping ratio, also foundation semi-dimension

C - electrical capacitance

C_u - undrained shear strength

C_v - consolidation coefficient

d - foundation diameter, also soil grain size

e - soil voids ratio

E - Young's Modulus

f - frequency of oscillation

f_n - natural frequency

F - magnitude of force

F_n - natural frequency of full size prototype

g - gravitational acceleration

G - shear modulus of soil

G_o - constant of proportionality

h - height of soil slope, also height of structure

H - maximum drainage path length

I - moment of inertia of structure

K - rotational stiffness of soil structure system, also general stiffness constant

ℓ - general dimension of length, also length of metal strips

M - mass of structure, also of accelerometer

MW - molecular weight of pore fluid

n - modelling scale

N_A - Avogadro's number

p' - mean effective confining pressure

p_o' - constant of proportionality

P - contact force

r - radius of structure base, also pore fluid molecular radius, also contact radius

R - centrifuge radius, also electrical resistance

R_o - ideal gas constant

t - time, also thickness of metal strips

T - absolute temperature, also torque

T_v - consolidation time factor*

v - velocity of motion

V - centrifuge tip velocity, also soil shear wave velocity

W - weight of package

x - general index

y - transverse co-ordinate of motion

z - depth of soil

α - fraction of soil pressure

β - ratio of horizontal to vertical acceleration

β_o - critical ratio of horizontal to vertical acceleration

ϕ - angle of torsional rotation

ϕ' - angle of soil friction

λ - wavelength

ν - Poisson's Ratio

ρ - density of soil, also of structure, also of pore fluid

σ - material stress

σ_H' - horizontal effective soil stress

σ_v' - vertical effective soil stress

θ - angle of rotation of structure, also slope angle

ω - angular velocity of oscillation

ω_n - angular velocity of natural oscillation

Ω - centrifuge angular velocity